SHALLOW-WATER HYDROTHERMAL VENTS

ECOSYSTEMS AND BIOTECHNOLOGICAL POTENTIAL

Ana Clara Pelliciari Silva

Doctoral Thesis

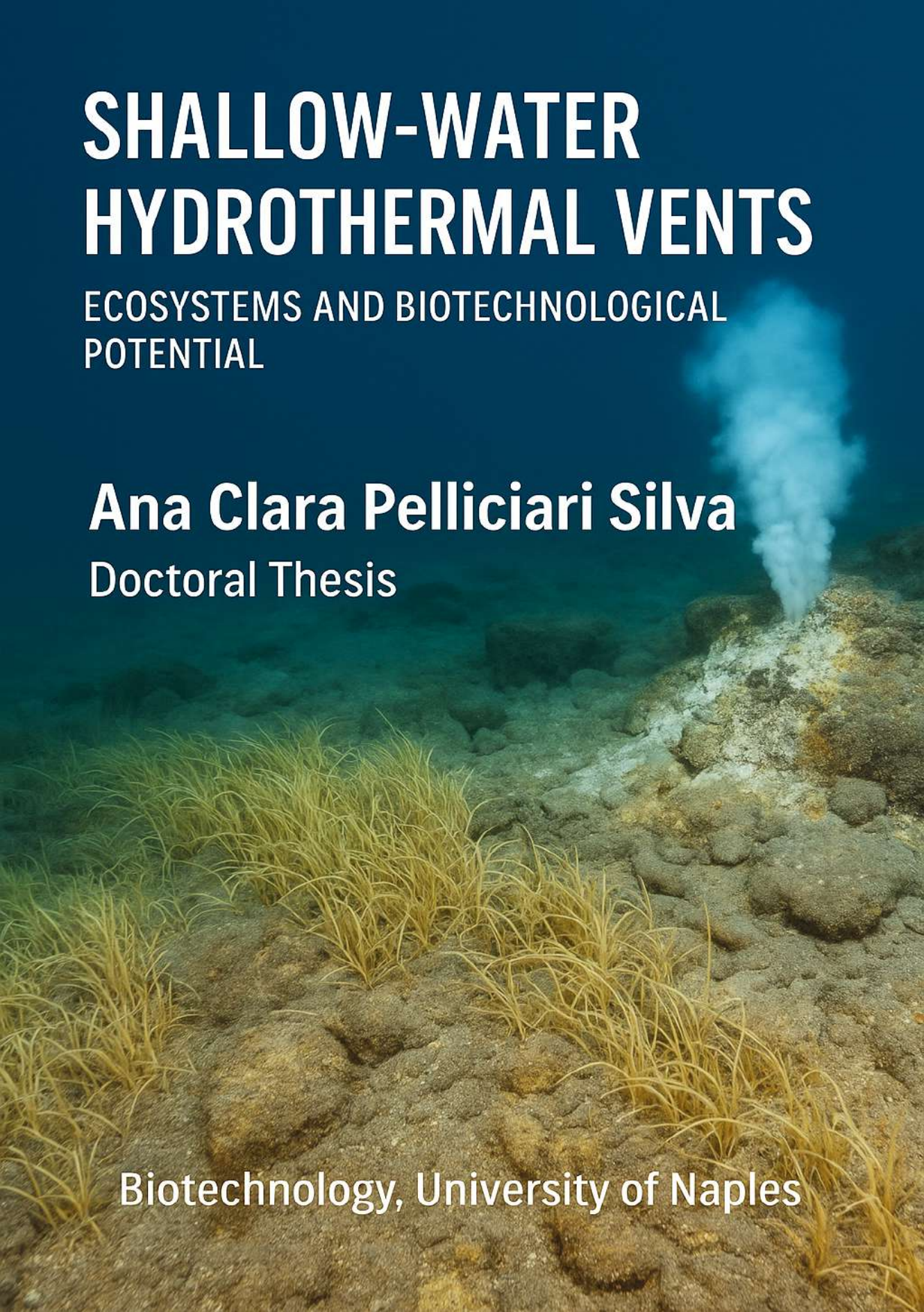

Biotechnology, University of Naples

Contents

Summary

Shallow-water hydrothermal vents (SHVs) are dynamic interfaces where geological activity, seawater chemistry, and microbial life converge, forming unique ecosystems shaped by steep gradients in temperature, chemistry, and light. Their accessibility compared to deep-sea vents makes them valuable natural laboratories, bridging terrestrial and marine influences while supporting both chemosynthesis and photosynthesis. Microbial communities here drive primary production, mediate mineral transformations, and produce metabolites with potential biotechnological applications. Yet, despite their relevance to global biogeochemical cycles, SHVs remain underexplored, particularly regarding microbial diversity, functional capacity, and environmental controls.

This thesis investigates SHVs as systems of ecological, evolutionary, and applied significance, integrating field observations, molecular approaches, and geochemical analyses. **Chapter 1** reviews the state of knowledge on SHV geochemistry, microbiology, and ecosystem services, identifying knowledge gaps in microbial ecology, viral communities, and cultivation approaches. **Chapter 2** presents a detailed case study from Milos Island, showing how hydrodynamic flow and benthic boundary layer interactions shape the composition and structure of white microbial mats. **Chapter 3** examines carbon fixation in the Gulf of Naples' Secca delle Fumose vent field, quantifying rates, and linking microbial processes to biosignature formation and carbon sequestration potential. **Chapter 4** explores SHVs and hot springs as untapped reservoirs for novel antibiotic discovery, highlighting biosynthetic gene clusters and underexplored microbiomes in extreme environments. Together, these studies advance our understanding of SHV microbiology, revealing their ecological roles and their promise for biotechnology, from climate change mitigation to new drug discovery.

Sommario

Le sorgenti idrotermali in acque basse sono interfacce dinamiche in cui l'attività geologica, la chimica dell'acqua marina e la vita microbica si incontrano, dando origine a ecosistemi unici modellati da forti gradienti di temperatura, composizione chimica e luce. La loro accessibilità, rispetto alle sorgenti idrotermali profonde, le rende preziosi laboratori naturali, in grado di collegare gli ambienti terrestri e marini e di sostenere sia la chemiosintesi sia la fotosintesi. Le comunità microbiche che vi abitano guidano la produzione primaria, mediano le trasformazioni minerali e producono metaboliti con potenziali applicazioni biotecnologiche. Tuttavia, nonostante la loro rilevanza nei cicli biogeochimici globali, le SHV rimangono poco esplorate, in particolare per quanto riguarda la diversità microbica, le capacità funzionali e i fattori ambientali che le regolano.
Questa tesi indaga le SHV come sistemi di rilevanza ecologica, evolutiva e applicata, integrando osservazioni sul campo, approcci molecolari e analisi geochimiche. Il **Capitolo 1** esamina lo stato delle conoscenze sulla geochimica, la microbiologia e i servizi ecosistemici delle SHV, individuando le lacune nella ricerca riguardanti l'ecologia microbica, le comunità virali e i metodi di coltivazione. Il **Capitolo 2** presenta uno studio di caso dettagliato sull'isola di Milo, mostrando come il flusso idrodinamico e le interazioni nello strato limite bentonico influenzino la composizione e la struttura dei tappeti microbici bianchi. Il **Capitolo 3** analizza la fissazione del carbonio nel campo di sfiati di Secca delle Fumose, nel Golfo di Napoli, quantificando i tassi di attività e collegando i processi microbici alla formazione di biofirme e al potenziale di sequestro del carbonio. Il **Capitolo 4** esplora le SHV e le sorgenti termali come riserve ancora poco sfruttate per la scoperta di nuovi antibiotici, evidenziando i cluster di geni biosintetici e i microbiomi poco studiati in ambienti estremi.Complessivamente, questi studi ampliano la comprensione della microbiologia delle SHV, rivelandone i ruoli ecologici e il potenziale biotecnologico, che spazia dalla mitigazione dei cambiamenti climatici alla scoperta di nuovi farmaci.

Objectives & Aims

The overarching aim of this PhD is to comprehend the ecological, functional, and biotechnological significance of microbial communities inhabiting shallow-water hydrothermal vents (SHVs). These environments form a bridge between terrestrial geothermal systems and deep-sea vents, offering a unique opportunity to study how geological processes and geochemical gradients influence microbial life, primary productivity, and metabolic potential.

This work integrates microbiological, geochemical, and bioinformatic approaches to address how microbial communities colonising SHVs interact with their environment, contribute to carbon cycling, and express biosynthetic potential. The main goals are:

1. To characterise the microbial diversity and community structure of SHV biofilms through 16S rRNA gene sequencing, metagenomics, and microscopic observations, linking microbial assemblages to local geochemical and hydrodynamic conditions.

2. To quantify carbon fixation rates in vent-associated biofilms using ^{13}C–bicarbonate incubation assays and isotope ratio mass spectrometry, providing direct estimates of autotrophic productivity and its role in sustaining vent ecosystems.

3. To compare shallow-vent microbiomes with continental geothermal systems, using a global dataset to identify common and divergent biosynthetic capacities across volcanic provinces.

4. To develop and apply an analytical workflow for estimating carbon fixation rates, including isotopic corrections and dilution factors, ensuring methodological consistency across vent sites.

5. To assess the biosynthetic potential of microbial communities through large-scale identification of biosynthetic gene clusters (BGCs), evaluating how geological and chemical factors shape natural product diversity.

Chapter 1

1 Shallow water hydrothermal vents: microbiology, geochemistry and coevolution

Abstract

Shallow-water hydrothermal vents (SHVs) represent dynamic biogeochemical systems situated at the interface between terrestrial and deep-sea environments. Unlike their deep-sea counterparts, SHVs are shaped by both subsurface geothermal processes and surface influences such as terrigenous inputs, photic zone exposure, and hydrodynamic forcing. This chapter synthesizes the current understanding of SHV microbiology and geochemistry, highlighting their complex co-evolution and ecological distinctiveness. SHVs support metabolically diverse microbial communities, including chemolithoautotrophs, phototrophs, heterotrophs, and extremophiles, which mediate key transformations in carbon, nitrogen, and sulfur cycles. The presence of both light and hydrothermal energy enables unique primary production modes that combine photosynthesis and chemosynthesis, thereby influencing microbial composition and function in ways distinct from deep-sea hydrothermal systems.Through a comparative framework, this chapter distinguishes SHVs from deep-sea hydrothermal vents based on depth thresholds, terrigenous organic inputs, and the role of light. Key environmental gradients, temperature, pressure, and redox chemistry, are identified as critical drivers of microbial diversity and spatial structuring within SHV habitats. Despite the increasing recognition of SHVs as biogeochemically significant and biotechnologically promising, substantial gaps persist in our knowledge. Notably, biases in sampling depth, limited culture-based studies, and underexplored functional genomics have hindered a holistic understanding of microbial ecology in these systems.This chapter also highlights novel avenues for research, including the roles of viral communities, symbiosis, and microbial polysaccharide production, as well as the relevance of SHVs to astrobiology, origin-of-life studies, and climate change mitigation. Emphasizing the need for integrative approaches that couple high-resolution geochemical data with advanced

'omics' techniques, this chapter advocates for SHVs to be studied as distinct ecological entities. In doing so, it provides the conceptual and empirical groundwork for understanding how these environments contribute to global biogeochemical cycles and how their microbiomes may inform future biotechnological innovation.

1.1 Exploring the Geochemistry and Microbiology of Marine Shallow-Water Hydrothermal Vents

Localized areas where water heated by geothermal processes emerges through openings in the Earth's crust, either above or below water surfaces, are called hydrothermal vents, another widely used noun for these geological environments is hot springs (e.g Figures 1 and 4). These fascinating phenomena occur in regions abundant in thermal energy sources that facilitate the movement of fluids (Jannasch and Taylor [1984]; Pichler et al. [2006]; Sievert and Vetriani [2012a]; Price et al. [2015]). On our planet, these energy sources primarily stem from dynamic geological events occurring in proximity to boundaries where tectonic plates interact, involving processes such as the formation of molten rock or the occurrence of geological faults (Jannasch and Taylor [1984]).

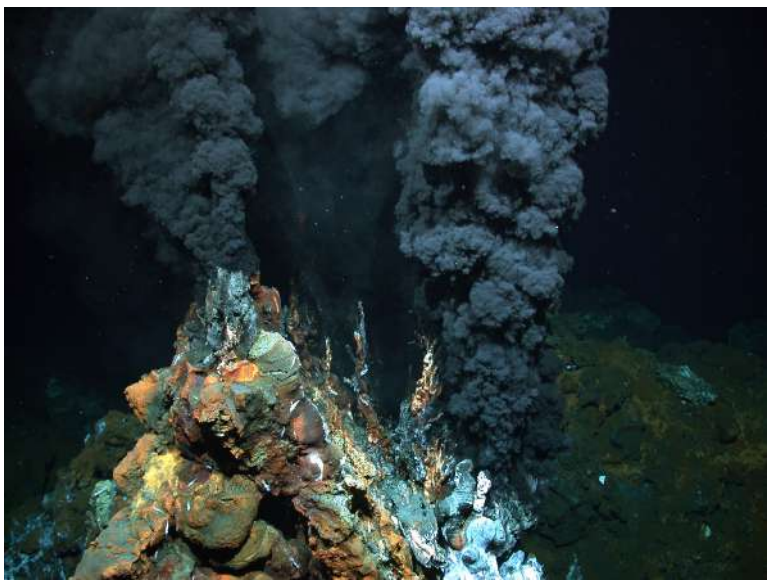

Figure 1: Hydrothermal vents present at over 3 Km below sea level in the Galapagos Rift. Photograph by MARUM - Zentrum für Marine Umwelt.

In this thesis, shallow-water hydrothermal vents (SHVs) are defined as hydrothermal systems occurring at depths shallower than 200 m, where volcanically or tectonically driven fluid circulation intersects the photic zone and oxygenated seawater. The scope of this work is to synthesize current knowledge of SHV geochemistry and microbiology, while identifying major gaps that distinguish these environments from deep-sea hydrothermal systems. The following chapters combine geological context, microbial community analyses, and targeted case studies to establish a coherent framework for understanding SHVs as unique, transitional ecosystems with both ecological and biotechnological relevance.
While the generation of molten rock can take place at various types of plate boundaries, including transform, divergent, and convergent boundaries, it is worth noting that hydrothermal venting mainly occurs at divergent boundaries along mid-ocean ridges, and convergent boundaries associated with island arc volcanoes and seamounts (Jannasch and Taylor [1984]). Furthermore, the circulation of hydrothermal fluids at transform fault boundaries can be attributed to heat generated through frictional processes (Jannasch and Taylor [1984]). Another potential driving force behind hydrothermal circulation is the occurrence of geochemical reactions, such as serpentinization (Lowell and Rona [2002]).
Within these complex hydrothermal systems, the fluids discharged from the vents often display a high concentration of inorganic chemical species that serve as electron donors. As the heated fluids intermingle with oxygen-rich seawater, which is rich in electron acceptors, a fundamental chemical interplay occurs, resulting in the formation of aqueous solutions marked by a multitude of imbalances within the realm of redox reactions. These chemical imbalances offer valuable resources that are effectively utilized by microbial communities comprised of bacteria and archaea (Jannasch and Taylor [1984]; Pichler et al. [2006]; Sievert and Vetriani [2012a]; Price et al. [2015]). Notably, these deep-sea hydrothermal vent environments harbor microbial communities that exploit these energy sources, forming the foundation of highly diverse ecosystems (Felbeck and Somero [1982]; Hügler and Imhoff [2009]; Lutz and Kennish [1993]).
Nonetheless, the mixing processes of hydrothermal systems described earlier are not solely limited to the deeper regions of the oceans. Shallow-water hydrothermal vents, also known as ”shallow-sea” vents (SHVs), can be found at shallower depths, encompassing coastal marine environments and shallow lakes, provided there exists a sufficient heat

source to stimulate hydrothermal circulation. New studies suggest that SHVs are not as scarce as previously thought worldwide (Figure 2). Despite sharing several resemblances with deep-sea hydrothermal vents (DHVs), SHVs exhibit significant differences mainly attributed to their presence at lesser depths. This literature review aims to provide a concise overview of SHV geochemistry and microbiology, highlighting unexplored research areas and acknowledging the current limitations in our understanding of these unique systems.

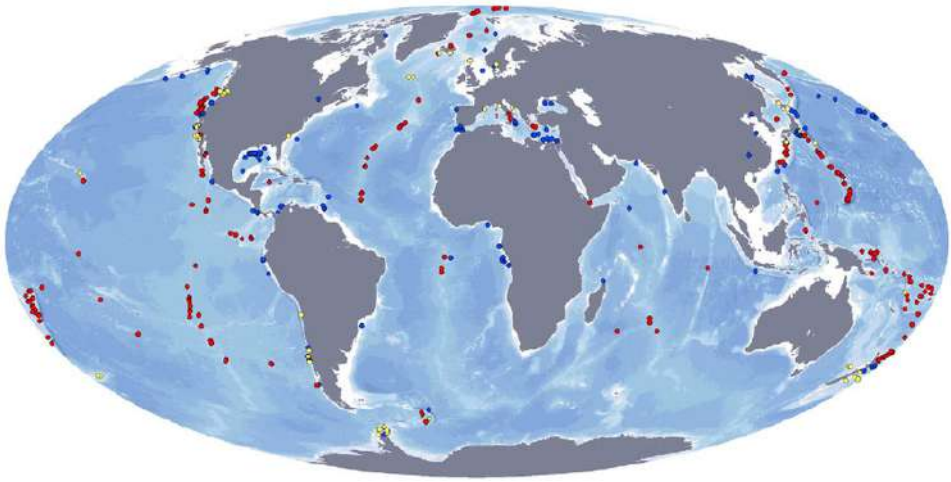

Figure 2: Global distribution of hydrothermal vents (red), cold seeps (blue) and whale falls (yellow). Diagram by German et al. [2003]. New studies suggest that SHV are as widespread as deep-sea vents, however significantly understudied.

1.1.1 Deep-sea vents versus shallow-sea vents

Three factors seem to be the most essential when distinguishing DHVs and SHVs. These are depth, terriginous input, and light.

1.1.1.1 How deep is deep?

Up until now, the recognized definition of SHVs is associated with water depths less than 200 m (Tarasov and et al. [2005]). This specific depth choice serves multiple purposes. Firstly, it approximately aligns with the maximum extent of the photic zone, beyond which light penetration into the ocean is significantly limited, even though certain conditions may allow light to reach deeper depths (Garrison [2016]). Additionally, qualitative observations indicate that around 200 m, there is a noticeable shift

in the slope of the seawater boiling curve (Price and Giovannelli [2017]), which has been utilized to distinguish between "deep" and "shallow" vent systems (Bischoff and Rosenbauer [1985]; Tarasov and et al. [2005]). However, these distinctions are somewhat arbitrary when considering the classification of hydrothermal venting as a whole. In a pioneering study conducted by Price and Giovannelli [2017], precise calculations were conducted to determine the exact point where the slope of the temperature versus depth seawater boiling curve transitions to a 1:1 ratio (Figure 3). This delineates the point at which changes in pressure become more influential than changes in temperature regarding boiling. Based on the calculations conducted, it has been determined that this pivotal threshold occurs at a depth of 212 meters, having in mind a consistent salinity level (Price and Giovannelli [2017]). Hence, 212 m may be regarded as a more accurate depth threshold for differentiating between "deep-sea" and "shallow-sea" hydrothermal vents (Price and Giovannelli [2017]).

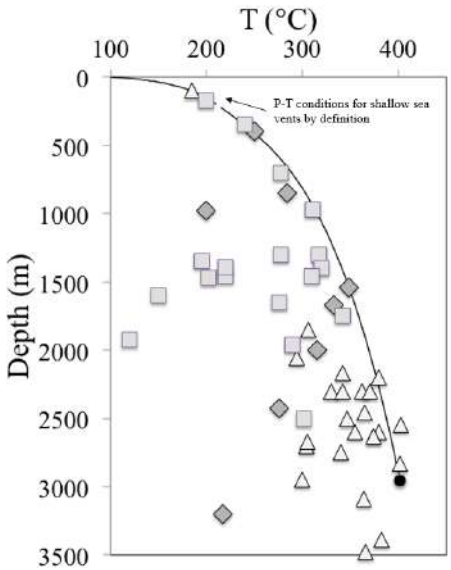

Figure 3: Two phase curve for seawater compiled by Price and Giovannelli [2017]. Data points by Havig [2009], all represent seawater hydrothermal vent systems. It is worth noting that below $\sim$ 200 m, the curve shallows signficantly indicating that beyond this point changes in pressure will dominate changes in temperature.

1.1.1.2 SHVs, a way to communicate between terrestrial and deep vents

SHV communities are characterized by the frequent presence of Cyanobacteria (Dávila-Ramos et al. [2014]; Giovannelli et al. [2013]; Kamenev et al. [1993]; Maugeri et al. [2013]; Roeselers et al. [2007]), anoxygenic phototrophs (Dando et al. [1999]; Hirayama et al. [2007b]; Lentini et al. [2014]), and abundant aerobic and anaerobic heterotrophs (Gugliandolo and Maugeri [1998]; Hoaki et al. [1995]; Sievert et al. [2000]). These communities benefit from the presence of sunlight and high organic carbon loads (Tarasov and et al. [2005]). Unlike deep-sea vents, shallow-sea vents often receive meteorically derived groundwater discharging into the marine realm, especially in tropical areas with high precipitation. This transitional nature between terrestrial and deep-sea vents is a defining and distinctive characteristic of shallow-sea vents.
However, there is a notable research gap concerning microbial diversity in shallow-water vent communities. Only a limited number of studies have investigated the microbial composition, revealing the presence of a range of mesophilic, thermophilic, and hyperthermophilic Archaea and Bacteria (e.g., Alfredsson et al. [1988]; Dando et al. [1999]; Hirayama et al. [2007b]; Sievert et al. [2000]) in subsurface and surface sediments, as well as on the hard substrate surrounding hydrothermal emissions. The high input of organic carbon in shallow-water vents likely contributes to their rich microbial diversity.

1.1.1.3 Temperature and light affecting the microbiome of SHVs

Temperature plays a crucial role in shaping the abundance of prokaryotes in the vents, as observed in previous studies (Giovannelli et al. [2013]; Manini et al. [2008]; Maugeri et al. [2009]). In a comprehensive investigation conducted by Giovannelli et al. [2013] at Milos (Greece), a decline in the number of cells was noted in the sediments surrounding the vents, with a gradual decrease from the background areas characterized by temperatures around 20 ℃, reaching the central region of the vent patch with temperatures around 90 ℃ (Sievert et al. [1999]; Giovannelli et al. [2013]). These findings suggest that the distribution of different microbial taxa within each vent is primarily influenced by temperature, as well as the presence of suitable electron donors and acceptors, as highlighted in previous studies (Giovannelli et al. [2013]; Price

and Giovannelli [2017]; Sievert et al. [2000]; Yücel et al. [2013]).
The designation of SHVs is partially based on their occurrence within the upper limit of the photic zone, approximately 200 meters deep, as mentioned in the previous subsection of this report. These unique environments, characterized by the coexistence of light and geothermally reduced compounds, exhibit high energy levels that support both photosynthesis and chemosynthesis (Dando et al. [1999]; Gugliandolo and Maugeri [1998]; Tarasov and et al. [2005]; Price et al. [2013]). This phenomenon finds similarity with terrestrial vents, such as the colorful pools observed in Yellowstone National Park (Figure 4), which owe their vibrancy to phototrophic bacteria boasting diverse pigments. The presence of light and the substantial inputs of photosynthetically derived organic carbon make SHVs truly exceptional in the realm of hydrothermal vent ecosystems (Figure 5). These factors profoundly shape the microbiology of SHVs, distinguishing them from deep-sea vents and highlighting the remarkable influence of light in these environments (Dando et al. [1999]; Giovannelli et al. [2013]; Gugliandolo and Maugeri [1998]).

Figure 4: Grand Prismatic Spring, Yellowstone National Park – the vivid rings of blue, green, yellow, and orange are created by temperature-dependent microbial mats. Thermophilic bacteria and archaea thrive in distinct zones around the spring, with pigments and metabolic activity changing as water cools from the deep, sterile blue center toward the cooler, more biologically active edges. Photo credit by Officers Row, Yellowstone National Park.

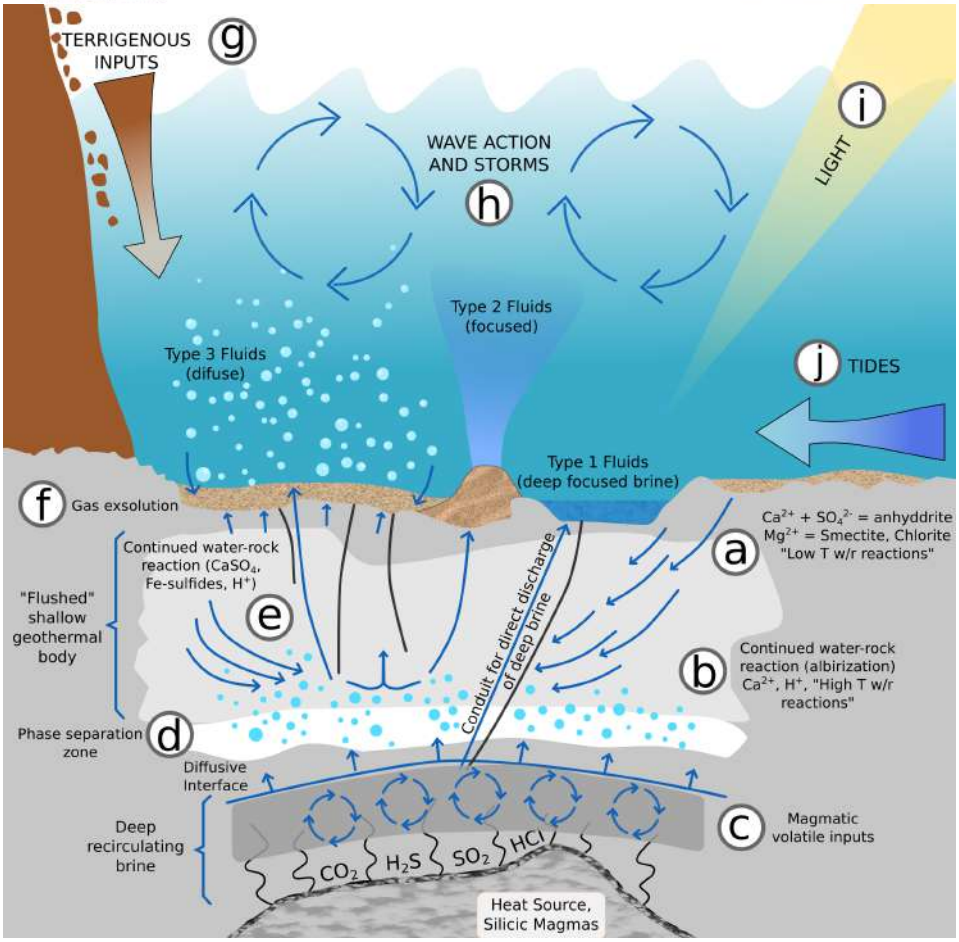

Figure 5: Conceptual model of shallow-water hydrothermal vent systems, highlighting their distinct position between terrestrial and deep-sea ecosystems. In addition to subsurface magmatic inputs and water–rock reactions, these environments are shaped by surface influences such as terrigenous inputs (g), wave action and storms (h), light penetration (i), and tidal forces (j). This combination of deep geochemical drivers and dynamic surface processes creates unique physical and chemical gradients that support diverse microbial and macrofaunal communities. Scheme from Giovannelli et al. [2013].

Shallow submarine hydrothermal systems exposed to sunlight are expected to harbor more diverse microbial communities compared to dark deep-sea hydrothermal systems. This is because these systems support in situ primary production by both chemolithotrophs and phototrophs. One such intriguing system associated with a subtropical coral reef has been discovered off Taketomi Island in the Southern Ryukyu Archipelago, Japan (Hirayama et al. [2007b]). This hydrothermal system

is located within a craterlike basin structure within barrier reefs, with visible fluid emissions and gas bubbles mainly composed of CH_4 and N_2. Extensive microbial communities, including white microbial mats at the deepest vent site and colored microbial mats at shallower vent sites, have been observed (Hirayama et al. [2007b]).
Analysis of the microbial communities in the Taketomi system reveals the predominance of chemolithoautotrophs and methanotrophs, including members of the *Epsilonproteobacteria* and unique members of the *Gammaproteobacteria*. Previous investigations in shallow submarine hydrothermal systems are limited, but Sievert et al. [2000] also found higher numbers of heterotrophs than autotrophs in the sediment community of the Milos, Greece shallow hydrothermal system, despite the presence of chemolithoautotrophic sulfur-oxidizing bacteria. In the Taketomi system, phototrophic microorganisms are not prominent components of the communities around the main vent site at a 23 m depth. This may be attributed to the lower energy input from sunlight compared to the greater input of inorganic energy sources from the hydrothermal fluid. It is noteworthy that the combination of light availability and the geological features, such as the crater basin, significantly influences the metabolic diversity of the microbiome in shallow submarine hydrothermal vents.

1.2 What are we still to discover about SHV?

1.2.1 Depth as a bias in the SHV realm

The scientific exploration of SHVs has been predominantly focused on a specific subset of sites. This bias can be attributed to the significant attention given to deep-sea vents located at depths exceeding 1000 meters. Additionally, the exploration of SHVs has primarily centered around those vents accessible to recreational SCUBA diving depths, typically around 50 meters or shallower. As a result, there is a significant expanse of depth encompassing hydrothermal venting that remains largely uncharted (Price and Giovannelli [2017]). To ensure a comprehensive understanding of SHVs, it is crucial to conduct investigations that encompass the depths ranging from approximately 50 to 1000 meters, thereby mitigating any potential knowledge biases associated with these ecosystems.

1.2.2 Studying SHV as its own entity

SHV exhibit various characteristics, encompassing focused vent structures that bear a resemblance, though less pronounced, to the well-known black smokers found in deep-sea vents (Figure 1 and 6). Additionally, they include areas where gas discharges appear predominantly as free gas with minimal fluid content, as well as regions where venting occurs diffusively through sediment. The temperatures within these vents can reach levels approaching the boiling point on the seawater boiling curve, with higher temperatures observed at greater depths. Notably, a SCUBA diver recorded an extreme temperature of 135.2℃ at a depth of approximately 22 meters in a shallow-sea vent off the coast of Panarea (Price et al. [2015]).

Figure 6: Diver approaching the shallow water vent Secca delle Fumose in the Gulf of Naples, present at 13 m depth. It is noticeable that light is still readily present at these depths in the ocean. Here we notice Secca delle Fumose as a diffused gas emission zone.

Shallow-sea vents associated with magmatic systems often display enrichment in either iron or sulfur. The dominance of iron or sulfur in

surface manifestations depends on the intricate interplay between these elements in the subsurface, wherein the abundance of one element influences the enrichment pattern (Price and Giovannelli [2017]). However, the specific processes driving the initial enrichment of one element over the other remain uncertain. Interestingly, shallow-sea vents can be sourced from meteoric water, which tends to have lower sulfate levels. It seems that vents originating from meteoric water sources are more inclined towards iron enrichment rather than sulfur enrichment. This discrepancy may arise from the substantial initial supply of sulfate in vents sourced from seawater, enabling sustained elevated sulfur concentrations until all iron is depleted (Price and Giovannelli [2017]). Nevertheless, further investigation and supporting evidence focused specifically on SHVs are necessary to corroborate this hypothesis.

Extensive research has been conducted to unravel the complex underground processes that govern the chemical composition of hydrothermal fluids discharged at deep-sea vents (Alt [1995]; Berndt et al. [1988]; Bischoff and Rosenbauer [1985]; Dzurisin and Fournier [2007]; Foustoukos and Seyfried Jr [2007]; German et al. [2003]; Hannington et al. [2005]; Hedenquist and Lowenstern [1994]; Rusk et al. [2004]; Henley and Ellis [1983]; Seyfried Jr and Mottl [1982]; Tivey [2007]). These intricate processes involve the interaction between fluids and minerals, separation of different phases, input of volatile substances from magmatic sources, precipitation of minerals at varying depths, and the mixing of seawater (Alt [1995]). While significant strides have been made in understanding DHV systems along mid-ocean ridges and back-arc basins (Gamo et al. [1997]; Reeves and Johnson [2011]), our knowledge of the subsurface mechanisms occurring at SHV remains limited. In fact, the current understanding of SHV is often inferred from studies conducted on deep-sea vents (Price and Giovannelli [2017]), highlighting the urgent need for dedicated investigations into the unique characteristics of shallow-sea hydrothermal vents. It is imperative to bridge this knowledge gap and gain insights into the distinct properties of SHV, particularly considering the alkaline SHV, which are very distinct from their deep-sea counterparts. In-depth examinations of shallow-sea hydrothermal vents can provide valuable insights into the origins of life on Earth, given the possibilities associated with alkaline systems as potential environments for the emergence of life (Herschy and Smith [2014]).

1.2.3 SHV parameters in need of more investigation

1.2.3.1 Low Pressure

SHVs inherently operate at considerably lower pressures compared to their deep-sea counterparts. The critical transition point, where pressure changes surpass temperature changes in influencing the ascending hydrothermal fluids, occurs around 212 meters (Giovannelli et al. [2013]). Consequently, SHVs systems commonly exhibit free gas phases, which have previously earned them the name "gasohydrothermal" vents (Dando et al. [1995]). The presence of free gas bubbles or degassing, resulting from enhanced gas exsolution (Caracausi et al. [2005]; Lupton et al. [2008]), is altered by gas scrubbing (process where gases present in a fluid, such as hydrothermal vent fluids, interact and exchange with the surrounding liquid phase. In the context of SHVs, the process involves the removal or absorption of certain gases from the fluid by the surrounding water). This phenomenon was observed in hydrothermal vent fluids off Panarea Island (Price et al. [2015]), it suggests that vent fluids, which have undergone gas scrubbing, show similar patterns of energy production to fluids present in DHV systems. This suggests that gas scrubbing may have a comparable impact on the overall characteristics of the fluids in hydrothermal vents. However, further research and evidence are required to delve deeper into this potential similarity between SHVs and DHVs.
It is interesting to notice that even within the hydrothermal system, depth within sediments can alter the local microbiome. In a research conducted by Molari and Manini [2012], the quantity of prokaryotes was shown to decrease the deeper the depth of shallow marine sediments. The reverse was also true, as prokaryotes increased in number in the vicinity of SHVs. A report written on the Milos Island (Greece) by Sievert et al. [2000] identifies that deeper sediments are also the hottest. Therefore, it is plausible to confirm the inversely correlated relationship between prokaryote quantity and temperature. Phytopigments seem to follow the same pattern as prokaryotes (Giovannelli et al. [2013]), therefore there is an increase of phototrophic organisms as temperature decreases. Following this hypothesis, temperature and pressure would be far more significant in affecting the microbial distribution than external terriginous input. The different bacteria present on the surface and deep in the sediments indicates a variety of regional environments in SHVs and reflects on the distinct thermal regimes present in these ecosys-

tems.

1.2.3.2 Terrigenous input and the sedimentary nature of SHVs

Svensson et al. [2004] conducted measurements of dissolved amino acids in various shallow-water vents and found that the composition of organic matter in these vents is greatly influenced by the surrounding geological conditions. Gomez-Saez et al. [2015] demonstrated that dissolved organic matter near shallow-water hydrothermal vents can bond with iron through coprecipitation. This process specifically removes aromatic compounds, leading to significant changes in the molecular composition of the remaining dissolved organic matter. As a result, the availability of more easily degradable organic compounds to microbial consumers may be affected. Shallow-water vents, being close to land masses, come into direct contact with inputs of terrigenous primary production, phytodetritus, and organic carbon (Figure 7). Compared to deep-sea vents, the presence of terrigenous inputs in shallow-water vents is significantly higher, which can have important implications for carbon cycling and primary productivity in these environments. Nevertheless, there has been limited research on the fate of terrigenous organic carbon in shallow vents, and the role of microbial communities in the diagenesis of organic carbon and the breakdown of both external and internally produced organic carbon sources remains largely unexplored (Gomez-Saez et al. [2015]; Svensson et al. [2004]).

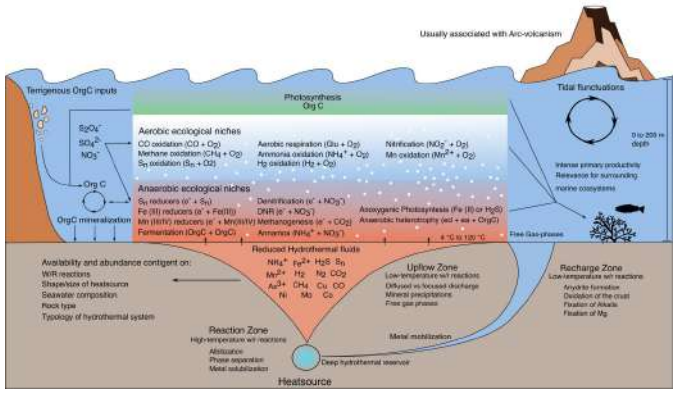

Figure 7: Cartoon illustrating range of processes taking place in SHV. Including terrigenous inputs, photosynthesis and magmatic inputs. Cartoon made by Bernardo Barosa.

The distinct characteristics of SHVs compared to DHVs, such as exposure to light, input of terrestrial materials, presence of free gas phases, influence of waves, storms, and tides, and variability in salinity due to meteoric water inputs, create a diverse and intricate environment for microbial communities to thrive. These systems, often composed of sediments and hosting a wide range of minerals, exhibit remarkable spatial and temporal dynamics in their microbial populations. Despite recent efforts to investigate these interactions, our understanding of the complex nature of SHV ecosystems is still in its early stages. There is a significant knowledge gap regarding the factors that drive microbial diversity in these ecosystems, as well as the metabolic pathways and activities of the microbial communities involved. Additionally, no studies to date have explored the contribution of these ecosystems to global biogeochemical cycles, highlighting the need for further research in this area (Pichler et al. [2006]; Godelitsas et al. [2015]; Becke et al. [2009]; Dando et al. [1995]; Yücel et al. [2013]).

1.2.4 The microbiome of SHVs

1.2.4.1 Functional diversity

The majority of research conducted to explore the microbial community of SHVs has relied on traditional molecular biology techniques, such as clone libraries or most probable numbers (Brinkhoff et al. [1999]; Giovannelli et al. [2013]; Miranda et al. [2016]; Price et al. [2013]).
In SHVs, similar to DHVs, specific pathways are used by microorganisms to obtain energy through chemical reactions instead of relying on sunlight. These pathways include the reductive tricarboxylic acid (rTCA) cycle for converting carbon and the sulfur oxidation pathway for processing sulfur compounds (Price and Giovannelli [2017]; Hügler and Sievert [2011]; Sievert and Vetriani [2012b]). The genetic makeup of microorganisms found in these vents supports such findings (Brinkhoff et al. [1999]; Giovannelli et al. [2013]; Hirayama et al. [2007a]; Price et al. [2013]).
As the temperature changes along the vent, there are interesting shifts in how the microorganisms get their energy. They switch from using the rTCA cycle to the more well-known process of the Calvin cycle for converting carbon. Additionally, the types of bacteria that process sulfur compounds change from one group called *Epsilonproteobacteria* to another group called *Gammaproteobacteria* (Giovannelli et al. [2013];

Tang et al. [2013]). This suggests that the microorganisms adapt to their environment and use different strategies to survive as conditions change. These results also show us that the metabolic diversity of the microbial community in SHVs can be greatly diversified depending on which area they occupy in the hydrothermal vent system. In the same study, it was shown that the high quantity of prokaryotes in SHV is comparable to the abundance found in DHVs. Moreover, because temperature changes in different microregions of the SHV, it is noticeable that the prokaryotic abundance and the presence of photoautrotophics increase in the surrounds of the vents -low temperature regions-.
However, it is important to note that only a limited number of studies have used advanced sequencing techniques to explore the variety of microorganisms in these environments (Gugliandolo et al. [2015]; Marziah et al. [2016]; Lentini and Rye [2014]; Zhang et al. [2012]). In fact, there is only one study that has used shotgun metagenomic sequencing (Tang et al. [2013]).
To gain a deeper understanding of the importance of different pathways and energy sources in shallow vent ecosystems, future research should combine various sequencing methods like metagenomics (studying the genetic material of the entire microbial community), metatranscriptomics (examining the active genes being expressed), and metaproteomics (analyzing the proteins produced by the microorganisms). These studies should be conducted alongside measurements of the local chemistry and efforts to isolate specific microorganisms for further study.

1.2.4.2 Are SHVs a place for symbiosis?

In DHV communities, the symbiotic relationship between prokaryotes and metazoa is worth to be highlighted (Tarasov and et al. [2005], Figure 8). These communities exhibit a shift in species composition from endemic symbiont-bearing metazoans in SHVs to opportunistic species capable of tolerating extreme conditions (Tarasov and et al. [2005]). Within these environments, the meiofauna, which refers to small benthic invertebrates, play a significant role in terms of abundance and diversity (Zeppilli and Danovaro [2009]).

Figure 8: Dense aggregation of giant tubeworms (*Riftia pachyptila*) at a hydrothermal vent. These tubeworms host chemosynthetic bacterial symbionts in a specialized organ (the trophosome), enabling them to thrive in the absence of sunlight by relying on the oxidation of reduced sulfur compounds for nutrition. The image highlights the key role of symbiosis in sustaining complex communities at deep-sea hydrothermal vents. Photograph by BBC.

The vent meiofauna is primarily composed of nematodes, particularly those belonging to the Onchalaimidae family, which have been repeatedly observed near emission points of diverse shallow hydrothermal vents (Dando et al. [1995]; Zeppilli and Danovaro [2009]). Notably, these organisms have also been found in sedimentary environments such as harbors and are associated with bivalve byssuses in the deep sea (Bellec et al. [2018]; Bellec et al. [2019]).
Recent studies have uncovered potential symbiotic associations between nematodes and sulfur-oxidizing bacteria affiliated with the *Epsilonproteobacteria* group. The presence of the AprA gene, which is involved in sulfur metabolism, in the nematode microbial communities suggests a close relationship between nematodes and chemosynthesis—a mechanism through which organisms derive energy from inorganic compounds. This association appears to be particularly significant in shallow-water environments (Bellec et al. [2019]).
SHVs are commonly found in the Mediterranean Sea due to the volcanic activity in the region. While microbial communities in these vents have been studied to some extent, there is limited research on the biological aspects. Examining the microbial communities associated with

Nematoda can contribute to our understanding of these ecosystems. In a recent study by Bellec et al. [2020], the bacterial community of a free-living marine nematode and its surrounding environment in a shallow hydrothermal vent near Naples, Italy, was investigated. The findings indicate that nematode-associated bacteria from shallow vents exhibit more similarities with those from deep-sea vents, across different invertebrate host taxa. This suggests that the associations between nematodes and bacteria may be influenced by habitat and environmental factors rather than co-evolutionary mechanisms. These findings open up new avenues for future research and raise important questions about bacterial dispersal between shallow and deep-sea vent systems, as well as the independent development of symbiotic relationships in these distinct environments, both in terms of depth and geographical location. It is worth remembering, however, that it is still very challenging to identify patterns or compare the microbiome and macrofauna of SHV because the majority of studies in SHV focus distinctively on single environmental features such as biofilms, sediments or fluid/gas samples. A more holistic approach is necessary when studying SHV, including all possible drivers of the diverse metabolic functioning of bacteria in SHV.

1.2.5 Culture Isolation, a necessary but overlooked mean to study SHVs

In the early 1980s, pioneering studies on the microbiology of shallow-sea vent systems started with the culturing efforts conducted by Stetter et al. [1983] in the shallow-water vents off Vulcano Island in Sicily. Researchers successfully isolated *Pyrodictium*, an organism capable of optimal growth above 100℃, and *Pyrolobus*, which can thrive at temperatures up to 113℃ (Stetter et al. [1983]; Stetter et al. [1987]). These discoveries sparked significant interest in isolating thermophiles and hyperthermophiles from shallow-water hydrothermal vents. While a few subsequent studies have been carried out over the years, it is important to note that the systematic investigation of microbial community diversity and functioning in shallow-water geothermal areas has lagged behind the research conducted in deep-sea hydrothermal vents.
Due to the limited research conducted on the operational dynamics of microbial communities in shallow-water volcanic systems, our understanding of the microbial diversity associated with SHVs remains incomplete. Studies, encompassing both experimental and observational

approaches, have identified certain commonalities between DHVs and SHVs in terms of their microbial communities. However, nuanced distinctions exist beyond the mere presence of photosynthetic organisms in SHVs. To gain deeper insights, future investigations should focus on unraveling the influence of organic matter influx and the dynamic geological factors inherent in shallow environments on the taxonomic and functional diversity of microbial communities in SHVs (Gomez-Saez et al. [2015]; Yücel et al. [2013]).

Early explorations of SHVs were predominantly guided by methodologies employed in deep-sea ecosystems (Sievert and Vetriani [2012b]). Such research was heavily based on investigating sulfur-oxidizing bacteria and their role in the microbial community, while other metabolic strategies were overlooked (Dávila-Ramos et al. [2014]; Miranda et al. [2016]). Consequently, the importance of sulfur-based metabolisms in shaping shallow-water hydrothermal vent systems has been confirmed by several studies.

Latest research has revealed that *Epsilonproteobacteria* are the dominant microbial group in shallow-water hydrothermal vent fluids and sediments (Giovannelli et al. [2013]; Tang et al. [2013]; Miranda et al. [2016]) found in regions characterized by high temperatures (up to 55 ℃) and elevated hydrogen sulfide concentrations. *Epsilonproteobacteria* are well-adapted to thrive in sulfidic conditions and are commonly found in DHVs, where they often form the predominant microbial communities (Sievert and Vetriani [2012b]). Even though they are a dominant microbial form in SHVs (Giovannelli et al. [2013]), no study managed to successfully isolate *Epsilonproteobacteria* from these environments.

Very little studies have been written on the functioning of genes and substrate utilization rates in energy-conserving reactions within SHVs. Research suggests that alternative electron acceptors such as nitrate, may be crucial for the ecosystem of SHV (Meyer-Dombard and Amend [2014]). Nevertheless, more work is necessary to comprehend the significance of these alternative electron acceptors.

One evidence provided by molecular studies is that *Epsilonproteobacteria* are genetically adapted to perform nitrate reduction (Vetriani et al. [2014]). Nevertheless, the fact that *Epsilonproteobacteria* was never able to be sucessfully isolated in laboratory, and the majority of the isolates on SHV have not been confirmed as nitrate reducers, adds to our current lack of knowledge of the microbiome of SHV.

1.2.6 Viral communities: a niche to be explored in SHVs

Viral communities in shallow-water hydrothermal vents are poorly understood, despite the key roles viruses play in marine ecosystems (Suttle [2007]). They can shape microbial diversity and distribution, redirect large fractions of microbial biomass through lysis, and drive horizontal gene transfer, influencing microbial evolution on both short and long timescales. While some work has explored viral abundance, diversity, and function in deep-sea hydrothermal vents (DHVs), almost nothing is known about these aspects in SHVs (Anderson et al. [2011]; Manini et al. [2008]; Rohwer and Thurber [2009]; Sharon et al. [2009]; Rastelli et al. [2017]; Williamson et al. [2008]).

In SHVs, viruses coexist with archaeal and bacterial hosts across steep thermal, chemical, and physical gradients. Many of these microbes inhabit biofilms attached to hard substrates, vent chimneys, or sediments, dense communities that can act as hotspots for viral activity. Evidence from other environments shows that viruses readily accumulate within biofilms (Skraber et al. [2005]),and that viral lysis can be common during biofilm development (Resch et al. [2005]). This makes SHVs promising sites to study virus–host dynamics under extreme conditions.

Understanding viruses in SHVs is also relevant to astrobiology and early Earth research. Hydrothermal systems provide natural laboratories for examining adaptation to extreme environments, which may resemble settings on other worlds. During the Hadean eon ($\sim$ 4 billion years ago), hydrothermal activity was likely more widespread due to intense tectonic and volcanic processes. These systems created geological, physical, and chemical gradients (Baross and Hoffman [1985]) capable of supporting complex, interconnected prebiotic reactions. Models suggest that such gradients, combined with confined mineral pores, could have fueled early metabolic processes such as CO_2 reduction by H_2 (Koonin and Martin [2005]; Lane and Archibald [2010]). These gradients provide favorable conditions for the development of diverse and interconnected processes that could have facilitated the origin and evolution of life on Earth.

Within this framework, viruses may have been present from the earliest stages of life's evolution. The "Virus World" hypothesis proposes that self-replicating RNA molecules, possibly precursors to modern viruses, emerged within these hydrothermal environments and played a central role in shaping early biological systems (Koonin and Martin [2005]).

By studying viral diversity, abundance, and ecological roles in present-day SHVs, we may gain new insights not only into their contemporary ecosystem functions but also into the ancient evolutionary processes that shaped life on Earth.

1.3 Why is it relevant to study SHVs?

1.3.1 SHV as accessible analogs to DHV

Shallow-water hydrothermal vents offer a unique window into the biological, chemical, and physical processes that shape organic matter in the hot subsurface. By studying these systems, we can gain insights into carbon cycling in the deep hot biosphere, which is far less accessible. In particular, the sudden introduction of labile organic carbon (organic matter readily broken down by microbes) can shift dominant microbial metabolisms toward heterotrophy, the use of organic compounds as an energy source (Bianchi [2011]). Such shifts can rapidly alter community composition and activity.

Laboratory studies with pure cultures from both deep-sea and shallow-water vents have shown that organic compounds in the growth medium can inhibit chemolithoautotrophic bacteria (Takai et al. [2006]; Voordeckers et al. [2005]). In contrast, certain substrates, such as Fe and humic substances, can stimulate specific species, like *Thiobacillus denitrificans*, which performs nitrate-dependent iron oxidation (Kanaparthi and Conrad [2015]). These results suggest that organic carbon availability strongly influences the balance between heterotrophic and chemolithoautotrophic processes in vent ecosystems.

Understanding how organic matter interacts with SHV processes, and how inputs from nearby land sources shape microbial communities, requires further targeted research (Bianchi [2011]). Such work could shed light in to the complex feedbacks between organic carbon, microbial metabolism, and geochemical cycling in both shallow and deep hydrothermal environments.

Physical forcing also differs markedly between SHVs and deep hydrothermal vents. While temperature fluctuations in DHVs may follow tidal cycles (Williams III and Tivey [2001]), SHVs, being much shallower—are additionally influenced by storms, waves, and more pronounced tidal changes. These dynamic conditions make SHVs excellent natural laboratories for studying how physical energy inputs interact with hydrother-

mal chemistry and biology.
As analogs to DHVs, SHVs share many fundamental processes but also introduce unique environmental variables that remain understudied. Their accessibility and lower operating costs compared to deep-sea expeditions make them ideal for high-resolution, long-term investigations. However, our understanding of how their variability drives chemical composition and microbial (including viral and macrobenthic) diversity is still in its early stages.

1.3.2 Biotechnological applications

1.3.2.1 Exopolysaccharides

Microbial polysaccharides, including polysaccharides produced by marine bacteria, have gained significant attention in various industries. While many marine bacteria are known to produce exopolysaccharides (EPS), there is ongoing exploration to discover new microorganisms capable of producing polysaccharides. The exploration of DHVs has shown promise in uncovering novel EPS. Screening efforts have identified several mesophilic heterotrophic bacteria from various vent locations as potential sources of these polysaccharides (Guezennec [2002]).
Polysaccharides occur as important constituents of plant and microbial cell walls, either as storage polysaccharides or as biopolymers known as exopolysaccharides (EPS) secreted by microorganisms. In recent years, there has been a growing interest in the isolation and identification of new microbial polysaccharides that might have novel uses such as gelling agents, viscosifiers, emulsifiers, stabilizers, and texture enhancers. Bacterial polysaccharides offer a diverse range of characteristics that may not be present in conventional plant-based polymers. While they may compete with polysaccharides derived from algae (such as alginates), crustaceans (like chitin), or plants, their production is less susceptible to fluctuations caused by marine pollution, crop failure, or climate-related factors (Guezennec [2002]). They possess a wide range of fascinating physical and chemical properties, such as their ability to stabilize, suspend, thicken, gel, coagulate, form films, and retain water (Sutherland [1996]). As a result, they have found applications in various industrial sectors, including detergents, textiles, adhesives, paper, paint, food and beverage industries (Sutherland [1996]). Polysaccharides also play a role in pharmaceuticals and cancer therapy, drug delivery (Benedetti et al. [1989]), and in the formulation of cell culture media

(Sutherland [1996]). In some cases, polysaccharides are chemically modified to enhance or introduce specific functional properties (Roller and Dea [1992]).

The discovery of novel polysaccharides with biotechnological significance has led to the recognition that extremophilic microorganisms offer valuable resources for both novel biotechnological processes and the study of biomolecule stability under extreme conditions. In the last 15 years, there has been a growing isolation of new genera and species of hyperthermophilic and mesophilic bacteria from DHVs. This increased bacterial diversity includes strains that have the capacity to produce new molecules such as enzymes, polymers, and other bioactive compounds. This exploration may uncover and characterize innovative molecules that hold promise for various industries (Guezennec [2002]).

Bacteria found in deep-sea hydrothermal environments have shown their ability to produce unique extracellular polymers when grown in aerobic carbohydrate-based conditions. So far, three main producers of these polymers have been identified: *Pseudoalteromonas*, *Alteromonas*, and *Vibrio* (Guezennec [2002]). Microbes isolated from extreme environments offer a wide range of chemical and physical properties in their polymers that are not typically found elsewhere in nature. The exploration of bacteria in remote areas, particularly hydrothermal vents, holds great potential for discovering microorganisms of biotechnological importance. Strains that produce novel EPS with unique properties can be transferred to private industries for further evaluation and potential commercial development. However, factors such as yield, cost, and market demand will ultimately determine the commercial viability of these polysaccharides, despite their interesting properties and potential applications.

For example, the polysaccharide expelled by *Alteromonas macleodii* subsp. *fijensis* -found in a deep hydrothermal vent of the coast of Fiji- presented an excellent metal-binding maximum capacity, which suggests that such polymer can be promising for wastewater and polluted water treatment (Loaec et al. [1998], Loaëc et al. [1997]). This EPS also had the characteristic of being hydrophobic and when used to promote the attachment of osteoblastic cells in in vivo rat calvaria experiments, the surfaces it was able to provide with hydrophobic coating allowed for significant bone healing, demonstrating that the use of EPS found in bacteria inhabiting hydrothermal vents has potential to extend to the medical domain (Zanchetta and Guezennec [2001]).

1.3.2.1.1 EPS from DHV applied in medicine

EPS produced by bacteria from deep-sea hydrothermal vents have shown significant potential for medical applications due to their unique chemical structures and biological activities. These EPS often mimic glycosaminoglycans (GAGs), which are important in human biology for roles such as tissue regeneration and cancer treatment. EPS from vent bacteria are rich in hexosamines, uronic acids, and sometimes sulfate groups, giving them properties similar to GAGs and making them promising candidates for regenerative medicine and as anti-cancer agents (Delbarre-Ladrat et al. [2017], Akoumany et al. [2019], Zykwinska et al. [2019]). Some EPS derivatives have demonstrated the ability to modulate the human complement system, which is involved in immune defense and inflammation, suggesting possible uses in immunotherapy or as anti-inflammatory agents (Courtois et al. [2014]).
Additionally, EPS from these environments have shown antioxidant activity and the ability to bind heavy metals, which could be relevant for detoxification therapies or as protective agents against oxidative stress (Ahamed et al. [2024]). The biocompatibility and biodegradability of these molecules further enhance their appeal for biomedical use (Nichols et al. [2005]). While some EPS have already found applications in cosmetics, their full biotechnological and pharmaceutical potential remains largely untapped, with ongoing research aiming to discover new strains and optimize EPS production for medical use (Guezennec [2002], Cambon-Bonavita et al. [2002]).

1.3.2.2 Using SHVs to investigate ocean acidification

SHVs can and have also been investigated for reasons that expand beyond understanding their basic geochemistry, ecology, and functioning. In addition, given the growing concerns regarding global warming and ocean acidification, these vents offer valuable insights. For instance, certain marine SHVs, characterized by the absence of hydrogen sulfide and lacking steep temperature gradients (e.g., Milne Bay Province, Papua New Guinea; Azores, Portugal), are now being utilized as natural laboratories to study the effects of ocean acidification on the biota and microbiota (Engel et al. [2015]; Fabricius et al. [2011]; Hall-Spencer et al. [2008]; Kerfahi et al. [2014]). It has been observed that increased acidity resulting from dissolved CO_2 (and/or H_2S) can have detrimental effects on nearby carbonate-secreting organisms, leading to potentially

drastic shifts in the coastal marine ecosystem. Investigations conducted at shallow-sea vents not only helps us understand their unique characteristics but also provides valuable knowledge and understanding regarding the impacts of global warming and ocean acidification.

1.3.2.3 Climate change mitigation

In the last century and a half, there has been a roughly 30% rise in atmospheric CO_2 levels (Vitousek et al. [1997]). Biotechnological approaches have been employed to mitigate atmospheric CO_2 in two primary ways: through biological fixation using microorganisms and through the capture of carbon dioxide using enzymes, specifically carbonic anhydrase. The enzymes present in hydrothermal vents have been hypothesised to help with carbon sequestration, also helping to mitigate global warming (Minic and Thongbam [2011]).
DHVs are situated near active volcanic regions along the mid-ocean ridge system, where tectonic plates diverge. Seawater enters the cracks in the volcanic bed and becomes heated by magma. This heated water ascends to the surface, carrying dissolved minerals that serve as an energy and nutrient source for chemoautotrophic organisms. Despite the extreme conditions in this environment, including the absence of photosynthesis, high temperature, high pressure, acidic pH, and chemical toxicity, a wide range of microorganisms and animal species have adapted to thrive in this hostile habitat. These organisms have developed highly efficient metabolic processes to utilize inorganic CO_2 from the surrounding environment (Wankel et al. [2012]). Given the need to develop technologies for carbon dioxide capture and reduction of greenhouse gases in the atmosphere, the enzymes involved in CO_2 fixation and assimilation found in these organisms hold great potential for application.
There are microalgae, such as Cyanophyceae (blue-green algae), Chlorophyceae (green algae), Bacillariophyceae (including diatoms), and Chrysophyceae (comprising golden algae), that exhibit remarkable proficiency in harnessing atmospheric CO_2 through the process of photosynthesis (Kumar et al. [2010]). Through the application of genetic modification and advanced technology, novel strains of these microalgae have been developed, enhancing their resilience in environments characterized by elevated CO_2 levels (Kumar et al. [2010]). Concurrently, ongoing endeavors are exploring the potential fusion of wastewater treatment with

the cultivation of microalgae, with the overarching objective of biofuel production (Kumar et al. [2010]). In a recent milestone, scientists have genetically engineered a cyanobacterium called *Synechococcus elongatus* PCC7942 to directly synthesize isobutyraldehyde and isobutanol from CO_2. Isobutyraldehyde serves as a precursor for diverse chemical synthesis pathways, while isobutanol holds promise as a biofuel source. Nevertheless, the creation of a bioreactor that can attain peak productivity and optimal energy efficiency within specific operational budget constraints remains an unaccomplished goal (Kumar et al. [2010]). A primary challenge associated with these reactors stems from the suboptimal effectiveness of carbon fixation through the microalgae's inherent Calvin cycle (Milne et al. [2009]). To engineer an innovative reactor that can augment the CO_2 fixation capacity of microalgae, it becomes imperative to enhance the efficiency of the Calvin cycle. A possible solution for such problem also includes utilization of carboxylase enzymes or even other CO_2 fixation pathways.

We can consider, for instance, the diverse bacteria strains that harness energy through chemical oxidation in the absence of light. These microorganisms exhibit proficiency in the capture of CO_2 and its subsequent conversion into fuel. They harbor the genetic blueprints for pivotal enzymes responsible for synthesizing ethanol from pyruvate. Numerous investigations have illustrated the potential for Rhodobacter species to transform CO_2 into ethanol, whether in illuminated anoxygenic environments or under dark aerobic cultivation environments (Wahlund et al. [1996], Conway et al. [1987]) . Consequently, microorganisms sourced from the depths of hydrothermal vents, capable of converting CO_2 into biomass, hold promise in advancing technologies for biofuel production and the synthesis of various compounds.

There has been successful case studies in the industry of companies which transformed CO_2 emissions into fuels and raw material. Carbon Sciences Inc. has created a technique for artificial generation of precipitated calcium carbonate (PCC) that finds applications in multiple sectors such as paper manufacturing, pharmaceuticals, and plastics production. Additionally, they developed technology that serves to convert CO_2 emissions into the fundamental components essential for producing fuels like gasoline, diesel, jet fuel, and others. Circular economy alternatives have also been implemented by CO_2 Solution Inc in cement factories. This consists of capturing the CO_2 emissions of cement factories and convert them into bicarbonate ions. Such ions are the raw

material for limestone production, which can be reintroduced in the cement factories (Gaill [1993]).
However, the current carbonic anhydrases (CAs) available are costly due to their expensive production, and they suffer from low activity and stability issues. Most of the enzymes tend to lose their activity or become completely inactive when exposed to temperatures above 50 °C (Conway et al. [1987]). Since most industrial CO_2 elimination processes require elevated temperatures, the challenge lies in finding immobilization techniques that can preserve biocatalyst activity at these higher temperature ranges (Lee et al. [2010]).
In contrast, microorganisms thriving in the extreme conditions of deep-sea hydrothermal vents have developed adaptations to survive in high-temperature environments, and cope with toxic substances like H_2S and heavy metals. Hence, biomolecules sourced from these organisms hold significant promise for various biotechnological applications (Minic and Thongbam [2011]). Consequently, investigating carbonic anhydrases sourced from these environments for carbon capture could present an appealing avenue for novel biotechnological advancements.

1.3.3 Origin of life research

Early research into the origin of life focused heavily on ancient deep-sea "black smoker" vents, where mineral-rich fluids emerge at high temperature and low pH. While these environments are rich in chemical energy, their extreme acidity and heat make them less likely analogs for the stable conditions that may have fostered prebiotic chemistry. More recent attention has shifted toward serpentinization-driven vent systems—both deep and shallow—that generate more moderate, alkaline conditions thought to be more favorable for the emergence of life (Amend et al. [2011]).
Serpentinization occurs when ultramafic rocks such as olivine and pyroxene react with water, producing molecular hydrogen (H_2). This hydrogen can then react abiotically with carbon monoxide or carbon dioxide to form methane, short-chain hydrocarbons, formate, and acetate (Seewald et al. [2006]; Bradley et al. [2009]; Etiope and Sherwood Lollar [2013]). These reactions also create proton and redox gradients—natural energy sources that could have been harnessed by primitive biochemical systems (Lane [2010]; Lane and Martin [2010]).
One well-studied deep-sea example is the Lost City Hydrothermal Field

(LCHF), located on the Mid-Atlantic Ridge flanks at $\sim$ 800 m depth (Kelley et al. [2001]). LCHF emits alkaline fluids (pH up to 11) enriched in H_2 and abiotic methane, making it a compelling analog for early Earth hydrothermal systems (Bradley et al. [2009]).
Importantly, similar serpentinization-driven systems also occur in shallow-water settings, providing more accessible, cost-effective opportunities for study. The Prony Hydrothermal Field (PHF), located in Prony Bay, New Caledonia, is one such example. Here, meteoric water infiltrates ultramafic rocks, driving serpentinization and producing warm (up to 41 ℃), highly alkaline (pH up to 11.2) fluids rich in H_2 and CH_4. These fluids discharge directly into a coastal marine environment, precipitating spectacular carbonate–brucite towers up to 38 m tall (Cox and Rye [1982]; Launay and Fontes [1985]; Figure 9).

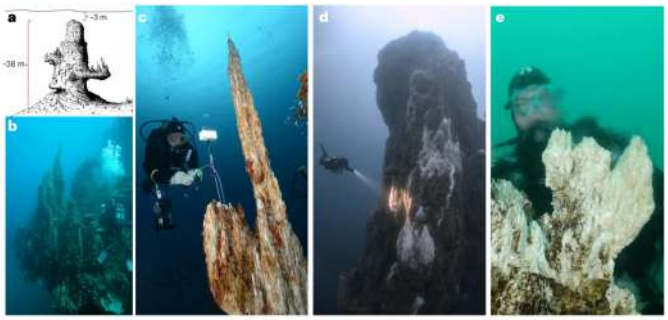

Figure 9: Hydrothermal carbonate structures at shallow-sea vent systems. (a) Schematic of the Prony Needle, a 38-m-high carbonate chimney formed by the precipitation of minerals as alkaline, calcium-rich vent fluids mix with seawater. (b) SCUBA diver exploring the large flange of the Prony tower illustrated in (a). (c) Diver collecting hydrothermal fluids from an active venting site on the Prony Needle. (d) The Big Strytan carbonate tower at the Strytan Hydrothermal Field, Iceland. (e) The most active venting zone located at the summit of the Big Strytan structure shown in (d). Image from Barge and Price [2022].

Shallow systems like PHF bridge the environmental gap between terrestrial serpentinizing springs and deep-sea fields such as LCHF. Microbial communities at PHF share features with both the deep-sea Lost City microbiome and terrestrial sites like The Cedars, California (Frouin et al. [2018], Postec et al. [2015], Quéméneur et al. [2014]) . This overlap suggests that shallow serpentinizing vents could preserve, in a single location, chemical and biological characteristics relevant to multiple stages of Earth's early geochemical evolution.

1.4 Current debates on the microbiome of SHVs

1.4.1 Photosynthesis on SHVs

The productivity of photosynthesis directly above the emissions of hydrothermal vents is typically reduced compared to the surrounding areas. This decrease in photosynthetic rates can be attributed to the presence of higher concentrations of hydrogen sulfide, metals, and elevated temperatures (Tarasov et al. [1999]). For instance, a research study conducted by Gomez-Saez et al. [2017] demonstrated that in sediments with a temperature of 55 ℃ in Dominica, although photosynthesis played a significant role, there was often a dominant reliance on chemotrophy, which refers to the utilization of chemical energy sources. This chemotrophic process accounted for up to 65% of the carbon fixation observed. Conversely, other studies have distinct findings and have reported elevated photosynthetic rates in the immediate vicinity of the vents (Dando et al. [1995]). This increase in photosynthesis is believed to be linked to the release of CO_2, ammonia, and phosphate from the venting system. The debate of whether hydrothermal emissions enhance or inhibit photosynthesis becomes even more complex because the presence of light as a controlling agent in the microbial diversity SHVs has not yet been studied in depth.
In order to investigate the enhancement or inhibition of photosynthesis on SHVs, we might want to recur to the microbiome of sulfidic caves, these environments provide a valid analog to DHVs parameters while also being in the shallow water realm (Canganella and Wiegel [2007]). They form a propitious experimental setting to study even more the significance of light in hydrothermal vents. The coexistence of sunlight, hydrogen sulfide, and other forms of reduced sulfur in shallow-water vents can create a favorable environment to understand more about anoxygenic phototrophic microorganisms.

1.4.2 Metabolic Diversity & Culture Isolations

Early investigations in shallow-water hydrothermal vents were primarily guided by approaches employed in deep-sea ecosystems (e.g. Sievert and Vetriani [2012b]). These studies focused extensively on examining the presence and role of sulfur-oxidizing bacteria as important constituents of the microbial community, while other metabolic strategies received comparatively less attention (Dávila-Ramos et al. [2014]; Mi-

randa et al. [2016]). As a consequence, the significance of sulfur-based metabolisms in shaping the functioning of shallow-water hydrothermal vent systems has been supported by several investigations.

In recent studies, *Epsilonproteobacteria* have emerged as the prevailing microbial group in SHV fluids and sediments (Giovannelli et al. [2013]; Tang et al. [2013]; Miranda et al. [2016]) found in regions characterized by elevated temperatures (35-55℃) and high concentrations of hydrogen sulfide. *Epsilonproteobacteria* are well-suited to thrive in sulfidic conditions and are frequently observed in surveys of DHVs, where they often dominate the microbial communities (Sievert and Vetriani [2012b]). Despite their abundance in SHVs (Giovannelli et al. [2013]), no isolates of *Epsilonproteobacteria* have been obtained from these environments. The lack of pure cultures of *Epsilonproteobacteria* from shallow-water hydrothermal vents highlights a significant knowledge gap regarding the ecological understanding of these dominant microbial community members.

Limited research has been conducted on the range of functional genes and the utilization rates of different substrates in energy-conserving reactions in shallow-water vents. The existing studies indicate that alternative electron acceptors such as nitrate, nitrite, manganese, and iron (III) might play a significant role in SHVs (Meyer-Dombard and Amend [2014]). However, further investigation is needed to fully understand the importance and contribution of these alternative electron acceptors.

Molecular evidence (Tang et al. [2013]) suggests that a considerable portion of chemolithoautotrophic production in SHVs may be linked to nitrate reduction, similar to DHVs communities (Sievert and Vetriani [2012b]). This observation is supported by both thermodynamic calculations (Price et al. [2015]) and the abundance of genetic sequences closely related to *Epsilonproteobacteria*, a class known to possess a conserved pathway for nitrate reduction (Vetriani et al. [2014]). However, the limited number of isolates obtained from shallow-water vents that have been confirmed as nitrate reducers adds to the ongoing debate. Furthermore, *Epsilonproteobacteria* have never been successfully isolated from SHVs.

Our current understanding of the metabolic diversity present in SHVs is debatable because firstly there is a research bias in investigating sulfur metabolisms in SHVs, and secondly some bacteria, such as *Epsilonproteobacteria*, which was never successfully isolated in laboratory, does not show a pathway for nitrate reduction when isolated (Vetriani

et al. [2014]), whereas studies suggest that chemolithoautotrophic organisms should be able to perform nitrate reduction (Sievert and Vetriani [2012b]). In order to solve the ongoing debate, it is essential to tackle these two major problems.

In light of the knowledge gaps outlined in this chapter, particularly the limited understanding of microbial metabolic diversity, the following chapter focuses on addressing these open questions within a well-characterized shallow-water hydrothermal vent system. Chapter 2 therefore presents a detailed investigation of the vents at Milos Island, Greece, where white microbial mats are used as a model habitat to explore taxonomic and functional diversity, evaluate carbon, sulfur, and nitrogen cycling, and assess community responses to short-term physical disturbances. By integrating high-resolution geochemical measurements with metagenomic analyses, this study aims to bridge current gaps in linking environmental variability to microbial function in shallow-vent ecosystems.

References

Johnthini Munir Ahamed, Hans-Uwe Dahms, and Yeou-Lih Huang. Heavy metal tolerance, and metal biosorption by exopolysaccharides produced by bacterial strains isolated from marine hydrothermal vents. *Chemosphere*, page 141170, 2024. doi: 10.1016/j.chemosphere.2024.141170.

Katy Akoumany, A. Zykwinska, C. Sinquin, L. Marchand, M. Fanuel, D. Ropartz, H. Rogniaux, M. Pipelier, C. Delbarre-Ladrat, and S. Colliec-Jouault. Characterization of new oligosaccharides obtained by an enzymatic cleavage of the exopolysaccharide produced by the deep-sea bacterium alteromonas infernus using its cell extract. *Molecules*, 24, 2019. doi: 10.3390/molecules24193441.

Gudni A Alfredsson, Jakob K Kristjansson, Sigridur Hjrleifsdottir, and Karl O Stetter. Rhodothermus marinus, gen. nov., sp. nov., a thermophilic, halophilic bacterium from submarine hot springs in iceland. *Microbiology*, 134(2):299–306, 1988.

Jeffrey C Alt. Sulfur isotopic profile through the oceanic crust: Sulfur mobility and seawater-crustal sulfur exchange during hydrothermal alteration. *Geology*, 23(7):585–588, 1995.

Jan P Amend, Thomas M McCollom, Michael Hentscher, and Wolfgang Bach. The origin of life in alkaline hydrothermal vents. *Astrobiology*, 11(12):97–110, 2011.

Rika E Anderson, William J Brazelton, and John A Baross. Using crisprs as a metagenomic tool to identify microbial hosts of a diffuse flow hydrothermal vent viral assemblage. *FEMS microbiology ecology*, 77 (1):120–133, 2011.

Laura M Barge and Roy E Price. Diverse geochemical conditions for prebiotic chemistry in shallow-sea alkaline hydrothermal vents. *Nature Geoscience*, 15(12):976–981, 2022.

J.A. Baross and S.E. Hoffman. Submarine hydrothermal vents and associated gradient environments as sites for the origin and evolution of life. *Origins of Life and Evolution of Biospheres*, 15(4):327–345, 1985.

Michael Becke, Alastair H Robertson, and Gernold Zulauf. Hydrothermal activity related to postcollisional magmatism and orogenic collapse in the eastern pontides, northeastern turkey. *International Journal of Earth Sciences*, 98(1):53–76, 2009.

Laure Bellec, Marie-Anne Cambon-Bonavita, Valerie Cueff-Gauchard, and Francois H Lallier. Chemosymbiotic bivalves from deep-sea vents and seeps: From the atlantic ocean to the mediterranean sea. *Frontiers in Marine Science*, 5:206, 2018.

Laure Bellec, Marie-Anne Cambon-Bonavita, Valerie Cueff-Gauchard, and Francois H Lallier. Harbor shallow-water vents reveal extreme k-rich hydrothermal fluids and novel sulfur-oxidizing bacteria. *Frontiers in Microbiology*, 10:1561, 2019.

Laure Bellec, Marie-Anne Cambon-Bonavita, Lucile Durand, Johanne Aube, Nicolas Gayet, Roberto Sandulli, Christophe Brandily, and Daniela Zeppilli. Microbial communities of the shallow-water hydrothermal vent near naples, italy, and chemosynthetic symbionts associated with a free-living marine nematode. *Frontiers in Microbiology*, 11:2023, 2020.

Laura M. Benedetti, E. Topp, and V.J. Stella. A novel drug delivery system: microspheres of hyaluronic acid derivatives. In V. Crescenzi,

I.C.M. Dea, S. Paoletti, S. Stivala, and I.W. Sutherland, editors, *Biomedical and Biotechnological Advances in Industrial Polysaccharides*, pages 27–33. Gordon and Breach, New York, 1989.

Michael E Berndt, William E Seyfried Jr, and J Warren Beck. Hydrothermal alteration processes at midocean ridges: experimental and theoretical constraints from ca and sr exchange reactions and sr isotopic ratios. *Journal of Geophysical Research: Solid Earth*, 93(B5):4573–4583, 1988.

Thomas S Bianchi. The role of terrestrially derived organic carbon in the coastal ocean: A changing paradigm and the priming effect. *Proceedings of the National Academy of Sciences*, 108(49):19473–19481, 2011.

James L Bischoff and Robert J Rosenbauer. Biogeochemical cycling of sulfur in hydrothermal systems: A review. *Chemical Geology*, 53 (1-2):225–244, 1985.

Adrian S. Bradley, David M. Reay, Anthony E. Fallick, Melanie J. Leng, Hayley Guy, and Albert Galy. Fluid–rock interaction in the active shallow hydrothermal system of the taupo volcanic zone, new zealand: mineralogical and stable isotope studies of sinters and hydrothermal calcite. *Chemical Geology*, 259(3-4):230–248, 2009.

Thorsten Brinkhoff, Jan Kuever, Gerard Muyzer, and Holger W Jannasch. Phylogenetic diversity and widespread occurrence of marine cytophaga-like bacteria. *Applied and Environmental Microbiology*, 65 (1):317–325, 1999.

M. Cambon-Bonavita, G. Raguénès, J. Jean, P. Vincent, and J. Guézennec. A novel polymer produced by a bacterium isolated from a deep-sea hydrothermal vent polychaete annelid. *Journal of Applied Microbiology*, 93, 2002. doi: 10.1046/j.1365-2672.2002.01689.x.

Francesco Canganella and Juergen Wiegel. Extremophiles: from abyssal to terrestrial ecosystems and possibly beyond. *Nature Reviews Microbiology*, 5(9):759–769, 2007.

Antonio Caracausi, Axel W Hofmann, Cornel EJ de Ronde, Robert A Zierenberg, Catherine Zimmermann, Shaun K Frape, Bruce K Nelson, Hitoshi Chiba, Akira Kudo, and Oleg S Pokrovsky. Hydrothermal vent fluid sulfur isotopes and the presence of isotope exchange reactions. *Geochimica et Cosmochimica Acta*, 69(18):4559–4572, 2005.

T Conway, YA Osman, JI Konnan, EM Hoffmann, and LO211885 Ingram. Promoter and nucleotide sequences of the zymomonas mobilis pyruvate decarboxylase. *Journal of bacteriology*, 169(3):949–954, 1987.

A. Courtois, C. Berthou, J. Guézennec, C. Boisset, and A. Bordron. Exopolysaccharides isolated from hydrothermal vent bacteria can modulate the complement system. *PLoS ONE*, 9, 2014. doi: 10.1371/journal.pone.0094965.

D L Cox and R O Rye. Hydrothermal origin for the giant calcite veins in the alpine-type fissure veins. *Economic Geology*, 77(2):285–297, 1982.

P R Dando, M Thomm, S I Bühring, V Brüchert, F Janssen, T Comtet, M Zabel, D Wagner, T Stührmann, and O Pfannkuche. Hydrothermal vent fauna in the northeastern pacific ocean: species composition, biogeography, and affinities. *Deep Sea Research Part I: Oceanographic Research Papers*, 42(8):1855–1876, 1995.

Paul R Dando, Alan J Southward, Eve C Southward, and Greg H Rau. A large population of *Hydrogenimonas*-like bacteria in the oxic and anoxic waters of the black sea. *Deep Sea Research Part II: Topical Studies in Oceanography*, 46(4-5):857–868, 1999.

Santiago Dávila-Ramos, Héctor G Castelán-Sánchez, Ricardo Cruz-López, and Alejandra Escobar-Zepeda. Draft genome sequence of a cyanobacterial symbiont from the gulf of california bivalve *Solemya velum*. *Genome Announcements*, 2(2):e00385–14, 2014.

C. Delbarre-Ladrat, Marcia Leyva Salas, C. Sinquin, A. Zykwinska, and S. Colliec-Jouault. Bioprospecting for exopolysaccharides from deep-sea hydrothermal vent bacteria: Relationship between bacterial diversity and chemical diversity. *Microorganisms*, 5, 2017. doi: 10.3390/microorganisms5030063.

Daniel Dzurisin and Robert O Fournier. Hydrothermal systems and volcano geochemistry. *Volcano deformation: Geodetic monitoring techniques*, pages 323–341, 2007.

Anja Engel, Richard Bellerby, Jelle Bijma, Kai G Schulz, and Ulf Riebesell. Ecological consequences of ocean acidification. *Interactions of the Ocean and Fresh Water: Impacts on Coastal Ecosystems*, 206: 179–201, 2015.

Giuseppe Etiope and Barbara Sherwood Lollar. Abiotic methane on earth. *Reviews of Geophysics*, 51(2):276–299, 2013.

Katharina E Fabricius, Chris Langdon, Sven Uthicke, Craig Humphrey, Sam Noonan, Glenn De'ath, Ryuji Okazaki, Nancy Muehllehner, Martin S Glas, and Janice M Lough. Losers and winners in coral reefs acclimatized to elevated carbon dioxide concentrations. *Nature Climate Change*, 1(3):165–169, 2011.

Horst Felbeck and George N. Somero. Primary production in deep-sea hydrothermal vent organisms: roles of sulfide-oxidizing bacteria. *Marine Biology*, 68(2):309–311, 1982.

Dionysis I Foustoukos and William E Seyfried Jr. Fluid phase separation processes in submarine hydrothermal systems. *Reviews in Mineralogy and Geochemistry*, 65(1):213–239, 2007.

E. Frouin, M. Bes, B. Ollivier, M. Quéméneur, A. Postec, D. Debroas, F. Armougom, and G. Erauso. Diversity of rare and abundant prokaryotic phylotypes in the prony hydrothermal field and comparison with other serpentinite-hosted ecosystems. *Frontiers in Microbiology*, 9, 2018. doi: 10.3389/fmicb.2018.00102.

Françoise Gaill. Aspects of life development at deep sea hydrothermal vents. *The FASEB journal*, 7(6):558–565, 1993.

Toshitaka Gamo, Kei Okamura, Jean-Luc Charlou, and Yves Fouquet. Hydrothermal plumes in the southern okinawa trough: Geological control of rare-earth elements and implications for the origin of the ree in seawater. *Earth and Planetary Science Letters*, 152(1):51–60, 1997.

James L Garrison. A statistical model and simulator for ocean-reflected gnss signals. *IEEE Transactions on Geoscience and Remote Sensing*, 54(10):6007–6019, 2016.

CR German, KL Von Damm, HD Holland, and KK Turekian. Treatise on geochemistry. 2003.

Donato Giovannelli, Giuseppe d'Errico, Elena Manini, Michail M Yakimov, and Costantino Vetriani. Diversity and phylogenetic analyses of bacteria from a shallow-water hydrothermal vent in milos island (greece). *Frontiers in Microbiology*, 4:184, 2013.

Athanasios Godelitsas, Theo J Mertzimekis, George E Christidis, and Christos Kanellopoulos. Mineralogy and geochemistry of the hydrothermal vent deposits from the kolumbo submarine volcano, greece. *Marine Geology*, 363:184–196, 2015.

Gonzalo V Gomez-Saez, Petra Pop Ristova, Stefan M Sievert, Marcus Elvert, and Kai-Uwe Hinrichs. Microbial ecology of the 'marichrom' black smoker chimney. *Environmental microbiology*, 17(3):1146–1161, 2015.

Gonzalo V Gomez-Saez, Petra Pop Ristova, Stefan M Sievert, Marcus Elvert, Kai-Uwe Hinrichs, and Solveig I Bühring. Relative importance of chemoautotrophy for primary production in a light exposed marine shallow hydrothermal system. *Frontiers in microbiology*, 8:702, 2017.

J Guezennec. Deep-sea hydrothermal vents: a new source of innovative bacterial exopolysaccharides of biotechnological interest? *Journal of Industrial Microbiology and Biotechnology*, 29(4):204–208, 2002.

Concetta Gugliandolo and Teresa L Maugeri. Distribution of bacteria in shallow hydrothermal vents of panarea island (italy). *Microbial Ecology*, 35(3):186–194, 1998.

Concetta Gugliandolo, Sergio Bellomo, Lorenzo Brusca, Rodolfo Neri, Fatima Viveiros, Paolo Censi, Paola Donato, and Francesco Italiano. The flegrei hydrothermal system: Geochemical characterization of vent fluids from the agnano-monte spina eruption (4.1 ka), naples, italy. *Journal of Volcanology and Geothermal Research*, 296:50–61, 2015.

Jason M Hall-Spencer, Riccardo Rodolfo-Metalpa, Sophie Martin, Emma Ransome, Maoz Fine, Suzanne M Turner, Sonia J Rowley, Danilo Tedesco, and Maria Cristina Buia. Volcanic carbon dioxide vents show ecosystem effects of ocean acidification. *Nature*, 454 (7200):96–99, 2008.

Mark D Hannington, Cornel EJ De Ronde, and Sven Petersen. Sea-floor tectonics and submarine hydrothermal systems. 2005.

Jeff Robert Havig. *Geochemistry of hydrothermal biofilms: composition of biofilms in a siliceous sinter-deposition hot spring*. Arizona State University, 2009.

Jeffrey W Hedenquist and Jacob B Lowenstern. The role of magmas in the formation of hydrothermal ore deposits. *Nature*, 370(6490): 519–527, 1994.

Richard W Henley and Alan John Ellis. Geothermal systems ancient and modern: a geochemical review. *Earth-science reviews*, 19(1): 1–50, 1983.

Barbel Herschy and Daniel Smith. Hydrothermal vents: An overview. *Geochemical Journal*, 48(4):355–370, 2014.

Hisako Hirayama, Michinari Sunamura, Ken Takai, and Takuro Nunoura. Kinetic and phylogenetic analysis of aerobic carbon monoxide oxidation by rubisco-like proteins of unknown function within the Engelmanniaceae. *Journal of Bacteriology*, 189(12):4295–4304, 2007a.

Hisako Hirayama, Michinari Sunamura, Ken Takai, Takuro Nunoura, Tamao Noguchi, Hanako Oida, Yasuo Furushima, Hiroyuki Yamamoto, and Fumio Inagaki. Culture-dependent and-independent characterization of microbial communities associated with a shallow submarine hydrothermal system occurring within a coral reef off taketomi island, japan. *Applied and Environmental Microbiology*, 73(21): 6616–6629, 2007b.

Toshiyuki Hoaki, Yuichi Nogi, Takehiko Itoh, and Takeo Hori. Sulfuricurvum kujiense gen. nov., sp. nov., another sulfur-oxidizing bacterium isolated from deep-sea hydrothermal vent polychaete nests. *International Journal of Systematic Bacteriology*, 45(2):327–330, 1995.

Michael Hügler and Johannes Imhoff. Life at deep sea hydrothermal vents—oases under water. *The International Journal of Marine and Coastal Law*, 24(2):201–208, 2009.

Michael Hügler and Stefan M Sievert. Beyond the calvin cycle: autotrophic carbon fixation in the ocean. *Annual Review of Marine Science*, 3(1):261–289, 2011.

Holger W Jannasch and Craig D Taylor. Deep-sea microbiology. *Annual review of microbiology*, 38(1):487–487, 1984.

G. M. Kamenev, V. M. Gorlenko, T. P. Tourova, V. V. Kuznetsov, and G. M. Frolova. Thiorhodospira sibirica sp. nov., a new alkaliphilic purple sulfur bacterium. *Microbiology*, 62(4):483–490, 1993.

Dinesh Kanaparthi and Ralf Conrad. Stimulation of thiobacillus denitrificans growth by fe (i) and humic substances. *Frontiers in microbiology*, 6:1212, 2015.

Deborah S. Kelley, Jeffrey A. Karson, Gretchen L. Fruüh-Green, Dana R. Yoerger, Timothy M. Shank, David A. Butterfield, John M. Hayes, Matthew O. Schrenk, Eric J. Olson, Giora Proskurowski, et al. An off-axis hydrothermal vent field near the mid-atlantic ridge at 30° n. *Nature*, 412(6843):145–149, 2001.

Dorsaf Kerfahi, Binu M Tripathi, Ke Dong, Rusea Go, and Jonathan M Adams. Microbial biogeography of six salt lakes in inner mongolia, china, and a salt lake in argentina. *Applied and Environmental Microbiology*, 80(6):1940–1951, 2014.

Eugene V Koonin and William Martin. On the origin of cells and viruses: primordial virus world scenario. *Annals of the New York Academy of Sciences*, 1178(1):47–64, 2005.

Amit Kumar, Sarina Ergas, Xin Yuan, Ashish Sahu, Qiong Zhang, Jo Dewulf, F Xavier Malcata, and Herman Van Langenhove. Enhanced co2 fixation and biofuel production via microalgae: recent developments and future directions. *Trends in biotechnology*, 28(7): 371–380, 2010.

Christopher E Lane and John M Archibald. Did an ancient chlamydial endosymbiosis facilitate the establishment of primary plastids? *Genome biology*, 11(5):R51, 2010.

Nick Lane. The origin of membrane bioenergetics. *Cell*, 142(6):887–899, 2010.

Nick Lane and William F. Martin. Reply to 'the reductive evolution of mitochondrial electron transport' and 'the origin and diversification of mitochondria'. *Nature*, 467(7313):E1–E4, 2010.

Gilbert Launay and Jean-Charles Fontes. Origin of carbon dioxide and hydrocarbons in natural gases from the troodos ophiolite, cyprus. *Chemical Geology: Isotope Geoscience section*, 52(1-2):1–11, 1985.

Seung-Woo Lee, Seung-Bin Park, Soon-Kwan Jeong, Kyoung-Soo Lim, Si-Hyun Lee, and Michael C Trachtenberg. On carbon dioxide storage based on biomineralization strategies. *Micron*, 41(4):273–282, 2010.

Christopher J Lentini and Robert O Rye. Geochemistry of the lassen hydrothermal system, california, usa. *Geochimica et Cosmochimica Acta*, 124:220–247, 2014.

Valeria Lentini, Concetta Gugliandolo, Teresa L. Maugeri, and Francesca Italiano. Anoxygenic phototrophic bacteria from extreme marine environments. *Journal of Marine Science and Engineering*, 2 (3):570–597, 2014.

M Loaec, R Olier, and J Guezennec. Chelating properties of bacterial exopolysaccharides from deep-sea hydrothermal vents. *Carbohydrate polymers*, 35(1-2):65–70, 1998.

Martine Loaëc, René Olier, and Jean Guezennec. Uptake of lead, cadmium and zinc by a novel bacterial exopolysaccharide. *Water Research*, 31(5):1171–1179, 1997.

RP Lowell and PA Rona. Seafloor hydrothermal systems driven by the serpentinization of peridotite. *Geophysical Research Letters*, 29(11): 26–1, 2002.

John E Lupton, Marvin D Lilley, David A Butterfield, Leigh J Evans, Robert W Embley, Eric J Olson, Giora Proskurowski, Joseph A Resing, Kevin K Roe, Rochelle R Greene, et al. Hydrothermal helium plumes in the pacific ocean. *Journal of Geophysical Research: Solid Earth*, 113(B8), 2008.

Richard A Lutz and Michael J Kennish. Ecology of deep-sea hydrothermal vent communities: A review. *Reviews of Geophysics*, 31(3):211–242, 1993.

Elena Manini, Gian M Luna, C Corinaldesi, D Zeppilli, G Bortoluzzi, G Caramanna, F Raffa, and Roberto Danovaro. Prokaryote diversity and virus abundance in shallow hydrothermal vents of the mediterranean sea (panarea island) and the pacific ocean (north sulawesi-indonesia). *Microbial Ecology*, 55:626–639, 2008.

M Marziah, Punyasloke Bhadury, Bipin K Pal, Sourav Roy, Jimit Polara, Saroj K Barik, Surajit Das, Sandipan Maiti, Sudip Mandal, Sandip Sarkar, et al. Microbial diversity of hydrothermal sediments in the bay of bengal using next generation sequencing. *Genomics Data*, 7: 102–104, 2016.

Teresa L. Maugeri, Daniela Caccamo, Concetta Gugliandolo, and Erko Stackebrandt. Two new phototrophic sulfur bacteria from marine microbial mats: *Thiorhodospira microaerophila* sp. nov. and *Thiorhodospira sibirica* sp. nov. *Archives of Microbiology*, 195(3):159–165, 2013.

Teresa Luciana Maugeri, Valeria Lentini, Concetta Gugliandolo, Francesco Italiano, Sylvie Cousin, and Erko Stackebrandt. Bacterial and archaeal populations at two shallow hydrothermal vents off panarea island (eolian islands, italy). *Extremophiles*, 13:199–212, 2009.

D'Arcy R Meyer-Dombard and Jan P Amend. Geochemistry and microbial ecology in alkaline hot springs of ambitle island, papua new guinea. *Extremophiles*, 18:763–778, 2014.

Jennifer L Milne, Jeffrey C Cameron, Lawrence E Page, Sally M Benson, and Himadri B Pakrasi. Report from workshop on biological capture and utilization of co2, charles f. knight center, washington university in st. louis, september 1–2, 2009, 2009.

Zoran Minic and Premila D Thongbam. The biological deep sea hydrothermal vent as a model to study carbon dioxide capturing enzymes. *Marine drugs*, 9(5):719–738, 2011.

Rafael Miranda, Brandy M Toner, Alex L Sessions, and Matthew O Schrenk. Hydrothermal vents and organic synthesis: a recipe for prebiotic chemistry? *Trends in Microbiology*, 24(3):161–172, 2016.

Massimiliano Molari and Elena Manini. Reliability of card-fish procedure for enumeration of archaea in deep-sea surficial sediments. *Current microbiology*, 64:242–250, 2012.

C. Nichols, J. Guézennec, and J. Bowman. Bacterial exopolysaccharides from extreme marine environments with special consideration of the southern ocean, sea ice, and deep-sea hydrothermal vents: A review. *Marine Biotechnology*, 7:253–271, 2005. doi: 10.1007/s10126-004-5118-2.

T. Pichler, T. Fuchs, and R. Huber. Nitrogen fixation in the dead sea water column. *Limnology and Oceanography*, $51(1_{part_2}) : 177 - -186, 2006.$

A. Postec, M. Quéméneur, M. Bes, Nan Mei, Fatma Benaïssa, C. Payri, B. Pelletier, C. Monnin, Linda Guentas-Dombrowsky, B. Ollivier, E. Gérard, C. Pisapia, M. Gérard, B. Ménez, and G. Erauso. Microbial diversity in a submarine carbonate edifice from the serpentinizing hydrothermal system of the prony bay (new caledonia) over a 6-year period. *Frontiers in Microbiology*, 6, 2015. doi: 10.3389/fmicb.2015.00857.

R. E. Price, I. P. Savov, B. Planer-Friedrich, and S. I. Bühring. Controls on the stable isotope composition of shallow-water hydrothermal vent fluids at ambitle island, papua new guinea. *Chemical Geology*, 396:238–251, 2015.

Roy E Price and Donato Giovannelli. A review of the geochemistry and microbiology of marine shallow-water hydrothermal vents. 2017.

Roy E Price, Ivan Savov, Britta Planer-Friedrich, Solveig I Bühring, Jan Amend, and Thomas Pichler. Processes influencing extreme as enrichment in shallow-sea hydrothermal fluids of milos island, greece. *Chemical Geology*, 348:15–26, 2013.

M. Quéméneur, M. Bes, A. Postec, Nan Mei, J. Hamelin, C. Monnin, V. Chavagnac, C. Payri, B. Pelletier, Linda Guentas-Dombrowsky,

M. Gérard, C. Pisapia, E. Gérard, B. Ménez, B. Ollivier, and G. Erauso. Spatial distribution of microbial communities in the shallow submarine alkaline hydrothermal field of the prony bay, new caledonia. *Environmental microbiology reports*, 6 6:665–74, 2014. doi: 10.1111/1758-2229.12184.

Eugenio Rastelli, Cinzia Corinaldesi, Antonio Dell'Anno, Michael Tangherlini, Eleonora Martorelli, Michela Ingrassia, Francesco L Chiocci, Marco Lo Martire, and Roberto Danovaro. High potential for temperate viruses to drive carbon cycling in chemoautotrophy-dominated shallow-water hydrothermal vents. *Environmental microbiology*, 19(11):4432–4446, 2017.

Robert R. Reeves and Harriet P. Johnson. Hydrothermal vents: A review. *Oceanography*, 24(4):36–45, 2011.

Alexander Resch, Stefan Leicht, Mirko Saric, László Pásztor, Alexander Jakob, Friedrich Götz, and Alfred Nordheim. Comparative proteome analysis of staphylococcus aureus biofilm and planktonic cells and correlation with transcriptome profiling. *Proteomics*, 5(18):4802–4815, 2005.

Guus Roeselers, Thomas B Norris, Richard W Castenholz, Søren Rysgaard, Ronnie Glud, Michael Kühl, and Gerard Muyzer. Diversity of phototrophic bacteria in microbial mats from arctic hot springs (greenland). *Environmental Microbiology*, 9(1):26–38, 2007.

Forest Rohwer and Rebecca Vega Thurber. Microbes in the marine environment: Viruses. *Encyclopedia of Microbiology*, 5:260–275, 2009. doi: 10.1016/B978-012373944-5.00272-7.

S. Roller and I.C.M. Dea. Biotechnology in the production and modification of biopolymers for food. *Critical Reviews in Biotechnology*, 12(3):261–277, 1992.

Brian G Rusk, Mark H Reed, John H Dilles, Leonhard M Klemm, and Christoph A Heinrich. Compositions of magmatic hydrothermal fluids determined by la-icp-ms of fluid inclusions from the porphyry copper–molybdenum deposit at butte, mt. *Chemical Geology*, 210(1-4):173–199, 2004.

Jeffrey S. Seewald, Kelly W. Doherty, Tracy R. Hammar, Scott P. Liberatore, Heath J. Mills, Barbara Sherwood Lollar, Giora Proskurowski, Eoghan P. Reeves, Wayne C. Shanks, and Peter R. Girguis. Vent fluids support hydrogenotrophic methanogenesis across broad thermal and geochemical gradients offshore nicaragua. *Chemical Geology*, 229(4): 331–343, 2006.

William E Seyfried Jr and Michael J Mottl. Hydrothermal alteration of basalt by seawater under seawater-dominated conditions. *Geochimica et Cosmochimica Acta*, 46(6):985–1002, 1982.

Itai Sharon, Amnon Alperovitch, Forest Rohwer, Matthew Haynes, Fabian Glaser, Nof Atamna-Ismaeel, Ron Pinter, Frédéric Partensky, Eugene V Koonin, Yuri I Wolf, et al. Virus infection of h2-oxidizing bacteria controls hydrothermal vent biofilm dynamics. *Environmental Microbiology*, 11 (10):2585–2597, 2009.

S. M. Sievert and C. Vetriani. Chemoautotrophy at deep-sea vents: past, present, and future. *Oceanography*, 25(1):218–233, 2012a.

Stefan M Sievert and Costantino Vetriani. Chemoautotrophy at deep-sea vents: past, present, and future. *Oceanography*, 25(1):218–233, 2012b.

Stefan M Sievert, Thorsten Brinkhoff, Gerard Muyzer, Wiebke Ziebis, and Jan Kuever. Spatial heterogeneity of bacterial populations along an environmental gradient at a shallow submarine hydrothermal vent near milos island (greece). *Applied and environmental microbiology*, 65(9):3834–3842, 1999.

Stefan M Sievert, Jan Kuever, and Gerard Muyzer. Identification of 16s ribosomal dna-defined bacterial populations at shallow and deep hydrothermal vents of the logatchev area, 14 degrees 45'n, mid-atlantic ridge. *FEMS Microbiology Ecology*, 32(2):101–113, 2000.

Stane Skraber, Oliver Schlosser, Marjan Veber, Martina Oder, Branka Gassilloud, and Jean-Claude Block. Comparative analysis of biofilm development in drinking water distribution systems in two different countries. *FEMS Microbiology Ecology*, 51(1):161–171, 2005.

Karl O Stetter, Gerta Lauerer, Michael Thomm, and Annemarie Neuner. Isolation of extremely thermophilic sulfate reducers: evidence for a novel branch of archaebacteria. *Science*, 236(4803):822–824, 1987.

Karl Otto Stetter, Helmut König, and Erko Stackebrandt. Sulfolobus metalloprotease i: a new metalloprotease from the extremely thermophilic archaebacterium sulfolobus solfataricus: purification, characterization, and determination of the n-terminal sequence. *Molecular & General Genetics MGG*, 191(1):21–25, 1983.

Ian W. Sutherland. Biotechnology. In Hans-Jürgen Rehm and Gerald Reed, editors, *Products of Primary Metabolism*, volume 6, pages 613–657. VCH, Weinheim, 2nd edition, 1996.

Curtis A. Suttle. Marine viruses — major players in the global ecosystem. *Nature Reviews Microbiology*, 5(10):801–812, 2007. doi: 10.1038/nrmicro1750.

Andreas Svensson, Carl-Magnus Mörth, Nils Odling, Alex N Halliday, Alexander Charkin, Yang Yu, Elsa Dahlin, Per Andersson, Johan Gelting, Johan Ingri, et al. Hydrothermal iron and manganese crusts from the pacific ocean: Elemental composition, mineralogy, and formation. *Geochimica et Cosmochimica Acta*, 68(23):4773–4793, 2004.

Ken Takai, Masae Suzuki, Satoshi Nakagawa, Masayuki Miyazaki, Yohey Suzuki, Fumio Inagaki, and Koki Horikoshi. Sulfurimonas paralvinellae sp. nov., a novel mesophilic, hydrogen-and sulfur-oxidizing chemolithoautotroph within the epsilonproteobacteria isolated from a deep-sea hydrothermal vent polychaete nest, reclassification of thiomicrospira denitrificans as sulfurimonas denitrificans comb. nov. and emended description of the genus sulfurimonas. *International Journal of Systematic and Evolutionary Microbiology*, 56(8):1725–1733, 2006.

Jing Tang, Gaosen Wang, Li Zhuang, Yao Zhang, Shuangfeng Wang, Shungui Zhou, Christopher J. van der Gast, and Lixin Shen. Life at the hyperarid margin: novel bacterial diversity in arid soils of the atacama desert, chile. *Extremophiles*, 17(4):553–566, 2013.

VG Tarasov, AV Gebruk, VM Shulkin, GM Kamenev, VI Fadeev, VN Kosmynin, VV Malakhov, DA Starynin, and AI Obzhirov. Effect of shallow-water hydrothermal venting on the biota of matupi harbour (rabaul caldera, new britain island, papua new guinea). *Continental Shelf Research*, 19(1):79–116, 1999.

Vladimir G. Tarasov and et al. Exploration of deep-sea hydrothermal vents. *Deep Sea Research Part II: Topical Studies in Oceanography*, 52(23-26):2260–2279, 2005.

Margaret Kingston Tivey. Generation of seafloor hydrothermal vent fluids and associated mineral deposits. *Oceanography*, 20(1):50–65, 2007.

Constantino Vetriani, Holger W Jannasch, Barbara J MacGregor, David A Stahl, and Anna-Louise Reysenbach. Deep-sea hydrothermal vents: Lessons in extreme physiology. *Oceanography*, 27(1):222–245, 2014.

Peter M Vitousek, Harold A Mooney, Jane Lubchenco, and Jerry M Melillo. Human domination of earth's ecosystems. *Science*, 277(5325):494–499, 1997.

John W Voordeckers, Edward H Kim, Eva van der Zande, Maria P de Miranda, Hermen P Jong, Roel Goldschmeding, Thomas M Jovin, Emile E Voest, and René H Verheijen. Catalyzed reporter deposition, a novel method of signal amplification. ii. application to membrane immunoassays. *Journal of Immunological Methods*, 305(1):14–22, 2005.

TM Wahlund, T Conway, and FR Tabita. Bioconversion of co {sub 2} to ethanol and other compounds. *Preprints of Papers, American Chemical Society, Division of Fuel Chemistry*, 41(CONF-960807-), 1996.

Scott D Wankel, Meghan M Adams, David T Johnston, Colleen M Hansel, Samantha B Joye, Peter R Girguis, and James J Moran. Anaerobic methane oxidation in metalliferous hydrothermal sediments: influence on carbon flux and decoupling from sulfate reduction. *Environmental microbiology*, 14(10):2726–2740, 2012.

Albert J Williams III and Margaret K Tivey. Tidal currents at hydrothermal vents, juan de fuca ridge-dr. albert j. williams iii and dr. margaret k. tivey (woods hole oceanographic institution) outline how at main endeavour field, modular. *Sea Technology*, 42(6):62–64, 2001.

Shannon J Williamson, S Craig Cary, Kurt Williamson, Rachel R Helton, Paul T Johnson, and Brian L Barber. Ecology and detection methods of viruses in unexplored environments: The deep seas and hydrothermal vents. *Deep Sea Research Part II: Topical Studies in Oceanography*, 55 (14-15):1516–1524, 2008.

Mustafa Yücel, Stefan M Sievert, Costantino Vetriani, Dionysis I Foustoukos, Donato Giovannelli, and Nadine Le Bris. Eco-geochemical dynamics of a shallow-water hydrothermal vent system at milos island, aegean sea (eastern mediterranean). *Chemical Geology*, 356:11–20, 2013.

Philippe Zanchetta and Jean Guezennec. Surface thermodynamics of osteoblasts: relation between hydrophobicity and bone active biomaterials. *Colloids and Surfaces B: Biointerfaces*, 22(4):301–307, 2001.

Daniela Zeppilli and Roberto Danovaro. Meiofaunal diversity and assemblage structure in a shallow-water hydrothermal vent in the pacific ocean. *Aquatic Biology*, 5(1):75–84, 2009.

Yunlin Zhang, David J Burdige, Shuai Ma, and Clare E Reimers. Hydrothermal venting in lake tanganyika, east africa. *Geochimica et Cosmochimica Acta*, 86:252–267, 2012.

A. Zykwinska, L. Marchand, Sandrine Bonnetot, C. Sinquin, S. Colliec-Jouault, and C. Delbarre-Ladrat. Deep-sea hydrothermal vent bacteria as a source of glycosaminoglycan-mimetic exopolysaccharides. *Molecules*, 24, 2019. doi: 10.3390/molecules24091703.

Chapter 2

2 Hydrodynamic Flow and Interaction with the Benthic Boundary Layer Shape the Microbial Community in the White Mats of Milos' Shallow Water Hydrothermal Vents

Ana Clara Pelliciari Silva[1], Flavia Migliaccio[1], Bernardo Barosa[1], Luigi Gallucci[2], Mustafa Yücel[3], Dionysis Foustoukos[4], Nadine Le Bris[5], Stuart J. Bartlett[6], Valerio D'Alessandro[7], Costantino Vetriani[8,9] and Donato Giovannelli[8,9,10,11,12]

1- Department of Biology, University of Naples "Federico II", Naples, Italy
2- Department of Molecular Ecology, Max Planck Institute for Marine Microbiology, Bremen, Germany
3- Institute of Marine Sciences, Middle East Technical University, Mersin, Turkey
4- Earth and Planets Laboratory, Carnegie Institution of Washington, Washington, District of Columbia, USA
5- Institute of Systematics Biodiversity and Evolution, Sorbonne University, Paris, France
6-Division of Geological and Planetary Sciences, California Institute of Technology, Pasadena, USA
7-Industrial Engineering and Mathematical Sciences Department, Polytechnic University of Marche, 60100 Ancona, Italy
8- National Research Council - Institute of Marine Biological Resources and Biotechnologies - CNR-IRBIM, Ancona, Italy
9- Marine Chemistry and Geochemistry Department - Woods Hole Oceanographic Institution, MA, U.S.A
10- Earth-Life Science Institute, Tokyo Institute of Technology, Tokyo, Japan
11- Department of Marine and Coastal Science, Rutgers University, New Brunswick, NJ, U.S.A
12- Department of Biochemistry and Microbiology, Rutgers University, New Brunswick, NJ, U.S.A

Chapter available as a paper in Frontiers Microbiology: doi.org/10.3389/fmicb.2025.1649514, see Appendix V: Selected papers & preprints

Chapter 3

3 High rates of carbon fixation in chemosynthetic microbial mats from a shallow-water hydrothermal vents in the Campi Flegrei volcano (Italy)

Ana Clara Pelliciari Silva[1], Flavia Migliaccio[1,2], Jacopo Brusca[1,3], Sara Diana[1,4], Isabel Bassolino[1], Bernardo Barosa[1], Veerle Troelstra[5], Luciano di Iorio[1], Angelina Cordone[1], Julie Brown[6], Andres Velasquez[7], Alessandro Aiuppa[7], Donato Giovannelli[1,8,9,10,11]

1 Department of Biology, University of Naples "Federico II", Naples, Italy
2 National Biodiversity Future Center, Italy
3 National PhD program in Polar Sciences, Ca' Foscari University of Venice, Venice Mestre, Italy
4 Department of Earth and Sea Sciences, University of Palermo, Italy National Biodiversity Future Center, Palermo, Italy
5 Department of Water Management, Faculty of Civil Engineering, Delft University of Technology, Delft, Netherlands
6 Department of Earth Sciences, Bloomsbury Environmental Isotope Facility Laboratory, University College London, UK
7 DiSTeM, Università degli Studi di Palermo, Palermo, Italy
8 Department of Biochemistry and Microbiology, Rutgers University, New Brunswick, NJ, USA
9 Istituto per le Risorse Biologiche e Biotecnologiche Marine, Consiglio Nazionale delle Ricerche, CNR-IRBIM, Ancona, Italy
10 Earth-Life Science Institute, Tokyo Institute of Technology, Ookayama, Tokyo, Japan
11 Marine Chemistry Geochemistry Department - Woods Hole Oceanographic Institution, MA, USA

Abstract

Shallow-water hydrothermal systems represent underexplored analogues of early Earth ecosystems with substantial implications for both microbial ecology and carbon cycling. This study investigates the carbon fixation potential of microbial mats at Secca delle Fumose, a hydrothermal vent field within the Campi Flegrei volcanic complex in the Gulf of Naples. Using *in situ* ^{13}C–bicarbonate incubations, coupled with stable isotope probing and geochemical profiling, we quantified light-dependent and chemoautotrophic carbon assimilation in two distinct microbial biofilms: a filamentous, sediment-bound white biofilm located in diffuse vent emissions and a mat-forming, rock-attached orange biofilm situated proximal to active venting. Results revealed significantly higher dark carbon fixation rates in the white biofilm (4.16 µg C g^{-1} organic C h^{-1}), primarily associated with *Aquificota*-dominated communities, in

contrast to markedly lower rates in the orange mat under both photic and aphotic conditions. These findings underscore the ecological significance and metabolic flexibility of filamentous chemoautotrophs in thermally dynamic, oxygen-rich vent zones. Furthermore, morphological characteristics emerged as key determinants of productivity, with filamentous structures enhancing gas exchange and metabolic rates, despite their lower fossilization potential. The high carbon fixation rates observed in these microbial systems not only challenge assumptions about biosignature preservation in the geologic record but also highlight their potential for biotechnological applications in carbon capture and resource-efficient bioengineering under extreme conditions.

3.1 Introduction

Microbial communities today exhibit various physical structures such as filaments, microbial mats, and stromatolites. These formations are prevalent in different environments, including hydrothermal areas, and consist of diverse microbial groups. Notably, filaments, microbial mats, and stromatolites have been identified in ancient rock records, with studies conducted by Logan [1964], Schopf [1993], Allwood [2006], Noffke [2006], Schopf [2007]. Also hydrothermal systems, are present in a wide depth range (Tarasov and et al. [2005], Hawkes [2014]) and are starting to be more recognisable in deep time (Dodd et al. [2017]). Marine shallow-water hydrothermal systems, located at depths of less than 200 meters, are relatively accessible extreme environments characterized by distinctive biogeochemical conditions (Tarasov and et al. [2005]). These systems derive energy for primary production from the interaction between hot, reduced hydrothermal fluids and cold, oxygenated seawater (Amend and Shock [1998]). Unlike deep-sea hydrothermal vents, shallow-water vents support not only chemosynthetic processes but also photosynthetic primary production due to the presence of light (Tarasov and et al. [2005]).
Present day research has underlined the importance of studying microscopic and macroscopic morphologies and their respective biosignatures in ancient and modern environments (Berelson et al. [2011]). Shallow-water hydrothermal vent systems are mostly understudied in terms of microbial diversity, potential biosignature formation, and biotechnology in comparison to their deep counterparts -deep hydrothermal vents present beyond 200 m depth such as the well known vents in the

East Pacific Rise (Damm et al. [1995]) or in mid-oceanic ridges in the Atlantic (Desbruyères et al. [2001])-. The lack of studies in this domain underscore the need to investigate deeper into the microbial communities making these modern environments, knowing their metabolic pathways, and knowing their carbon fixation rates; the latter can be significant for both, biosignatures research (Blumenberg et al. [2007]), and for biotechnology purposes in terms of carbon sequestration (Jo et al. [2014]).
In the Mediterranean Sea, numerous shallow-water hydrothermal vents have been discovered, stemming from the collision between the African and European tectonic plates. These unique vent environments are distinguished by the presence of major compounds such as carbon dioxide, sulfur dioxide, hydrogen sulfide, methane, and hydrogen (Dando et al. [1999]. In the Gulf of Naples, we investigated the small submarine relief Secca delle Fumose (Figure 10), which is the largest degassing structure offshore of Campi Flegrei (Di Napoli et al. [2016], Figure 11). It has been suggested that Secca delle Fumose was formed on the edge of a N-S graben-like structure during dike emplacement (Di Napoli et al. [2016]). The Secca delle Fumose relief now preferentially facilitates the upward movement of hot brines, which have an equilibrium temperature of 179 ℃, thereby maintaining hydrothermal degassing on the seafloor (Di Napoli et al. [2016]).
Here, we examined the rate of carbon fixation in two biofilms present in the Secca delle Fumose surroundings, analysing how photosynthesis as well as chemoautotrophy can contribute to carbon fixation within the same microbial morphology.

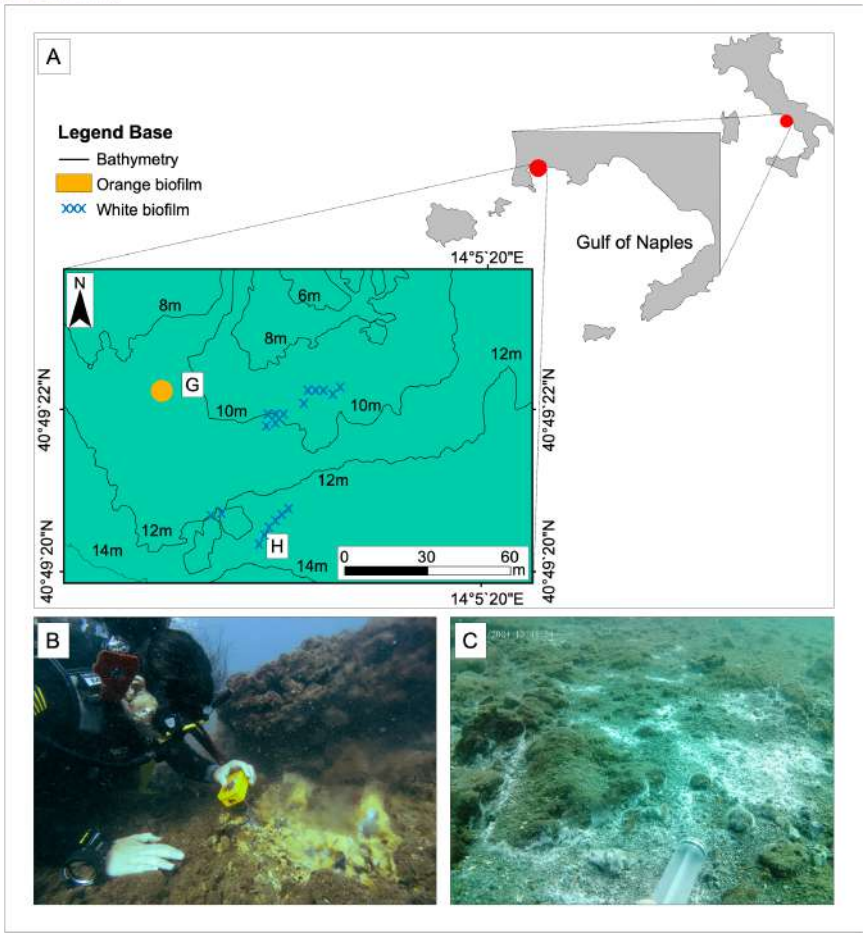

Figure 10: Map collocation of Secca delle Fumose geyser (G), and diffused hydrothermal vent with white biofilm location (H). Map addapted from Appolloni et al. [2020].

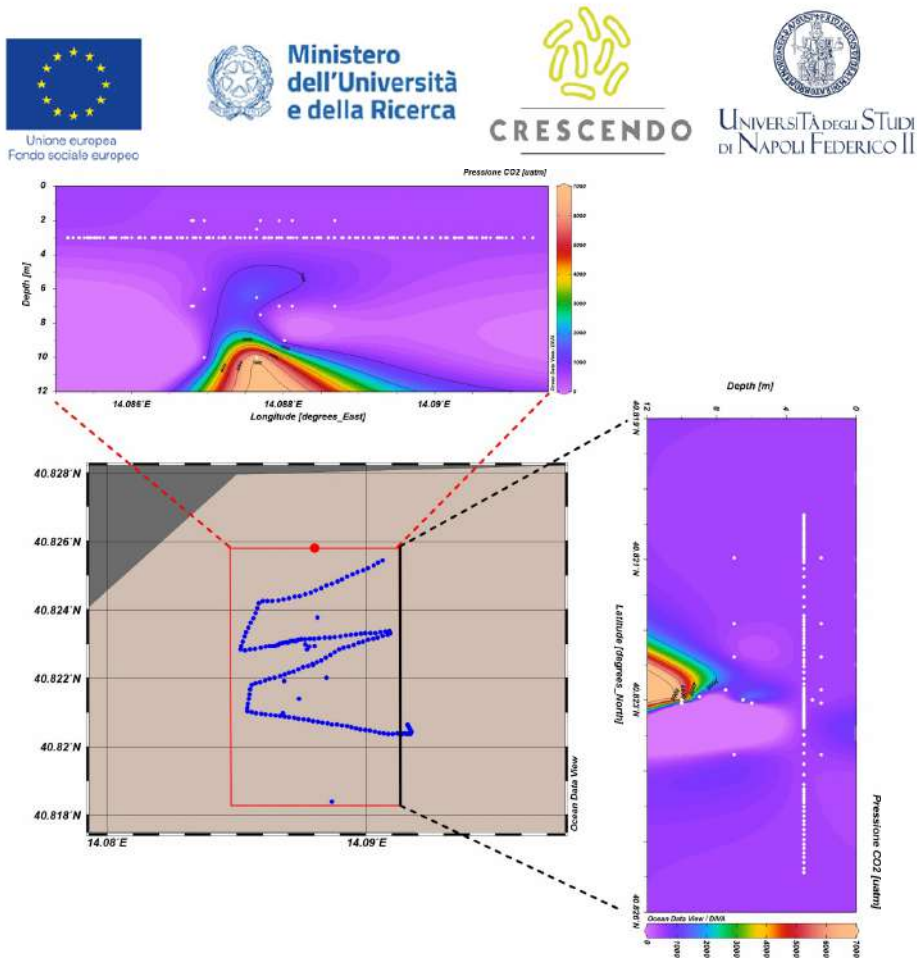

Figure 11: Figure illustrating the pCO_2 according to depth, and longitudinal and latitudinal location in relation to the Secca delle Fumose vent. We notice that the pCO_2 is greater from 8 m to 12 m deep in the immediate vicinity of the vent.

3.2 Materials & Methods

3.2.1 Microbial Community Morphology Descriptions

The two collected biofilms had different colours. They can be differentiated into WSB (White Smooth Biofilm, Figure 12), and OB (Orange Biofilm, Figure 13). The biofilms might contain different textures due to diverse substrate attachments, WSB was attached to sediment, whereas the orange biofilm was rock-attached. It is interesting to notice that WSB was very fragile, and as soon as scuba divers approached this morphology, a slight movement of water would be enough for spreading out the biofilm. Therefore, care needed to be taken when nearing it. The carbon fixation experiment was performed on both kinds of biofilm, being the orange one the nearest biofilm to the geyser, and the white one the furthest away from the geyser.

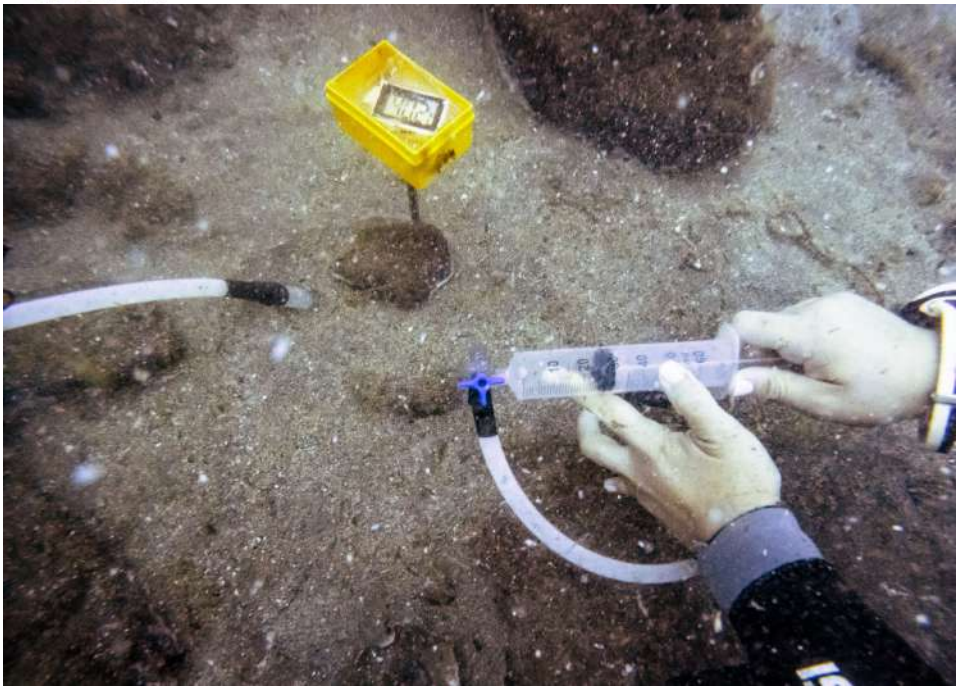

Figure 12: Sampling of the white biofilm. In the image, we can observe patches of the biofilm around sediments. This biofilm was located further away from the geyser.

Figure 13: Orange biofilm located near the geyser. The Secca delle Fumose geyser is in the bottom right corner of the image.

3.2.2 Sample Collection & Geochemistry

All measurements, samples, and in situ microcosms (described below) were performed and collected on November 2024. Samples for C content and δ^{13}C determination (n = 1) were collected using 60 mL syringes. Samples were filtered through an ADVANTEC 25mm diameter 0.22 μm glass fibre filters, also known as GFF (Tokyo Roshi Kaisha Ltd.), with the flow-through being placed in a 15 mL falcon tube and stored at 4 ℃. The GFF containing the filtered biofilms were then placed for 10 minutes in -80 ℃ to ensure incubation was ceased. After drying up the filters on a 60 ℃ incubator for one week, they were then processed for IRMS analysis. Temperature, pH and conductivity were measured onsite using a WTW 330i meter and probe (Hanna probe). Sulfide, Fe^{2+} and dissolved silica were measured onsite using a DR1900 portable spectrophotometer.

Water samples were filtered through 25 mm diameter 0.2µm polyethersulfone syringe filters (VWR International, Radnor, PA, USA). For ion chromatography analysis of anions, water was filtered into 15-mL cen-

trifuge tubes (pre-soaked in 18.2 MΩ/cm DI water). Samples were stored at 4◦C until analysis.

3.2.3 CO_2 Assimilation

A microcosm-based method was used to evaluate the potential for inorganic carbon absorption directly in the environment by adding $NaH^{13}CO_3$. These in situ microcosms were conducted between noon and 4 PM under full or partial sunlight. Samples were collected using 60mL syringes and was injected into overnight acid-washed (0.5 M HCl), precombusted (2h, 180 ℃), autoclaved, gas-tight black butyl rubber septa 10mL vials, which already contained a solution of $NaH^{13}CO_3$ 0.01 M (100 μM final concentration). Care was taken to maintain the structure of the biofilms. Samples were filled completely by their respective biofilms. All serum vials were performed in triplicate.
We assessed the potential for photoautotrophic (light) and chemoautotrophic (dark) $NaH^{13}CO_3$ uptake. To assess CO_2 assimilation in the dark, vials (n = 3 replicates) were amended with $NaH^{13}CO_3$ and completely wrapped in black tape. Assays were stopped by freezing GFFs with filtered biofilms on -80℃. Reported values of ^{13}C-labeled DIC uptake (carbon fixation rates) reflect the difference in uptake between the biomass in the assays that received $NaH^{13}CO3$ and the natural abundance biomass samples described below.

3.2.4 C and Stable Isotopes Concentrations

Natural abundance samples were collected at the time of sampling. These control vials did not contain any pre-injected $NaH^{13}CO_3$, and went through the same steps as samples enriched in $NaH^{13}CO_3$. Biofilms were filtered through GFF and left to dry for a week (60℃). At the time of analysis, half of the GFF were cut and used for determination of C concentration and placed into tin boats, sealed, and analyzed via a Costech Instruments Elemental Analyzer (EA) periphery connected to a Thermo Scientific Delta V Advantage Isotope Ratio Mass Spectrometer (IR-MS) at the Stable Isotope Geochemistry Lab in the Department of Geology at the University College of London, and δ^{13}C values were calibrated using reference standards USGS-40 and USGS-41 and checked with a laboratory working standard (glycine). Total uptake of DIC was calculated using DIC numbers determined for the source water (described above). All stable isotope results are given in delta formation expressed

as per mil (‰). Carbon stable isotopes are calculated as:

$$\delta^{13}C = [((R_a)_{sample}/(R_a)_{standard}) - 1] \times 10^3 \quad (1)$$

where R_a is the $^{13}C/^{12}C$ ratio of the sample or standard, and are reported vs. the Vienna Pee Dee Belemnite (VPDB) standard.
Precautions were taken to minimize cross contamination of natural abundance samples with incubation assays. Natural abundance samples were processed and analyzed in turn, prior to incubation assays. All laboratory processing and weighing equipment was cleaned with 80% ethanol between each sample.
Assimilation rates were calculated from the following parameters: Absolute isotopic stable carbon ratios were used to determine the difference between the total amount of ^{13}C in natural abundance samples and incubation assay replicates. The difference represents total mass of ^{13}C-labeled DIC taken up during incubations. Incubation duration times were recorded in the field. Using the organic carbon content, the uptake rate is then calculated from the total μg C taken up divided by the grams of organic C, and that was divided by the number of hours the incubation was carried out over (typically $\sim$ 3 h).

3.2.4.1 Full workflow of calculations

Since we are investigating how much ^{13}C-labeled the sample has uptaken, we calculate the total ^{13}C-labeled mass as follows:

$$^{13}\mathrm{C}_{\text{sample}}\,(\mathrm{mg}) = ^{13}\,\mathrm{C}_{\text{mass}} \times \left(\frac{(R_a)_{\text{sample}}}{1 + (R_a)_{\text{sample}}}\right) \quad (2)$$

Having in mind that R_{sample} is calculated as:

$$R_{\text{sample}} = R_{\text{standard}} \times \left(1 + \frac{\delta^{13}\mathrm{C}}{1000}\right) \quad (3)$$

In order to calculate the amount of ^{13}C accumulated in the sample, we first compute the ^{13}C in the control experiment (no ^{13}C-labeled bicarbonate added). Formulas used were:

$$^{13}\mathrm{C}_{\text{control}}\,(\mathrm{mg}) = \left(\frac{R_{\text{control}}}{1 + R_{\text{control}}}\right) \times \text{total C in sample} \tag{4}$$

$$^{13}\mathrm{C}_{\text{accumulated}}\,(\mathrm{mg}) = ^{13}\,\mathrm{C}_{\text{sample}} - ^{13}\,\mathrm{C}_{\text{control}} \tag{5}$$

We further convert the result to μg:

$$^{13}\mathrm{C}_{\text{accumulated}}\,(\mu\mathrm{g}) = ^{13}\,\mathrm{C}_{\text{accumulated}}\,(\mathrm{mg}) \times 10^3 \tag{6}$$

We calculate the carbon fixation rate (pre-dilution factor) as:

$$\text{CF} = \frac{^{13}\mathrm{C}_{\text{accumulated}}\,(\mu\mathrm{g})}{\text{net weight sample (g)} \times \text{incubation time (h)}} \tag{7}$$

The incubation time (h) and the net weight of the sample (g) were used to normalize the accumulation rate.

However, because the added ^{13}C–bicarbonate mixes with the natural dissolved inorganic carbon (DIC) already present in the incubation water, only a small fraction of the total DIC inside each vial is labeled. To correct for this dilution, a label dilution factor (DF) was calculated as:

$$\text{DF} = \frac{[\mathrm{DIC}_{\text{total}}]}{[^{13}\text{C-HCO}_3^-]_{\text{final}}} \tag{8}$$

where: $[\mathrm{DIC}_{\text{total}}]$ is the total inorganic carbon concentration derived from the total alkalinity (in mM); $[^{13}\text{C-HCO}_3^-]_{\text{final}}$ is the final concentration of labeled bicarbonate in the incubation water (in mM).

The corrected rate, accounting for this dilution, was then calculated as:

$$\text{Rate}_{\text{corrected}} = \text{CF} \times \text{DF} \tag{9}$$

Normalizing the results to the organic carbon (OC) content in the total sample mass (m) follows as:

$$\frac{\text{OC (g)}}{m_{\text{sample}}} = \frac{\text{mass of C in sample (mg)}}{1000 \times \text{net sample mass (g)}} \tag{10}$$

Final rate normalized to organic carbon:

$$\text{Rate}_{\text{OC-normalised}} = \frac{\text{Rate}_{\text{corrected}}}{\text{OC (g)}} \tag{11}$$

Full workflow of calculations can be visualised in the diagram below:

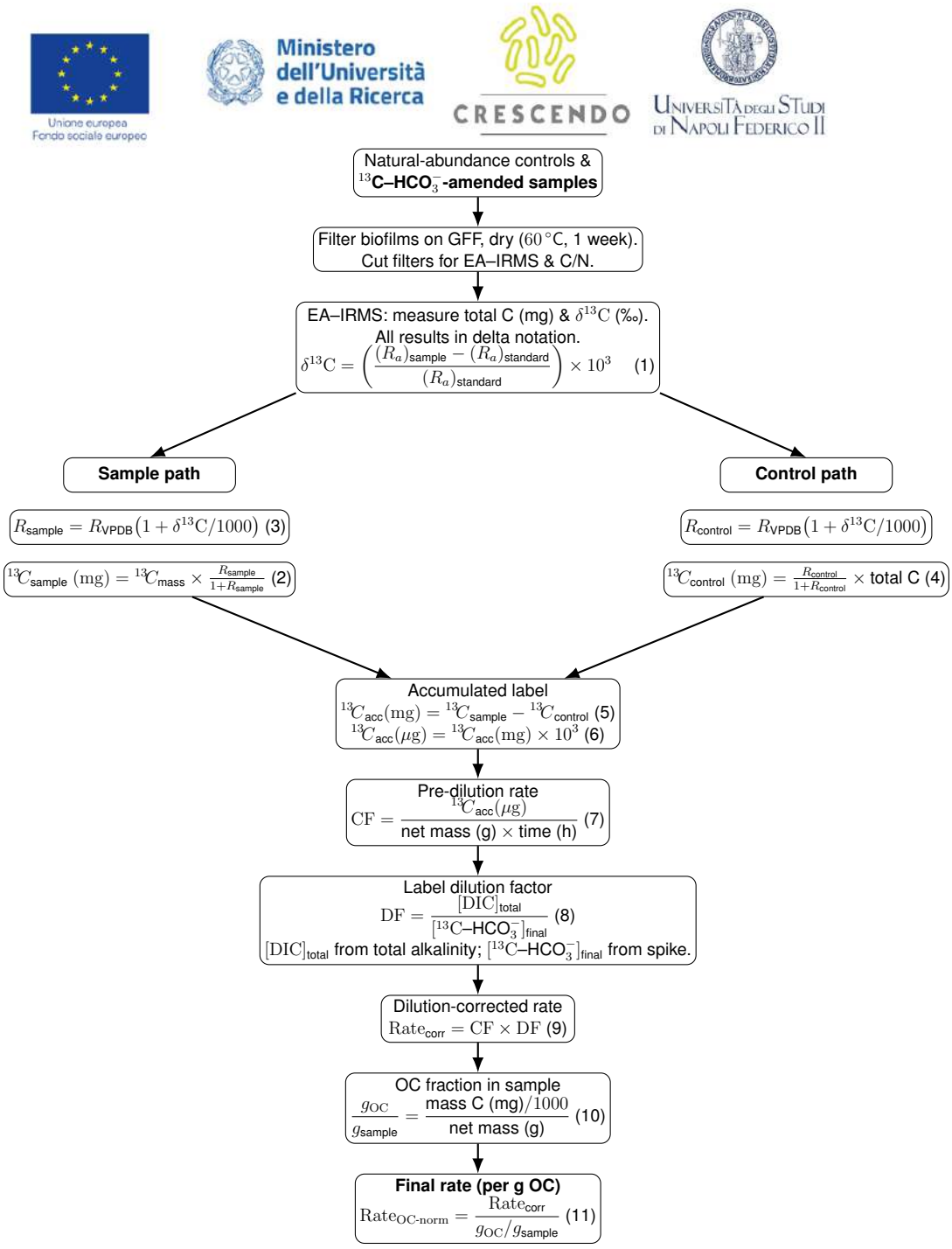

3.2.5 DNA Extraction and Amplicon Sequencing

DNA extraction was performed using the DNeasy PowerSoil Kit (QIAGEN), following the manufacturer's instructions, with an additional elution step. When low DNA yields were obtained, a modified phenol–chloroform DNA extraction method was applied, adapted for shallow-water hydrother-

mal vent conditions Giovannelli et al. [2013].
Briefly, 850 µl of extraction buffer (50 mM Tris-HCl pH 8, 20 mM EDTA pH 8, 100 mM NaCl) was added to 0.5 g of sediment and Sterivex filters. Then, 100 µl of lysozyme (100 mg/ml) and 5 µl of proteinase K were added sequentially, each followed by incubation at 37 ℃ for 30 min and a 1 min vortexing step. Subsequently, 50 µl of 20% SDS was added to the samples and incubated for 30 min at 65 ℃ with regular mixing, followed by a 1 min vortexing step. Samples were then centrifuged for 3 min at 14,000 $\times$ g.
The supernatant was collected and transferred to a phenol:chloroform:isoamyl alcohol (25:24:1) solution, followed by centrifugation for 3 min at 14,000 $\times$ g. The aqueous phase was then transferred to a chloroform:isoamyl alcohol (24:1) solution and centrifuged for 3 min at 14,000 $\times$ g. The resulting supernatant was collected and supplemented with sodium acetate (0.1 vol) and isopropanol (0.7 vol), then incubated at -20 ℃ for 2 h. The precipitated DNA was washed with 70% cold ethanol and re-suspended in 50 µl of Tris-HCl.
DNA quality was verified by agarose gel electrophoresis and quantified both spectrophotometrically and spectrofluorimetrically using NanoDrop and Qubit instruments, respectively. Successfully extracted DNA was sequenced at the Integrated Microbiome Resource (https://imr.bio) using primers targeting the V4–V5 region (515FB: `GTGYCAGCMGCCGCGGTAA` and 926R: `CCGYCAATTYMTTTRAGTTT`) of the 16S rRNA gene, on an Illumina MiSeq platform (V3 chemistry).

3.3 Bioinformatic analysis

The raw sequencing data were analysed using the DADA2 package Callahan et al. [2016]. Quality profile analysis was performed after trimming primers and adapters, retaining only sequences with a per-base quality score between 20 and 40 for downstream analysis. Amplicon sequencing variants (ASVs) were inferred through error profiling, and taxonomy was assigned to each ASV using the SILVA database, release 138 Quast et al. [2013].
Amplicon variant abundance tables and taxonomic assignments were imported into a `phyloseq` object to calculate diversity indices and assess microbial diversity, as previously described Cordone et al. [2022, 2023], Barosa et al. [2023]. Sequences assigned to mitochondria, eukaryotes, chloroplasts, groups related to human pathogens, and known

DNA extraction contaminants Sheik et al. [2018], as well as sequenced blanks, were removed from the dataset. The remaining reads represented 95% of the original dataset, with a total of 178,671 reads assigned to 4,612 ASVs.
ASV taxonomic classification was further refined using the EzBioCloud database Yoon et al. [2017], and verified by comparison against the nucleotide database of the National Center for Biotechnology Information (NCBI) using BLAST searches. All the sequences analysed in this study are available through the European Nucleotide Archive (ENA) under project accession PRJEB67762, under the ENA Umbrella project CoEvolve PRJEB55081.

3.4 Results

We strategically targeted the OB, which was the biofilm near-most the Secca delle Fumose geyser, and the WSB which was present far away from the geyser, around diffused emissions in the sand. OB was rock-attached, while WSB was sediment-attached. Near the geyser, temperatures reached up to 74.9 ^{o}C and the recorded pH was 5.74. Dissolved oxygen reached 51.7% and conductivity 51.62 mS/cm. Around the diffused emissions where WSB was present, temperature reached 46.6 ^{o}C, and pH of 6.34. Dissolved oxygen reached 93.7% and conductivity 56.04 mS/cm.

3.4.1 C Content and δ^{13}C Natural Abundance

The orange mat site contained highest overall carbon content, with an average of 9.06 mg of C being present in the samples, white biofilm samples had an average of 0.96 mg of C. Natural abundance δ^{13}C values of the white biomass ranged from -19.94 ‰ for the white chemoautotroph community (dark-taped vial incubated around diffused emissions), to -17.87 ‰ for the white photosynthetic community (clear vial incubated around diffused emissions). For the orange biomass values ranged from -18.82 ‰ for the orange chemoautotroph community, to -19.07 ‰ for the orange photosynthetic community. All the incubation assays with 13C label added had δ^{13}C values more positive than the natural abundance samples (Table 1 and Figure 14).

3.4.2 Carbon Assimilation

A microcosm-based approach was employed to assess the potential for inorganic carbon uptake in-situ across biofilm morphologies in the Secca delle Fumose area through the addition of $NaH^{13}CO_3$. We assessed light-dependent and light-independent inorganic carbon uptake in white and orange microbial mats.

Biofilm description	Type of incubation	Replicates	Net weight sample (g)	d13C	Incubation time (h)	13C accumulated (ug)	Carbon uptake rates (ug/g OC/h)
Orange Biofilm	Photosynthetic	1	0,3909	-17,29	3	0,225451	0,68
		2	0,0884	-17,4	3	0,056776	0,64
		3	0,2380	-18,52	3	0,040934	0,21
		Control	0,0415	-19.07	3		
Orange Biofilm	Chemosynthetic	1	0,5539	ND	3	ND	ND
		2	0,1144	-18,26	3	0,021967	0,21
		3	0,7629	-18,51	3	0,052303	0,12
		Control	0,2186	-18,82	3		
White Biofilm	Chemosynthetic	1	0,0092	9,22	3	0,026404	5,22
		2	0,0142	-6,16	3	0,035498	1,10
		3	0,0160	-13,81	3	0,065141	2,47
		Control	0,0415	-19,94	3		
White Biofilm	Photosynthetic	1	0,0576	ND	3	ND	ND
		2	0,0476	-12,24	3	0,087211	1,01
		3	0,0490	-16,31	3	0,021514	0,28
		Control	0,0193	-17,87	3		

Table 1: Carbon uptake rates and isotope composition of orange and white biofilms under photosynthetic and chemosynthetic incubation. Values show replicate measurements for net sample weight, δ^{13}C, incubation time, ^{13}C accumulation, and calculated carbon uptake rates. “ND” indicates no data; control samples were not enriched.

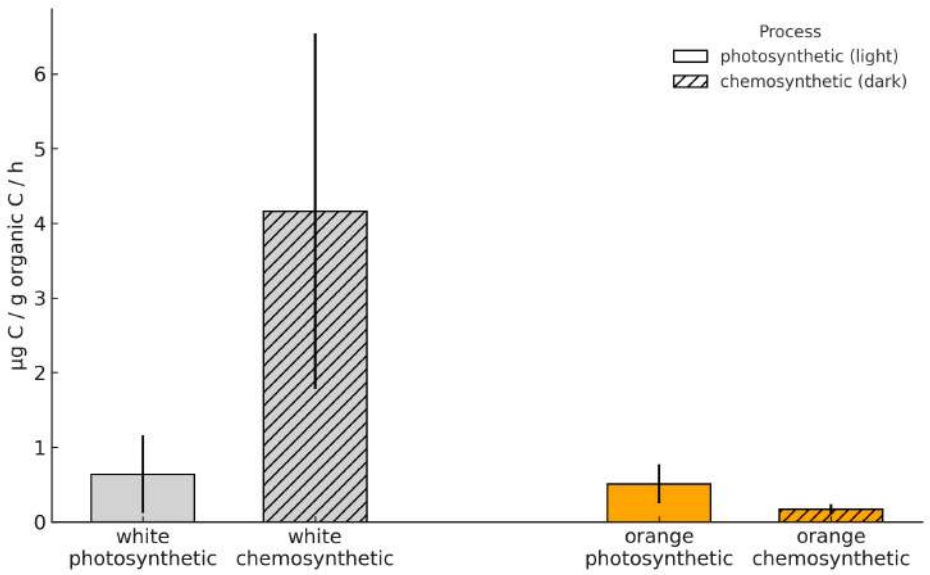

Figure 14: Carbon fixation rates across color treatments and metabolic processes. Bars show mean carbon fixation rates (μg C g^{-1} organic C h^{-1}) for white and orange treatments under photosynthetic (clear bars) and chemosynthetic (hatched bars) conditions. Error bars represent standard deviations ($n = 3$). The legend indicates both color treatments (white and orange) and metabolic processes (photosynthetic and chemosynthetic).

The highest rates of inorganic carbon uptake are observed in the white biofilm when not exposed to light (chemosynthetic incubation), comprising a mean of 4.16 ug C/ g organic C/ hour. It is also possible to observe elevated values of carbon fixation for the light dependent incubation of the white biofilm (mean 0.64 ug/ g organic C/ hour). The OB seems to have a distinct trend in which the light-dependent incubation scored higher values of carbon uptake than the light-independent essays (0.51 mean vs 0.17 mean ug/ g organic C/ hour).
Nevertheless, it must be remarked that the potential for light-independent primary productivity (chemolithoautotrophy) was observed in all sites.

3.4.2.1 Comparison to other geothermal systems worldwide

When normalized to biomass ($\mu g\ C\ g^{-1}\ h^{-1}$), carbon fixation rates measured in microbial mats from SdF occupy an intermediate range relative to other geothermal systems in the light incubations (Figure 15a).

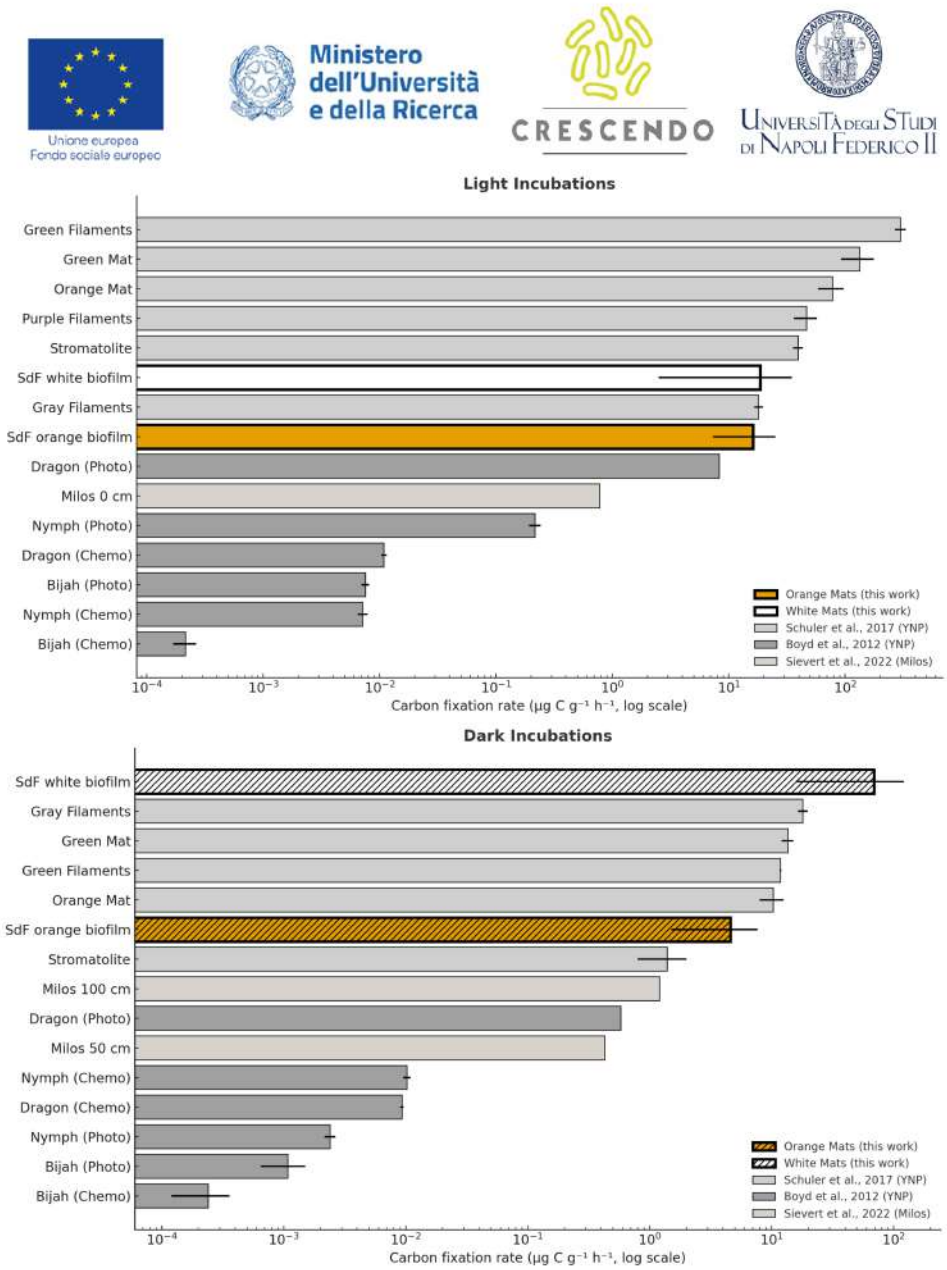

Figure 15: Comparison of carbon fixation rates across geothermal microbial communities worldwide in light-exposed and dark incubations. Carbon fixation rates ($\mu g\ C\ g^{-1}\ h^{-1}$, log scale) for microbial mats from Secca delle Fumose (SdF) are compared with published data from Yellowstone National Park (YNP; Boyd et al. [2012]; Schuler et al. [2017]) and Milos hydrothermal sediments (Sievert et al. [2022]). .

Both the orange and white SdF mats exhibited higher dark-incubation activities than the chemoautotrophic biofilms reported for Nymph and Bijah Springs in Yellowstone National Park (Boyd et al. [2012],Figure 15). The orange mat at SdF remained lower than the highly phototrophic mats and higher than the stromatolites characterized by Schuler et al.

[2017]. The SdF white mat displayed fixation rates that were the highest reported for dark incubations amongst both terrestrial and marine ecosystems.

3.5 Discussion

3.5.1 Carbon Fixation, Microbial Morphology, and Biotechnological Relevance

The rock record contains diverse microbially generated structures, from filaments to bacterial mats, and the classic stromatolites, that represent some of the oldest biosignatures of life on Earth. Among these, stromatolites are the most commonly preserved, with well-documented occurrences dating back to 3.5 Ga (Noffke et al. [2013]) and putative forms identified even earlier (Lepot [2020]). Traditionally, stromatolites are associated with phototrophic microbial activity in shallow aquatic environments (Schuler et al. [2017]), microbial mats and filamentous structures, though often less preserved, also provide valuable insights into past biological productivity (Lehn et al. [2024]). It is worth noting that both photoautotrophic and chemoautotrophic communities can give rise to similar morphologies, complicating efforts to interpret their metabolic origins in the geological record.

In this study, we investigated modern analogues of ancient microbial systems in the shallow-water hydrothermal field of Secca delle Fumose in the Gulf of Naples. Specifically, we targeted microbial mats with contrasting visual morphologies (orange, rock-attached biofilms near active venting, and white, sediment-bound biofilms farther from the geyser) to assess their potential for carbon fixation under light and dark conditions. By combining morphological observation, stable isotope probing, and quantitative measurements of carbon uptake, our goal was to better understand the ecological roles of these communities, and to clarify how photoautotrophic versus chemoautotrophic processes contribute to their productivity.

Importantly, microbial communities inhabiting extreme environments such as shallow hydrothermal systems are increasingly recognized not only as analogues for early Earth ecosystems, but also as promising candidates for biotechnological applications, including natural carbon sequestration, biofilm engineering, and metabolic resource harvesting (Rawat et al. [2024]. Assessing their fixation capacity and metabolic flexibility

under natural conditions is therefore crucial for both paleoenvironmental interpretation and emerging climate-oriented technologies.

The marked difference in carbon fixation rates between the white and orange biofilms can be largely explained by their contrasting microbial community structures, morphologies, and local geochemical settings. The white biofilm, located in diffuse emission zones farther from the main geyser, developed under moderately warm conditions (46.6 ℃, pH 6.34) with high dissolved oxygen (93.7%). This habitat supports a community dominated by Aquificota (Aquificae, 88.9%), well-known thermophilic chemolithoautotrophs that oxidize hydrogen or reduced sulfur compounds to fix CO_2 (Barosa et al., *in revision*; Figure 16). Field observations showed that the white biofilm exhibited a distinctly filamentous morphology, loosely attached to sediment and easily disrupted by water movement. Such a morphology has been suggested to enhance nutrient and gas exchange with the surrounding water column, increasing the effective surface area for CO_2 uptake (Havig [2009]; Barthelmeß et al. [2021]). This is consistent with the high dark incubation uptake rates observed (0.54 ug C/ g/ h) and relatively modest light–dark differences. The Yellowstone study by Havig [2009] proposed that filamentous communities are generally more effective in carbon fixation than mat-like structures, although they have a lower preservation potential in the rock record, which may bias interpretations of ancient productivity (Figure 17).

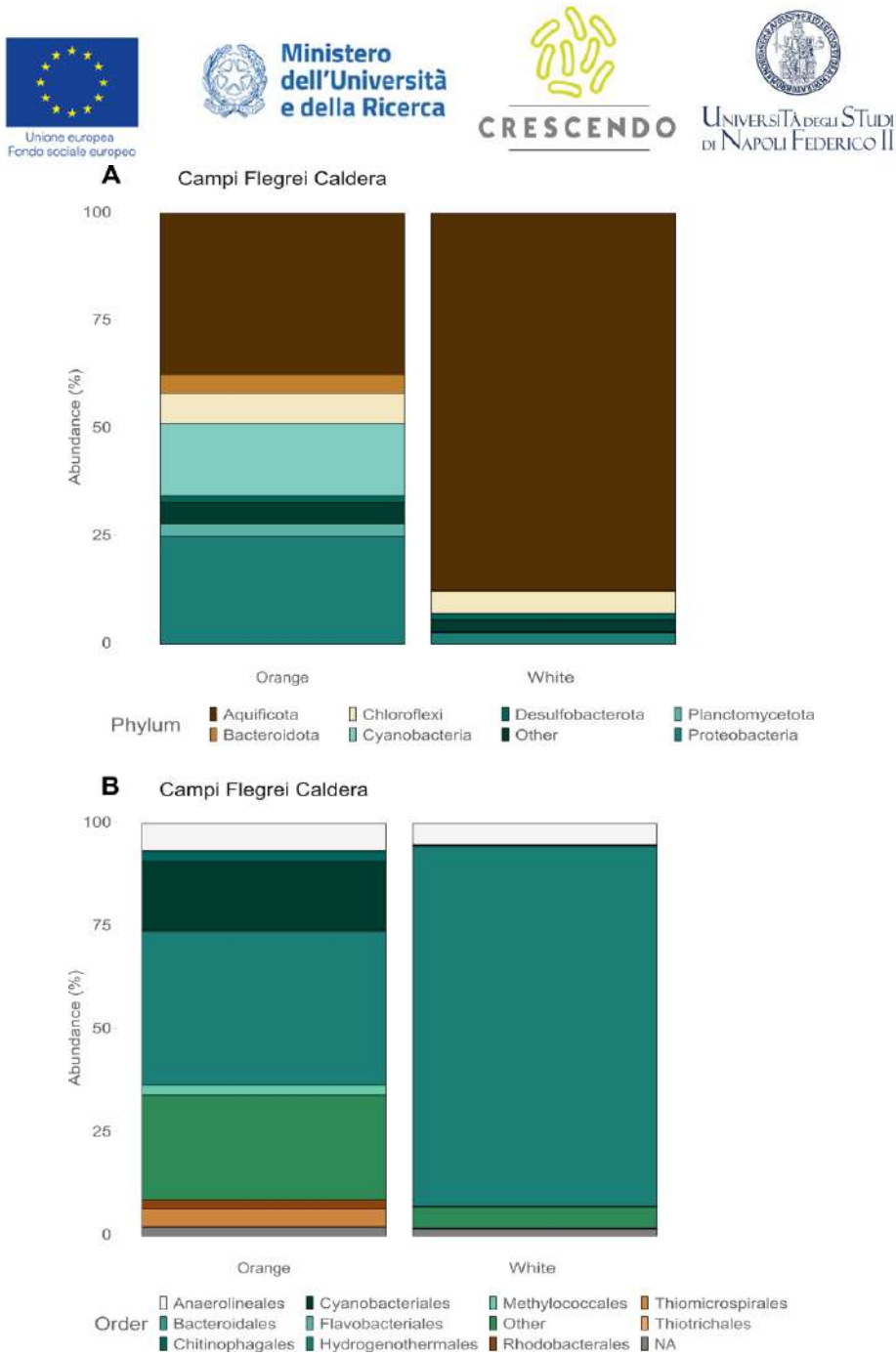

Figure 16: Microbial community composition of the biofilms sampled around the shallow-water hydrothermal vents studied here: A) Phylum taxonomic rank; B) Order taxonomic rank. Figure adapted from Barosa et al., *in prep.*

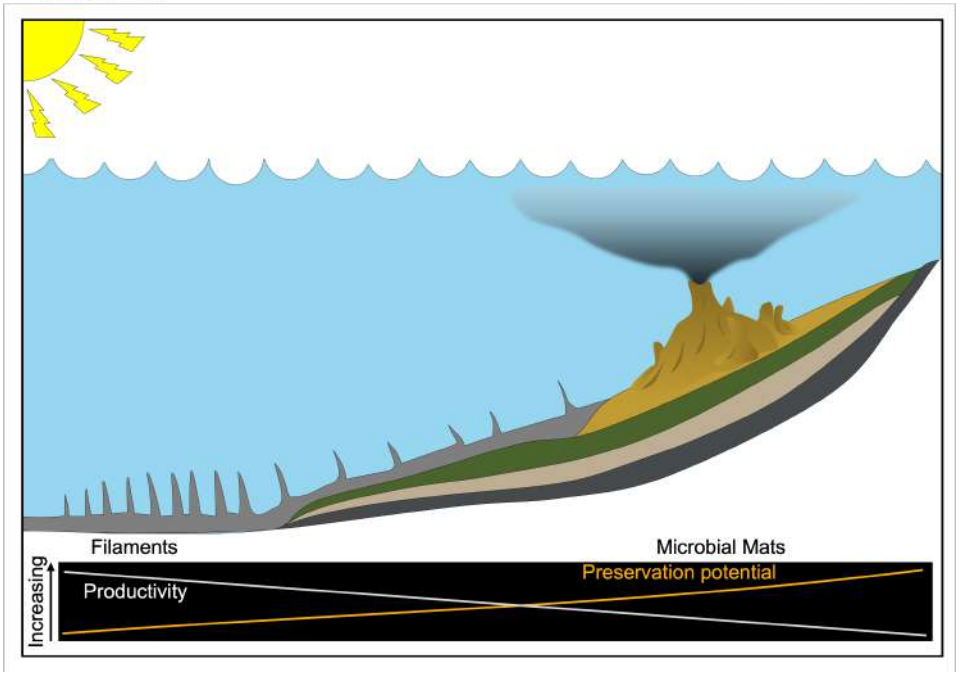

Figure 17: Cartoon illustrating the relationship between productivity and preservation potential for microbial community morphologies, adapted from Schuler et al. [2017].

In contrast, the orange biofilm, located immediately adjacent to the vent, was morphologically mat-like, densely bound to rocky substrates. It experienced more extreme thermal (74.9 ℃) and acidic (pH 5.74) conditions with lower dissolved oxygen (51.7%). Despite hosting phototrophic Cyanobacteria (16.6%) and photosynthetic Alphaproteobacteria (Figure 24), carbon uptake rates in both light and dark conditions were very low ($\sim$ 0.51 ug C/g/h and $\sim$ 0.17 ug C/g/h, respectively), and δ^{13}C enrichment was negligible. This reduced activity may reflect the thicker, stratified mat structure, which can limit light penetration, nutrient exchange, and gas diffusion to active phototrophic layers, especially under physiologically stressful geochemical conditions (Stal et al. [1985]; Lichtenberg et al. [2020]). Additionally, environmental stress near the geyser, such as elevated sulfide and temperature, likely suppresses metabolic activity or channels energy into stress responses rather than growth.

Together, these observations support the notion that morphology is not merely a passive outcome of community composition, but a functional trait influencing carbon fixation potential. Filamentous forms, as in the

white biofilm, can enhance metabolic rates through increased interface with the water column, while mat structures may confer stability under harsh conditions but at the cost of lower metabolic efficiency. These functional trade-offs have important implications for interpreting the rock record: the preferential preservation of mats and stromatolites over filaments (Schuler et al. [2017]) may underestimate past primary productivity, especially in hydrothermal or marginal marine environments where filaments could have played a dominant role.

Despite these insights, several limitations should be acknowledged. Sampling was limited to a single moment in time, preventing assessment of short-term or seasonal variability in venting, geochemistry, or microbial physiology. The sealed microcosm incubations, although necessary for in-situ isotope probing, may not perfectly reproduce natural diffusion and redox gradients, particularly for loosely structured filamentous mats. DIC concentrations can fluctuate rapidly around vents, introducing uncertainty in dilution-factor corrections. Future work should include repeated temporal sampling, continuous microsensor profiling, and flow-through or open-chamber incubation systems that better mimic natural conditions. Complementary metagenomic and metatranscriptomic analyses would directly link metabolic pathways to measured uptake, while nanoSIMS or microautoradiography could reveal fine-scale spatial heterogeneity in carbon fixation within each morphology.

Microbially generated structures such as stromatolites have been readily preserved in the rock record since the Archean (Awramik [1992]), yet filamentous and mat-like morphologies are far less frequently preserved, potentially obscuring their contribution to past carbon fixation and oxygen production. By studying distinct microbial community macrostructures within the same shallow-water hydrothermal system, we demonstrate a clear link between morphology, community composition, and carbon uptake potential. The orange biofilm, exhibiting a dense mat-like structure and located under high-temperature, low-oxygen, acidic conditions near the vent, showed the lowest rates of carbon uptake in both light and dark incubations, paralleling the lower productivity often observed in some stromatolitic forms. In contrast, the white biofilm, characterized by a loosely attached filamentous morphology in cooler, oxygen-rich diffuse flows, displayed the highest dark carbon uptake rates, nearly an order of magnitude greater than the orange mat, and substantial light-dependent activity. These findings support the idea, also observed in Yellowstone hot springs, that filamentous phototrophic or

chemolithoautotrophic communities can be highly productive but have low preservation potential, while mat-like or stromatolitic forms may be more robust in the rock record despite lower metabolic rates. This negative correlation between preservation potential and productivity suggests that the rock record may systematically underestimate the role of fast-growing, high-uptake microbial forms in early carbon cycling. Beyond paleoenvironmental reconstruction, the high carbon fixation efficiency and environmental resilience of filamentous biofilms highlight their potential for biotechnological applications. Their capacity to sustain high productivity under elevated temperatures, variable pH, and fluctuating redox conditions positions them as promising candidates for engineered carbon sequestration systems in geothermal or industrial contexts, as well as sources of thermostable enzymes, bioactive compounds, and metabolic pathways that can be harnessed for sustainable bioprocessing in extreme environments.

3.6 Conclusion

Here we present primary productivity, morphology, geochemistry, and community composition data for filamentous and mat-like biofilms from a shallow-water hydrothermal vent system. We demonstrate pronounced differences in carbon fixation rates between these morphologies despite their shared hydrothermal origin and overlapping dominant taxa at the phylum level. Filamentous white biofilms, dominated by Aquificota, exhibited the highest dark carbon fixation rates and substantial light-dependent activity, while mat-like orange biofilms showed minimal uptake under both light and dark conditions. These results reinforce the view that morphological form strongly influences productivity, with filamentous communities representing high-productivity but low-preservation end members, and mat-like structures acting as low-productivity but more preservation-prone analogues. Collectively, our findings suggest that the contribution of filamentous microbial forms to carbon cycling in ancient hydrothermal systems may be underrepresented in the rock record, with implications for both the reconstruction of early biospheres and the identification of microbial taxa of interest for biotechnological carbon capture in extreme environments.

3.7 Supplementary Figures

Figure 18: Photograph of white smooth biofilm present in the Gulf of Naples.

References

Walter Malcolm R. Kamber Balz S. Marshall Craig P. Burch Ian W. Allwood, Abigail C. Stromatolite reef from the early archaean era of australia. *Nature*, 441:714–718, 2006.

Jan P. Amend and Everett L. Shock. Energetics of overall metabolic reactions of thermophilic and hyperthermophilic archaea and bacteria. *FEMS Microbiology Reviews*, 22(4):389–414, 1998.

Luca Appolloni, Daniela Zeppilli, Luigia Donnarumma, Elisa Baldrighi, Elena Chianese, Giovanni Fulvio Russo, and Roberto Sandulli. Seawater acidification affects beta-diversity of benthic communities at a shallow hydrothermal vent in a mediterranean marine protected area (underwater archaeological park of baia, naples, italy). *Diversity*, 12 (12):464, 2020.

Stanley M Awramik. The history and significance of stromatolites. In *Early organic evolution: implications for mineral and energy resources*, pages 435–449. Springer, 1992.

Joana Barosa, Jeffrey J. Marlow, Costantino Vetriani, Gaetano D'Errico, Giulia Grasso, Alessandro Cordone, Laura Giuliano, and Donato Giovannelli. Comparative metagenomics of microbial mats from shallow hydrothermal vents reveals functional differentiation across venting systems. *Microbiome*, 11(1):134, 2023. doi: 10.1186/s40168-023-01566-3.

Theresa Barthelmeß, Florian Schütte, and Anja Engel. Variability of the sea surface microlayer across a filament's edge and potential influences on gas exchange. *Frontiers in Marine Science*, 8:718384, 2021.

William M Berelson, Frank A Corsetti, Charles PEPE-RANNEY, DE Hammond, William Beaumont, and John R Spear. Hot spring siliceous stromatolites from yellowstone national park: assessing growth rate and laminae formation. *Geobiology*, 9(5):411–424, 2011.

M Blumenberg, R Seifert, Sven Petersen, and W Michaelis. Biosignatures present in a hydrothermal massive sulfide from the mid-atlantic ridge. *Geobiology*, 5(4):435–450, 2007.

Eric S Boyd, Kristopher M Fecteau, Jeff R Havig, Everett L Shock, and John W Peters. Modeling the habitat range of phototrophs in yellowstone national park: toward the development of a comprehensive fitness landscape. *Frontiers in Microbiology*, 3:221, 2012.

Benjamin J. Callahan, Paul J. McMurdie, Michael J. Rosen, Andrew W. Han, Amy Jo A. Johnson, and Susan P. Holmes. Dada2: High-resolution sample inference from illumina amplicon data. *Nature Methods*, 13(7):581–583, 2016. doi: 10.1038/nmeth.3869.

Alessandro Cordone, David J. Martínez-Cano, Fabio Gamberi, Silvia Pelosi, Costantino Vetriani, Laura Giuliano, Angelina Lo Giudice, and Donato Giovannelli. Microbial community structure and function in shallow-water hydrothermal vents of the aeolian archipelago (italy). *Frontiers in Microbiology*, 13:892731, 2022. doi: 10.3389/fmicb.2022.892731.

Alessandro Cordone, David J. Martínez-Cano, Costantino Vetriani, Laura Giuliano, Angelina Lo Giudice, and Donato Giovannelli. Environmental drivers of microbial diversity and function in mediterranean shallow-water hydrothermal vents. *Environmental Microbiology*, 25 (6):2735–2752, 2023. doi: 10.1111/1462-2920.16345.

KL Von Damm, SE Oosting, R Kozlowski, LG Buttermore, DC Colodner, HN Edmonds, JMm Edmond, and JM Grebmeier. Evolution of east pacific rise hydrothermal vent fluids following a volcanic eruption. *Nature*, 375(6526):47–50, 1995.

PR Dando, D Stüben, and SP Varnavas. Hydrothermalism in the mediterranean sea. *Progress in Oceanography*, 44(1-3):333–367, 1999.

D Desbruyères, M Biscoito, J-C Caprais, A Colaço, T Comtet, Ph Crassous, Y Fouquet, A Khripounoff, N Le Bris, K Olu, et al. Variations in deep-sea hydrothermal vent communities on the mid-atlantic ridge near the azores plateau. *Deep Sea Research Part I: Oceanographic Research Papers*, 48(5):1325–1346, 2001.

R Di Napoli, A Aiuppa, A Sulli, S Caliro, G Chiodini, V Acocella, G Ciraolo, MA Di Vito, F Interbartolo, C Nasello, et al. Hydrothermal fluid venting in the offshore sector of c ampi f legrei caldera: A geochemical, geophysical, and volcanological study. *Geochemistry, Geophysics, Geosystems*, 17(10):4153–4178, 2016.

Matthew S. Dodd, Dominic Papineau, Tor Grenne, John F. Slack, Martin Rittner, Franco Pirajno, Jonathan O'Neil, and Crispin T.S. Little. Evidence for early life in earth's oldest hydrothermal vent precipitates. *Nature*, 543:60–64, 2017.

Donato Giovannelli, Giuseppe d'Errico, Elena Manini, Michail M Yakimov, and Costantino Vetriani. Diversity and phylogenetic analyses of bacteria from a shallow-water hydrothermal vent in milos island (greece). *Frontiers in Microbiology*, 4:184, 2013.

Jeff Robert Havig. *Geochemistry of hydrothermal biofilms: composition of biofilms in a siliceous sinter-deposition hot spring*. Arizona State University, 2009.

Connelly D.P. Gledhill M. Achterberg E.P. Hawkes, J.A. The stabilisation and transportation of dissolved iron from high temperature hydrothermal vent systems. *Earth and Planetary Science Letters*, 375: 280–290, 2014.

Byung Hoon Jo, Jeong Hyun Seo, and Hyung Joon Cha. Bacterial extremo-α-carbonic anhydrases from deep-sea hydrothermal vents as potential biocatalysts for co2 sequestration. *Journal of Molecular Catalysis B: Enzymatic*, 109:31–39, 2014.

Ilana Lehn, Paulo Sérgio Gomes Paim, and Farid Chemale Jr. From the sea to the land: How microbial mats dominated marine and continental environments in the ediacaran camaquã basin, brazil. *Geosystems and Geoenvironment*, 3(3):100283, 2024.

Kevin Lepot. Signatures of early microbial life from the archean (4 to 2.5 ga) eon. *Earth-Science Reviews*, 209:103296, 2020.

Mads Lichtenberg, Paulo Cartaxana, and Michael Kühl. Vertical migration optimizes photosynthetic efficiency of motile cyanobacteria in a coastal microbial mat. *Frontiers in Marine Science*, 7:359, 2020.

Rezak R. Ginsburg R.N. Logan, B.W. Classification and environmental significance of algal stromatolites. *The Journal of Geology*, 72(1): 68–83, 1964.

Hazen Robert M. Nhleko Nontombi Noffke, Nora. Earth's earliest microbial mats in a siliciclastic marine environment (2.9 ga mozaan group, south africa). *Geology*, 34(4):253–256, 2006.

Nora Noffke, Daniel Christian, David Wacey, and Robert M Hazen. Microbially induced sedimentary structures recording an ancient ecosystem in the ca. 3.48 billion-year-old dresser formation, pilbara, western australia. *Astrobiology*, 13(12):1103–1124, 2013.

Christian Quast, Elmar Pruesse, Pelin Yilmaz, Jan Gerken, Timmy Schweer, Pablo Yarza, Jörg Peplies, and Frank Oliver Glöckner. The silva ribosomal rna gene database project: improved data processing and web-based tools. *Nucleic Acids Research*, 41(D1):D590–D596, 2013. doi: 10.1093/nar/gks1219.

Manvi Rawat, Mansi Chauhan, and Anita Pandey. Extremophiles and their expanding biotechnological applications. *Archives of Microbiology*, 206(6):247, 2024.

J. William Schopf. Microfossils of the early archean apex chert: New evidence of the antiquity of life. *Science*, 260(5108):640–646, 1993.

Kudryavtsev Anatoliy B. Czaja Andrew D. Tripathi Abhishek B. Schopf, J. William. Evidence of archean life: Stromatolites and microfossils. *Precambrian Research*, 158(3-4):141–155, 2007.

Caleb G Schuler, Jeff R Havig, and Trinity L Hamilton. Hot spring microbial community composition, morphology, and carbon fixation: implications for interpreting the ancient rock record. *Frontiers in Earth Science*, 5:97, 2017.

Cody S. Sheik, Brandi K. Reese, Kathryn I. Twing, Jason B. Sylvan, Sharon L. Grim, Matthew O. Schrenk, Mitchell L. Sogin, Frederick S. Colwell, Beth N. Orcutt, and Stefan M. Sievert. Identification and removal of contaminant sequences from ribosomal gene databases: lessons from the census of deep life. *Frontiers in Microbiology*, 9: 840, 2018. doi: 10.3389/fmicb.2018.00840.

Stefan M Sievert, Solveig I Bühring, Lara K Gulmann, Kai-Uwe Hinrichs, Petra Pop Ristova, and Gonzalo V Gomez-Saez. Fluid flow stimulates chemoautotrophy in hydrothermally influenced coastal sediments. *Communications Earth & Environment*, 3(1):96, 2022.

Lucas J Stal, Hans van Gemerden, and Wolfgang E Krumbein. Structure and development of a benthic marine microbial mat. *FEMS Microbiology Ecology*, 1(2):111–125, 1985.

Vladimir G. Tarasov and et al. Exploration of deep-sea hydrothermal vents. *Deep Sea Research Part II: Topical Studies in Oceanography*, 52(23-26):2260–2279, 2005.

Sung-Min Yoon, Seung-Beom Ha, Sojeong Kwon, Jongsik Lim, Young-Do Kim, Mincheol Kim, and Jongsik Chun. Introducing ezbiocloud: a taxonomically united database of 16s rrna gene sequences and whole-genome assemblies. *International Journal of Systematic and Evolutionary Microbiology*, 67(5):1613–1617, 2017. doi: 10.1099/ijsem.0.001755.

Chapter 4

4 Hot Springs and Shallow Vents as New Niche for Antibiotic Discovery

Ana Clara Pelliciari Silva[1], Benoit de Pins[1], Francesco Montemagno[1], Flavia Migliaccio[1,2], Martina Cascone[1], Deborah Bastoni[1], Bernardo Barosa[1], Matteo Selci[1,3], Costantino Vetriani[3,4], Agostina Chiodi[5], Federico A[6]. Vignale, Maria Garcia Alai[6], Alberto Vitale Brovarone[7,8], Gerdhard L. Jessen[9], Jenny M. Blamey[10], J. Maarten de Moor[11], Karen G. Lloyd[12], Peter Barry[13], Donato Giovannelli[1,3,4,14,15,16]

1- Department of Biology, University of Naples "Federico II", Naples, Italy

2- National Biodiversity Future Center, Palermo, Italy

3- Department of Marine and Coastal Science, Rutgers University, New Brunswick, NJ, USA

4- Department of Biochemistry and Microbiology, Rutgers University, New Brunswick, NJ, USA

5- CONICET Instituto de Bio y Geociencias del NOA (IBIGEO), Rosario de Lerma, Argentina

6- European Molecular Biology Laboratory - Hamburg Unit, Hamburg, Germany

7- Department of Biology and Geology, BIGEA, University of Bologna "Alma Mater Studiorum", Bologna, Italy

8- CNRS

9- Instituto de Ciencias Marinas y Limnológicas, Universidad Austral de Chile, Valdivia, Chile Centro de Investigación Oceanográfica COPAS COASTAL, Universidad de Concepción, Chile

10- Fundación Biociencia Universidad de Santiago de Chile

11-Observatorio Vulcanológico y Sismológico de Costa Rica, Universidad Nacional, Heredia, Costa Rica

12- Department of Earth and Planetary Sciences, University of New Mexico, Albuquerque, NM, USA

13- Earth Science Department, University of Southern California, Los Angeles, CA, USA

14- Marine Chemistry Geochemistry Department, Woods Hole Oceanographic Institution

15- National Research Council - Institute of Marine Biological Resources and Biotechnologies - CNR-IRBIM, Ancona, Italy

16- Earth-Life Science Institute, Tokyo Institute of Technology, Tokyo, Japan

Abstract

Microbial communities in geothermal environments constitute an underexplored reservoir of biosynthetic gene clusters with significant biotechnological potential. Here, we investigate the secondary metabolite potential of 219 microbial communities across marine and continental geothermal field sites, encompassing broad environmental gradients in temperature (4.7 °C to 93.5 °C), pH (0.85 to 10.3), and tectonic setting, includ-

ing convergent margins, divergent margins at mid-ocean ridges, and paleo-convergent intraplate plume systems. We identified 37,178 new biosynthetic gene clusters and demonstrated that volcanic arc systems consistently harbor the most biosynthetically diverse communities. Intraplate plume systems exhibit a terpene-enriched profile, with terpenes comprising 47 % of their biosynthetic repertoire, whereas divergent margins were dominated by nonribosomal peptide synthetases and ribosomally synthesized and post-translationally modified peptides pathways, together accounting for 64 % of their total potential. These findings position tectonics as a key driver of microbial secondary metabolism and offer a geobiological framework for guiding natural product discovery in extreme geothermal ecosystems.
Chapter partially available as a preprint in BioXirv:
doi.org/10.1101/2025.09.14.675129

4.1 Introduction

Microorganisms produce a vast repertoire of specialized (secondary) metabolites that mediate interactions with neighbouring cells and the surrounding environment and have profoundly impacted medicine and biotechnology (Sayed et al. [2020], Chen et al. [2020]). The genes encoding them are typically not required for the organism survival and growth, but confer critical adaptive advantages, for example, inhibiting competitors, scavenging nutrients, or tolerating stress, thereby enhancing the overall fitness of the producing organism (Chen et al. [2020]). Notably, natural products derived from microorganisms remain indispensable as drug leads; indeed, 70 % of clinically used anti-infectives originate from naturally occurring microbial metabolites (Berdy [2005]). Among these, many well-known antibiotics such as penicillin (from *Penicillium* spp.), streptomycin (from *Streptomyces griseus*), and vancomycin (from *Amycolatopsis orientalis*) are direct microbial products that have transformed clinical medicine (Fleming [1929], Kudo and Eguchi [2009]). Beyond anti-infectives, microbial metabolites also contribute to the food industry: for example, nisin, a bacteriocin produced by *Lactococcus lactis*, is widely used as a natural food preservative (Gharsallaoui et al. [2016]). Likewise, psychrophilic microorganisms have yielded enzymes with unique catalytic properties at low temperatures, such as cold-active lipases and proteases, which are valuable in dairy processing and biotechnology (Gerday et al. [2000]).

Biosynthetic gene clusters (BGCs) encode the enzymatic pathways that assemble specialized metabolites (Kwon et al. [2021]). Key classes of BGCs include those for nonribosomal peptide synthetases (NRPS), which encode siderophores and other metallophores (Le Govic et al. [2019]). These compounds serve dual ecological functions: in nutrient-limited systems they scavenge essential metals such as Fe, Cu, and Zn (Ghssein and Ezzeddine [2022], Ohlemacher et al. [2018]), whereas in metal-rich or toxic settings they chelate and detoxify excess metals (e.g., As, Cd, Hg) (Alexander et al. [2025], Avalon et al. [2024]), enabling microbial survival under contrasting geochemical regimes. Polyketide synthases (PKS) generate a wide spectrum of bioactive molecules, including many clinically important antibiotics (Chen et al. [2020], Le Govic et al. [2019]). Ribosomally synthesized and post-translationally modified peptides (RiPPs) encompass bacteriocins, lantibiotics, and archaeocins, which frequently act as antimicrobials that shape microbial communities, particularly in dense biofilms (Vagstad [2023], Hudson and Mitchell [2018], Li and Rebuffat [2020], Novotny Jr and Perry [1992]). It is worth highlighting archaeocins specifically, as they often exhibit remarkable stability under extreme environmental conditions such as high temperature and salinity (Besse et al. [2015], O'connor and Shand [2002]), making them relevant for biofilm formation in geothermal spring systems (Li and Rebuffat [2020],Besse et al. [2015]). Finally, terpene synthase clusters produce structurally diverse metabolites involved in signaling, membrane stabilization, and oxidative stress protection (Avalos et al. [2022]). Because terpenes are chemically stable and can persist in sediments, they might also serve as potential geobiological markers, linking modern microbial activity to ancient Earth environments and potentially offering insights into other planetary environments (Finkel et al. [2023], Thiago et al. [2018]). For instance, studies using Mars soil analogs, including those from the Atacama Desert, have demonstrated that complex microbial communities can persist under conditions analogous to extraterrestrial environments. These studies also suggest that terpene-related compounds may be detectable using advanced analytical techniques (Finkel et al. [2023], Aerts et al. [2020]).

Prior work has highlighted geothermal extremophiles as an untapped source of natural products (Barosa et al. [2023], Nagar et al. [2023]), with environmental stressors often correlating with enrichment of specific BGC classes in the microbiome: for example, chronic metal exposure favors NRPS-linked metallophores that detoxify metals (Nagar

et al. [2023]), whereas extremely acidic, heat-stressed systems dominated by few chemolithotrophs often show a dearth of large NRPS/PKS clusters (Liu et al. [2016], Tiquia-Arashiro and Rodrigues [2016]). These patterns suggest that BGC repertoires reflect the selective pressures of their environment. It is important to notice, however, that the geochemical landscapes in which microbial communities adapt to are not random but are firmly rooted in the geological settings from which they arise (Fullerton et al. [2021]). The mineral content, redox potential, temperature and ionic composition of each environment are shaped by underlying tectonic and geological processes, which in turn influence microbial community structure and function (Fullerton et al. [2021], Upin et al. [2023]).

Traditionally, the search for new BGCs (and the metabolites they encode) has focused on readily culturable organisms such as soil *Streptomyces* (Lee et al. [2020]). However, the continued emergence of drug-resistant pathogens and the frequent rediscovery of known compounds underscore the urgent need to access untapped biosynthetic diversity in less conventional sources (Miethke et al. [2021]).

Extreme environments have emerged as especially promising reservoirs of novel BGCs and chemistry (Andreani-Gerard et al. [2024]). Harsh conditions, for example, the desiccation and intense ultraviolet radiation of hyper arid deserts, immense pressures of deep-sea trenches, or the acidity of geothermal springs, impose unique selective pressures on resident microbial communities (Sayed et al. [2020]). There is now compelling evidence supporting this premise: extremophilic microbes have yielded a wealth of previously unknown natural products in the past decade (Amina and Lotfi [2024]). For instance, a recent review documented 186 new secondary metabolite structures isolated from 129 extremophilic strains collected between 2010 and 2018 (Sayed et al. [2020]). Among these discoveries are novel antimicrobial and cytotoxic compounds from desert actinomycetes, including 46 new molecules identified from Atacama Desert isolates alone (Andreani-Gerard et al. [2024]). Likewise, organisms from other extreme biomes, such as Antarctic soil communities and deep-sea sediments, have revealed extraordinary biosynthetic richness, often with little overlap to known chemical space (Medeiros et al. [2024]). Even archaeal lineages once thought devoid of secondary metabolism have been found to harbor BGCs in extreme settings: for example, *Heimdallarchaeota* and *Lokiarchaeota* from hypersaline microbial mats were recently shown to possess puta-

tively novel BGCs, expanding the phylogenetic range of natural product producers (Chen et al. [2020]).

In spite of the increasing evidence suggesting the high potential of extreme environments in harboring new biosynthetic pathways and metabolites, large scale BGCs surveys across diverse ecosystems are lacking. Advances in genomics and metagenomics are now enabling the systematic exploration of BGC potential in these inaccessible ecosystems (Du et al. [2023]). Many extremophiles remain uncultivated, but culture-independent genome mining approaches, including high-throughput sequencing of environmental DNA and reconstruction of metagenome-assembled genomes (MAGs), allow researchers to recover biosynthetic genes directly from environmental samples (Paoli et al. [2022]). Using these approaches, recent works explored the biosynthetic potential of microbiomes on a global scale, across terrestrial and marine environments (Nayfach et al. [2021], Paoli et al. [2022]) and in more localized settings such as the extreme microbial mats of Shark Bay (Chen et al. [2020]), Antarctic soils (Waschulin et al. [2022]), glacier-fed stream biofilms (Geers et al. [2025]), or the Tibetan Plateau extreme aquatic microbiomes (Cheng et al. [2024]). Geothermal environments are the source of a large number of active compounds and enzymes used in industry (Giordano [2020]). Despite this, we lack systematic investigations of the biosynthetic potential of geothermal systems and how the diversity of secondary metabolites is influenced by environmental factors.

Here, we address this knowledge gap by investigating the biosynthetic potential of global geothermal extreme environments. We combine comprehensive analyses of 219 microbial communities from marine and continental geothermal sites to map the diversity and distribution of BGCs across diverse tectonic settings. Our results show that the geological and geochemical complexity of geothermal systems translate into diversity of microbial natural products. This work lays a foundation for future bioprospecting efforts and expands our understanding of how Earth's subsurface drives chemical innovation in the microbial world.

4.2 Sample Location & Acquisition

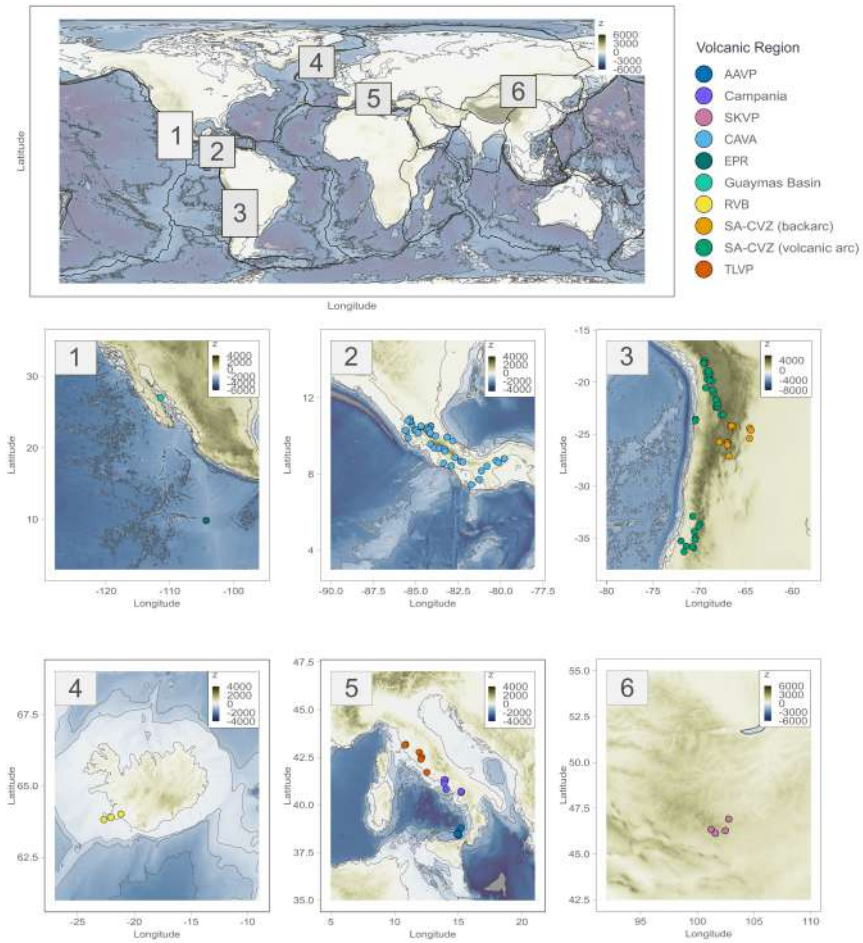

Figure 19: Geographic distribution of sampled geothermal extreme environments included in this study. Locations span diverse volcanic provinces in the Central America Volcanic Arc (CAVA), the Guaymas basin, East Pacific Rise (EPR), the South American Central Volcanic Zone (SA-CVZ), the Reykjkanes Volcanic Belt (RVB), the South Khangai Volcanic Province (SKVP) and the TLVP (Tuscan-Latium Volcanic Province), the Campania region, and the Aeolian Arc Volcanic Province (AAVP).

4.3 Methods

4.3.1 Sample acquisition and locations

The present work encompasses sampling campaigns spanning different tectonics settings distributed worldwide, and following a large-scale

sampling approach described in Giovannelli et al. [2022] (Figure 19). Environmental metadata and geological context were integrated based on the extended geochemical and tectonic framework outlined in Giovannelli et al. [2022], which emphasizes the role of deep subsurface inputs in structuring microbial communities. This broader context allowed us to systematically categorize geothermal sites by their underlying tectonic regime (backarc, volcanic arc, forearc, outer forearc and on axis ridges), facilitating standardized comparisons across disparate geographic regions.

At each site, the primary venting point was identified based on temperature and pH gradients in combination with visual cues (e.g., gas bubbling, mineral precipitates), as described by Giovannelli et al. [2022]. Fluids were collected directly from the venting orifice using silicone tubing attached to a portable peristaltic pump, and passed through Sterivex 0.22 μm cartridges (MilliporeSigma). Up to 2 L of hydrothermal fluid was filtered at each site. To preserve sample integrity for molecular applications, fluids were immediately filtered through 0.22 μm MilliporeSigma membranes and stored at –20 °C on-site. Subsamples of the filtered fluids were reserved for major ion analysis, and aliquots were stored in 12 mL gas-tight vials for δ^{13}C analysis of the dissolved inorganic carbon content. Samples were later maintained under controlled storage conditions to ensure the stability of microbial and geochemical features. Gas-phase and water samples for dissolved gases were collected in pre-evacuated 250 mL Giggenbach bottles containing 50 mL of 4 N NaOH, following the method of Stix and de Moor [2018], to minimize atmospheric contamination. Additionally, copper tubes were used to sample noble gases at each site, as detailed by Barry et al. [2022].

Sediment samples were collected in close proximity (within centimeters) to the fluid vents using sterile, acid-washed PTFE spatulas and transferred into 50 mL Falcon tubes. Sediment aliquots were also sampled for subsequent analysis of trace elements concentration and CNS content in each site. The use of PTFE spatulas was chosen to avoid metal contamination, as Teflon prevents the release of metals during sampling. Adjacent background soils were also sampled as controls (when present) from areas with no apparent geothermal influence, typically upsloping from the vent. Approximately 40–45 mL of sediment was transferred into 50 mL Falcon tubes. Collected sediment samples were immediately frozen at –20 °C and kept at this temperature during transport to the laboratory, where they were stored until further analyses. To

identify and count cells by using flow cytometry, we sampled both fluids and sediments into 2 mL cryovials, preserved them with 2 % formalin and stored at 4 ℃.
Physicochemical parameters of the fluids were measured in situ using a thermocouple and a multiparameter probe (HANNA, HI98196). The thermocouple was used to record pool temperatures directly at the main vent inlet. Freshly venting fluids were analyzed with the multiprobe, which measured pH, oxidation-reduction potential, specific conductivity, dissolved oxygen, and total suspended solids. For fluid temperatures exceeding 65℃, the maximum operating limit of the dissolved oxygen sensor, samples were cooled in a closed container prior to measurement. This cooling may have affected the accuracy of the dissolved oxygen readings, potentially resulting in overestimated values for high-temperature sites.

4.3.2 Geochemical analysis

In situ environmental parameters were recorded using a multiparametric probe (HANNA HI98196), field thermometer, and Fisherbrand™ refractometer. Core measurements included temperature, pH, conductivity, redox potential, dissolved oxygen, and total suspended solids. To characterize the ionic composition of geothermal fluids, we conducted ion chromatography (IC) on filtered water samples using a Metrohm ECO IC system, following the standardized procedures detailed in Correggia et al. [2024]. In the field, fluids were collected in acid-washed plastic containers and immediately filtered through 0.22 um membrane filters. To prevent contamination and ensure analytical accuracy, both filters and collection vessels were rinsed with sample fluid three times prior to use. Samples were stored at 4 ℃ and processed within recommended holding times depending on target analytes. For chloride preservation, ethylenediamine (EDA) was added in accordance with Jackson [2000], when applicable.
Cation and anion analyses were performed in separate runs using Metrosep C 4 and A Supp 5 columns, respectively. Samples were diluted with ultrapure water (typically 1:10) to maintain conductivity below 600 uS/cm, which is critical for optimal chromatographic resolution and column longevity. Where necessary, additional pretreatment steps were applied, such as silver ion exchange to reduce chloride interference and solid-phase extraction (C18) to remove excess organic compounds.

Chromatographic runs included a protective guard column, followed by the analytical column and conductivity detector. For anion analysis, chemical suppression was used to minimize background conductivity and enhance analyte signals. Retention times were matched against certified standards, and quantification was performed through multipoint calibration curves. This workflow allowed precise quantification of environmentally relevant ions (e.g., sulfate, chloride, sodium, potassium, calcium, magnesium), facilitating site comparisons and enabling downstream ecological interpretations 83. All samples were analyzed in technical triplicates, and quality control included routine injections of blank and standard reference solutions.

Concentrations of trace elements were determined by inductively coupled plasma mass spectrometry (ICP–MS) following the protocols described by Correggia et al. [2024]. Briefly, filtered and acidified hydrothermal fluid samples were analyzed on an Agilent 7900 ICP–MS equipped with a collision/reaction cell to minimize polyatomic interferences. Calibration was carried out using multi-element standards spanning 0.01–100 µg/L, with internal standards (e.g., Rh, In) added to correct for instrumental drift. Accuracy and precision were verified against certified reference materials and matrix-matched standards, ensuring reliable quantification even in high-salinity geothermal fluids. The procedure allows detection of trace metals of biological relevance (e.g., Fe, Mn, Co, Ni, Cu, Mo, W, V, As) at sub-ppb levels.

Gas composition analysis was performed at the Volcano Observatory of the Universidad Nacional de Costa Rica. Headspace gases (He, H_2, O_2, Ar, N_2, CH_4) were analyzed using an Agilent 7890a gas chromatograph equipped with two HP-molesieve columns (Agilent 19095P-MSO) maintained at 30 °C. Methane was detected with a flame ionization detector, while the remaining gases were quantified using thermal conductivity detectors. Following gas chromatograph analysis, the NaOH solution from the Giggenbach bottles was titrated with 0.1 N HCl to determine CO_2 content. The CO_2/CH_4 ratio was calculated by determining the total moles of CO_2 and CH_4 in each sample. Carbon isotope compositions (δ^{13}C) of gas samples were measured using a Picarro G2201-I analyzer, following acidification of the NaOH solutions extracted from the Giggenbach bottles. δ^{13}C values (reported in ‰ relative to the PDB standard) were calibrated against a set of eight reference standards ranging from +2.42‰ to 37.21‰, including internationally recognized standards such as NBS19 and Carrara Marble.

The analysis of carbon (C), nitrogen (N), and sulfur (S) content (expressed as percentages) was performed using a vario PYRO cube elemental analyzer (Elementar) operating in combustion mode. Samples were first dried at 70 ℃ for 48 hours and then homogenized using an agate mortar. Approximately 2–10 mg of the dried, ground sample was weighed into tin capsules, which were then loaded into the autosampler for CNS analysis. Sulphanilamide was used as the reference material for quantification. In the vario PYRO cube system, samples are combusted in a high-temperature combustion tube operating at 1150 ℃. The resulting gases are then passed through a reduction tube maintained at 850 ℃ and packed with copper, which facilitates the reduction of NO_x and SO_3. Following these reactions, the analytes are fully converted into their target gaseous forms: N_2, CO_2, and SO_2.

4.3.3 DNA extraction, metagenomic sequencing and BGC analysis

DNA was extracted with a combination of the DNeasy PowerSoil Kit (QIAGEN), and a modified phenol-chloroform DNA extraction method adapted for low biomass samples (Fullerton et al. [2021]). Sequencing was carried out by NOVOGENE using Illumina MiSeq platforms. For all the campaigns used here, the same metagenomics pipeline was used to ensure uniformity of the data. We applied therefore the GEOMOSAIC pipeline (github.com/giovannellilab/Geomosaic), made to integrate state of art metagenomic softwares for analysis. Briefly, all the raw reads were trimmed using fastp, set to default parameters. The trimmed reads were then assembled using metaSPAdes (v. 3.15.5) (Nurk et al. [2017]), with k-mers -k 33, 55, 77, and 127, and filtering for minimum contig length of 2000 base pairs. Read mapping to the assemblies was carried out using Bowtie2 (v. 2.5.4) (Langmead and Salzberg [2012]) set to default parameters. Gene coverage was obtained by using hidden Markov model search as implemented in GEOMOSAIC.
All the generated 219 assemblies were analyzed with antiSMASH 7.0 (Blin et al. [2019]), using default settings, including KnownClusterBlast/MIBiG (Minimum Information about a Biosynthetic Gene cluster) 4.0 (Terlouw et al. [2023]) matching and the product/substrate prediction modules to investigate the richness of biosynthetic potential in geothermal environments. AntiSMASH detects BGC classes by rule-based domain profiling and, when possible, predicts candidate product scaffolds. Each BGC

was compared against the MIBiG repository of experimentally characterized clusters; we report the best MIBiG hit of some terpene BGCs in Figure 20. Results were combined into a single feature table and imported in R (v. 4.3, R Core Team 2024). The subsequent statistical analyses, data processing and plotting were carried out using the phyloseq package (McMurdie and Holmes [2013]), vegan (Oksanen et al. [2013]), and ggplot2 (Wickham [2011]) packages. Alpha diversity of BGCs was quantified using Shannon's diversity index, calculated from antiSMASH-derived BGC profiles. Differences among tectonic settings (volcanic arc, backarc, post-subduction) were tested with the Kruskal–Wallis test followed by pairwise Wilcoxon rank-sum tests with Benjamini–Hochberg correction. To test for differences in BGC repertoires, we calculated unweighted and weighted Jaccard distance matrices. Ordination was performed using principal coordinate analysis (PCoA), and community-level differences among groups were assessed using analysis of similarities (ANOSIM). In addition to our PCoA, k-means clustering of ordination scores was used to identify data-driven sample clusters. Environmental vector fitting (envfit) was then applied to the PCoA to identify the geochemical variables most strongly correlated with cluster structure. To assess how continuous environmental variables (e.g., temperature, pH, sulfate, crustal thickness) explain variation in BGC profiles, we used permutational multivariate analysis of variance (PERMANOVA, adonis2) based on Jaccard distances. Prior to analysis, conductivity (spc), chloride, and sulfate were $\log_{10}$-transformed to reduce skew. Finally, differences among clusters in individual environmental variables were tested using the non-parametric Kruskal–Wallis test with Dunn's post hoc comparisons and Benjamini–Hochberg correction.

4.4 Results

We analyzed metagenomic assemblies from 219 geothermal features across ten major volcanic provinces, summarized in Figure 19. These include environments in present-day convergent tectonics settings, including volcanic arcs (e.g., the South American Central Volcanic Zone (SA-CVZ), Central America Volcanic Arc (CAVA), and Aeolian Arc Volcanic Province (AAVP)), adjacent back-arc regions (e.g., part of the SA-CVZ), and transitional post-subduction extensional arcs (Campania, southern Italy and the Tuscan-Latium Volcanic Province, (TLVP) in central Italy); plume-influenced mid-ocean ridge settings (Reykjanes

Volcanic Belt, RVB); intracontinental magmatic systems in paleoaccretionary environments in the South Khangai Volcanic Province (SKVP); and deep-sea vents in the Guaymas basin and the East Pacific Rise (EPR) (Figure 19). BGCs predicted from these metagenomes revealed distinct patterns linked to tectonic context and geochemical regimes (Figure 20). Thus, volcanic arc samples preferentially occupy distinct clusters from those of back-arc, post-subduction extensional volcanics, and mid-oceanic ridge (MOR) spreading systems. This structure held across both unweighted and weighted ordinations (ANOSIM, unweighted Jaccard: $R = 0.7$, $n = 219$, $p \leq 0.001$; weighted Jaccard: $R = 0.5$, $n = 219$, $p \leq 0.001$), showing that the geothermal systems located in diverse tectonic systems differ both in the most abundant BGCs as well their overall biosynthetic potential (Figure 20 and Supplementary Supplementary Figure 26).

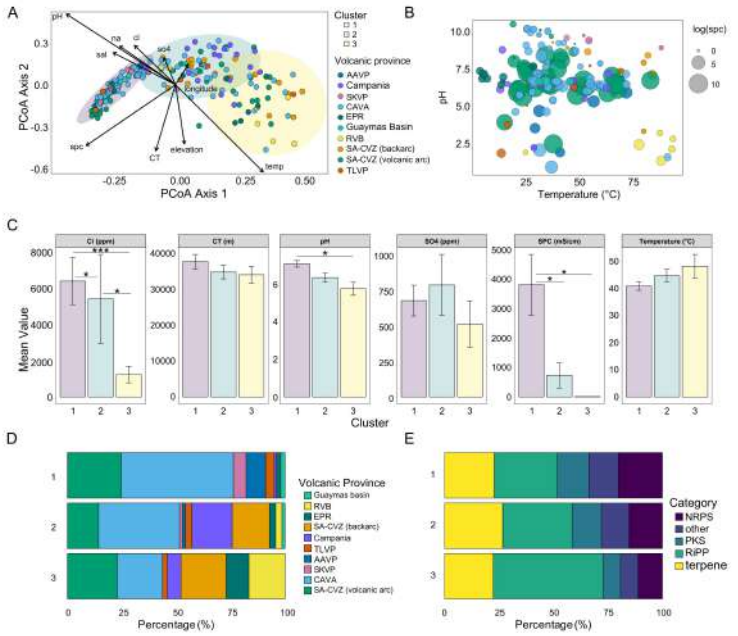

Figure 20: Biosynthetic gene cluster (BGC) composition across geothermal sites. (a) Principal Coordinates Analysis (PCoA) based on unweighted Jaccard similarity of BGC presence/absence across samples. Cluster 1: majorly composed of subduction-driven volcanic arc geothermal sites, Cluster 2: subduction-driven volcanic arc and a strong presence of SA-CVZ backarc sites. Cluster 3: diverse tectonic settings such as backarc, volcanic arc, along with a notable share of on-axis MOR settings. vari Points are colored by volcanic province of origin: CAVA (Central American Volcanic Arc), SA-CVZ (South American Central Volcanic Zone), RVB (Reykjanes Volcanic Belt), TLVP (Tuscan-Latium Volcanic Province), AAVP (Aerolian Arc Volcanic Province), Campania region, SKVP (South Khangai Volcanic Province), the Guaymas basin, and the EPR (East Pacific Rise). Arrows represent environmental variables (e.g., pH, temperature, salinity, conductivity (spc), crustal thickness (CT), elevation, Cl- content, SO4 content, longitude and latitude) fitted post hoc using envfit; arrow length and direction indicate strength and orientation of correlation with ordination space. Colored convex hulls illustrate the spatial distribution of three k-means clusters, used here to highlight compositional similarities. (b) pH as a function of temperature scatter plot. Size of samples are correlated with their log conductivity values (spc), and coloured by volcanic province of origin. (c) Environmental variables by cluster. Mean ± standard error (SE) values are shown for six key environmental parameters across microbial community clusters (1–3). Colors represent cluster identity: pale yellow (Cluster 1), pale teal (Cluster 2), and pale purple (Cluster 3). Statistical differences were tested using the Kruskal-Wallis test followed by Dunn's post-hoc comparisons with Benjamini-Hochberg correction. Asterisks indicate significant pairwise differences between clusters (*$p \leq 0.05$, **$p \leq 0.01$, ***$p \leq 0.001$). (d) Volcanic province origin across tectonic clusters. Stacked horizontal bar plots show the proportion of each volcanic province represented within each k-means-derived cluster. (e) Relative abundance of major BGC classes across sample clusters defined by unweighted Jaccard distances, reflecting presence/absence of biosynthetic profiles. Cluster 1 (volcanic arc majorly) exhibits a more even distribution across BGC classes, with notable enrichment in NRPSs (nonribosomal peptide synthetases). Cluster 2 (backarc and volcanic arc majorly) shows a higher relative proportion of terpenes and RiPPs (ribosomally synthesized and post-translationally modified peptides), in comparison to the remaining categories of secondary metabolites. Cluster 3 (rich in on-axis MOR) is dominated by RiPPs with minor contributions from terpenes, NRPSs, and PKSs (polyketide synthases).

Three major environmental clusters were identified, each aligned with different geochemical profiles and tectonic regimes (Figure 20a).

Cluster 1, was dominated by volcanic arc samples (90 %) along the primary geochemical gradient (Figure 20a). CAVA samples contributed the most (51.4 %), followed by the volcanic arc of the SA-CVZ at 24.8 %, AAVP at 8.9 %, TLVP at 3.9 %, and Campania at 1 %. In addition, 6 % of the samples come from the SKVP, and the young spreading system of the Guaymas Basin and EPR contribute 2 % each. This cluster was associated with higher pH, electrical conductivity (spc), and crustal thickness (CT) values (Figure 20b-c). Cluster 2, which occupied the central portion of the ordination, was associated with elevated sulfate concentrations and was also primarily composed of volcanic arc samples (73.8 %). However, its internal composition differed from that of Cluster 1. CAVA remained the main contributor (37 %), but Campania samples show a stronger presence (18.6 %), equaled by the SA-CVZ backarc, also at 17.6 %. TLVP contributes 2.9 %, while AAVP, SKVP and the Guaymas Basin contribute 1.3 % each. EPR contribution rises by 1 % in comparison to Cluster 1 (3 %). Notably, the proportion of SA-CVZ volcanic arc samples show a 10.8 % decrease compared to Cluster 1 (14 % vs. 24.8 %). The remaining 3 % of the samples come from the RVB. Cluster 3, located on the far right of the ordination along the primary geochemical gradient, is characterized by a stronger presence of volcanic provinces associated with divergent tectonic margins. The RVB accounts for 16.6 % of the sample pool, the highest among divergent settings, and EPR samples account for 10.4 %. Despite this, volcanic arc provinces related to convergent margins still dominate the cluster. The SA-CVZ volcanic arc contributes 23 % to the sample pool, CAVA and the SA-CVZ backarc contribute 21 % each. Campania contributes 6 %, and the TLVP adds 2 %. Overall, there is a noticeable decrease in the proportion of volcanic arc samples from Cluster 1 to Cluster 3, dropping from 90 % to 52 %. Cluster 3 aligns closely with high-temperature environments, suggesting it includes predominantly sites that could host thermophilic microbes.

We next examined the biosynthetic composition across clusters, focusing on the relative abundance of BGCs. Cluster 1 showed the highest representation of nonribosomal peptide synthetases (NRPSs), accounting for 20 % of its BGC pool, compared to 15 % in Cluster 2 and 12 % in Cluster 3. Terpenes were most abundant in Cluster 2 (27 %), followed by Cluster 1 (23 %) and Cluster 3 (22 %). Ribosomally synthesized and post-translationally modified peptides (RiPPs) were the most dominant BGC category across all clusters, forming more than half of the BGC

pool in Cluster 3 (51 %), and representing 32 % and 29 % in Clusters 2 and 1, respectively. Polyketide synthases (PKSs) were less prevalent, contributing 14 % in Cluster 1, 13 % in Cluster 2, and only 8 % in Cluster 3. The remaining BGCs, which included hybrid BGCs, rare or unusual RiPPs that have not yet been fully categorised or recognised and BGC fragments that do not contain enough hallmark genes for a confident type call, grouped as "Other," comprised 14 % of Cluster 1, 13 % of Cluster 2, and 7 % of Cluster 3 (Figure 20).

Among the environmental variables tested, crustal thickness (CT) explained the largest proportion of variance in BGC profiles (PERMANOVA, Jaccard distance; R^2 = 0.8, F = 1.4, $p \leq 0.001$; Supplementary Figure 27 a), followed by temperature (R^2 = 0.7, F = 1.5, $p \leq 0.001$; Supplementary Figure 27 b) and pH (R^2 = 0.6, F = 1.6, $p \leq 0.001$; Supplementary Figure 27 c). When analysing samples in active convergent margins, volcanic arc geothermal systems exhibit greater diversity in comparison to backarc and post-subduction extensional arcs (volcanic arc: 2.18 $\pm$ 0.69; backarc: 1.85 $\pm$ 0.57; post-subduction extensional arcs: 1.88 $\pm$ 0.41; Kruskal–Wallis ^{2} = 17.35, p = 1.7 $\times$ 10^{-4}, Supplementary Figure 28). The strong, non-linear underlying environmental gradient driving the differences between samples is reflected in this classic visual artifact (i.e., horseshoe-shaped pattern) observed in the PCoA ordination. Specifically, the gradient separates samples from metal-rich subduction zone arc volcanoes at one end, to high temperature/silica-rich mid-ocean ridge environments at the other, underscoring the influence of geological/tectonic setting in shaping microbial biosynthetic potential.

4.5 Discussion

4.5.1 BGCs, geology and geochemistry

The extreme conditions and metal bioavailability in geothermal systems not only select which microbes thrive (Basili et al. [2024]), but also the BGC repertoire those communities harbor. In our study, geothermal systems of volcanic arcs in subduction zones exhibit high potential for microbial BGC richness (Cluster 1, Figures 20, Supplementary Figure 28). This is exemplified by Cluster 1, which consists of over 90 % volcanic arc samples from active convergent margins and contains a diverse BGC pool. The SA-CVZ volcanic arc can serve as an example and accounts for 25 % of samples within Cluster 1. Here, deeply sourced springs fed

by surrounding arc volcanism carry waters with high arsenic concentrations (often $>$ 1 mg/L, Supplementary Table 2) derived from arc geothermal inputs (Romero et al. [2003]), along with several metals (e.g., Sb, Cu) mobilized by magmatic fluids (Tapia et al. [2021]). Despite the toxicity, the resident microbial community in the hot springs of the SA-CVZ volcanic arc is metabolically rich (Castro-Severyn et al. [2021]). This is consistent with our metagenomic surveys of microbial BGC potential in volcanic arcs exhibiting broad BGC diversity (Supplementary Figure 28). In the AAVP, geothermal fields likewise produce acidic, sulfur-rich emissions with significant heavy metal enrichment in Cu, Zn, Hg, and Co (Bargagli et al. [1991]). Accordingly, the microbial communities from volcanic arc springs reveal significantly higher NRPS prevalence compared with all other sites (Figure 21), suggesting prolific metallophore production and metal-microbe interactions in this environment (Zelaya-Molina et al. [2025]).

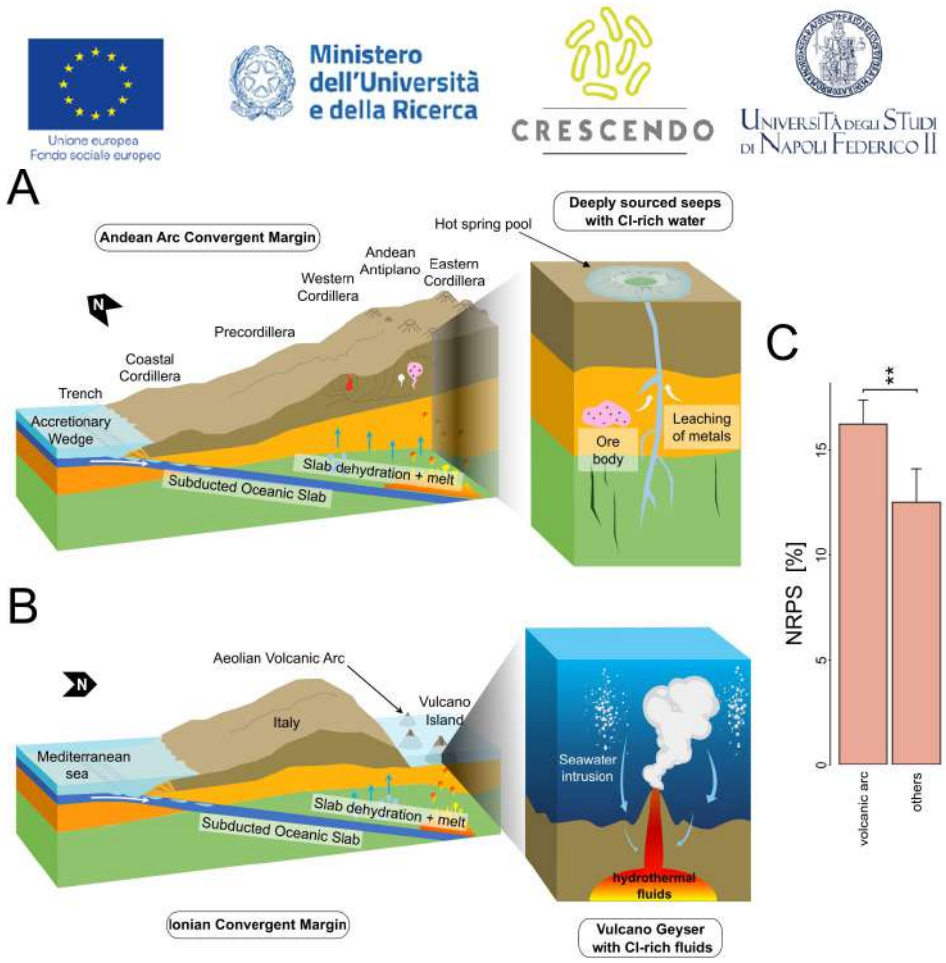

Figure 21: Schematic representation of volcanic arcs at convergent margins and their influence on microbial biosynthetic potential. (a) Schematic representation of the SA-CVZ (South American Central Volcanic Zone) volcanic arc and its influence on microbial biosynthetic potential. On the macro scale, the steeply dipping oceanic slab dehydrates, releasing Cl-enriched fluids from altered oceanic crust. These fluids migrate upward through faults and fractures in the continental crust. Metal leaching in these environments favor NRPS-rich (nonribosomal peptide synthetases) microbial communities. Macro-scale cross-section of the SA-CVZ adapted from (Tapia et al. [2021]) (b) Schematic of the Ionian convergent margin tectonic system and its role in shaping microbial biosynthetic potential in the AAVP (Aeolian Arc Volcanic Province). The subduction of the Ionian slab beneath the Aeolian Arc fuels arc magmatism and geothermal activity across southern Italy, and enhances mantle input in hydrothermal fluids. Beneath Vulcano Island, CO2 and chloride-bearing fluids ascend through permeable structures, mixing with meteoric water or seawater to form acidic, and metal-rich environments, selecting for a microbiome capable of withstanding heavy metal toxicity. Cross-section of the Vulcano Geyser adapted from Rizzo et al. [2022]. (c) At the microbiological level, volcanic arc microbiomes carry a biosynthetic gene cluster repertoire rich in NRPS, that support survival through metal chelation and detoxification. The bar plots show the per-sample relative abundance of NRPS BGCs (number of NRPS contigs divided by the total number of BGC contigs in each sample, expressed as %) in 125 volcanic arc samples versus the remaining 87 samples within active plate tectonic settings. Differences between the two groups ("volcanic arc" vs "others") were evaluated with the non-parametric two-sided Wilcoxon rank-sum (Mann–Whitney U) test. Significance is coded as $p \leq 0.05$ (*), $p \leq 0.01$ (**).

4.5.2 Metal-Poor Volcanic Fluids Drive Terpene-Enriched BGC pool

The metagenomic BGC profile of backarc sites is accordingly less diverse (Supplementary Figure 28), and specialized in terpenes com-

pared to other sites (Figure 22). High levels of terpenes might suggest a specific strategy of membrane fortification and stress quenching mechanisms (Simon et al. [2025]). A comparable trend is observed in the shallow degassing system of the Campi Flegrei in the Campania region in Italy,where shallow CO_2 degassing can reach up to 4000–5000 tones per day (Cardellini et al. [2017]), and the Solfatara crater and surrounding fumaroles (e.g., Pisciarelli) continuously emit CO2-rich, sulfurous fumes (Cardellini et al. [2017]). Despite such geochemical harshness, cultivation efforts have yielded spore-forming isolates (e.g., *Alicyclobacillus mali* from Pisciarelli mud) whose genomes encode enzymes for unusual isoprenoid terpene biosynthesis (Aulitto et al. [2021]). It is worth highlighting this cultivation evidence aligned with our metagenomic data from these Campania systems, which similarly reveals abundant terpene biosynthetic clusters (Figure 22). Both the SA-CVZ backarc and Italian Campania cases illustrate that when volcanic systems skew toward high volatile (CO_2 and H_2S) flux and away from direct input of metal-rich magmatic fluids, microbial secondary metabolism might shift toward a terpene-enriched repertoire.

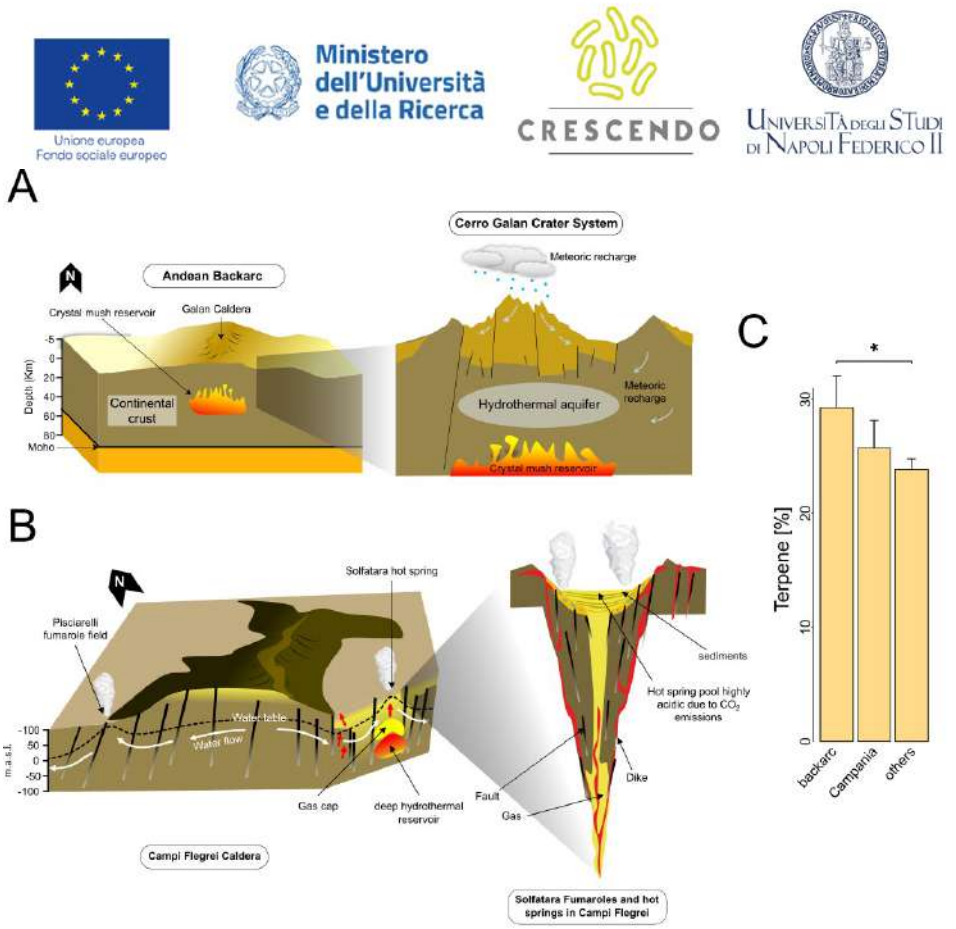

Figure 22: Schematic representation of backarc and post-subduction extensional volcanic systems in active plate tectonic settings and their influence on the microbial biosynthetic potential. (a) Schematic representation of the Galán system in the SA-CVZ (South American Central Volcanic Zone) backarc and its influence on the local microbial biosynthetic potential. The Galán Caldera overlies a large crystal mush reservoir within the continental crust. In contrast to volcanic arcs, backarc systems experience fewer direct discharge of magmatic gases to the surface and therefore are more scarce in the primary metal-rich fluids associated with direct magmatic degassing. They are majorly controlled by the hydrothermal circulation of deep hydrothermal reservoirs, receiving less direct input from the subducting slab, and hence their fluid chemistry is comparatively restricted. Accordingly the BGC potential diversity is lower and specialised in terpenes, likely involved in membrane stabilization. Geological and regional scale cartoons were adapted from Chiodi et al. [2024]). (b) Schematic representation of Campi Flegrei Caldera (post-subduction extensional arc), in the Campania region, Italy; "m.a.s.l." refers to meters above sea level. At the macro scale, Campi Flegrei is influenced by a deep hydrothermal reservoir within the continental crust. The system is high in volatiles such as CO_2 and H_2S. These conditions support microbial communities adapted to high acidity, elevated CO_2, and sulfide concentrations. Cross sections adapted from Isaia et al. [2021]) (c) At the microbiological level, the BGC potential in backarc systems and Campania is high in terpenes, which may aid in stress tolerance, cellular protection, and adaptation to volatile-rich environments. The bar plots show the per-sample relative abundance of terpene BGCs (number of terpene contigs divided by the total number of BGC contigs in each sample, expressed as %) in 34 backarc samples, versus 17 Campania samples and the remaining 161 samples within active plate tectonic settings. Group differences in terpene proportions were evaluated with the non-parametric two-sided Wilcoxon rank-sum (Mann–Whitney U) test. Significance is coded as p $\leq$0.05 (*), p $\leq$ 0.01 (**).

4.5.3 Microbial strategies for metal homeostasis and competition in Mid-Ocean Ridge Ecosystems

Tectonic settings at spreading centers, such as at mid-ocean ridges (MORs), generate biosynthetic profiles distinct from both volcanic arcs and backarc systems. In the RVB, geothermal fields like Gunnuhver lie directly atop the Mid-Atlantic Ridge, tapping basaltic magmas and mantle-derived volatiles. At Gunnuhver, subsurface temperatures reach 290 ℃, with localized zones exceeding 300 ℃ (Fridriksson et al. [2006]). Previous studies of (plume influenced) Icelandic solfataric fields have reported enrichment in RiPPs, such as archaeocins (Besse et al. [2015]), and our RVB hot spring microbiomes likewise show the highest relative abundance of both RiPP and NRPS pathways (Supplementary Figure 29), together accounting for 64 % of their total BGC pool. The prevalence of RiPP BGCs suggests that antimicrobial production plays an important role in these communities: many thermophiles produce heat-stable bacteriocins and related peptides that help maintain competitiveness within dense biofilm assemblages coating sinter deposits in hot springs (Li and Rebuffat [2020], Novotny Jr and Perry [1992]). The NRPS enrichment likely reflects a dual adaptation to the environment of MOR hot springs where basalt-hosted fluids are indeed enriched in metals such as Fe, Cu, Zn, and various trace elements, primarily due to intense fluid-rock interaction and magmatic degassing at depth (Zeng et al. [2021], Saby et al. [2022]). However, the bioavailability of these metals is highly variable, largely because of rapid mineral precipitation, which removes metals from the fluid phase as the fluids ascend and cool (Saby et al. [2022], Clark et al. [2020]). In this context, NRPS metallophores may serve a dual role: scavenging essential trace nutrients under limitation (Alexander et al. [2025], Avalon et al. [2024]), and detoxifying excess metals when concentrations become inhibitory (Kraemer et al. [2015], Gomes et al. [2024]). The resulting BGC profile thus can represent a strategy shaped by MOR geochemistry, which creates a complex system for metal bioavailability (Zeng et al. [2021], Saby et al. [2022], Allen and Seyfried Jr [2005]).

Overall, our findings suggest that tectonic setting exerts a strong influence on microbial biosynthetic repertoires. The volcanic arc BGC potential is enriched in NRPS pathways that respond to magmatic metal inputs, while backarc systems, especially those located at high elevation, are characterized by less diverse, stress-adaptive terpenoid metabo-

lites. In divergent settings such as MOR, the tilt toward NRPS- and RiPP-dominated profiles likely reflects strategies for metal scavenging and microbial competition. Thus crustal thickness, which emerged as the strongest environmental correlate of BGC variation, might be understood as a geophysical proxy for the diverse tectonic regimes investigated in this study. By influencing magmatic differentiation (Alasino et al. [2022]), pressure of mineral stabilization (Tang et al. [2020], Park et al. [2021]), and fluid-rock interaction pathways (Filiberto et al. [2023]), crustal thickness indirectly structures the chemical and thermal conditions that subsurface microbial communities experience in geothermally influenced ecosystems. The strong crustal thickness–BGC diversity signal reinforces that large-scale geodynamic context, rather than any single physicochemical factor, underlies the observed patterns in microbial biosynthetic potential.

4.5.4 Microbial terpenes as potential biosignatures in modern and ancient geothermal systems

While our analysis focuses on broad-scale patterns in BGC abundance and composition, we observed notable structural diversity within terpene biosynthetic clusters across the sampled sites. Gene clusters from multiple volcanic provinces and tectonic settings encode a wide range of predicted products, including carotenoids, sesterterpenes, and smaller cyclic terpenes such as pristinol and sodorifen (Figure 23), many of which hold potential as molecular indicators of past life and environmental conditions (Finkel et al. [2023]). Although most biomarker applications to-date rely on plant-derived terpenes (e.g., triterpenoids) preserved in sedimentary archives from the mid-Paleozoic onwards (Nakamura [2019], Pańczak et al. [2023]), recent work has highlighted the presence of microbial terpenes in modern and ancient hydrothermal deposits (Summons et al. [2022], Finkel et al. [2023]).

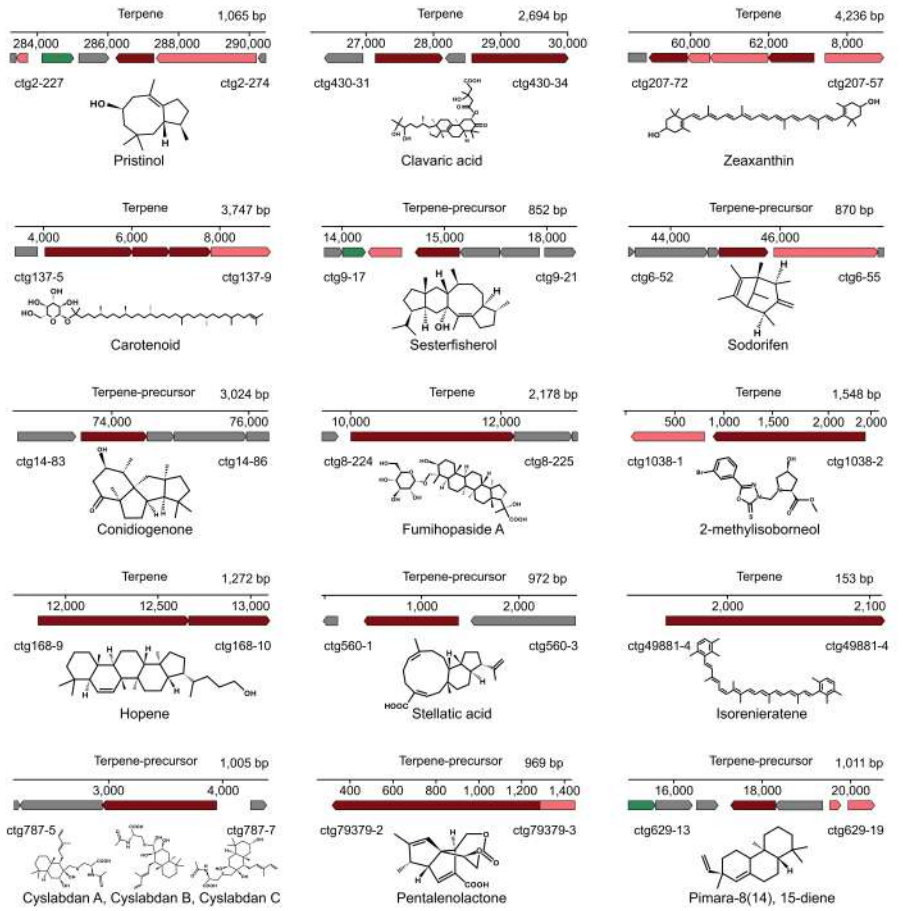

Figure 23: Variety of terpene biosynthetic gene clusters (BGC) present within our geothermal samples, demonstrating the variety of potential biomarkers. Genes are colored by predicted function: red for core biosynthetic genes, pink for accessory biosynthetic, green for regulatory, and grey for non-biosynthetic or unknown function. The first and last genes in each BGC are labeled.

Fossilized microbial lipids, including terpenes, serve as molecular fossils (biomarkers) that show the history of microbial life on Earth (Summons et al. [2022], Jia et al. [2016]). For example, carotenoids (a subset of terpenes) in ancient sediments are used to infer the presence and ecological roles of phototrophic microbes in past environments (Meyer et al. [2011]). The structural diversity and recurrence of microbial terpene BGCs in our geothermal samples reinforces the view that these compounds could serve as biomarkers not only in modern geothermal

environments but also in ancient settings where microbial biomass dominated, as already suggested by Avalos et al. [2022], Finkel et al. [2023]). As very early Earth environments were often geothermal (Nisbet and Sleep [2001], Westall et al. [2018]), the rich terpene diversity present today in these systems may reflect a long-standing association between geothermal activity and microbial terpene biosynthesis (Kompanichenko [2017], Kietäväinen et al. [2025], Álvaro et al. [2021]). It is also worth remarking that the biosynthetic pathways for terpenoids are equally ancient and widespread among microorganisms (Kuzuyama [2017], Zhang et al. [2023]). If preserved in the rock record, microbial terpenes extend the application beyond the plant-derived molecules typically used, broadening both the range of environments and the geological time periods that can be reconstructed (Finkel et al. [2023]).

Among our sites, the SKVP stands out as particularly relevant for the study of palaeoenvironments and the preservation of microbial biosynthetic signatures on Earth and potentially beyond. These hydrothermal systems are linked to Late Cenozoic intraplate volcanism driven by mantle plume–lithosphere interaction, which generated widespread volcanic centers and elevated regional heat flow (Savatenkov et al. [2010], Windley and Allen [1993]). Unlike hydrothermal systems at convergent margins, the SKVP is hosted in a tectonically inactive, paleo convergent, intracontinental plume setting but still shows evidence of long-lived geothermal activity and elevated regional heat flow (Rychkova and Kalnaya [2023]). Geothermal springs in the region are largely fed by meteoric waters, and there is minimal evidence for the contribution of magmatic gases or metals, which contrasts with present-day subduction-related hydrothermal systems where such inputs diversify the chemistry of the fluids (Oyuntsetseg et al. [2015], Meng et al. [2018]).

Continental plume volcanism has been hypothesised in other planetary bodies (Broquet and Andrews-Hanna [2022], Broquet and Andrews-Hanna [2023], Fuller and Head Iii [2003]) and directly inferred on Mars (Broquet and Andrews-Hanna [2023]). These systems could offer prolonged heat sources that might have potentially sustained subsurface hydrothermal habitats even as surface waters waned (Crandall et al. [2021]). The SKVP plume-heated, meteoric-fed springs (Figure 24a) thus might provide a terrestrial analogue for such environments, emerging as an intraplate-hosted simple hydrothermal circuit, driven by volcanic heat but with limited magmatic metal flux.

Interestingly, our analysis of the SKVP geothermal sites revealed the

strongest terpene enrichment across our global dataset (47 %), a value nearly double that observed in tectonically active convergent margins at volcanic arcs, where terpene contributions never exceeded 25 % (Figure 24b, Supplementary Figure 29). Comparable enrichments in terpenes and volatile organic compounds have also been documented in the Outokumpu deep drill site in Finland, which is hosted within a paleoserpentinized ultramafic complex, emplaced and metamorphosed during the Svecofennian orogeny (Kietäväinen et al. [2025]). The recurrence of terpene-dominated signatures in inactive plate tectonic locations either plume-related (e.g SKVP), or ancient intraplate settings (e.g Outokumpu) might suggest that long-lived hydrothermal circulation with limited magmatic metal inputs can foster modern microbial communities that preferentially invest in membrane-protective and stress-mitigating terpene pathways. Such parallels point to the potential persistence of terpene biosynthetic strategies in hydrothermal systems over geological timescales, as terpene signatures can be constantly present even if plate tectonics ceases.

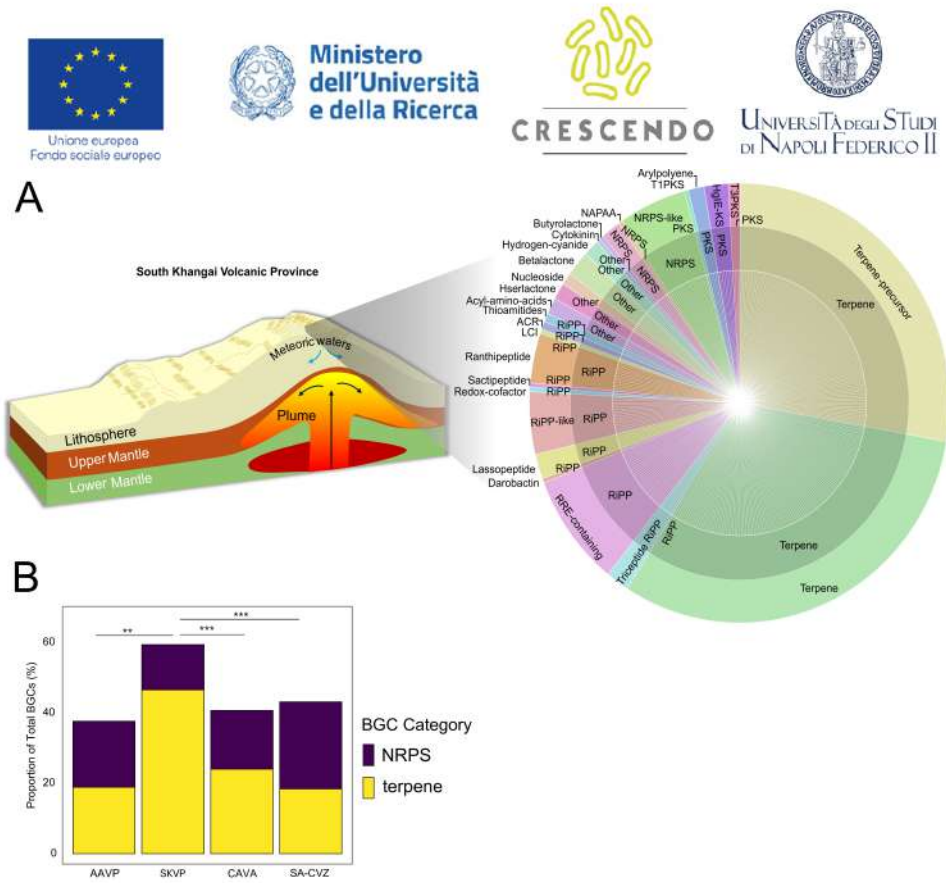

Figure 24: Geological context and distribution of biosynthetic gene clusters (BGCs) across the South Khangai Volcanic Province (SKVP). (a) Conceptual cross-section of the plume–lithosphere interaction in the SKVP, modified from Savatenkov et al. [2010], where meteoric waters circulate through the lithosphere sitting above a mantle plume. The adjacent donut plot depicts the diversity of BGC categories recovered from a representative SKVP metagenome (Taragat hot spring), with each segment corresponding to a contig. Terpene and terpene-precursor BGCs dominate the biosynthetic repertoire. The full list of BGCs present in this site is available in Supplementary Table 3. (b) Proportions of NRPS (nonribosomal peptide synthetase) and terpene BGCs across different volcanic provinces: AAVP (Aeolian Arc Volcanic Province, n=10), SKVP (n=7), CAVA (Central American Volcanic Arc, n=88), and SA-CVZ volcanic arc (South American Central Volcanic Zone, n=46). Significant differences in BGC proportions amongst volcanic provinces evaluated with the non-parametric two-sided Wilcoxon rank-sum (Mann–Whitney U) test. Significance is coded as p $\leq$0.05 (*), p $\leq$ 0.01 (**), p $\leq$ 0.001(***).

The enrichment of terpene biosynthetic clusters in the SKVP plume-related geothermal systems highlights a functional contrast with the active convergent margin tectonics of volcanic arcs, where NRPS pathways dominate (Figure 42). In arc settings such as the SA-CVZ, CAVA, and AAVP, hydrothermal fluids are directly influenced by magmatic degassing (Kleint et al. [2019]), and subducting slab metal input (Castillo

[2023]). Under these conditions, NRPS systems provide a selective advantage by producing metal-binding metabolites that mitigate toxicity (Carroll and Moore [2018], Alves et al. [2022]), Similar NRPS enrichment is observed in other tectonically active volcanic settings, such as the Kolumbo submarine volcano (Santorini) (Bourbouli et al. [2015]), shallow-water hydrothermal vents in the Azores (Ramasamy et al. [2020]), and the Barren Islands volcanic arc in Southeast Asia (Meena et al. [2019]). In contrast, the SKVP hot springs are primarily fed by meteoric waters circulating through the continental crust, with limited magmatic input but constant heat-flux from remnants of the intraplate plume. Here, other environmental factors, such as the local thermal regime and the arid, high altitude desert like nature of the region, might favor the protective and stabilizing functions of terpenes (Gershenzon and Dudareva [2007]). These compounds are well-suited to mitigate oxidative stress (Borisov et al. [2021], Bosak et al. [2008]), maintain membrane integrity under variable temperature and pH conditions (Willdigg and Helmann [2021], Hoshino and Villanueva [2023], Santana-Molina et al. [2022]), and enhance UV protection (Avalos et al. [2022]). Thus, intraplate inactive tectonic systems hosting residual geothermal activity have the potential to foster microbial communities that harbor terpene-enriched strategies of stress resilience, in contrast to the NRPS-driven metal response typical of volcanic arcs in active convergent margins of subduction zones.

4.6 Conclusion

Altogether, understanding how geological processes shape microbial secondary metabolism over large planetary scales not only sheds light on microbial adaptation on Earth but also informs on planetary biosignatures exploration. Our results exemplify how the large-scale geological context can influence the natural product potential of regional microbiomes, positioning tectonics as a fundamental yet underexplored driver of microbial BGC repertoires and biosynthetic signatures (Figure 25). Future efforts to map microbial function at the planetary scale will further increase our understanding of the extent of tectonics influence, may expand the repertoire of known microbial natural products, and even refine molecular tools for reconstructing ancient environments on Earth and other planets that undergo plate tectonics.

Figure 25: Schematic cross-section of representative tectonic regimes and associated geothermal systems in this study, illustrating large-scale geodynamics shaping microbial biosynthetic gene cluster (BGC) diversity. In volcanic arcs, fluids sourced from subducting slabs and magmatic degassing support NRPS-linked (nonribosomal peptide synthetases) to metallophore production. Back-arc springs, with reduced direct magmatic input, shift toward stress-adaptive terpene pathways. Mid-ocean ridge (MOR) systems, influenced by divergent tectonics and mantle plumes, display NRPS- and RiPP-dominated (ribosomally synthesized and post-translationally modified peptides) repertoires reflecting metal-microbe interactions and microbial competition. Intraplate plume-influenced settings are characterized by pronounced terpene enrichment potentially reflecting scarce direct magmatic input in this system. BGC charts represent the relative proportions of BGC categories within the SA-CVZ (South American Central Volcanic Zone) volcanic arc, SA-CVZ backarc, RVB (Reykjanes Volcanic Belt) and SKVP (South Khangai Volcanic Province) respectively. Moho and 122 ℃ isotherm are representative general changes across tectonic settings. Cross section adapted from Giovannelli et al. [2022].

4.7 Supplementary Figures

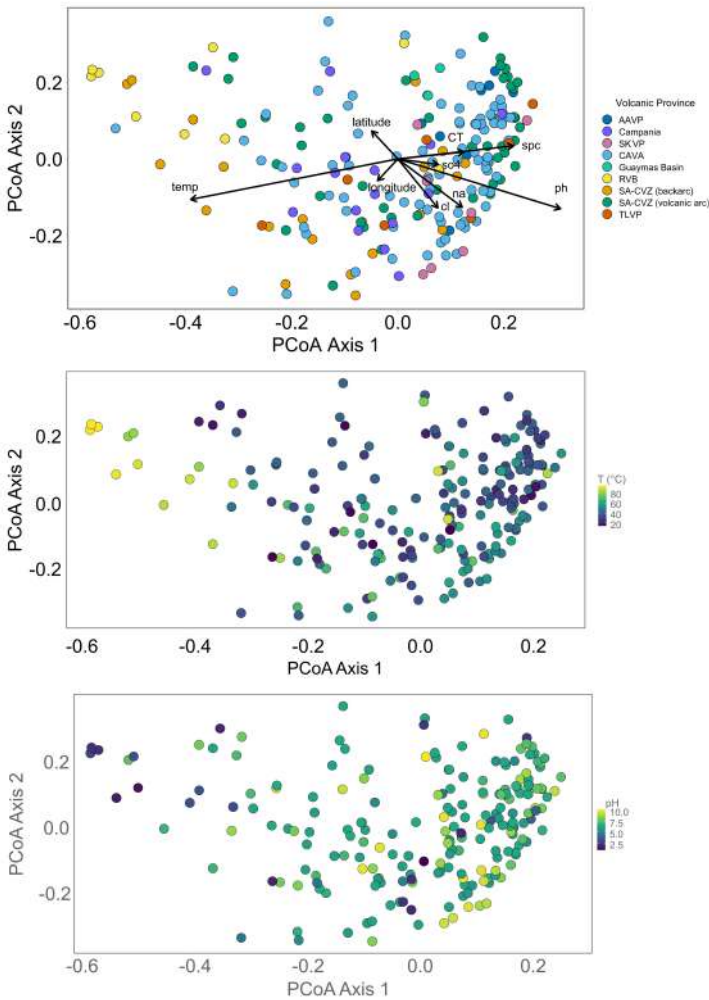

Figure 26: Weighted Jaccard principal coordinate analysis (PCoA) of biosynthetic gene cluster (BGC) community structure across geothermal sites. Top: PCoA plot with environmental vector fitting (envfit) showing the direction and strength of selected geochemical variables (temperature, pH, chloride, conductivity, crustal thickness, etc.) alongside sample symbols colored by tectonic regime and shaped by volcanic zone of origin: CAVA (Central American Volcanic Arc), SA-CVZ (South American Central Volcanic Zone), RVB (Reykjanes Volcanic Belt), AAVP (Aerolian Arc Volcanic Province), TLVP (Tuscan-Latium Volcanic Province), and SKVP (South Khangai Volcanic Province). Middle: The same ordination with point color scaled by in situ temperature (°C), illustrating a gradient aligned with Axis 1. Bottom: The same ordination colored by pH, showing a similar transition in geochemical conditions along the ordination space.

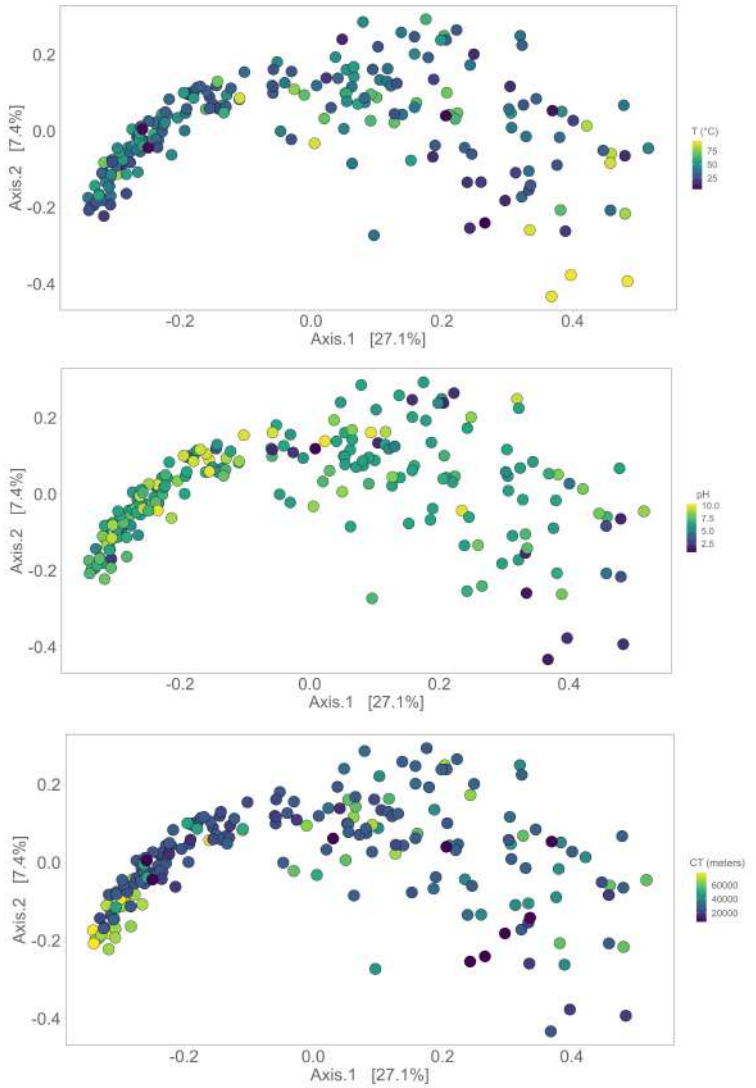

Figure 27: Environmental gradients shaping microbial BGC composition across geothermal systems. Top: Principal Coordinate Analysis (PCoA) showing ordination of microbial biosynthetic gene cluster (BGC) profiles constrained by crustal thickness (CT). Middle: PCoA constrained by temperature, showing a diffuse gradient across samples. Bottom: PCoA constrained by pH. Environmental variables tested for impact in the dataset using PERMANOVA (adonis2, Jaccard distance).

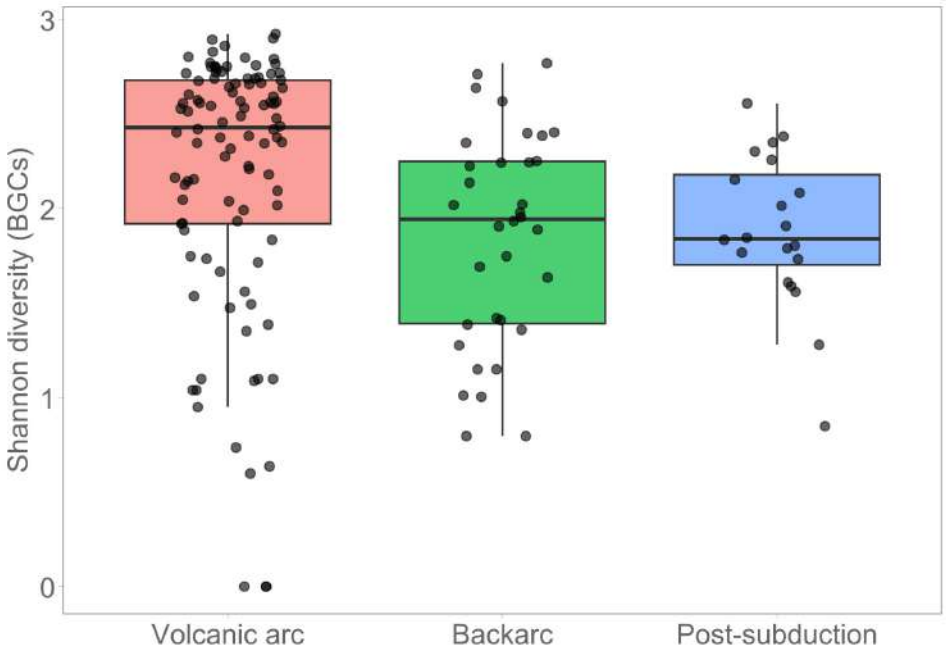

Figure 28: Alpha diversity of biosynthetic gene clusters (BGCs) across tectonic settings. Shannon diversity indices were calculated from BGC profiles of geothermal samples grouped by tectonic context (volcanic arc, backarc, post-subduction). Diversity differed significantly among groups (Kruskal–Wallis χ^2 = 17.35, p = 1.7 × 10^{-4}). Volcanic arc sites (n = 125) showed the highest diversity (mean ± SD = 2.18 ± 0.69), significantly greater than both backarc (n = 34, 1.85 ± 0.57; p = 0.0026) and post-subduction sites (n = 17, 1.88 ± 0.41; p = 0.0026). Backarc and post-subduction sites did not differ significantly (p = 0.99). Box plots display medians (horizontal line), interquartile range (box), and full range (whiskers), with individual samples shown as jittered points.

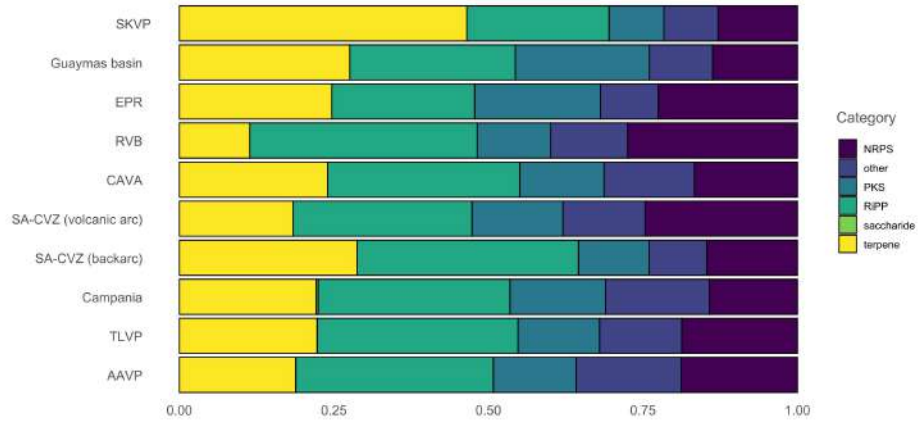

Figure 29: Biosynthetic gene cluster (BGC) composition across geothermal and volcanic regions. Stacked bar plots show the relative abundance of BGC categories in metagenomic assemblies from different global sites. Variations in BGC profiles reflect distinct microbial adaptations to the geochemical and geological characteristics of each location. At the volcanic province scale, the same patterns as of our Clusters are possible to be seen. SA-CVZ (South American Central Volcanic Zone) volcanic arc samples (most abundant in Cluster 1) exhibit high proportions of NRPS (nonribosomal peptide synthetases) (24.7 %) and RiPP (ribosomally synthesized and post-translationally modified peptides) (29.0 %) BGCs, consistent with environments characterized by heavy metal input. Terpenes contribute 18.4 %, PKSs (polyketide synthases) account for 14.7 %, and other BGC types make up the remaining 13.2 %. In contrast, SA-CVZ back-arc samples (most abundant in Clusters 2 and 3) display a more streamlined BGC profile, with RiPPs further elevated to 35.8 % and terpenes rising to 28.7 %, and NRPSs drop to 14.7 %, a notable 10 % decrease relative to the volcanic arc counterpart. PKS and other categories share the remaining 20.4 % of the SA-CVZ backarc BGC pool. Samples from the CAVA (Central American Volcanic Arc) reveal a relatively balanced biosynthetic landscape. RiPPs still dominate (31.1 %), followed by terpenes (24.0 %), NRPSs (16.7 %), PKSs (13.6 %), and other clusters (14.6 %). In Italy, which spans diverse tectonic regimes, from subduction-related island arcs (e.g., AAVP (Aeolian Arc Volcanic Province)) to post-subduction extensional arcs (e.g., Campania and TLVP (Tuscan-Latium Volcanic Province)), the BGC distribution is varied. AAVP samples show the lowest terpene contribution to BGC pool amongst Italian samples (18.8 %, while Campania and TVLP had a contribution of 23 % both), and Campania samples show a modest NRPS contribution (14 % in comparison to 19 % for both AAVP and TVLP). TVLP samples show a slightly elevated RiPP proportion 33 %, followed by AAVP 32 % and Campania 31 %. PKS show small contributions in all Italian samples, reaching no more than 15 % for each of them. Other BGCs contribute 17 % for Campania and AAVP, and 13 % for TVLP. Geothermal springs in the RVB (Reykjanes Volcanic Belt), located along the active Mid-Atlantic Ridge, as well as deep-sea hydrothermal vents in the Guaymas Basin and deep seeps in the SKVP (South Khangai Volcanic Province), show distinctly different biosynthetic profiles compared to all other sample sites. In the RVB (most abundant in Cluster 3), biosynthetic gene clusters (BGCs) are dominated by RiPPs (36.8 %) and NRPSs (27.5 %), while all other categories each account for less than 12 %. The EPR BGC pool is relatively well balanced containing 24 % terpene, 23 % RiPP, 22 % NRPS and 20 % PKS, other BGCs occupy the remaining 10 %. The Guaymas Basin microbiome shows the highest PKS representation across all sampled volcanic provinces (22 %), terpenes were the most abundant BGC category in these samples (28 %), followed by RiPPs (27 %) and NRPSs (14 %). Other BGCs contributed modestly at 9 %. SKVP samples exhibit strongest terpene enrichment across our global dataset (47 %). RiPPs contribute 22 %, NRPSs 13 %, and the remaining categories together comprise the final 18 %. These distributions suggest a focused yet distinct biosynthetic specialization across such geothermal systems.

References

Joost W Aerts, Andreas Riedo, Daniel J Melton, Simone Martini, Jessica Flahaut, Uwe J Meierhenrich, Cornelia Meinert, Iuliia Myrgorodska, Robert Lindner, and Pascale Ehrenfreund. Biosignature analysis of mars soil analogs from the atacama desert: Challenges and implications for future missions to mars. *Astrobiology*, 20(6):766–784, 2020.

Pablo Horacio Alasino, SR Paterson, M Kirsch, and Mariano Alexis Larrovere. The role of crustal thickness on magma composition in arcs: An example from the pre-andean, south american cordillera. *Gondwana Research*, 106:191–210, 2022.

Kelsey L Alexander, C Benjamin Naman, Arihiro Iwasaki, Alfonso Mangoni, Tiago Leao, Raphael Reher, Daniel Petras, Hyunwoo Kim, Eva Ternon, Eduardo JE Caro-Diaz, et al. Fatuamide a, a hybrid pks/nrps metallophore from a leptolyngbya sp. marine cyanobacterium collected in american samoa. *Journal of natural products*, 88(2):322–335, 2025.

Douglas E Allen and WE Seyfried Jr. Ree controls in ultramafic hosted mor hydrothermal systems: an experimental study at elevated temperature and pressure. *Geochimica et Cosmochimica Acta*, 69(3): 675–683, 2005.

Jose Javier Álvaro, Mónica Sánchez-Román, Klaas GJ Nierop, and Francien Peterse. Multiscale microbial preservation and biogeochemical signals in a modern hot-spring siliceous sinter rich in co2 emissions, krỳsuvík geothermal field, iceland. *Minerals*, 11(3):263, 2021.

Ana RA Alves, Qifan Yin, Rui S Oliveira, Eduardo F Silva, and Luís AB Novo. Plant growth-promoting bacteria in phytoremediation of metal-polluted soils: current knowledge and future directions. *Science of the Total Environment*, 838:156435, 2022.

Meglali Amina and Ghellai Lotfi. An overview of extremophile: microbial diversity, adaptive strategies, and potential applications. 2024.

Constanza M Andreani-Gerard, Verónica Cambiazo, and Mauricio González. Biosynthetic gene clusters from uncultivated soil bacteria of the atacama desert. *Msphere*, 9(10):e00192–24, 2024.

Martina Aulitto, Giovanni Gallo, Rosanna Puopolo, Angela Mormone, Danila Limauro, Patrizia Contursi, Monica Piochi, Simonetta Bartolucci, and Gabriella Fiorentino. Genomic insight of alicyclobacillus mali fl18 isolated from an arsenic-rich hot spring. *Frontiers in Microbiology*, 12:639697, 2021.

Nicole E Avalon, Mariana A Reis, Christopher C Thornburg, R Thomas Williamson, Daniel Petras, Allegra T Aron, George F Neuhaus, Momen Al-Hindy, Jana Mitrevska, Leonor Ferreira, et al. Leptochelins a–c, cytotoxic metallophores produced by geographically dispersed leptothoe strains of marine cyanobacteria. *Journal of the American Chemical Society*, 146(27):18626–18638, 2024.

Mariana Avalos, Paolina Garbeva, Lisa Vader, Gilles P van Wezel, Jeroen S Dickschat, and Dana Ulanova. Biosynthesis, evolution and ecology of microbial terpenoids. *Natural Product Reports*, 39(2):249–272, 2022.

R Bargagli, C Barghigiani, BZ Siegel, and SM Siegel. Trace metal anomalies in surface soils and vegetation on two active island volcanoes: Stromboli and vulcano (italy). *Science of the total environment*, 102:209–222, 1991.

Bernardo Barosa, Alessandra Ferrillo, Matteo Selci, Marco Giardina, Alessia Bastianoni, Monica Correggia, Luciano di Iorio, Giulia Bernardi, Martina Cascone, Rosaria Capuozzo, et al. Mapping the microbial diversity associated with different geochemical regimes in the shallow-water hydrothermal vents of the aeolian archipelago, italy. *Frontiers in Microbiology*, 14:1134114, 2023.

PH Barry, JM De Moor, A Chiodi, F Aguilera, MR Hudak, DV Bekaert, SJ Turner, J Curtice, AM Seltzer, GL Jessen, et al. The helium and carbon isotope characteristics of the andean convergent margin. *Frontiers in Earth Science*, 10:897267, 2022.

Marco Basili, Timothy J Rogers, Mayuko Nakagawa, Mustafa Yücel, J Maarten de Moor, Peter H Barry, Matthew O Schrenk, Gerdhard L Jessen, Ricardo Sánchez-Murillo, Sabin Zahirovic, et al. Subsurface microbial community structure shifts along the geological features of the central american volcanic arc. *PLoS One*, 19(11):e0308756, 2024.

Janos Berdy. Bioactive microbial metabolites. *The Journal of antibiotics*, 58(1):1–26, 2005.

Alison Besse, Jean Peduzzi, Sylvie Rebuffat, and Alyssa Carre-Mlouka. Antimicrobial peptides and proteins in the face of extremes: Lessons from archaeocins. *Biochimie*, 118:344–355, 2015.

Kai Blin, Simon Shaw, Kat Steinke, Rasmus Villebro, Nadine Ziemert, Sang Yup Lee, Marnix H Medema, and Tilmann Weber. antismash 5.0: updates to the secondary metabolite genome mining pipeline. *Nucleic acids research*, 47(W1):W81–W87, 2019.

Vitaliy B Borisov, Sergey A Siletsky, Martina R Nastasi, and Elena Forte. Ros defense systems and terminal oxidases in bacteria. *Antioxidants*, 10(6):839, 2021.

Tanja Bosak, Richard M Losick, and Ann Pearson. A polycyclic terpenoid that alleviates oxidative stress. *Proceedings of the National Academy of Sciences*, 105(18):6725–6729, 2008.

Maria Bourbouli, Efstathios A Katsifas, Evangelos Papathanassiou, and Amalia D Karagouni. The kolumbo submarine volcano of santorini island is a large pool of bacterial strains with antimicrobial activity. *Archives of microbiology*, 197(4):539–552, 2015.

A Broquet and JC Andrews-Hanna. Geophysical evidence for an active mantle plume underneath elysium planitia on mars. nat. astron, 2022.

Adrien Broquet and Jeffrey C Andrews-Hanna. Plume-induced flood basalts on hesperian mars: An investigation of hesperia planum. *Icarus*, 391:115338, 2023.

Carlo Cardellini, Giovanni Chiodini, F Frondini, R Avino, E Bagnato, S Caliro, Matteo Lelli, and Angelo Rosiello. Monitoring diffuse volcanic degassing during volcanic unrests: the case of campi flegrei (italy). *Scientific Reports*, 7(1):6757, 2017.

Cassandra S Carroll and Margo M Moore. Ironing out siderophore biosynthesis: a review of non-ribosomal peptide synthetase (nrps)-independent siderophore synthetases. *Critical reviews in biochemistry and molecular biology*, 53(4):356–381, 2018.

Paterno R Castillo. An alternative new view of convergent margin magmatism. *Journal of Asian Earth Sciences*, 256:105834, 2023.

Juan Castro-Severyn, Coral Pardo-Esté, Katterinne N Mendez, Jonathan Fortt, Sebastian Marquez, Franck Molina, Eduardo Castro-Nallar, Francisco Remonsellez, and Claudia P Saavedra. Living to the high extreme: unraveling the composition, structure, and functional insights of bacterial communities thriving in the arsenic-rich salar de huasco altiplanic ecosystem. *Microbiology spectrum*, 9(1):10–1128, 2021.

Ray Chen, Hon Lun Wong, Gareth S Kindler, Fraser Iain MacLeod, Nicole Benaud, Belinda C Ferrari, and Brendan P Burns. Discovery of an abundance of biosynthetic gene clusters in shark bay microbial mats. *Frontiers in Microbiology*, 11:1950, 2020.

Mingyue Cheng, Shuai Luo, Peng Zhang, Guangzhou Xiong, Kai Chen, Chuanqi Jiang, Fangdian Yang, Hanhui Huang, Pengshuo Yang, Guanxi Liu, et al. A genome and gene catalog of the aquatic microbiomes of the tibetan plateau. *Nature Communications*, 15(1):1438, 2024.

A Chiodi, W Báez, F Tassi, Emilce Bustos, R Filipovich, J Murray, AL Rizzo, O Vaselli, G Giordano, and Jose German Viramonte. Fluid geochemistry of the cerro galán geothermal system (southern puna, argentina): Implications for the geothermal potential of one of the youngest giant calderas in the andes. *Journal of Volcanology and Geothermal Research*, 450:108089, 2024.

Deirdre E Clark, Eric H Oelkers, Ingvi Gunnarsson, Bergur Sigfússon, Sandra Ó Snæbjörnsdóttir, Edda S Aradottir, and Sigurur R Gíslason. Carbfix2: Co2 and h2s mineralization during 3.5 years of continuous injection into basaltic rocks at more than 250 c. *Geochimica et Cosmochimica Acta*, 279:45–66, 2020.

Monica Correggia, Luciano Di Iorio, Alessia Benedicta Bastianoni, Mustafa Yücel, Angelina Cordone, and Donato Giovannelli. Standard operating procedure for the determination of trace elements in hydrothermal fluids by inductively coupled plasma mass spectrometry (icp-ms). *Open Research Europe*, 3:90, 2024.

Jake R Crandall, Justin Filiberto, Nicholas Castle, Sally L Potter-McIntyre, Susanne P Schwenzer, Karen Olsson-Francis, and Scott Perl. Habitability of martian noachian hydrothermal systems as constrained by a terrestrial analog on the colorado plateau. *The Planetary Science Journal*, 2(4):138, 2021.

Rubing Du, Wu Xiong, Lei Xu, Yan Xu, and Qun Wu. Metagenomics reveals the habitat specificity of biosynthetic potential of secondary metabolites in global food fermentations. *Microbiome*, 11(1):115, 2023.

Lorena H Filiberto, Christine V Putnis, and Maude Julia. Factors controlling reaction pathways during fluid–rock interactions. *Contributions to Mineralogy and Petrology*, 178(8):53, 2023.

Pablo L Finkel, Daniel Carrizo, Victor Parro, and Laura Sánchez-García. An overview of lipid biomarkers in terrestrial extreme environments with relevance for mars exploration. *Astrobiology*, 23(5):563–604, 2023.

Alexander Fleming. On the antibacterial action of cultures of a penicillium, with special reference to their use in the isolation of b. influenzae. *British journal of experimental pathology*, 10(3):226, 1929.

Thráinn Fridriksson, Bjarni Reyr Kristjánsson, Halldor Armannsson, Eygerur Margrétardóttir, Snjólaug Ólafsdóttir, and Giovanni Chiodini. Co2 emissions and heat flow through soil, fumaroles, and steam heated mud pools at the reykjanes geothermal area, sw iceland. *Applied geochemistry*, 21(9):1551–1569, 2006.

Elizabeth R Fuller and James W Head Iii. Olympus mons, mars: detection of extensive preaureole volcanism and implications for initial mantle plume behavior. *Geology*, 31(2):175–178, 2003.

Katherine M Fullerton, Matthew O Schrenk, Mustafa Yücel, Elena Manini, Marco Basili, Timothy J Rogers, Daniele Fattorini, Marta Di Carlo, Giuseppe d'Errico, Francesco Regoli, et al. Effect of tectonic processes on biosphere–geosphere feedbacks across a convergent margin. *Nature Geoscience*, 14(5):301–306, 2021.

Aileen Ute Geers, Grégoire Michoud, Susheel Bhanu Busi, Hannes Peter, Tyler J Kohler, Leïla Ezzat, Vanishing Glaciers Field Team, and

Tom J Battin. Deciphering the biosynthetic landscape of biofilms in glacier-fed streams. *MSystems*, 10(2):e01137–24, 2025.

Charles Gerday, Mohamed Aittaleb, Mostafa Bentahir, Jean-Pierre Chessa, Paule Claverie, Tony Collins, Salvino D'Amico, Joelle Dumont, Genevieve Garsoux, Daphne Georlette, et al. Cold-adapted enzymes: from fundamentals to biotechnology. *Trends in biotechnology*, 18(3):103–107, 2000.

Jonathan Gershenzon and Natalia Dudareva. The function of terpene natural products in the natural world. *Nature chemical biology*, 3(7): 408–414, 2007.

Adem Gharsallaoui, Nadia Oulahal, Catherine Joly, and Pascal Degraeve. Nisin as a food preservative: part 1: physicochemical properties, antimicrobial activity, and main uses. *Critical reviews in food science and nutrition*, 56(8):1262–1274, 2016.

Ghassan Ghssein and Zeinab Ezzeddine. A review of pseudomonas aeruginosa metallophores: Pyoverdine, pyochelin and pseudopaline. *Biology*, 11(12):1711, 2022.

Daniela Giordano. Bioactive molecules from extreme environments. *Marine Drugs*, 18(12):640, 2020.

Donato Giovannelli, Peter H Barry, J Maarten De Moor, Gerdhard L Jessen, Matthew O Schrenk, and Karen G Lloyd. Sampling across large-scale geological gradients to study geosphere–biosphere interactions. *Frontiers in Microbiology*, 13:998133, 2022.

Ana FR Gomes, Mariana C Almeida, Emília Sousa, and Diana ISP Resende. Siderophores and metallophores: Metal complexation weapons to fight environmental pollution. *Science of The Total Environment*, 932:173044, 2024.

Yosuke Hoshino and Laura Villanueva. Four billion years of microbial terpenome evolution. *FEMS Microbiology Reviews*, 47(2):fuad008, 2023.

Graham A Hudson and Douglas A Mitchell. Ripp antibiotics: biosynthesis and engineering potential. *Current opinion in microbiology*, 45: 61–69, 2018.

Roberto Isaia, Maria Giulia Di Giuseppe, Jacopo Natale, Francesco D'Assisi Tramparulo, Antonio Troiano, and Stefano Vitale. Volcano-tectonic setting of the pisciarelli fumarole field, campi flegrei caldera, southern italy: insights into fluid circulation patterns and hazard scenarios. *Tectonics*, 40(5):e2020TC006227, 2021.

Peter E Jackson. Ion chromatography in environmental analysis. *Encyclopedia of analytical chemistry*, 2779, 2000.

Qidong Jia, Guanglin Li, Tobias G Köllner, Jianyu Fu, Xinlu Chen, Wangdan Xiong, Barbara J Crandall-Stotler, John L Bowman, David J Weston, Yong Zhang, et al. Microbial-type terpene synthase genes occur widely in nonseed land plants, but not in seed plants. *Proceedings of the National Academy of Sciences*, 113(43):12328–12333, 2016.

Riikka Kietäväinen, Mari Nyyssönen, Maija Nuppunen-Puputti, and Malin Bomberg. Naturally occurring volatile organic compounds in deep bedrock groundwater. *Communications Earth & Environment*, 6(1): 64, 2025.

Charlotte Kleint, Wolfgang Bach, Alexander Diehl, Nico Fröhberg, Dieter Garbe-Schönberg, Jan F Hartmann, Cornel EJ de Ronde, Sylvia G Sander, Harald Strauss, Valerie K Stucker, et al. Geochemical characterization of highly diverse hydrothermal fluids from volcanic vent systems of the kermadec intraoceanic arc. *Chemical Geology*, 528: 119289, 2019.

Vladimir N Kompanichenko. Organic matter in the hydrothermal systems of kamchatka peninsula and nearby area. In *Thermodynamic Inversion: Origin of Living Systems*, pages 249–271. Springer, 2017.

Stephan M Kraemer, Owen W Duckworth, James M Harrington, and Walter DC Schenkeveld. Metallophores and trace metal biogeochemistry. *Aquatic Geochemistry*, 21(2):159–195, 2015.

Fumitaka Kudo and Tadashi Eguchi. Biosynthetic genes for aminoglycoside antibiotics. *The Journal of antibiotics*, 62(9):471–481, 2009.

Tomohisa Kuzuyama. Biosynthetic studies on terpenoids produced by streptomyces. *The Journal of antibiotics*, 70(7):811–818, 2017.

Min Jin Kwon, Charlotte Steiniger, Timothy C Cairns, Jennifer H Wisecaver, Abigail L Lind, Carsten Pohl, Carmen Regner, Antonis Rokas, and Vera Meyer. Beyond the biosynthetic gene cluster paradigm: genome-wide coexpression networks connect clustered and unclustered transcription factors to secondary metabolic pathways. *Microbiology Spectrum*, 9(2):e00898–21, 2021.

Ben Langmead and Steven L Salzberg. Fast gapped-read alignment with bowtie 2. *Nature methods*, 9(4):357–359, 2012.

Yohann Le Govic, Nicolas Papon, Solène Le Gal, Jean-Philippe Bouchara, and Patrick Vandeputte. Non-ribosomal peptide synthetase gene clusters in the human pathogenic fungus scedosporium apiospermum. *Frontiers in microbiology*, 10:2062, 2019.

Namil Lee, Woori Kim, Soonkyu Hwang, Yongjae Lee, Suhyung Cho, Bernhard Palsson, and Byung-Kwan Cho. Thirty complete streptomyces genome sequences for mining novel secondary metabolite biosynthetic gene clusters. *Scientific data*, 7(1):55, 2020.

Yanyan Li and Sylvie Rebuffat. The manifold roles of microbial ribosomal peptide–based natural products in physiology and ecology. *Journal of Biological Chemistry*, 295(1):34–54, 2020.

Lan Liu, Nimaichand Salam, Jian-Yu Jiao, Hong-Chen Jiang, En-Min Zhou, Yi-Rui Yin, Hong Ming, and Wen-Jun Li. Diversity of culturable thermophilic actinobacteria in hot springs in tengchong, china and studies of their biosynthetic gene profiles. *Microbial Ecology*, 72(1): 150–162, 2016.

Paul J McMurdie and Susan Holmes. phyloseq: an r package for reproducible interactive analysis and graphics of microbiome census data. *PloS one*, 8(4):e61217, 2013.

William Medeiros, Kelly Hidalgo, Tiago Leão, Lucas Miguel de Carvalho, Nadine Ziemert, and Valeria Oliveira. Unlocking the biosynthetic potential and taxonomy of the antarctic microbiome along temporal and spatial gradients. *Microbiology Spectrum*, 12(6):e00244–24, 2024.

Balakrishnan Meena, Lawrance Anburajan, Nambali Valsalan Vinithkumar, Ramalingam Kirubagaran, and Gopal Dharani. Biodiversity and antibacterial potential of cultivable halophilic actinobacteria from the

deep sea sediments of active volcanic barren island. *Microbial Pathogenesis*, 132:129–136, 2019.

Fan-chao Meng, Inna Safonova, Shuang-shuang Chen, and Patrick Rioual. Late cenozoic intra-plate basalts of the greater khingan range in ne china and khangai province in central mongolia. *Gondwana Research*, 63:65–84, 2018.

KM Meyer, Jennifer L Macalady, JM Fulton, LR Kump, I Schaperdoth, and KH Freeman. Carotenoid biomarkers as an imperfect reflection of the anoxygenic phototrophic community in meromictic fayetteville green lake. *Geobiology*, 9(4):321–329, 2011.

Marcus Miethke, Marco Pieroni, Tilmann Weber, Mark Brönstrup, Peter Hammann, Ludovic Halby, Paola B Arimondo, Philippe Glaser, Bertrand Aigle, Helge B Bode, et al. Towards the sustainable discovery and development of new antibiotics. *Nature Reviews Chemistry*, 5(10):726–749, 2021.

Shekhar Nagar, Meghali Bharti, and Ram Krishan Negi. Genome-resolved metagenomics revealed metal-resistance, geochemical cycles in a himalayan hot spring. *Applied Microbiology and Biotechnology*, 107(10):3273–3289, 2023.

Hideto Nakamura. Plant-derived triterpenoid biomarkers and their applications in paleoenvironmental reconstructions: chemotaxonomy, geological alteration, and vegetation reconstruction. *Researches in Organic Geochemistry*, 35(2):11–35, 2019.

Stephen Nayfach, Simon Roux, Rekha Seshadri, Daniel Udwary, Neha Varghese, Frederik Schulz, Dongying Wu, David Paez-Espino, I-Min Chen, Marcel Huntemann, et al. A genomic catalog of earth's microbiomes. *Nature biotechnology*, 39(4):499–509, 2021.

EG Nisbet and NH Sleep. The habitat and nature of early life. *Nature*, 409(6823):1083–1091, 2001.

JAMES F Novotny Jr and JEROME J Perry. Characterization of bacteriocins from two strains of bacillus thermoleovorans, a thermophilic hydrocarbon-utilizing species. *Applied and Environmental Microbiology*, 58(8):2393–2396, 1992.

Sergey Nurk, Dmitry Meleshko, Anton Korobeynikov, and Pavel A Pevzner. metaspades: a new versatile metagenomic assembler. *Genome research*, 27(5):824–834, 2017.

Em O'connor and RF Shand. Halocins and sulfolobicins: the emerging story of archaeal protein and peptide antibiotics. *Journal of Industrial Microbiology and Biotechnology*, 28(1):23–31, 2002.

Shannon I Ohlemacher, Yiquan Xu, Daniel L Kober, Mahnoor Malik, Jay C Nix, Tom J Brett, and Jeffrey P Henderson. Ybtt is a low-specificity type ii thioesterase that maintains production of the metallophore yersiniabactin in pathogenic enterobacteria. *Journal of Biological Chemistry*, 293(51):19572–19585, 2018.

Jari Oksanen, F Guillaume Blanchet, Roeland Kindt, Pierre Legendre, Peter R Minchin, RB O'hara, Gavin L Simpson, Peter Solymos, M Henry H Stevens, Helene Wagner, et al. Package 'vegan'. *Community ecology package, version*, 2(9):1–295, 2013.

Dolgorjav Oyuntsetseg, Darmaa Ganchimeg, Amgalan Minjigmaa, Akira Ueda, and Minoru Kusakabe. Isotopic and chemical studies of hot and cold springs in western part of khangai mountain region, mongolia, for geothermal exploration. *Geothermics*, 53:488–497, 2015.

Jan Pańczak, Paweł Kosakowski, and Adam Zakrzewski. Biomarkers in fossil resins and their palaeoecological significance. *Earth-Science Reviews*, 242:104455, 2023.

Lucas Paoli, Hans-Joachim Ruscheweyh, Clarissa C Forneris, Florian Hubrich, Satria Kautsar, Agneya Bhushan, Alessandro Lotti, Quentin Clayssen, Guillem Salazar, Alessio Milanese, et al. Biosynthetic potential of the global ocean microbiome. *Nature*, 607(7917):111–118, 2022.

Jung-Woo Park, Ian H Campbell, Massimo Chiaradia, Hongda Hao, and Cin-Ty Lee. Crustal magmatic controls on the formation of porphyry copper deposits. *Nature Reviews Earth & Environment*, 2(8):542–557, 2021.

Kesava Priyan Ramasamy, Raju Rajasabapathy, Inga Lips, Chellandi Mohandass, and Rathinam Arthur James. Genomic features and copper biosorption potential of a new alcanivorax sp. vbw004 isolated

from the shallow hydrothermal vent (azores, portugal). *Genomics*, 112(5):3268–3273, 2020.

Carmen Rizzo, Erika Arcadi, Rosario Calogero, Valentina Sciutteri, Pierpaolo Consoli, Valentina Esposito, Simonepietro Canese, Franco Andaloro, and Teresa Romeo. Ecological and biotechnological relevance of mediterranean hydrothermal vent systems. *Minerals*, 12(2):251, 2022.

Leonardo Romero, Hugo Alonso, Patricio Campano, Luca Fanfani, Rosa Cidu, Claudia Dadea, Thomas Keegan, Iain Thornton, and Margaret Farago. Arsenic enrichment in waters and sediments of the rio loa (second region, chile). *Applied Geochemistry*, 18(9):1399–1416, 2003.

KM Rychkova and OI Kalnaya. Isotopic composition for helium in late cenozoic south-baikal and south-khangai volcanic areas. , (4):39–51, 2023.

Marion Saby, Vincent van Hinsberg, Daniele L Pinti, Kim Berlo, Bjarni Gautason, Ásgerur Sigurardóttir, Kevin Brown, and Océane Rocher. The behaviour of metals in deep fluids of ne iceland. *Scientific Reports*, 12(1):21952, 2022.

Carlos Santana-Molina, Valentina Henriques, Damaso Hornero-Méndez, Damien P Devos, and Elena Rivas-Marin. The squalene route to c30 carotenoid biosynthesis and the origins of carotenoid biosynthetic pathways. *Proceedings of the National Academy of Sciences*, 119(52):e2210081119, 2022.

VM Savatenkov, VV Yarmolyuk, EA Kudryashova, and AM Kozlovskii. Sources and geodynamics of the late cenozoic volcanism of central mongolia: evidence from isotope-geochemical studies. *Petrology*, 18 (3):278–307, 2010.

Ahmed M Sayed, Marwa HA Hassan, Hani A Alhadrami, Hossam M Hassan, Michael Goodfellow, and Mostafa E Rateb. Extreme environments: microbiology leading to specialized metabolites. *Journal of applied microbiology*, 128(3):630–657, 2020.

Gwénola Simon, Laurie Casalot, Corinne Valette, Christopher Burot, Jean François Rontani, and Patricia Bonin. Do carotenoids protect

phytodetritus-associated bacteria from oxidative stress? *Environmental Science and Pollution Research*, 32(17):11167–11178, 2025.

John Stix and J Maarten de Moor. Understanding and forecasting phreatic eruptions driven by magmatic degassing. *Earth, Planets and Space*, 70(1):83, 2018.

Roger E Summons, Paula V Welander, and David A Gold. Lipid biomarkers: molecular tools for illuminating the history of microbial life. *Nature Reviews Microbiology*, 20(3):174–185, 2022.

Ming Tang, Cin-Ty A Lee, Wei-Qiang Ji, Rui Wang, and Gelu Costin. Crustal thickening and endogenic oxidation of magmatic sulfur. *Science Advances*, 6(31):eaba6342, 2020.

J Tapia, B Schneider, M Inostroza, F Álvarez-Amado, JA Luque, F Aguilera, S Parra, and M Bravo. Naturally elevated arsenic in the altiplano-puna, chile and the link to recent (mio-pliocene to quaternary) volcanic activity, high crustal thicknesses, and geological structures. *Journal of South American Earth Sciences*, 105:102905, 2021.

Barbara R Terlouw, Kai Blin, Jorge C Navarro-Munoz, Nicole E Avalon, Marc G Chevrette, Susan Egbert, Sanghoon Lee, David Meijer, Michael JJ Recchia, Zachary L Reitz, et al. Mibig 3.0: a community-driven effort to annotate experimentally validated biosynthetic gene clusters. *Nucleic acids research*, 51(D1):D603–D610, 2023.

Monfredini Thiago, Manoel Gustavo P Homem, and Douglas Galante. Volatile organic compounds stability at exoplanetary atmospheres. *Proceedings of the International Astronomical Union*, 14(S345):273–275, 2018.

Sonia Tiquia-Arashiro and Debora Rodrigues. Alkaliphiles and acidophiles in nanotechnology. In *Extremophiles: applications in nanotechnology*, pages 129–162. Springer, 2016.

Heather E Upin, Dennis L Newell, Daniel R Colman, and Eric S Boyd. Tectonic settings influence the geochemical and microbial diversity of peru hot springs. *Communications Earth & Environment*, 4(1):112, 2023.

Anna L Vagstad. Engineering ribosomally synthesized and posttranslationally modified peptides as new antibiotics. *Current Opinion in Biotechnology*, 80:102891, 2023.

Valentin Waschulin, Chiara Borsetto, Robert James, Kevin K Newsham, Stefano Donadio, Christophe Corre, and Elizabeth Wellington. Biosynthetic potential of uncultured antarctic soil bacteria revealed through long-read metagenomic sequencing. *The ISME journal*, 16 (1):101–111, 2022.

Frances Westall, Keyron Hickman-Lewis, Nancy Hinman, Pascale Gautret, Kathleen A Campbell, Jean-Gabriel Bréhéret, Frédéric Foucher, Axelle Hubert, Stephanie Sorieul, Avinash Vicholous Dass, et al. A hydrothermal-sedimentary context for the origin of life. *Astrobiology*, 18(3):259–293, 2018.

Hadley Wickham. ggplot2. *Wiley interdisciplinary reviews: computational statistics*, 3(2):180–185, 2011.

Jessica R Willdigg and John D Helmann. Mini review: bacterial membrane composition and its modulation in response to stress. *Frontiers in Molecular Biosciences*, 8:634438, 2021.

Brian F Windley and Mark B Allen. Mongolian plateau: Evidence for a late cenozoic mantle plume under central asia. *Geology*, 21(4):295–298, 1993.

Lily X Zelaya-Molina, Ismael F Chávez-Díaz, José A Urrieta-Velázquez, Marco A Aragón-Magadan, Cristo O Puente-Valenzuela, Mario Blanco-Camarillo, Sergio de los Santos-Villalobos, and Juan Ramos-Garza. Microbial metallophores in the productivity of agroecosystems. *Microbiology Research*, 16(3):67, 2025.

Zhigang Zeng, Xiaohui Li, Shuai Chen, Jeroen De Jong, Nadine Mattielli, Haiyan Qi, Christopher Pearce, and Bramley J Murton. Iron, copper, and zinc isotopic fractionation in seafloor basalts and hydrothermal sulfides. *Marine Geology*, 436:106491, 2021.

Xinyi Zhang, Xun Wang, Yu Zhang, Fei Wang, Congqiang Zhang, and Xun Li. Development of isopentenyl phosphate kinases and their application in terpenoid biosynthesis. *Biotechnology Advances*, 64: 108124, 2023.

5 Appendix I: Funding acknowledgments

This PhD was supported by H2020 (Horizon 2020) Marie Sklodowska-Curie project ”CRESCENDO”. This work received additional work from funding from the European Research Council (ERC) under the European Union’s Horizon 2020 research and innovation program Grant Agreement No. 948972—COEVOLVE—ERC-2020-STG. Additional individual funding to coauthors have been acknowledged in the respective publications submitted or in preparation.

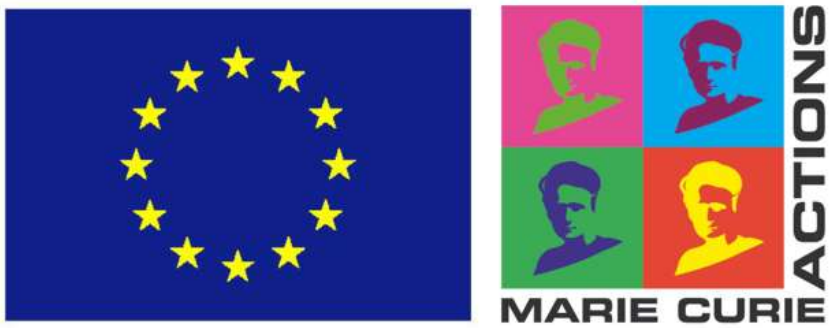

6 Appendix II: Sampling expeditions

6.1 Aeolian Islands July 2025 AEO25

I participated in the sampling expedition “AEO25” organized by Prof. Donato Giovannelli (donato.giovannelli@unina.it) in the framework of the ERC CoEvolve project. The expedition sampled several gas emissions sites particularly in Vulcano island, including both terrestrial and submarine locations. Sampled matrices included fluids, sediments, biofilms and gas that will be used for the characterization of the geochemistry and microbiology of the sites. I was involved in sample collection, sample processing and preservation in the field.

6.2 CN5 Expedition Gulf of Pozzuoli 2024

I participated in the sampling expedition “CN5” organized by Prof. Donato Giovannelli (donato.giovannelli@unina.it). The focus was on shallow-water hydrothermal vents in the Gulf of Pozzuoli, to analyze their microbial taxonomic and functional diversity and to unveil their impact on the surrounding ecosystem. Sampled matrices included fluids and biofilms that will be used for the characterization of the geochemistry and microbiology of the sites. I was involved in sample collection, sample processing and preservation in the field. This expedition happened in January 2024, May 2024, June 2024 and lasted 5-8 days each.

6.3 International Continental Drilling Program Drilling into the Ivrea-Verbano Zone November 2023

I participated in the expedition “ICP-DIVE” where the focus was sampling rock cores from the area of Ivrea-Verbano. I was involved in sample collection, sample processing and preservation in the field.

6.4 Bio Ocean 5D October 2023

I participated in the expedition Bio Ocean 5D where I was in charge of collecting macro and microfauna and sediment samples on seafloor and freezing some samples on liquid nitrogen after collection.

7 Appendix III: Publications

- **Ana Clara Pelliciari Silva**, Flavia Migliaccio, Bernardo Barosa, Luigi Gallucci, Mustafa Yücel, Dyonisius Foustoukos, Nadine le Bris, Constantino Vetriani, Donato Giovannelli (2025a). Hydrodynamic flow and benthic boundary layer interactions shape the microbial community in Milos shallow water hydrothermal vents. Front. Microbiol. 16, 1649514. *doi: 10.3389/fmicb.2025.1649514*

- Bernardo Barosa, Carmela Celentano, Flavia Migliaccio, Sara Claudia Diana, **Ana Clara Pelliciari Silva**, Matteo Selci, Luca Tonietti, Deborah Bastoni, Martina Cascone, Alessia Bastianoni, Monica Correggia, Luciano di Iorio, Roy Price, Stefano Caliro, Marco Milazzo, Alessandro Aiuppa, Costantino Vetriani, Angelina Cordone, Donato Giovannelli. The microbiology and geochemistry of the shallow-water hydrothermal vents of the Gulf of Naples, Italy, preprint at biorxiv
doi.org/10.1101/2025.10.02.679971.

- **Ana Clara Pelliciari Silva**, Benoit de Pins, Francesco Montemagno, Flavia Migliaccio, Martina Cascone, Deborah Bastoni, Bernardo Barosa, Matteo Selci, Costantino Vetriani, Agostina Chiodi, Federico A. Vignale, Maria Garcia Alai, Alberto Vitale Brovarone, Gerdhard L. Jessen, Jenny M. Blamey, J. Maarten de Moor, Karen G. Lloyd, Peter Barry, Donato Giovannelli (2025). Tectonic setting shapes microbial biosynthetic potential across global geothermal environments, preprint at biorxiv *doi.org/10.1101/2025.09.14.675129*

8 Appendix IV: Participations in congresses

- Italian Society of Microbial Biotechnology Congress - Rome, Italy September 2025 ”Geosphere-Biopshere coevolution: the role of trace metal availability in the evolution of biogeochemistry” contributed as coauthor, D. Giovannelli as first author

- Life and Planet 2025 (sponsored by The Geological Society) - London, UK July 2025 presenting ”Tectonic regime shapes microbial biosynthetic potential across global geothermal systems” as first author

- Goldschmidt 2025 - Prague, Czech Republic July 2025 presenting as first author ”Hydrodynamics and Benthic Boundary layer interactions shape the microbial community in Milos’ shallow water vents”
- Volcanic Gas Sampling Summer School in the Aeolian Islands, Sicily June 2025 joining as full-time participant
- Banff Geobiology - Banff, Canada April 2025 presenting ”Microbial mats as time capsules: lessons from modern hydrothermal systems” as first author
- Exploring Otherness on Earth and beyond: Bridging the gap between natural sciences, social sciences and humanities - Berlin, Germany April 2025 presenting as first author ”Organic matter and ferric ferrous minerals in Frutexites dubiofossils might support the search for life on Mars”
- American Geophysical Union - Washington D.C, USA December 2024 presenting ”Niche Differentiation in Freshwater Beggiatoa Mats” as first author
- 57th European Marine Biology Symposium - Naples, Italy September 2024 ”Multilevel analysis of the ecosystem effects of marine geothermalism - the case study of the Gulf of Pozzuoli (Italy)” contributed as coauthor, F. Migliaccio first author
- International Geobiology Summer Course June 2024-July 2024 hosted by Penn State University (Pennsylvania, USA) joining as full-time participant
- GRC Geobiology Conference, Galveston - Texas, USA January 2024 joining as funded participant
- Lyell Day, Royal Holloway University - London, UK February 2023 presenting ”Organic matter and ferric ferrous minerals in Frutexites dubiofossils might support the search for life on Mars” as first author

9 Appendix V: Selected papers and preprints

frontiers | Frontiers in Microbiology

TYPE Original Research
PUBLISHED 29 August 2025
DOI 10.3389/fmicb.2025.1649514

OPEN ACCESS

EDITED BY
Maxim Rubin-Blum,
Israel Oceanographic and Limnological Research (IOLR), Israel

REVIEWED BY
Julie L. Meyer,
University of Florida, United States
Andreas Teske,
University of North Carolina at Chapel Hill, United States

*CORRESPONDENCE
Costantino Vetriani
✉ vetriani@imcs.rutgers.edu
Donato Giovannelli
✉ donato.giovannelli@unina.it

RECEIVED 18 June 2025
ACCEPTED 08 August 2025
PUBLISHED 29 August 2025

CITATION
Silva ACP, Migliaccio F, Barosa B, Gallucci L, Yücel M, Foustoukos D, Le Bris N, Bartlett SJ, D'Alessandro V, Vetriani C and Giovannelli D (2025) Hydrodynamic flow and benthic boundary layer interactions shape the microbial community in Milos shallow water hydrothermal vents.
Front. Microbiol. 16:1649514.
doi: 10.3389/fmicb.2025.1649514

Hydrodynamic flow and benthic boundary layer interactions shape the microbial community in Milos shallow water hydrothermal vents

Ana Clara Pelliciari Silva[1], Flavia Migliaccio[1], Bernardo Barosa[1], Luigi Gallucci[1,2], Mustafa Yücel[3], Dionysis Foustoukos[4], Nadine Le Bris[5], Stuart J. Bartlett[6], Valerio D'Alessandro[7], Costantino Vetriani[8,9]* and Donato Giovannelli[1,8,9,10,11,12]*

[1]Department of Biology, University of Naples "Federico II", Naples, Italy, [2]Department of Molecular Ecology, Max Planck Institute for Marine Microbiology, Bremen, Germany, [3]Institute of Marine Sciences, Middle East Technical University, Mersin, Türkiye, [4]Earth and Planets Laboratory, Carnegie Institution of Washington, Washington, DC, United States, [5]Institute of Systematics Biodiversity and Evolution, Sorbonne University, Paris, France, [6]Division of Geological and Planetary Sciences, California Institute of Technology, Pasadena, CA, United States, [7]Industrial Engineering and Mathematical Sciences Department, Polytechnic University of Marche, Ancona, Italy, [8]Department of Marine and Coastal Science, Rutgers University, New Brunswick, NJ, United States, [9]Department of Biochemistry and Microbiology, Rutgers University, New Brunswick, NJ, United States, [10]National Research Council-Institute of Marine Biological Resources and Biotechnologies (CNR-IRBIM), Ancona, Italy, [11]Marine Chemistry and Geochemistry Department, Woods Hole Oceanographic Institution, Woods Hole, MA, United States, [12]Earth-Life Science Institute, Tokyo Institute of Technology, Tokyo, Japan

In shallow-water hydrothermal vents, the dynamic interface between the discharged reduced hydrothermal fluids and the oxidized seawater allows the establishment of gradients capable of supporting diverse and complex microbial mats. Due to their shallow depths and proximity to land masses, shallow vents are heavily influenced by dynamic forcing, tidal fluctuations, and episodic events (e.g., storms, tides, etc.). Although several studies have investigated the microbial communities inhabiting shallow vents in the last decades, less is known about how microbial communities respond to episodic events and how the complex interplay of physical and chemical drivers shapes the establishment and structure of microbial biofilms in these systems. Here we present data combining the taxonomic and functional diversity of the white microbial mats commonly found in sulfide rich shallow-water hydrothermal vents in Paleochori Bay (Milos Island, Greece), using a combined approach of 16S rRNA transcript amplicon sequencing (from RNA) and shotgun metagenomic sequencing (from which 16S rRNA genes were retrieved). We show that the white microbial mats of Milos shallow-water hydrothermal vents are dominated by Epsilonproteobacteria, now classified as Campylobacterota, with metabolic functions associated with chemolithoautotrophic lifestyles and exposed to a diverse array of viral communities. Taxonomic names follow the classification available at the time of analysis (2012). We explore how dynamic forcing and storm events influence microbial community restructuring and turn-over, and provide evidence that dynamic interactions with the benthic boundary layer play a key role in controlling the spatial distribution of taxa. Overall, our results show diverse processes through which geodynamic events influence microbial taxonomic and functional diversity.

KEYWORDS

shallow-water hydrothermal vents, microbial diversity, metagenomics, fluid-mixing, microbiome, ripples, storms, benthic boundary layer

1 Introduction

Shallow-water hydrothermal vents (SWHVs) are dynamic environments that form near tectonic plate boundaries and active volcanic areas, where geothermal heat drives the circulation of hydrothermal fluids (Price and Giovannelli, 2017). Upon discharge, hydrothermal fluids show unique chemical compositions, and are often enriched in carbon dioxide, sulfide, hydrogen, and iron among other compounds. Several of the compounds and elements released in the water column by SWHV, like iron, cobalt and reduced sulfur and nitrogen compounds, play a crucial role in marine ecosystems, supporting primary productivity and other metabolisms (Yücel et al., 2011; Price and Giovannelli, 2017; Schine et al., 2021; Gledhill and Buck, 2012; Frawley and Fang, 2014; Gomez-Saez et al., 2017). Additionally, the presence of sunlight in SWHVs fosters a dual-energy ecosystem, supporting both photosynthetic and chemosynthetic metabolisms. The availability of locally produced organic carbon, along with terrigenous and water column derived organic matter inputs, support complex heterotrophic microbial communities (Bellec et al., 2020; Arcadi et al., 2023).

Due to their shallow depths, SWHVs are also subject to unique dynamic physical and chemical forces that differ from their deep-sea counterparts. These include increased exposure to storm-induced turbulence, which enhances seawater–hydrothermal fluid mixing and creates steep chemical and thermal gradients across relatively short spatial scales (Yücel et al., 2013). For example, episodic storm events, driven by high wind velocity and surface shear stress, and resulting strong waves, can resuspend sediments in the Milos shallow vent system, altering fluid discharge patterns, and influencing both microbial and geochemical zonation (Yücel et al., 2013). These mixing processes result in the formation of localized microenvironments characterized by rapid changes in temperature, redox conditions, and electron donor/acceptor availability (Yücel, 2013). Such steep gradients strongly influence microbial colonization and niche differentiation. The thermodynamic disequilibria created at the interface of hydrothermal fluids and oxygenated seawater provide abundant energy sources for microbial metabolism, particularly for chemolithoautotrophs that exploit reduced compounds such as hydrogen and sulfide (Price and Giovannelli, 2017; Lu et al., 2020). As a result, SWHVs serve as natural laboratories for studying microbial processes shaped by both geochemical potential and hydrodynamic forces.

Biofilm formation is expected to be a dominant microbial strategy in shallow-water hydrothermal vents, given the dynamic mixing processes and steep physicochemical gradients described above. Biofilms and microbial mats are structured microbial communities embedded in self-produced extracellular polymeric substances that facilitate surface colonization, metabolic cooperation, and resilience to fluctuating environmental conditions (Dobretsov, 2009; Flemming and Wingender, 2010). While extensively studied in deep-sea hydrothermal vents, where they play critical roles in primary productivity and community stability under extreme thermal and chemical regimes (Alain et al., 2004; Gulmann et al., 2015; O'Brien et al., 2015), biofilms are also recognized as key features of microbial life in terrestrial hot springs, such as those in Yellowstone and Iceland, where similarly steep gradients drive spatial microbial stratification (Schuler et al., 2017). In shallow-water hydrothermal vents, however, these structures are likely even more significant due to increased environmental variability, including exposure to light, turbulence, and storm-induced mixing (Price and Giovannelli, 2017; Patwardhan et al., 2018; Sciutteri et al., 2022). Shifting physical and chemical conditions in SWHV selects for microbial assemblages capable of adhering to surfaces and rapidly adapting to changing redox and nutrient conditions, making biofilms not just prevalent but essential to microbial survival and ecosystem function in shallow vents.

The hydrothermal area of Milos Island, situated within the Aegean Volcanic Arc, is a region extending from the island of Kos close to the Turkish coast in the east to Methana in the west. The arc has been formed by the subduction of the African plate beneath the northeastern edge of the European plate, hosting Milos Island. Milos island spans a geo-active zone of vents covering approximately 35 km^2 and stands as one of the most extensively studied shallow-water geothermal systems globally (Dando et al., 1995, 2000; Price and Giovannelli, 2017; Nomikou et al., 2021). Within this area, Paleochori Bay, located on the southeast coast of Milos island (Figure 1), represents a venting site characterized by intense degassing, hydrothermal activity, and a pronounced thermal and redox vertical gradient (Dando et al., 1995, 2000; Yücel et al., 2013).

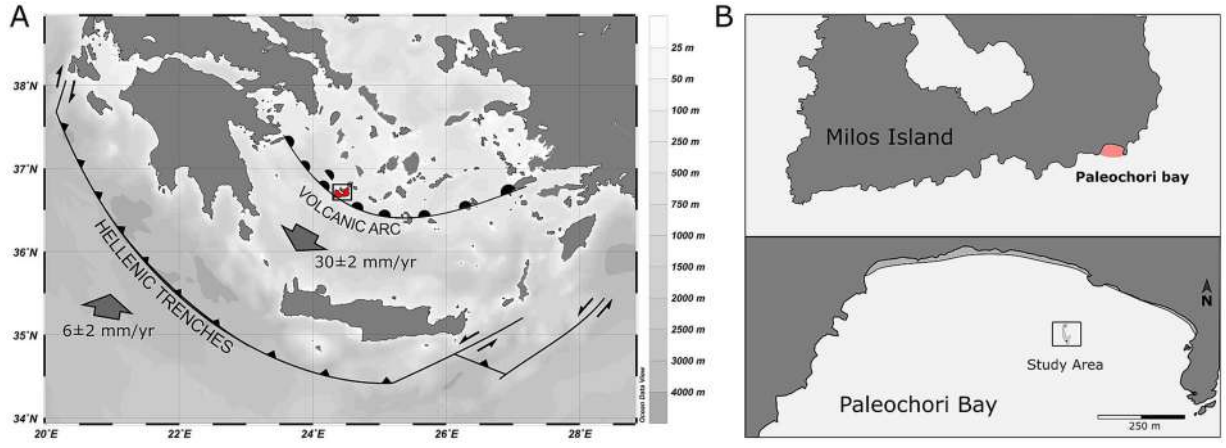

FIGURE 1
(A) Map of the Eastern Mediterranean Sea and Aegean Sea showing the position of the Hellenic Trenches and the Hellenic Volcanic Arc (adapted from Kokkalas et al., 2006). **(B)** Upper: Map of the south portion of Milos Island; lower: detail of the study area in Paleochori Bay.

The entire Paleochori Bay area manifests as regions of elevated temperature and degassing on the sandy seabed (Khimasia et al., 2020). Vertical gradients in temperature and redox are steep, with sediment depth correlating with temperature rise, whereas horizontal changes in temperature and redox are gradual and decrease as the distance from the venting center increases (Sievert et al., 1999; Sievert et al., 2000; Dando et al., 2000; Wenzhöfer et al., 2000). Reported temperatures of up to 119 °C at a vent site at 10-meter water depth underscore the extreme thermal conditions present (Botz et al., 1996). Venting fluids exhibit varying salinity levels, often mixed with freshwater. The CO_2 content in these fluids ranges between 54.9 and 91.9%, while the emissions of H_2S, CH_4 and H_2 comprise $\leq$ 8.1%, $\leq$ 9.7%, and $\leq$ 3%, respectively (Botz et al., 1996; Dando et al., 2000). Hydrothermal fluids have been found to contain elevated concentrations of reduced inorganic chemicals, including NH_4^+ (up to 1 mM), Mn^{2+} (up to 0.4 mM) (Fitzsimons et al., 1997), and arsenic primarily in the trivalent oxidation state [As(III)] (in the range of 30 uM) (Price et al., 2013). Common occurrences near vent orifices include arsenic minerals and elemental sulfur precipitates, while sediment depressions often harbor dense brines (Dando et al., 2000).

Within the extreme conditions found in the Milos hydrothermal systems, biofilms and microbial mats can attain thicknesses of several centimeters (Figure 2), representing the most abundant biomass structures (Hall-Stoodley et al., 2004). These biofilms offer homeostasis in fluctuating environments, potentially mitigating variations in pH, oxygen levels, exposure to ultraviolet radiation, and detoxifying heavy metals while concentrating nutrients. By confining cells in close proximity, biofilms facilitate inter- and intra-specific chemical signaling and nutrient exchange (Hall-Stoodley et al., 2004; Garnett and Matthews, 2012; Patwardhan et al., 2021). The presence of thick white microbial mats, which form at the interface of an oxygen-rich environment, such as in contact with both seawater and a H_2S-rich environment, where hydrothermal fluids are discharged, is a prominent feature of hydrothermal systems on the seafloor (Sievert and Vetriani, 2012; Giovannelli et al., 2013; Yücel et al., 2013).

Despite their importance and visual prominence, the taxonomic and functional diversity of white mats in the Paleochori Bay has never been explored in response to hydrodynamics events. In this study, we combined 16S rRNA amplicon sequencing, from DNA and RNA, and metagenomic sequencing to investigate microbial community composition before, during, and after major storm events in Paleochori Bay. We also investigated mat structuring following hydrodynamic interactions with the sandy bottom. By integrating these approaches, we unravel the extent to which environmental perturbations shape microbial communities in SWHVs and provide new insights into the resilience and adaptability of biofilm-associated microbiota in fluctuating conditions. Our findings contribute to a broader understanding of the complex geobiological interactions governing hydrothermal vent ecosystems and highlight the importance of considering dynamic events when studying microbial diversity in geothermal ecosystems.

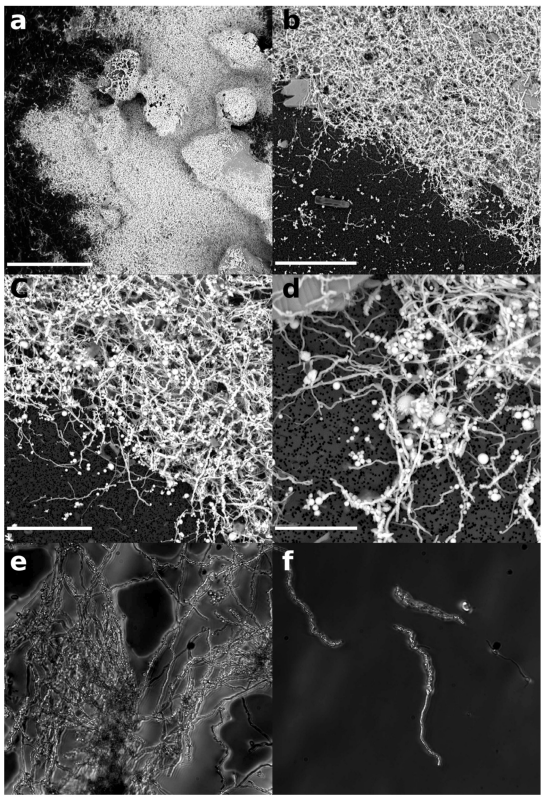

FIGURE 2
Scanning electron microscopy micrographs of Milos white microbial mats filtered onto a 0.22 µm filter. **(a)** A low-magnification overview of the microbial mats showing the high abundance of filamentous structures and the presence of large sand granules (scale bar 300 µm); **(b)** detail of a marginal section of the microbial mat structure showing the presence of long (20–50 µm) filaments and globular precipitates (scale bar 50 µm); **(c)** detail of the filamentous structures and globular precipitates. Each filaments is coated with a large number of small precipitates (scale bar 20 µm); **(d)** close up of the filamentous structures and globular precipitates (scale bar 10 µm); and **(e,f)** phase contrast micrograph of the filaments (1,000x). The globular precipitates are visible as bright spots under this light.

2 Materials and methods

2.1 Sites and sample collection

Samples were collected from May 21st to May 29th, 2012, from the shallow-water vents of Paleochori Bay in the island of Milos, Greece. The sampling site was characterized by shallow depth (9–13 meters) (Yücel et al., 2013) and the presence of thick microbial mats (Giovannelli et al., 2013; Puzenat et al., 2021; Le Moine Bauer et al., 2023), enabling close monitoring of the hydrodynamic disturbances impact on hydrothermal activity and microbial community (Figure 1). White mat samples used to assess the taxonomic and functional diversity were sampled during a period of calm sea state when the mats were mature and reached the thickness of a few centimeters. Samples for assessing the spatial changes in composition across small scales (i.e., at the scale of a single sand ripple) were acquired during the same period of time. Different coloured microbial mat samples were collected across sand ripples following the changes in the visual composition of the community from white, to yellow to brown. These changes occurred on sand ripples of 15–20 cm length from crest to crest. Samples used to analyze the microbial community composition after a major dynamic event were sampled before and after a 5 and 7 day period from a storm event with winds reaching up to 50 m s^{-1} (Yücel et al., 2013). All microbial mats samples were collected by SCUBA divers using sterile syringes and stored directly on the seafloor either in empty sealed hungate tubes or in hungate tubes pre-filled with RNAlater solution using a18G needle. Samples for molecular analysis were frozen 12 h after collection to allow for the

RNAlater solution to stabilize the mats. Aliquots of the mats were preserved in 2% glutaraldehyde for microscopy analysis.

2.2 Scanning electron microscopy and phase contrast microscopy

Fragments of the microbial mats preserved in glutaraldehyde (2% final concentration) were recovered on a 0.22 µm pore-size Nucleopore polycarbonate filter, then frozen at −20 °C, mounted on a temperature controlled sample holder, and visualized at −25 °C on a Phenom ProX microscope (Phenom World). Images were acquired at maximum resolution using either a 10 kV or 15 kV acceleration voltage. Energy-dispersive X-ray spectroscopy (EDS) was performed at 15 kV acceleration voltage using the Phenom ProX EDS module. Microbial biofilms were also observed under optical microscopy using phase contrast at 1,000x magnification.

2.3 RNA and DNA extractions

Community DNA was extracted from RNAlater-fixed biomass using a modified phenol:chloroform protocol, following the method outlined by Giovannelli et al. (2013). Briefly, biomass aliquots (ca. 0.5 mL) were centrifuged to remove the RNAlater solution, followed by the resuspension of the pellet in extraction buffer (100 mM Tris–HCl, 100 mM EDTA, 1.5 M NaCl pH 8.0) supplemented with lysozyme (10 mg mL^{-1}), and incubated at 37 °C for 30 min. Proteinase K (20 mg mL^{-1}) was added, followed by another 30 min-long incubation at 37 °C. The sample was then treated with 20% SDS and agitated at 60 °C for 1 h. Precipitates and cell debris were removed by centrifugation (5 min at 14,000 × g) and the supernatant was collected and extracted with 1 volume of phenol:chloroform:isoamyl alcohol (25:24:1, pH 8.0), followed by one extraction with chloroform:isoamyl alcohol (24:1). DNA was then precipitated overnight with sodium acetate and isopropanol, washed with 70% ethanol, and resuspended in PCR grade water. DNA was visualized on 1% agarose gel stained with ethidium bromide and quantified on a NanoDrop 2000 spectrophotometer (Thermo Scientific). RNA extraction was carried out using a similar procedure, with acidic phenol used instead of phenol:chloroform:isoamyl alcohol, and the pellet was resuspended in diethylpyrocarbonate (DEPC)-treated water. RNA samples were then treated with DNAse I TURBO DNA-free kit (Ambion) following the manufacturer protocol. This DNase treated RNA was reverse transcribed into cDNA using the Invitrogen cDNA synthesis kit (Invitrogen, Carlsbad, CA, United States), according to the manufacturer's specifications. Appropriate negative and no-RT control were carried out. Obtained cDNA was tested by PCR using 338F/517R bacterial primers targeting the 16S rRNA gene (Muyzer et al., 1993).

2.4 Pyrotag sequencing and analysis

Pyrotag amplicon sequencing was performed on the Roche 454 GS-FLX sequencer at MR DNA,[1] using the cDNA as template and the bacterial primer 27F mod and 530R (Dowd et al., 2008). White microbial mat samples collected before (on the 21st May 2012), during (on the 26th May 2012) and after the storm event (the 28th May 2012), along with samples of different mats collected across the sand ripple (yellow, orange and green) were subjected to DNA extraction and 16S rRNA gene amplicon sequencing, concluding a total of six samples. Pyrotag amplicon sequencing was performed as specified above, by targeting the variable regions V1-V3 with the Roche 454 GS-FLX sequencing platform at MR DNA (see text footnote 1) (Dowd et al., 2008).

Generated raw 16S rRNA gene sequences were processed and analyzed using the QIIME 1.8 software package (Caporaso et al., 2010). Pyrosequencing noise was removed by employing the Denoiser 0.91 (Reeder and Knight, 2010) included in QIIME. Chimeric sequences were removed using UCHIME (Edgar et al., 2011), included in USEARCH (6.0.152). We applied UCHIME in *de novo* mode to cluster sequences, as this has been shown to outperform closed reference clustering approaches (Westcott and Schloss, 2015). The determination of Operational taxonomic unit (OTUs) was performed with the UCLUST algorithm (Edgar, 2010) at 97% similarity, and a representative set was selected employing the QIIME scripts "pick_otus.py" and "pick_rep_set.py." Singleton were removed from the dataset. Taxonomic classification of selected reference sequences (OTUs) was performed by similarity searches using the Ribosomal Database Project naive Bayesian classifier, version 2.12 (Wang et al., 2007), included in QIIME with a cut off level of 0.80 on the assignment confidence. Therefore, all taxonomic affiliations used herein are based on those used at the time of the analysis. Individual OTUs represented by more than 10 sequences were searched against the EzTaxon database (Chun et al., 2007) in order to identify the closest cultured relative.

2.5 Metagenome sequencing and analysis

High quality community DNA extracted from the undisturbed microbial white microbial mat before the storm was submitted to MR DNA lab (see text footnote 1) for shotgun sequencing on the Roche 454 GS-FLX platform. Sequences obtained from the metagenomic shotgun sequencing were uploaded to MG-RAST webserver (Meyer et al., 2008), followed by a demultiplexing, quality and length filtering and dereplication steps. The obtained QC reads were analyzed using the built in MG-RAST pipeline and downloaded for downstream analysis. The raw fastq sequences were analyzed using webMGA (Wu et al., 2011) and Real Time Metagenomic (Edwards et al., n.d.) web servers. Sequences were screened for ribosomal RNA genes using RNAmmer (Lagesen et al., 2007) and Metaxa (Bengtsson et al., 2011). Obtained 16S rRNA sequences were clustered and classified using UCLUST and the RDP classifier as described above. Metaphlan2 (Truong et al., 2015) was used for taxonomic profiling of the entire metagenome. Quality checked reads downloaded from MG-RAST were assembled into contigs using the CLC genomic workbench. Gene calling was performed on the obtained contigs using prodigal (Hyatt et al., 2010). Obtained coding sequences were analyzed using NCBI blastp service (McGinnis and Madden, 2004) against the non-redundant database and the KEGG GostKOALA web service (Kanehisa and Goto, 2000). Given the high amount of reads assigned to viruses, the quality checked reads were uploaded to MetaVIR

1 http://www.mrdnalab.com

(Roux et al., 2011). All raw data is available through ENA Bioproject PRJEB88540.

To link taxonomic classification to functional potential, representative OTU sequences were analyzed using BLAST (McGinnis and Madden, 2004) against the NCBI non-redundant database, allowing for functional assignment based on sequence homology.

2.6 Fluid flow model generation

The effects of hydrodynamic forcing in sand ripples at the vicinity of the shallow-water hydrothermal systems were inferred by applying both the Lattice Boltzmann Method (LBM) and Finite Volume Method (FVM) to model the interaction between the tide and shear imposed fluid flow, thermal advection and an obstacle represented by a sand ripple. The FVM was adopted to solve the flow model, based on the Navier–Stokes equations with a momentum sink term to represent soil porosity. Specifically, a colocated unstructured FVM strategy was used (Greenshields and Weller, 2022). Furthermore, all diffusive terms and pressure gradients were approximated with second-order accuracy, while the convective terms were discretized using a linear-upwind approach. The aforementioned solution strategy was implemented within the well-known object-oriented OpenFOAM open-source library.

We performed lattice Boltzmann modeling (LBM) simulations to examine water flow around and through a simplified ripple geometry. Flow within the computational domain was driven by imposing a constant horizontal velocity at the upper boundary, simulating shear flow conditions. Both the ripple structure and the underlying sand bed were represented as porous media, permitting fluid penetration to a limited extent. In addition, a vertical temperature gradient was imposed throughout the domain. This gradient was deliberately set below the threshold required to induce natural convection, thereby ensuring that heat transport within the system occurred exclusively via advection associated with the imposed horizontal flow. Model parameters, including upper boundary flow velocity, sediment porosity, and the magnitude of the temperature gradient, were selected based on typical environmental conditions observed in sediment-water interaction scenarios (Precht and Huettel, 2004).

The code for implementing this LBM was written in C with MPI routines for parallelization. It can be found at the following github repository: https://github.com/giovannellilab/Milos_white_mats.

3 Results

3.1 Microbial mat structure and microscopic observations

A close association between the curved non-branching filaments and the small bright granules emerged from phase contrast observations of the microbial mat (Figure 2). Granules with diameters below 2 µm appeared to be attached to the outer surface of the filaments. The white microbial mat structure did not present classic evidence of well structured exopolysaccharides, but was composed of a network of loosely packed microbial filaments and mineral precipitates. EDS analysis of the larger granules revealed the presence of dominant sulfur peaks, suggesting the presence of sulfur-rich mineral phases, possibly including oxidized sulfur species and elemental sulfur precipitates. We also identified additional minerals embedded in the mat filaments, such as manganese oxide and arsenic sulphides. Individual cells shaped like elongated, curved rods and measuring 1.5–2 µm in length were visible under phase contrast, though they were not consistently present across all samples. The samples included a variety of microbial morphologies, such as vibroids, cocci, and rods. Filaments were the most abundant morphology observed. The granules were bright under phase contrast (Douglas, 2000; Kümpel et al., 2023).

3.2 Taxonomic and functional diversity of the white microbial mat community

The diversity and activity of the resident microbial community were investigated by analyzing and comparing the V1-V3 variable regions of the 16S rRNA gene transcripts, thus representing the actively transcribing community, with genes encoding for the 5S, 16S, and 23S rRNA extracted from the shotgun metagenomic sequencing (Figure 3). A total of 4,294 reads from the 16S rRNA gene transcripts sequencing passed quality control steps and were clustered in 804 unique OTUs at 97% similarity. The library is dominated by sequences belonging to the Proteobacteria (91%—all percentages refer to relative abundances), with the majority belonging to the Epsilonproteobacteria class (90.6%, now classified as Campylobacterota), and a small fraction not assigned to any known Proteobacteria class (0.4%; Figure 3a). The majority of the remaining sequences (8.5%) was not classified in any known bacterial phyla, while a very small fraction (0.5%) was classified into the candidate division GN02. Within the Epsilonproteobacteria, 23.8% was classified as belonging to the *Sulfurimonas* genus, 6.1% to *Arcobacter* genus, and 1.3% to the *Sulfurovum* genus. The remaining sequences within the Epsilonproteobacteria class were evenly classified as unidentified *Helicobacteraceae* (29.6%), and unidentified Epsilonproteobacteria (29.8%). A search of all the OTUs (each represented by more than 10 sequences) against the EzTaxon database revealed very low similarities (between 89 and 93%) against cultured strains, even for sequences for which the Ribosomal Database Project (RDP) classifier returned high confidence of assignment to specific genera.

A total of 559 partial 16S rRNA genes were recovered from the metagenomic library. The sequences were dominated by the Proteobacteria phylum (87.9% of the 16S rRNA sequences), followed by the Bacteroidetes (5.3%; Figure 3b). The remaining 16S rRNA sequences were represented by uncultured bacteria (6.9%). At the class level the Proteobacteria sequences were evenly assigned to the Epsilon- and Gammaproteobacteria class (41 and 36.9%, respectively), followed by unidentified Proteobacteria (9.4%), uncultured Bacteria (6.9%) and a small percentage of sequences assigned to the Alphaproteobacteria class (0.5%). The sequences belonging to the Epsilonproteobacteria were further assigned to the genera *Arcobacter* (21.9%), *Sulfurimonas* (11.6%), and *Sulfurospirillum* (2.1%), with the remaining sequences classified as either unidentified *Helicobacteraceae* (2.2%) or unidentified *Campylobacterales*. The sequences belonging to the Gammaproteobacteria were dominated by sequences closely related to the genera *Pseudoalteromonas* (11.8%), *Vibrio* (4.7%), *Marinomonas* (3.4%) and other unidentified *Vibrionales* (2.6%). The sequences

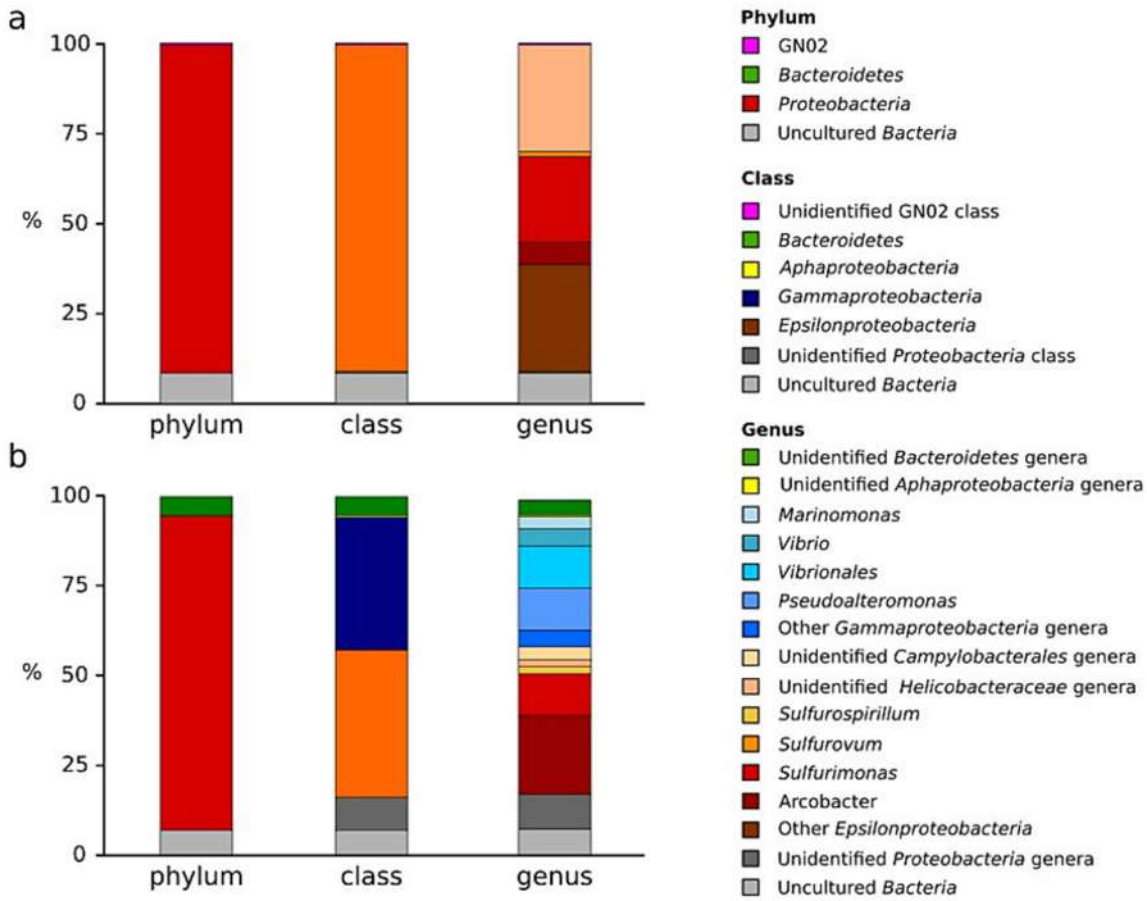

FIGURE 3
Comparison of the prokaryotic diversity in the single sample from the undisturbed microbial white mat before the storm event estimated using **(a)** the cDNA 16S rRNA pyrotags (active community) and **(b)** DNA (16S rRNA extracted from the metagenome). Taxonomic affiliation of the sequences is presented at the phylum, class and genus level.

related to the Alphaproteobacteria class of the Proteobacteria and the Bacteroidetes were not identified at the class or genus level.

Metagenomic shotgun sequencing of the white microbial mat resulted in 264,257,917 bp in 1,284,013 reads. These were assembled in a total of 3,988 contigs (N50 = 3,407 bp, total contigs length of 7,796,078 bp). Functional assignments made through the use of Kegg Orthologues (KO) and Enzyme Commission numbers (EC) on the MG-RAST database resulted in a diverse number of assigned reads (259,784 and 130,269 counts, respectively; Figure 4). By contrast, functional assignment using NCBI Protein Cluster through WebMGA and the RAST Subsystem database through Realtime MG yielded 149,920 and 3,205,896 assigned reads, respectively (Supplementary Table 1).

3.2.1 Carbon and energy metabolism

The high abundance of sequences assigned to genes encoding for ATP citrate (*Pro-S*) lyase (*aclA*; up to 476 reads), for 2-oxoglutarate:ferredoxin oxidoreductase (*korA*; up to 814 reads) and for pyruvate:ferredoxin oxidoreductase (*porA*; up to 788 reads), key genes for the rTCA cycle, suggests that carbon fixation through this pathway was highly represented in the white mat metagenome (Hügler et al., 2005; Fuchs, 2011). Likewise, the identification of sequences assigned to the bifunctional carbon monoxide dehydrogenase/acetyl-CoA synthase gene (*codH/acs*; up to 43 reads), and to the formate dehydrogenase complex (*fdh*; up to 788 reads) hint to the relevance of the Wood–Ljungdahl pathway, also known as the reductive acetyl coenzyme A pathway.

The high number of sequences assigned to genes encoding for the SOX (sulfur oxidation) complex (up to 550 reads), responsible for the oxidation thiosulfate and sulfide, suggests that all major prokaryotic sulfur oxidation pathways typical of geothermal environments were widespread in the white microbial mat community (Ghosh et al., 2009; Chen et al., 2022). All subunits of the SOX gene complex are detected in our dataset, suggesting the presence of a complete thiosulfate oxidation pathway in the white mat microbial community. In addition, genes associated with both assimilatory and dissimilatory sulfate reduction pathways are present, indicating that the community held the potential for multiple sulfur transformations (Figure 4) (Weissgerber et al., 2013; Dahl, 2017).

We retrieved a consistent set of nitrogen cycle-related sequences across all five annotation databases. Specifically, we identified sequences assigned to gene *nifH* (up to 178 reads) encoding one subunit of nitrogenase, the enzyme complex responsible for biological

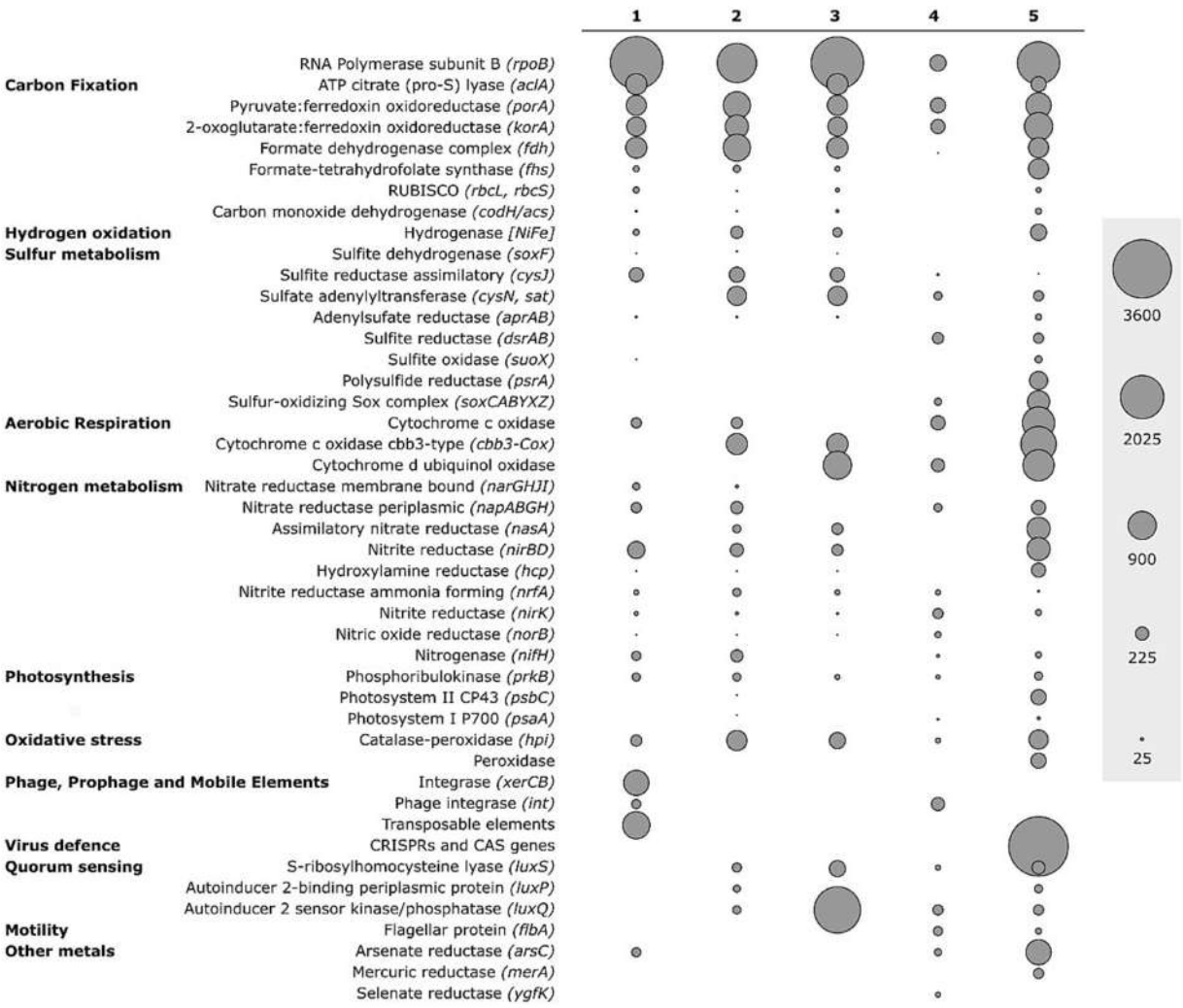

FIGURE 4
Abundance of reads assigned to key functional genes in the microbial mat metagenome using different approaches: (1) genes assigned to functions in the Kyoto Encyclopedia of Genes and Genomes (KEGG); (2) genes assigned to KEGG KO numbers using MG-RAST; (3) genes assigned to Enzyme Commission numbers using MG-RAST; (4) genes assigned to functions against the NCBI Protein Cluster database using WebMGA; (5) genes assigned to the RAST Subsystem database using Realtime MG. Raw gene counts are shown in Supplementary material.

nitrogen fixation under anaerobic or microaerobic conditions (Mehta et al., 2003; Chen et al., 2023). In addition, sequences assigned to genes involved in dissimilatory nitrate reduction and denitrification pathways were recovered, including *narGHJI* (up to 62 reads), *napA* (up to 215 reads), *nirB* (up to 565 reads), *nirK* (up to 112 reads), *nrfA* (up to 75 reads), and *norB* (up to 47 reads), indicating the potential for both respiratory and dissimilatory nitrate/nitrite reduction mechanisms (Pérez-Rodríguez et al., 2013; Reyes et al., 2017; Patwardhan et al., 2021, 2023). Sequences assigned to gene *nasA* (up to 589 reads), encoding the nitrate reductase involved in assimilatory nitrate reduction, were also present, supporting the role of nitrate as a nutrient source in this community.

Oxidative phosphorylation in the white mat microbial community appeared to be facilitated by the presence of multiple terminal oxidase complexes and oxidative stress defense enzymes. Of significance is the presence of the cytochrome c oxidase cbb3-type gene (*cbb3-Cox*; up to 506 reads). Furthermore, our analysis revealed the presence of sequences assigned to catalase-peroxidase gene (*hpi*, up to 435 reads) and bacterial cytochrome c peroxidase gene (*ccp1;* 249 reads).

3.2.2 Additional functions: mobile elements, quorum sensing and motility, and heavy metal detoxification

The analysis highlighted the presence of sequences assigned to phage integrase-related genes (*xerC*; 692 reads), which encode proteins mediating unidirectional site-specific recombination between the phage attachment site (attP) and the bacterial attachment site (attB) on two DNA recognition sequences (Groth and Calos, 2004).

Our read-based analysis revealed the presence of genes encoding for autoinducer ligands (*luxS*), which are released by bacteria to monitor cell density. The presence of the gene *flbA* encoding for a flagellar protein, further highlights motility related to quorum sensing.

Our sample shows the presence of sequences assigned to key genes involved in heavy metals detoxification pathways, such as arsenate reductase (*arsC*; up to 687 reads), mercury reductase (*merA*; up to 130 reads) and selenate reductase (*yfgK*; up to 32 reads).

3.2.3 Taxonomic affiliation of the functional genes

To better understand the diversity of the microorganisms involved in diverse biogeochemical pathways, we taxonomically annotated the main functional genes of each major element cycle, showing interesting relationships between microbial diversity and functions in the SWHV white mat (Figure 5). This analysis revealed that the genes involved in the rTCA cycle, dissimilatory nitrate reduction, denitrification, thiosulfate oxidation and *CAS* genes were assigned to Epsilonproteobacteria. The relative abundance of *aclA* is divided among *Sulfurimonas* (46.4%), *Sulfuricurvum* (32.9%), *Sulfurovum* (9.3%) and other related genera (11.3%). The taxonomic assignment of the functional genes was consistent with the microbial composition obtained with the 16S rRNA transcripts (Figure 5). Thiosulfate oxidation gene (*soxC*) sequences were assigned to *Sulfurimonas* (58.2%), *Arcobacter* (36.9%) and *Nitratifractor* (3.5%) taxonomic groups. Dissimilatory nitrate reduction and denitrification (*napA*) showed a similar distribution compared to *soxC*, with high dominance of *Sulfurimonas* (69.1%), and differed from the latter as *napA* is also consistently assigned to Gammaproteobacteria (*Vibrio* 16.1% and *Alteromonadales* 4.8%). In relative abundance, CAS genes were dominated by the genera *Campylobacter* (28%), *Sulfurospirillum* (20.5%) and *Arcobacter* (10.2%). The diversity data about transposon and phage integrase gene (*int*) showed, contrary to the others genes, a dominance of Gammaproteobacteria (59.5% of taxonomically annotated genes), followed by Epsilonproteobacteria (21.1%).

3.3 Changes in microbial community composition before and after a storm event

Field observations and microscopy analysis suggest that the microbial mat is loosely attached to the sandy seafloor, likely as a result of benthic deposition due to the presence of a high percentage of minerals attached to the microbial filaments and dispersed in the matrix. Rapid movements of the SCUBA divers or increased lateral fluid flow near the seafloor due to currents and waves can easily resuspend the mats that dissolve in seawater creating a milky resuspension (Figure 6). Hydrodynamic stress and water column mixing is minimal during periods of calm sea conditions, allowing the establishment of the white microbial mats around the outflow zones of the shallow vent, and leading to the creation of stable white patches that might grow to several cm thickness (Figures 2, 6A). Our data show that immediately prior to a storm, the white mat community was dominated by *Arcobacter* (78.3%), followed by a lower percentage of *Sulfurimonas* and unclassified bacteria (16.3 and 2.5%, respectively). During the storm events, the white mat disappeared due to blowing of South-East (SE) wind, characterized by velocities up to 50 m s^{-1}. The storm also determined a shift in the sulfide and temperature regime of the vent (Figure 6B; Yücel et al., 2013). The white mats reappeared as thin white layers one day after the storm. The samples taken one day after the disturbance

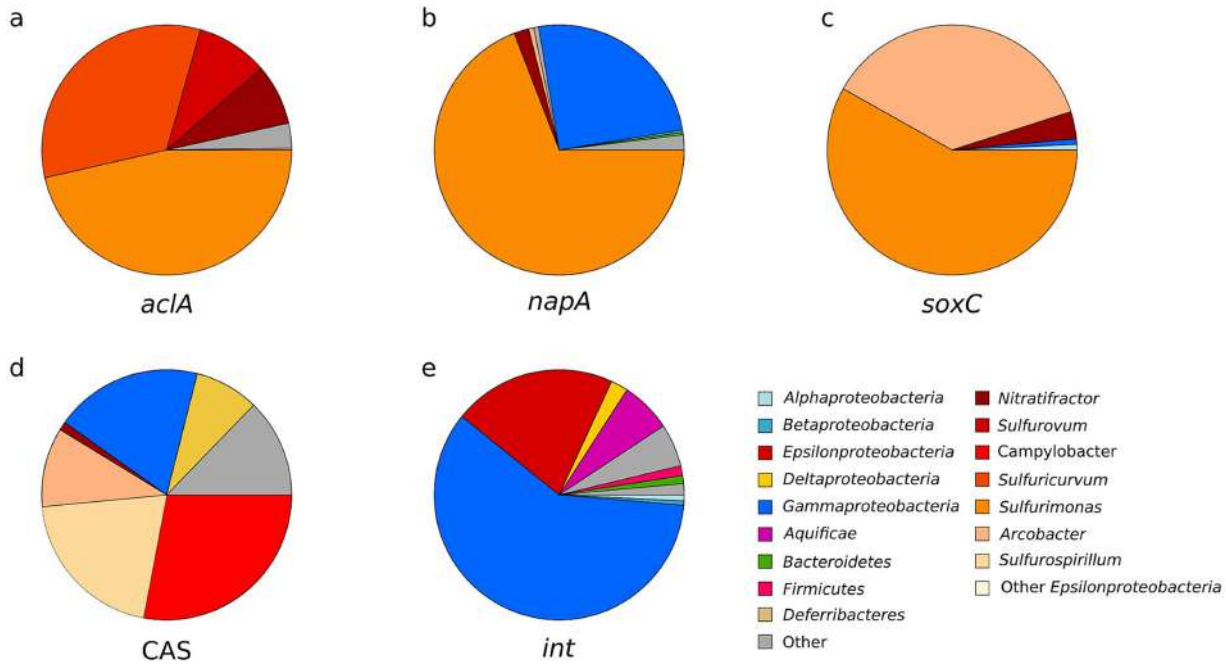

FIGURE 5
Taxonomic affiliation and relative abundance of key selected genes recovered in the metagenome. Diversity of recovered ATP citrate lyase alpha subunit gene *aclA* **(a)**; periplasmic nitrate reductase catalytic subunit gene *napA* **(b)**; thiosulfate oxidation protein coding gene *soxC* **(c)**; CRISPR associated sequences gene diversity **(d)**; and diversity of transposon and phage integrase gene *int* **(e)**. In all plots the diversity of sequences associated with the Epsilonproteobacteria is shown at the genus level, except in plot **(e)**, where the sequences are combined at the class level.

10.3389/fmicb.2025.1649514

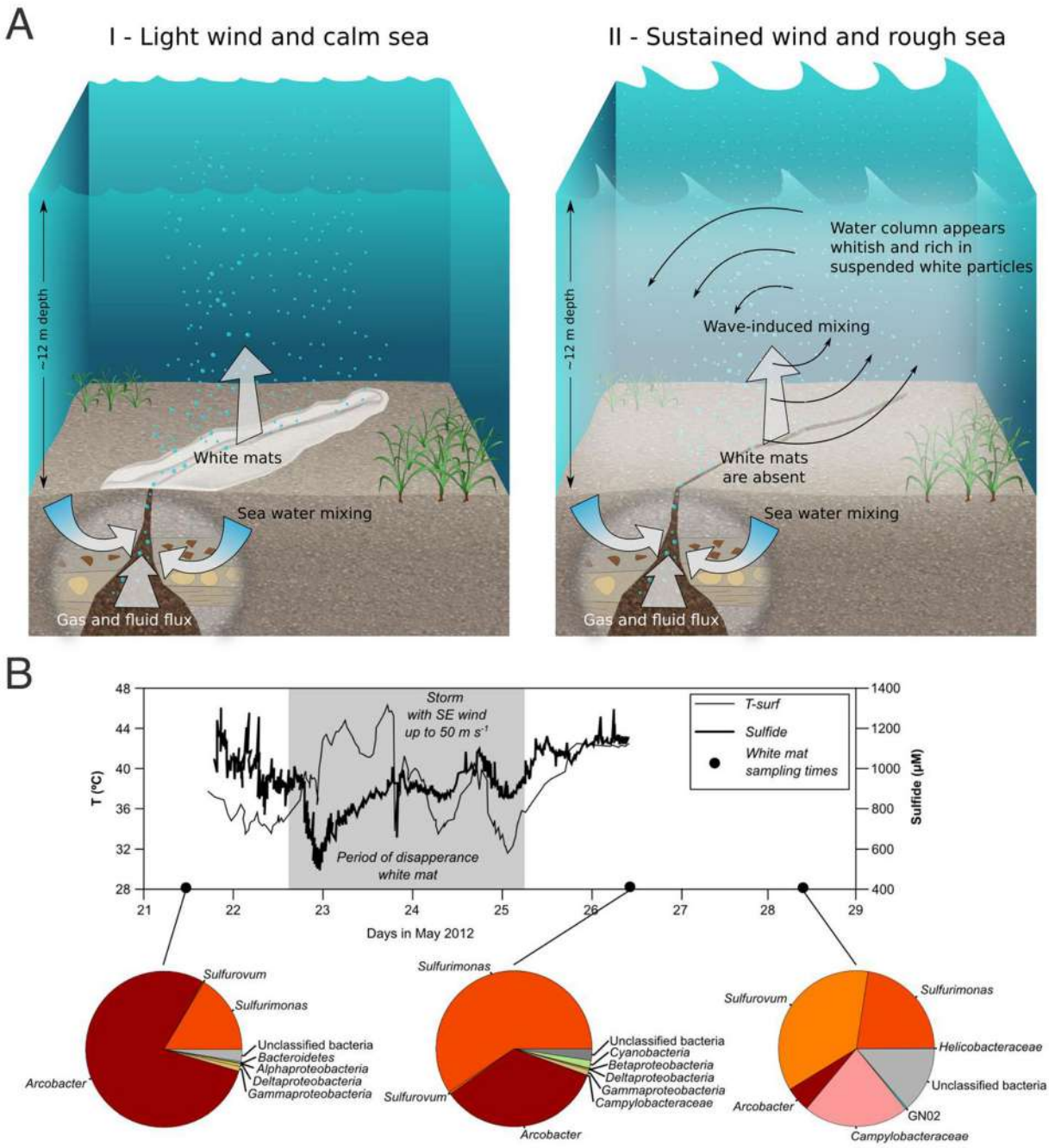

FIGURE 6
(A) Reproduction of establishment and disruption of white mat precipitate in response to hydrothermal fluid emissions. Dynamics of the site under light wind and calm sea (I), during which the SCUBA Divers observed the deposition of the white precipitate and fluid emissions unaffected by currents. Dynamics of the site under sustained wind and rough sea (II), during which the SCUBA Divers observed the disruption of the white mat precipitate and its related resuspension, resulting in a whitish water column rich in suspended material. **(B)** Time series of *in situ* sensor measurements coupled with temporal changes in the microbial community based on cDNA 16S rRNA amplicons. The gray area indicates the approximate timing of the high wind and wave conditions and the corresponding mat-free period. In this period, maximum wind speeds approaching 50 m s^{-1} were recorded on May 23rd. Temperature close to the surface of the sediment (10 mm depth, 0.5 m away from the vent center) is represented by a thin black line. The total dissolved sulfide time series at 10 mm below the sediment–water interface is indicated by a bold line. Sampling to understand the community composition and its variation over time are conducted, respectively, one day before disturbance (pre-storm conditions), one day after it (post-storm conditions—mats re-establishment) and three days after it (post-storm conditions—mats development).

event showed a shift in community toward dominance of *Sulfurimonas* (59.1%), with a lower abundance of *Arcobacter* (34.4%). Notably, *Cyanobacteria* relative abundance increased after the storm event (1.6% compared to pre-storm abundance of 0.3%). Three days after the disturbance event, there was a further shift to a community dominated by *Sulfurovum* (36.2%) and *Sulfurimonas* (22.5%), with an additional decrease of *Arcobacter* (5.2%), disappearance of *Cyanobacteria,* and higher abundance of

Campylobacteraceae (22.0%) and unclassified bacteria (13.8%) (Figure 6).

3.4 Fluid flow across the sandy bottom

The interaction of buoyancy-driven fluid flow discharge with ripple topography modifies the direction and mixing of vent fluids. As hot, buoyant fluid convects upward from subsurface conduits, it encounters lateral flow from bottom currents driven by regional circulation and surface wind forcing. When this convective upwelling intersects ripple crests and troughs, it generates heterogeneous flow regimes, including zones of focused upwelling, lateral shear, and recirculation eddies. It is very important to put evidence that ripple shape induces flow acceleration over the ripple crest and a consequent pressure drop in accordance with the Euler equation in streamlines coordinates (Supplementary Figure S1A). The deriving pressure field generates a vertical stream (Supplementary Figure S1B); on the contrary high pressure zones in the ripple troughs inhibit discharge or can produce a lateral flow. Moreover, the aforementioned pressure difference produces a mixing layer between the involved fluids and the resulting effect is chemical species gradients spatial variability.

Actually, ripple shape produces a particular flow field with a strong heterogeneity in fluid chemical composition, temperature, and redox conditions over centimeter scales. Crest regions may be more exposed to oxygenated seawater, while troughs trap reducing hydrothermal fluids, creating sharp horizontal and vertical gradients in electron donors and acceptors. As a result, the relative contribution of hydrothermal versus seawater inputs varies dramatically across the ripple, directly shaping the chemistry of porewater and the structure of microbial mats growing on the surface. These microscale variations help explain the spatial patchiness observed in microbial community structure and function described in Section 3.4.

We conducted LBM studies of the flow around and through a simplified ripple shape. The driving force of the flow was an assumed constant velocity (horizontal shear flow) upper boundary (the upper layer of grid cells). The ripple and sand bed are assumed porous so there is a modest flow through both. We see in Supplementary Figure S1 that there is boundary layer separation due to the ripple, and a subtle recirculation eddy on the lee side of the ripple. We impose a vertical temperature gradient, as shown in the lower panel of Supplementary Figure S1C. However, this temperature gradient is not sufficient to drive natural convection, hence advection of heat occurs only due to the flow past the ripple (the eddy described above).

3.5 Spatial variability in microbial community composition across a sand ripple

Near the venting location in the shallow-water hydrothermal systems in Paleochori Bay we observed microbial mats of different colours (e.g., white, yellow, light brown and brown mats) in close proximity following single sand ripples. Analysis performed on these differently coloured mats provide insights into the short-scale spatial variability of microbial communities in these systems (Figure 7). White colored mats were consistently present in the sand ripple valleys, and yellow and brown colors appeared to be preferentially located on the sand ripple flank and crest. This distribution suggested a physical control over the microbial composition of the mats.

White mat composition has been described in section 3.2 (Figures 3, 7). The yellow mat community was dominated by *Proteobacteria* (68.2%). At the class level, *Epsilonproteobacteria* dominated the community (64.0%), with a high abundance of *Arcobacter* (28.2%). In contrast, the light brown mat showed higher variability at the class level, with a similar abundance of *Proteobacteria* (66.6%), but a reduced proportion of *Epsilonproteobacteria* (46.7%), showing differences with the white mat due to a higher percentage of *Deltaproteobacteria* and *Gammaproteobacteria* (12.0% and 7.0%, respectively). The brown mat, compared to the other types, showed increased differences, with a lower proportion of *Proteobacteria* (36.4%) represented mainly by sequences belonging to the *Epsilonproteobacteria* class (27.2% of the total). The genus *Arcobacter* was less represented when compared to the other types of mat (18.5%). The *Cyanobacteria* abundance varied across the sand ripple surface, increasing from the yellow mat to the brown mat (26.6% in the yellow mat; 26.0% in the light brown mat; 57.6% in brown mat). Moreover, we observed a decreasing gradient of *Sulfurimonas* presence along the sand ripple surface, which lowered towards the brown mat (35.3% in the yellow mat; 18.1% in the light brown mat; 8.1% in the brown mat).

4 Discussion

4.1 White mat diversity and composition

Shallow-water hydrothermal vents are ubiquitous systems in coastal marine environments characterized by volcanic activity (Price and Giovannelli, 2017). The primary productivity in these systems is driven both by photosynthesis and chemosynthesis carried out by diverse microbial groups (Tarasov, 2006; Dando, 2010). The relative contribution of the two is controlled by complex physical and chemical interactions between the advecting fluids, the seafloor features and seawater column processes (Price and Giovannelli, 2017; Giovannelli and Price, 2019). Biofilm and microbial mats represent an important strategy for microorganisms to colonize these dynamic ecosystems and constitute the base of the food web sustaining local diversity and possibly exporting carbon and nutrients to neighboring ecosystems (O'Brien et al., 2015; Sciutteri et al., 2022). Milos shallow-water hydrothermal vents are dominated by white microbial mats loosely attached to the sandy bottom in areas of hydrothermal fluid discharge (Giovannelli et al., 2013; Price et al., 2013; Yücel et al., 2013). The mat exhibits a filamentous structure intertwined with sulfur-rich granules (Sievert et al., 1999), either attached to filaments or dispersed within the matrix. The composition of the biofilm communities shows similarities to those found in other shallow hydrothermal vent systems worldwide (Kamenev et al., 1993; Dando et al., 1999; Wenzhöfer et al., 2000; Cardigos et al., 2005; Lentini et al., 2014). Elemental analysis (EDS) of the sulfur granules confirms their composition (Figure 2). The detection of sulfur-oxidizing bacteria, particularly *Epsilonproteobacteria,* in the active fraction of the community, further supports their possible role in the biological mediated precipitation of sulfur granules. Members of this class, especially the genus *Arcobacter*, have been implicated in filamentous sulfur structures in similar environments (Sievert et al., 1999, 2007; Wirsen et al., 2002). This functional role is further corroborated by the abundance of *sox* gene

10.3389/fmicb.2025.1649514

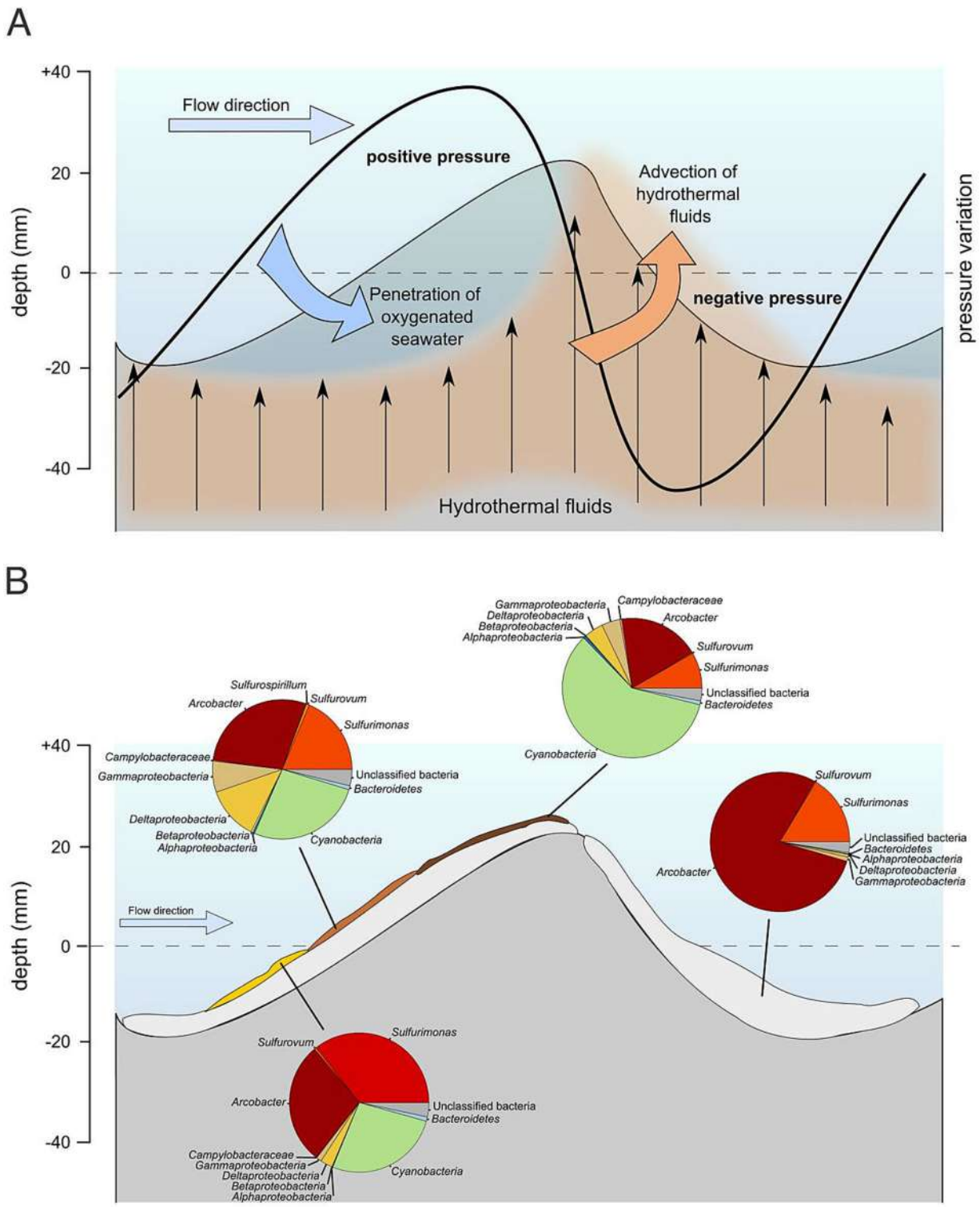

FIGURE 7
(A) Proposed model depicting the dynamics of water flow surrounding the vent structure and its interaction with vent fluid emissions. The area under consideration extends to a depth of 20–40 mm within the sediments. The outflow of hydrothermal fluids creates a void, generating negative pressure, which in turn establishes a positive pressure gradient from top to bottom inside the sand ripple. The flow direction of water currents facilitates the thinning of the benthic boundary layer over the gentle slope of the ripples, enabling increased oxygen penetration into the sediments and facilitating the growth of associated microbial mats. **(B)** Microbial community gradient established by different degree of oxygenation and its comparison with a community of the opposite side of the ripple (steep one) rich in H_2S. Differences regarding the composition in phototrophic players are created by different oxygenation of the geo-biological system. The light-grey layer beneath the colored microbial mats (yellow, Siena red, brown) represents the underlying white microbial mat that serves as a basal layer upon which the overlying colored microbial communities develop.

clusters identified in the metagenomic dataset, which include genes such as *soxB,* key components of the sulfur oxidation pathway known to lead to the accumulation of elemental sulfur as an intermediate (Friedrich et al., 2005; see below section 4.2). Altogether, given that both biotic and abiotic processes can generate such structures, the strong microbial activity observed in this site (Giovannelli et al., 2013) likely plays a key role in their formation.

The higher abundance of *Sulfurimonas* spp. in the 16S rRNA transcriptome (Figure 3a) could be related to their metabolic flexibility, such as the utilization of a wide range of electron donors of geothermal origin, including sulfide, sulfur, thiosulfate, sulfite, and hydrogen, while employing nitrate, nitrite, or oxygen as electron acceptors. *Sulfurimonas* spp. have been shown to use CO_2 as their primary carbon source, though some species have also been reported to metabolize acetate (Giovannelli et al., 2013; Labrenz et al., 2013). Similarly, *Arcobacter* and *Sulfurovum* genera exhibit wide metabolic flexibility in the usage of several electron donors and acceptors of hydrothermal origin (Xie et al., 2021). Previous studies have shown the *Arcobacter* spp. implication in sulfur filaments formation within the white mats of Milos shallow vents (Sievert et al., 2007). Additionally, members belonging to *Sulfurimonas* have been widely described in other shallow water and deep-sea hydrothermal systems (Wang et al., 2017, 2021). The presence of an active community with distinct members that use multiple species of sulfur as electron donors hints at their ecological adaptation to shallow water hydrothermal systems and at their crucial roles in the sulfur cycle therein. Notably, no sequences associated with the Gammaproteobacteria genus *Galenea* (Giovannelli et al., 2012), a chemolithoautotrophic thiosulfate oxidizing organism originally isolated from Milos shallow vents, have been found in the libraries. This could be due to its low abundance at the time of sampling, or to biases in the annotation database used.

In contrast to the active community revealed by 16S rRNA transcripts (Figure 3a), the total resident community captured by 16S rRNA genes in the metagenomes (Figure 3b) shows a higher abundance of *Gammaproteobacteria* and *Bacteroidetes*. Among *Gammaproteobacteria*, the genus *Pseudoalteromonas* is notably dominant, aligning with its known roles in organic matter degradation and metabolite production in marine hydrothermal systems (Sievert et al., 1999; Patwardhan et al., 2021; Lu et al., 2020; Price and Giovannelli, 2017; Holmström and Kjelleberg, 1999). Other notable genera include *Vibrio*, and *Marinomonas*, both associated with nutrient cycling and adaptability to hydrothermal fluid interactions (Huang et al., 2020; Huber et al., 2003). This comparison revealed that the active community represents only a fraction of the total resident microbial groups. The active taxonomic groups do correspond to a substantial proportion of the total community, while the low-abundance genera are metabolically inactive, quiescent.

The observed groups are well known members of the water column; their detection in the gene (but not transcript) dataset suggests they are delivered to the white mats by the short-scale circulation patterns reported by Yücel et al. (2013). This mechanism works in a way that microbial taxa present and active in the water column are trapped by short scale hydrothermal recharges in the white mats that act as a mechanical filter. This brings into the active mats, dominated by Epsilonproteobacteria, new trophic and genetic resources, potentially sustaining the heterotrophic community and favouring lateral gene transfer between the water column genetic pool and the hydrothermally sustained active white mat community. This hypothesis is supported by the presence of integrase and CAS associated genes in the white mat metagenome that are of gammaproteobacterial origin (Figure 5).

Viral analysis revealed the predominance of dsDNA viruses primarily from the order *Caudovirales*, including families *Siphoviridae*, *Myoviridae*, and *Podoviridae* (Supplementary Figure S2). These phages likely play a role in microbial population control and horizontal gene transfer, potentially influencing community structure and metabolic capacity (Howard-Varona et al., 2020).

4.2 White mat contribute to carbon, sulfur and nitrogen cycling in Milos shallow vents

The microbial communities inhabiting shallow-water hydrothermal vents off Milos, Greece, exhibit a diverse functional profile. The high abundance of genes involved in the rTCA cycle suggests this might be the primary pathway for carbon fixation, consistent with the dominance of Epsilonproteobacteria, particularly *Sulfurimonas*, *Sulfuricurvum*, *Sulfurovum* which rely on this cycle (Hügler and Sievert, 2011; Wang et al., 2017). This metabolic strategy, common in both shallow and deep-sea hydrothermal vents, likely reflects adaptation to CO_2-rich conditions from magmatic degassing and the microaerophilic to anaerobic conditions (Hügler and Sievert, 2011; Giovannelli et al., 2013; Wang et al., 2017). Epsilonproteobacteria have been previously identified as major chemoautotrophs in similar systems, supporting their role as primary producers (Tarasov et al., 2005; Giovannelli et al., 2013; Wang et al., 2015).

Sulfur metabolism is well-represented with a strong presence of *sox* genes associated with sulfur oxidizing bacteria, particularly Epsilonproteobacteria (Dahl, 2017; Patwardhan et al., 2021). Thermodynamic calculations of the Milos shallow water vents systems suggest thiosulfate/sulfide oxidation through the SOX pathway as highly energy-efficient for chemolithotrophs (Lu et al., 2020). Genes such as *soxCD* and polysulfide reductase indicate a mix of sulfur-storing and non-storing microorganisms, supporting the biogenic origin of sulfur globules seen microscopically (Dahl, 2017). The detection of genes involved in both sulfur oxidation (*sox* genes) and those typically linked to sulfate reduction (*sat*, *aprAB*, *dsrAB*) highlights the metabolic versatility of the community in adapting to sulfur-rich conditions. While these genes are commonly associated with dissimilatory sulfate-reducing pathways (Pereira et al., 2011; Müller et al., 2015), their potential bidirectional function, including use in oxidative sulfur metabolism (Dahl, 2017), prevents definitive assignment of functional direction. Nonetheless, their co-occurrence suggests the community harbors both oxidative and reductive sulfur metabolic potential, consistent with dynamic redox conditions at hydrothermal vents.

Nitrate reduction is another prominent pathway. The *napA* gene, involved in nitrate reduction, was the most abundant and mainly attributed to *Sulfurimonas*. Its presence is widespread in Epsilonproteobacteria from marine hydrothermal systems, and the enzyme's high affinity for nitrate may be related to the adaptation to environments with low nitrate concentrations, such as hydrothermal vents (Vetriani et al., 2014) and other nitrate-limited habitats (Han and Perner, 2015). This aligns with previous studies that have linked the process of denitrification to *Sulfurimonas denitrificans*. This process plays a critical role in balancing the nitrogen and carbon

cycles in hydrothermal vent ecosystems by regulating nitrogen availability and supporting microbial metabolism (Grote et al., 2012; Sievert and Vetriani, 2012). Additional genes for dissimilatory nitrate reduction, assimilatory nitrate reduction, and nitrogen fixation suggest flexible nitrogen cycling strategies with oxygen-limited zones (Vetriani et al., 2014; Sievert and Vetriani, 2012; Tang et al., 2013). Dissimilatory nitrate reduction and denitrification (n*apA*) have mainly been attributed to the genus *Sulfurimonas* (69.1%) in our reads, but these pathways differ as to the association to Gammaproteobacteria (*Vibrio* 16.1% and *Alteromonadales* 4.8%, respectively). These data indicate that a significant fraction of the chemolithoautotrophic production at shallow-water vents could be coupled to nitrate reduction.

Aerobic and microaerophilic oxygen respiration appears to be supported by cytochrome c oxidase (cbb_3-COX), which can be coupled with the oxidation of H_2S and thiosulfate found in white mat areas (Yücel et al., 2013). In these environments, microaerophilic bacteria thrive at the interface where oxygen (O_2) and hydrogen sulfide (H_2S) gradients meet (Yücel et al., 2013). The cbb3-type cytochrome c oxidase is particularly well adapted to these conditions as it has a high affinity for oxygen, allowing bacteria to efficiently respire in low-oxygen (microaerobic) zones while simultaneously oxidizing sulfide (Smirnov et al., 2009). Cytochrome c oxidase affiliated with the *Sulfurimonas* genus (Labrenz et al., 2013), and other Epsilonproteobacteria (Campbell et al., 2006) support its functional role as terminal enzymes in the bacterial respiratory chain (bd complex) (Borisov et al., 2011, 2021). The detection of cytochrome c (Cyt-c) further indicates a complete electron transport chain, acting as a soluble electron carrier that facilitates electron flow between dehydrogenases and terminal oxidases (Kranz et al., 2009). Together, the co-occurrence of cbb3-type, Cyt-bd, and Cyt-c enzymes supports the idea that these microbial communities are well-adapted to the fluctuating redox conditions typical of shallow-water hydrothermal vent systems (Borisov et al., 2021).

The predominance of the chemolithoautotrophic community, dominated by microorganisms of the Epsilonproteobacteria class and, more specifically, by the *Sulfurimonas* genus, highlights their key roles in the ecosystem functioning. Our sequence data depict a metabolic framework in which carbon fixation likely occurs alongside nitrate reduction, as already suggested by Tang et al. (2013) and observations made on chemoautotrophy in a deep-sea context (Sievert and Vetriani, 2012). This result is in line with what we observe in other studies performed on Milos shallow water vents (Lu et al., 2020; Sievert et al., 1999; Sievert et al., 2000; Giovannelli et al., 2013). While previous research has highlighted the dominance of Epsilonproteobacteria and their role in sulfur and carbon cycling, our findings further emphasize the functional adaptation of these microbial communities to low-nitrate environments and their genetic potential to oxidize molecular hydrogen (H_2) as a potential energy source, although hydrogen sulfide (H_2S) is likely the dominant electron donor in this environment.

We also detected viral genes in the white microbial mat community (Supplementary Figure S2) that could promote the transfer or exchange of genetic material (Jarett et al., 2020; Carreira et al., 2020). The integrase genes identified in our reads facilitate horizontal gene transfer by enabling the integration and excision of genetic elements, thereby promoting genetic diversity and adaptation to environmental stressors (Springael and Top, 2004). The high abundance of CRISPRs and Cas-related genes suggest that microbes in our samples developed a defense system against viral activity (Heidelberg et al., 2009), thus pointing to viral-host interactions and coevolution as a driver of microbial genetic diversity in hydrothermal vents ecosystems (Andersson and Banfield, 2008). Moreover, a high number of transposable element (TE) has been found in our reads, which can be significant in extreme environments, serving as a signal of cell stress and consequently facilitating movement of functional genes between genomes, thus serving as powerful means of adaptation (Vigil-Stenman et al., 2017). Specifically, in extreme environments such as hydrothermal vents, TEs play a crucial role in microbial evolution by facilitating genome plasticity, enabling rapid adaptation to fluctuating conditions, and increasing genetic diversity (Piednoël and Bonnivard, 2009). By mediating horizontal gene transfer, TEs can help microbes acquire beneficial traits, such as heavy metal resistance or enhanced metabolic capabilities, which are essential for survival in these extreme habitats (Casacuberta and González, 2013; Prieto-Barajas et al., 2018). The dense microbial aggregation within the mat creates microhabitats with distinct physicochemical gradients, fostering niche specialization and supporting a high diversity of metabolic functions (Meier et al., 2017). This structural complexity not only promotes microbial diversity but also enhances ecological resilience by enabling the exchange of adaptive genes through horizontal gene transfer, allowing microbes to rapidly respond to environmental fluctuations and stressors (Ghosh et al., 2015). In summary, our study reveals the presence of viral-associated genes and transposable elements, suggesting a potential for dynamic genetic exchange within the mat community, though further analysis is required to assess co-localization with functional genes.

4.3 White microbial mats are resilient to storm events

The hydrothermal activity reported in this region is linked to the mixing between the hydrothermal fluids and seawater (Yücel et al., 2013). A previous study on the shallow-water hydrothermal systems of the Gulf of Naples showed how different fluid mixing played a determining role in constraining microbial community structure in shallow-water hydrothermal systems (Bellec et al., 2020). Similarly, the distribution of the white mats of Milos islands is strongly influenced by hydrothermal fluid and seawater mixing patterns (Yücel et al., 2013), and by episodic hydrodynamic events (i.e., storms) which determine a shift in the mixing pattern and the transient disappearance of the white mats (Yücel et al., 2013).

The increase of *Sulfurimonas* related sequences with respect to *Arcobacter* during and after the storm (i.e., after a disturbance event) may reflect its resilience and competitive advantage under the new environmental conditions, possibly driven by temperature shifts, sulfide dynamics, and possibly other electron donor availability (e.g., hydrogen). These factors may have favored *Sulfurimonas* as an early colonizer in the re-establishing community, although the specific drivers of this shift remain difficult to untangle. This interpretation is supported by environmental data from Yücel et al. (2013), which were collected concurrently with the microbial samples analyzed in this study. Three days after the storm event, the microbial white mat was once again thick (up and over 1 cm) and the community diversified further, suggestive of an ecological succession already described in

shallow-water vents of Tor Caldara (Patwardhan et al., 2018), and deep-sea hydrothermal vent chemosynthetic biofilm colonization (O'Brien et al., 2015). Species belonging to *Sulfurovum* have been found in sulfidic habitats worldwide, including deep-sea and shallow-water hydrothermal vents (Dahle et al., 2013; Mino et al., 2014; Price and Giovannelli, 2017), and were reported in this study to be the most abundant bacterial genus at the late stage of storm recovery. The microbial community composition 3 days post storm was the most diverse, compared to both the mature community before, and the recently established community right after the storm event. This suggests that the storm (along with the following increased fluid mixing) and the re-establishment of the microbial mat, could have allowed the replenishment of essential nutrients (for instance, nitrogen species and organic carbon), expanding the ecological niches to be explored by the microbial communities, and therefore selecting for a more diverse microbial community in line with prediction from the intermediate disturbance theory (Giguère and Tunnicliffe, 2021). These temporarily available niches become exhausted overtime, and *Arcobacter* spp. become dominant prior to the next disturbance cycle. Disturbance events, such as storms and tides, with their transient nature, exert influence on the environment and, as a consequence, on the resident microbial communities. Such results underscore the interplay among episodic hydrodynamic events, geochemical gradients and niche differentiation created by the mixing of seawater and vent fluids and by disturbance events. These factors emerge as critical determinants shaping the dynamics of benthic microbial communities in shallow-water hydrothermal vents and additional research with focused time-series studies is necessary for an in-depth understanding of these processes.

4.4 Benthic boundary layer interactions shape the spatial distribution of microbial mats in shallow vents

Sand ripples in shallow-water hydrothermal vent fields such as Paleochori Bay are formed by the interaction between bottom currents and unconsolidated sediment. These bedforms arise as flow instabilities develop when current velocity exceeds a threshold, causing sediment to be entrained, transported, and redeposited in a rhythmic pattern (Blondeaux, 1990). In hydrothermal settings, these ripples are not only shaped by hydrodynamics due to current and waves, but also by hydrothermal fluid advection and the complex interaction between the two influence fluid–sediment interactions, creating microtopographies that affect both geochemical gradients and microbial community structure.

The sampled Milos microbial mats were characterized by a stratified layering of mat colors within a sand ripple near the venting location. Mat coloration transitioned from yellow at the base, through Siena red in the middle, to brown moving from the trough to the crest and were present only on one side of the ripple (Figure 7B; Supplementary Figure S3). These three colored mat layers overlaid a foundational white mat. The composition of the community varied according to the color, with the relative abundance of Cyanobacteria increasing along the side of the ripple and having the highest abundances in the brown mats at the top of the ripple (Figure 7B). A possible explanation for this distribution is the exposure to sunlight (facing south) on one of the ripple sides favoring phototrophic microorganisms. This hypothesis can be quickly eliminated as the ripples changed in direction during our sampling campaign in Milos, and the coloring of the mats was always present on the leading edge of the ripple, with respect to the main currents generating the ripples, rather than facing the same bearing. We therefore hypothesized that complex fluid interactions between the buoyant hydrothermal fluids, the dominant currents and the porous sandy bottom might account for the differential microbial distribution observed. In porous sediments the diffusion of O_2 can be modulated by the interactions of the benthic boundary layer with the sandy bottom (Jørgensen, 1994). The flow of seawater over the sandy sediments in the presence of sand ripple can favour the advective flow of deeper pore water (Precht and Huettel, 2004). This would contribute to a velocity gradient of oxygenated water through the sandy structure, which is reported to be lower at the basis of the ripple and higher in correspondence of the crest (Precht and Huettel, 2004). In addition, the presence of microbial mats, together with the porosity of the sediments, could affect the flow through sandy structures (Jørgensen and Revsbech, 1985; Precht and Huettel, 2004).

The Milos system is shaped by the interplay between lateral seawater flow, driven by tides and wave action, and the buoyant ascent of hydrothermal fluids characteristic of shallow-water hydrothermal vents. This interaction creates complex sediment structures such as sand ripples, which in turn generate dynamic boundary layer conditions influencing both fluid mixing and microbial colonization. In our initial modeling experiments, using a computational method known as the lattice Boltzmann approach, we explored how water flow interacts with a simplified sediment ripple shape (Supplementary Figure S1). We found that when water moves over this ripple structure, it creates a swirling, recirculating flow pattern—known as an eddy—just behind the ripple. This phenomenon occurs due to a process called boundary layer separation. Boundary layer separation happens when flowing water near a solid surface, such as the ripple, slows down and detaches from the surface, forming turbulent vortices or eddies downstream.

These eddies are important because they significantly influence how substances dissolved in water (known as passive scalars, such as nutrients or chemical signals) mix and distribute in the area around the ripple. Additionally, they control the transport and deposition of small particles, which could include sediment grains or microorganisms.

Interestingly, the microbial communities present in the sediment may also interact with these flow patterns. Microbes might alter the local environment, potentially changing sediment stability or flow characteristics, while at the same time, the flow could affect where and how microbes grow and thrive.

In future studies, we plan to expand our modeling to capture more complex interactions. This will include tracking how particles move within these flow patterns, understanding how erosion and deposition processes reshape the ripple structures, and examining how microbial communities directly impact the physical structure of the sediment and thereby influence the overall flow dynamics. When using combined FVM and LBM fluid flow to reconstruct the possible interactions in the Milos microbial mats system, our results show that, at the small scale of a single sand ripple, the primary mechanism driving the temperature-redox gradient is the mixing of hydrothermal fluids with the overlying seawater. This process, which governs the availability of electron donors and acceptors for the *in situ* microbial

community, is controlled by the relative speed of the lateral seawater flow. In conditions where lateral flow is reduced or near zero, the advection of hydrothermal fluids dominate the system creating complex microcirculation cells near the vent center (Yücel et al., 2013). This pressure-driven phenomenon, observed previously by Yücel et al. (2013) using in situ microsensors, generates an inward flux of oxygenated seawater in the area surrounding the vent center. When lateral flow of seawater reaches a threshold velocity capable of overcoming and interacting with the advective flow, complex boundary layer dynamics control mixing (Supplementary Figure S1). We observed the presence of a positive pressure area in the stoss side of the sand ripple, favouring the oxygenated, cold seawater flux in the ripple side and crest. This might lead to higher re-circulation of nutrients and oxygenated water, lower temperatures and lower concentrations of sulfide favouring the presence of microorganisms involved in aerobic respiration and photosynthesis (Figure 7A). Our results support this conclusion as the relative abundance of *Cyanobacteria* increases over the ripple stoss side, reaching its peak at the ripples crest, while the abundance of chemolithotrophic sulfur oxidizers like *Sulfurimonas* and related Epsilonproteobacteria genera decreases.

On the lee side of the sand ripple, the negative pressure generated by the lateral flow of seawater induces an increased flux of hydrothermal fluids, generating a pocket of higher temperature, reduced fluids in the trough between ripples. Microbial diversity data shows at this location the community is dominated by *Sulfurimonas* and related Epsilonproteobacteria genera, consistent with their physiology and preferred metabolisms (Campbell et al., 2006). The complex dynamics between microbial distribution and fluid dynamic interactions over the seafloor has been overlooked as a possible explanatory variable in describing small scale variability, especially in shallow-water hydrothermal vents (Esposito et al., 2018). Overall our results highlight the importance of considering the effects of dynamic events, both episodic events like storms and complex dynamic mixing across small scales to comprehend the factors controlling microbial community structuring in natural systems.

5 Conclusion

Our study demonstrates that hydrodynamic forces play a fundamental role in shaping microbial communities in the white mats of Milos shallow-water hydrothermal vents. These mat communities are dominated by chemolithoautotrophic *Epsilonproteobacteria* that thrive on the chemical energy of vent fluids, yet their population structure is highly dynamic in space and time. We found that a major storm disturbance caused a rapid but transient reorganization of the community, followed by a succession that restored the mat's characteristic sulfur-oxidizer dominance within days. Spatially, small-scale variations in fluid mixing created a patchwork of niches across the vent field: for example, oxygen-rich microhabitats generated by benthic boundary layer flow dynamics supported cyanobacterial growth in the sand ripple crests, whereas sulfide-rich small scale zones selected for *Sulfurimonas* and *Arcobacter*. Together, these results highlight that both transient events acting on a large spatial scale (storms) and persistent physical gradients affecting the local niches (flow and diffusion across the benthic boundary layer) drive the diversity and function of vent-associated biofilms. The close coupling between hydrodynamic processes (fluid flow, tides, waves and storms) and microbial ecology controls the distribution and contribution of these ecosystems to biogeochemical cycling, both at the local and regional scale. Understanding this interplay is crucial for predicting how shallow vent ecosystems respond to natural disturbances and environmental changes. Our findings provide a framework for how geodynamic events influence microbial succession and resilience in coastal hydrothermal systems, and underscore the need for further studies of these dynamic habitats. Future work targeting shallow-water vents will help refine our models of biogeochemical feedback in these systems and shed additional light on the strategies microbial communities use to persist amidst environmental variability.

Data availability statement

The original contributions presented in the study are publicly available. This data can be found here: https://www.ebi.ac.uk/ena/browser/home, accession number PRJEB8854. All data and code used in this paper is available on the GitHub repository: https://github.com/giovannellilab/Milos_white_mats and made available through Zenodo at: 10.5281/zenodo.15528839.

Author contributions

AS: Resources, Data curation, Conceptualization, Writing – review & editing, Writing – original draft, Supervision, Investigation. FM: Writing – review & editing, Investigation, Conceptualization, Writing – original draft, Visualization. BB: Writing – original draft, Investigation, Writing – review & editing, Conceptualization, Visualization. LG: Writing – review & editing, Writing – original draft, Investigation, Visualization, Data curation, Formal analysis. MY: Investigation, Visualization, Conceptualization, Methodology, Formal analysis, Writing – review & editing. DF: Investigation, Methodology, Writing – review & editing, Funding acquisition, Data curation, Formal analysis, Project administration. NB: Investigation, Formal analysis, Methodology, Conceptualization, Funding acquisition, Writing – review & editing. SB: Methodology, Visualization, Writing – review & editing, Investigation, Software. VD'A: Investigation, Visualization, Software, Writing – review & editing, Methodology. CV: Visualization, Supervision, Writing – original draft, Formal analysis, Data curation, Funding acquisition, Methodology, Conceptualization, Resources, Investigation, Validation, Writing – review & editing, Project administration. DG: Writing – review & editing, Supervision, Formal analysis, Project administration, Writing – original draft, Methodology, Data curation, Resources, Investigation, Conceptualization, Visualization, Funding acquisition, Validation.

Funding

The author(s) declare that financial support was received for the research and/or publication of this article. AS was supported by the Marie Curie Co Found Crescendo (grant agreement no. 101034245). CV and DF were supported by NSF grants OCE 11-24141, OCE 19-48623, and IOS 19-51690 and NASA grant 80NSSC21K0485 to

CV. FM was supported by the "National Biodiversity Future Center-NBFC," project code CN_00000033, concession decree no. 1034 of 17 June 2022 adopted by the Italian Ministry of University and Research. This work was supported by funding from the European Research Council (ERC) under the European Union's Horizon 2020 research and innovation program grant agreement no. 948972-COEVOLVE-ERC-2020-STG.

Conflict of interest

The authors declare that the research was conducted in the absence of any commercial or financial relationships that could be construed as a potential conflict of interest.

The author(s) declared that they were an editorial board member of Frontiers, at the time of submission. This had no impact on the peer review process and the final decision.

Generative AI statement

The author(s) declare that no Gen AI was used in the creation of this manuscript.

Any alternative text (alt text) provided alongside figures in this article has been generated by Frontiers with the support of artificial intelligence and reasonable efforts have been made to ensure accuracy, including review by the authors wherever possible. If you identify any issues, please contact us.

Publisher's note

All claims expressed in this article are solely those of the authors and do not necessarily represent those of their affiliated organizations, or those of the publisher, the editors and the reviewers. Any product that may be evaluated in this article, or claim that may be made by its manufacturer, is not guaranteed or endorsed by the publisher.

Supplementary material

The Supplementary material for this article can be found online at: https://www.frontiersin.org/articles/10.3389/fmicb.2025.1649514/full#supplementary-material

SUPPLEMENTARY FIGURE S1
(A) Streamwise velocity component field deriving from FVM model, [m/s]. Flow direction starting from left to right of the modelling mesh. The modeling domain is constrained within a 45x55 cm box. **(B)** Transverse velocity component field deriving from FVM model, [m/s]. **(C)** Steady state flow structure of our modelled ripple and porous bed. The units here are simply the number of simulation grid points, so the numerical simulation grid in this case was 5000x10000 grid points in size. These units are dimensionless as the only relevant parameters in the model are dimensionless number groups such as the Reynolds number (a dimensionless quantity in fluid dynamics that helps predict the flow pattern of a fluid), Rayleigh number (a dimensionless quantity that characterizes the buoyancy-driven flow, or free convection, of a fluid), Nusselt number (dimensionless number that describes the ratio of convective heat transfer to conductive heat transfer at the boundary between a solid surface and a fluid). Upper panel: fluid density, second panel: horizontal flow rate, third panel: vertical flow rate, lower panel: temperature. Steady fluid motion is imposed using a constant horizontal shear flow at the upper boundary, as seen in the colormap of horizontal momentum [second panel of **(C)**]. In the third panel we see the vertical velocity component, w. The lower panel shows temperature: convection has little impact in this particular configuration, but thermal energy is being advected by the flow, namely the boundary layer separation effect downstream of the ripple.

SUPPLEMENTARY FIGURE S2
Viral diversity in the microbial mat metagenome classified according to the Baltimore classification (inner circle), and the International Commission on Viral Taxonomy classification at the Order (median circle) and Family (outer circle) level. A total of 30,891 sequences were classified using MetaVIR with an e-value cutoff of 10^{-5} (a total of 50,050 sequences were classified using a less conservative e-value cutoff of 10^{-3}).

SUPPLEMENTARY FIGURE S3
Photograph of microbial mats at the hydrothermal venting area off Milos Island, Greece. The image shows a series of sand ripples coated with microbial mats displaying distinct surface coloration gradients: white, yellow, light reddish/orangish and brownish, with yellow mats often overlying white mats along ripple flanks. These mat colors reflect differences in microbial community composition and are consistent with stratified layering represented in Figure 7B. The coloration and distribution are influenced by venting intensity and hydrodynamic flow conditions. Image credit: Thanos Dailianis/Hellenic Centre for Marine Research (SeaBioTech project, FP7-KBBE.2012.3.2-01).

References

Alain, K., Zbinden, M., Le Bris, N., Lesongeur, F., Quérellou, J., Gaill, F., et al. (2004). Early steps in microbial colonization processes at deep-sea hydrothermal vents. *Environ. Microbiol.* 6, 227–241. doi: 10.1111/j.1462-2920.2003.00557.x

Andersson, A. F., and Banfield, J. F. (2008). Virus population dynamics and acquired virus resistance in natural microbial communities. *Science* 320, 1047–1050. doi: 10.1126/science.1157358

Arcadi, E., Rizzo, C., Calogero, R., Sciutteri, V., Fabiano, F., Consoli, P., et al. (2023). Microbial communities inhabiting shallow hydrothermal vents as sentinels of acidification processes. *Front. Microbiol.* 14:1233893. doi: 10.3389/fmicb.2023.1233893

Bellec, L., Cambon-Bonavita, M.-A., Durand, L., Aube, J., Gayet, N., Sandulli, R., et al. (2020). Microbial communities of the shallow-water hydrothermal vent near Naples, Italy, and chemosynthetic symbionts associated with a free-living marine nematode. *Front. Microbiol.* 11:2023. doi: 10.3389/fmicb.2020.02023

Bengtsson, J., Eriksson, K. M., Hartmann, M., Wang, Z., Shenoy, B. D., Grelet, G.-A., et al. (2011). Metaxa: a software tool for automated detection and discrimination among ribosomal small subunit (12S/16S/18S) sequences of archaea, bacteria, eukaryotes, mitochondria, and chloroplasts in metagenomes and environmental sequencing datasets. *Antonie Van Leeuwenhoek* 100, 471–475. doi: 10.1007/s10482-011-9598-6

Blondeaux, P. (1990). Sand ripples under sea waves part 1. Ripple formation. *J. Fluid Mech.* 218, 1–17. doi: 10.1017/S0022112090000908

Borisov, V. B., Gennis, R. B., Hemp, J., and Verkhovsky, M. I. (2011). The cytochrome *bd* respiratory oxygen reductases. *Biochimica et Biophysica Acta (BBA)* 1807, 1398–1413. doi: 10.1016/j.bbabio.2011.06.016

Borisov, V. B., Siletsky, S. A., Paiardini, A., Hoogewijs, D., Forte, E., Giuffrè, A., et al. (2021). Bacterial oxidases of the cytochrome bd family: redox enzymes of unique structure, function, and utility as drug targets. *Antioxid. Redox Signal.* 34, 1280–1318. doi: 10.1089/ars.2020.8039

Botz, R., Stüben, D., Winckler, G., Bayer, R., Schmitt, M., and Faber, E. (1996). Hydrothermal gases offshore Milos Island, Greece. *Chem. Geol.* 130, 161–173. doi: 10.1016/0009-2541(96)00023-X

Campbell, B. J., Engel, A. S., Porter, M. L., and Takai, K. (2006). The versatile ε-proteobacteria: key players in sulphidic habitats. *Nat. Rev. Microbiol.* 4, 458–468. doi: 10.1038/nrmicro1414

Caporaso, J. G., Kuczynski, J., Stombaugh, J., Bittinger, K., Bushman, F. D., Costello, E. K., et al. (2010). Qiime allows analysis of high-throughput community sequencing data. *Nat. Methods* 7, 335–336. doi: 10.1038/nmeth.f.303

Cardigos, F., Colaço, A., Dando, P. R., Ávila, S. P., Sarradin, P.-M., Tempera, F., et al. (2005). Shallow water hydrothermal vent field fluids and communities of the D. João de Castro seamount (Azores). *Chem. Geol.* 224, 153–168. doi: 10.1016/j.chemgeo.2005.07.019

Carreira, C., Lønborg, C., Kühl, M., Lillebø, A. I., Sandaa, R.-A., Villanueva, L., et al. (2020). Fungi and viruses as important players in microbial mats. *FEMS Microbiol. Ecol.* 96:fiaa187. doi: 10.1093/femsec/fiaa187

Casacuberta, E., and González, J. (2013). The impact of transposable elements in environmental adaptation. *Mol. Ecol.* 22, 1503–1517. doi: 10.1111/mec.12170

Chen, M., Li, Y., Tang, K., Hu, A., Fan, W., Wang, D., et al. (2023). Highly diverse diazotrophs drive high N2 fixation rates in a shallow submarine hydrothermal system. *Fundam. Res.* doi: 10.1016/j.fmre.2023.07.009

Chen, X., Tang, K., Zhang, M., Liu, S., Chen, M., Zhan, P., et al. (2022). Genome-centric insight into metabolically active microbial population in shallow-sea hydrothermal vents. *Microbiome* 10:170. doi: 10.1186/s40168-022-01351-7

Chun, J., Lee, J.-H., Jung, Y., Kim, M., Kim, S., Kim, B. K., et al. (2007). Eztaxon: a web-based tool for the identification of prokaryotes based on 16S ribosomal RNA gene sequences. *Int. J. Syst. Evol. Microbiol.* 57, 2259–2261. doi: 10.1099/ijs.0.64915-0

Dahl, C. (2017). "Sulfur metabolism in phototrophic Bacteria" in Modern topics in the phototrophic prokaryotes: Metabolism, bioenergetics, and omics. ed. P. C. Hallenbeck (Cham: Springer International Publishing), 27–66.

Dahle, H., Roalkvam, I., Thorseth, I. H., Pedersen, R. B., and Steen, I. H. (2013). The versatile in situ gene expression of an Epsilonproteobacteria-dominated biofilm from a hydrothermal chimney. *Environ. Microbiol. Rep.* 5, 282–290. doi: 10.1111/1758-2229.12016

Dando, P. R. (2010). "Biological communities at marine shallow-water vent and seep sites" in The vent and seep biota: Aspects from microbes to ecosystems. ed. S. Kiel (Dordrecht: Springer Netherlands), 333–378.

Dando, P. R., Aliani, S., Arab, H., Bianchi, C. N., Brehmer, M., Cocito, S., et al. (2000). Hydrothermal studies in the Aegean Sea. *Phys. Chem. Earth* 25, 1–8. doi: 10.1016/S1464-1909(99)00112-4

Dando, P. R., Hughes, J. A., Leahy, Y., Niven, S. J., Taylor, L. J., and Smith, C. (1995). Gas venting rates from submarine hydrothermal areas around the island of Milos, Hellenic volcanic arc. *Cont. Shelf Res.* 15, 913–929. doi: 10.1016/0278-4343(95)80002-U

Dando, P. R., Stüben, D., and Varnavas, S. P. (1999). Hydrothermalism in the Mediterranean Sea. *Prog. Oceanogr.* 44, 333–367. doi: 10.1016/S0079-6611(99)00032-4

Dobretsov, S. (2009). "Marine biofilms" in Biofouling (John Wiley & Sons, Ltd.), 123–136.

Douglas, S. (2000). Environmental scanning electron microscopy studies of colloidal sulfur deposition in a natural microbial community from a cold sulfide spring near Ancaster, Ontario, Canada. *Geomicrobiol J.* 17, 275–289. doi: 10.1080/01490450050192974

Dowd, S. E., Sun, Y., Wolcott, R. D., Domingo, A., and Carroll, J. A. (2008). Bacterial tag–encoded FLX amplicon pyrosequencing (bTEFAP) for microbiome studies: bacterial diversity in the ileum of newly weaned Salmonella-infected pigs. *Foodborne Pathog. Dis.* 5, 459–472. doi: 10.1089/fpd.2008.0107

Edgar, R. C. (2010). Search and clustering orders of magnitude faster than BLAST. *Bioinformatics* 26, 2460–2461. doi: 10.1093/bioinformatics/btq461

Edgar, R. C., Haas, B. J., Clemente, J. C., Quince, C., and Knight, R. (2011). Uchime improves sensitivity and speed of chimera detection. *Bioinformatics* 27, 2194–2200. doi: 10.1093/bioinformatics/btr381

Edwards, R., Olson, R., and Disz, T. (n.d.). Real time metagenomics: using k-mers to annotate metagenomes | bioinformatics | Oxford academic. Available online at: https://academic.oup.com/bioinformatics/article/28/24/3316/245032 (Accessed February 2, 2023).

Esposito, V., Andaloro, F., Canese, S., Bortoluzzi, G., Bo, M., Bella, M. D., et al. (2018). Exceptional discovery of a shallow-water hydrothermal site in the SW area of Basiluzzo islet (Aeolian archipelago, South Tyrrhenian Sea): an environment to preserve. *PLoS One* 13:e0190710. doi: 10.1371/journal.pone.0190710

Fitzsimons, M. f., Dando, P. R., Hughes, J. A., Thiermann, F., Akoumianaki, I., and Pratt, S. M. (1997). Submarine hydrothermal brine seeps off Milos, Greece. Observations and geochemistry. *Mar. Chem.* 57, 325–340. doi: 10.1016/S0304-4203(97)00021-2

Flemming, H.-C., and Wingender, J. (2010). The biofilm matrix. *Nat. Rev. Microbiol.* 8, 623–633. doi: 10.1038/nrmicro2415

Frawley, E. R., and Fang, F. C. (2014). The ins and outs of bacterial iron metabolism. *Mol. Microbiol.* 93, 609–616. doi: 10.1111/mmi.12709

Friedrich, C. G., Bardischewsky, F., Rother, D., Quentmeier, A., and Fischer, J. (2005). Prokaryotic sulfur oxidation. *Curr. Opin. Microbiol.* 8, 253–259. doi: 10.1016/j.mib.2005.04.005

Fuchs, G. (2011). Alternative pathways of carbon dioxide fixation: insights into the early evolution of life? *Ann. Rev. Microbiol.* 65, 631–658. doi: 10.1146/annurev-micro-090110-102801

Garnett, J. A., and Matthews, S. (2012). Interactions in bacterial biofilm development: a structural perspective. *Curr. Protein Pept. Sci.* 13, 739–755. doi: 10.2174/138920312804871166

Ghosh, W., Mallick, S., and DasGupta, S. K. (2009). Origin of the sox multienzyme complex system in ancient thermophilic bacteria and coevolution of its constituent proteins. *Res. Microbiol.* 160, 409–420. doi: 10.1016/j.resmic.2009.07.003

Ghosh, W., Roy, C., Roy, R., Nilawe, P., Mukherjee, A., Haldar, P. K., et al. (2015). Resilience and receptivity worked in tandem to sustain a geothermal mat community amidst erratic environmental conditions. *Sci. Rep.* 5:12179. doi: 10.1038/srep12179

Giguère, T. N., and Tunnicliffe, V. (2021). Beta diversity differs among hydrothermal vent systems: implications for conservation. *PLoS One* 16:e0256637. doi: 10.1371/journal.pone.0256637

Giovannelli, D., d'Errico, G., Manini, E., Yakimov, M., and Vetriani, C. (2013). Diversity and phylogenetic analyses of bacteria from a shallow-water hydrothermal vent in Milos island (Greece). *Front. Microbiol.* 4:184. doi: 10.3389/fmicb.2013.00184

Giovannelli, D., Grosche, A., Starovoytov, V., Yakimov, M., Manini, E., and Vetriani, C. (2012). *Galenea microaerophila* gen. Nov., sp. nov., a mesophilic, microaerophilic, chemosynthetic, thiosulfate-oxidizing bacterium isolated from a shallow-water hydrothermal vent. *Int. J. Syst. Evol. Microbiol.* 62, 3060–3066. doi: 10.1099/ijs.0.040808-0

Giovannelli, D., and Price, R. E. (2019). "Marine shallow-water hydrothermal vents: geochemistry" in *Encyclopedia of Ocean Sciences (Third Edition)*. eds. J. K. Cochran, H. J. Bokuniewicz and P. L. Yager (Oxford: Academic Press), 353–363.

Gledhill, M., and Buck, K. N. (2012). The organic complexation of iron in the marine environment: a review. *Front. Microbiol.* 3:69. doi: 10.3389/fmicb.2012.00069

Gomez-Saez, G. V., Pop Ristova, P., Sievert, S. M., Elvert, M., Hinrichs, K.-U., and Bühring, S. I. (2017). Relative importance of chemoautotrophy for primary production in a light exposed marine shallow hydrothermal system. *Front. Microbiol.* 8:702. doi: 10.3389/fmicb.2017.00702

Greenshields, C. J., and Weller, H. G. (2022). Notes on computational fluid dynamics: general principles. CFD Direct. Available online at: https://cir.nii.ac.jp/crid/1130570038682879362 (Accessed May 25, 2025).

Grote, J., Schott, T., Bruckner, C. G., Glöckner, F. O., Jost, G., Teeling, H., et al. (2012). Genome and physiology of a model *Epsilonproteobacterium* responsible for sulfide detoxification in marine oxygen depletion zones. *Proc. Natl. Acad. Sci. USA* 109, 506–510. doi: 10.1073/pnas.1111262109

Groth, A. C., and Calos, M. P. (2004). Phage integrases: biology and applications. *J. Mol. Biol.* 335, 667–678. doi: 10.1016/j.jmb.2003.09.082

Gulmann, L. K., Beaulieu, S. E., Shank, T. M., Ding, K., Seyfried, W. E., and Sievert, S. M. (2015). Bacterial diversity and successional patterns during biofilm formation on freshly exposed basalt surfaces at diffuse-flow deep-sea vents. *Front. Microbiol.* 6:901. doi: 10.3389/fmicb.2015.00901

Hall-Stoodley, L., Costerton, J. W., and Stoodley, P. (2004). Bacterial biofilms: from the natural environment to infectious diseases. *Nat. Rev. Microbiol.* 2, 95–108. doi: 10.1038/nrmicro821

Han, Y., and Perner, M. (2015). The globally widespread genus *Sulfurimonas*: versatile energy metabolisms and adaptations to redox clines. *Front. Microbiol.* 6:989. doi: 10.3389/fmicb.2015.00989

Heidelberg, J. F., Nelson, W. C., Schoenfeld, T., and Bhaya, D. (2009). Germ warfare in a microbial mat community: CRISPRs provide insights into the co-evolution of host and viral genomes. *PLoS One* 4:e4169. doi: 10.1371/journal.pone.0004169

Holmström, C., and Kjelleberg, S. (1999). Marine *Pseudoalteromonas* species are associated with higher organisms and produce biologically active extracellular agents. *FEMS Microbiol. Ecol.* 30, 285–293. doi: 10.1111/j.1574-6941.1999.tb00656.x

Howard-Varona, C., Lindback, M. M., Bastien, G. E., Solonenko, N., Zayed, A. A., Jang, H., et al. (2020). Phage-specific metabolic reprogramming of virocells. *ISME J.* 14, 881–895. doi: 10.1038/s41396-019-0580-z

Huang, F., Pan, L., He, Z., Zhang, M., and Zhang, M. (2020). Identification, interactions, nitrogen removal pathways and performances of culturable heterotrophic nitrification-aerobic denitrification bacteria from mariculture water by using cell culture and metagenomics. *Sci. Total Environ.* 732:139268. doi: 10.1016/j.scitotenv.2020.139268

Huber, J. A., Butterfield, D. A., and Baross, J. A. (2003). Bacterial diversity in a subseafloor habitat following a deep-sea volcanic eruption. *FEMS Microbiol. Ecol.* 43, 393–409. doi: 10.1111/j.1574-6941.2003.tb01080.x

Hügler, M., and Sievert, S. M. (2011). Beyond the Calvin cycle: autotrophic carbon fixation in the ocean. *Annu. Rev. Mar. Sci.* 3, 261–289. doi: 10.1146/annurev-marine-120709-142712

Hügler, M., Wirsen, C. O., Fuchs, G., Taylor, C. D., and Sievert, S. M. (2005). Evidence for autotrophic CO2 fixation via the reductive tricarboxylic acid cycle by members of the ε subdivision of Proteobacteria. *J. Bacteriol.* 187, 3020–3027. doi: 10.1128/JB.187.9.3020-3027.2005

Hyatt, D., Chen, G.-L., LoCascio, P. F., Land, M. L., Larimer, F. W., and Hauser, L. J. (2010). Prodigal: prokaryotic gene recognition and translation initiation site identification. *BMC Bioinform.* 11:119. doi: 10.1186/1471-2105-11-119

Jarett, J. K., Džunková, M., Schulz, F., Roux, S., Paez-Espino, D., Eloe-Fadrosh, E., et al. (2020). Insights into the dynamics between viruses and their hosts in a hot spring microbial mat. *ISME J.* 14, 2527–2541. doi: 10.1038/s41396-020-0705-4

Jørgensen, B. B. (1994). Sulfate reduction and thiosulfate transformations in a cyanobacterial mat during a diel oxygen cycle. *FEMS Microbiol. Ecol.* 13, 303–312. doi: 10.1111/j.1574-6941.1994.tb00077.x

Jørgensen, B. B., and Revsbech, N. P. (1985). Diffusive boundary layers and the oxygen uptake of sediments and detritus. *Limnol. Oceanogr.* 30, 111–122. doi: 10.4319/lo.1985.30.1.0111

Kamenev, G. M., Fadeev, V. I., Selin, N. I., Tarasov, V. G., and Malakhov, V. V. (1993). Composition and distribution of macro- and meiobenthos around sublittoral hydrothermal vents in the Bay of Plenty, New Zealand. *N. Z. J. Mar. Freshw. Res.* 27, 407–418. doi: 10.1080/00288330.1993.9516582

Kanehisa, M., and Goto, S. (2000). KEGG: Kyoto encyclopedia of genes and genomes. *Nucleic Acids Res.* 28, 27–30. doi: 10.1093/nar/28.1.27

Khimasia, A., Rovere, A., and Pichler, T. (2020). Hydrothermal areas, microbial mats and sea grass in Paleochori Bay, Milos, Greece. *J. Maps* 16, 348–356. doi: 10.1080/17445647.2020.1748131

Kokkalas, S., Xypolias, P., Koukouvelas, I., and Doutsos, T. (2006). Post-collisional contractional and extensional deformation in the Aegean region. In: *Post-Collisional Tectonics and Magmatism in the Mediterranean Region and Asia. Geological Society of America Special Paper*. (eds). Y. Dilek and S. Pavlides. 409, pp 97–123.

Kranz, R. G., Richard-Fogal, C., Taylor, J.-S., and Frawley, E. R. (2009). Cytochrome c biogenesis: mechanisms for covalent modifications and trafficking of heme and for heme-iron redox control. *Microbiol. Mol. Biol. Rev.* 73, 510–528. doi: 10.1128/mmbr.00001-09

Kümpel, C., Grein, F., and Dahl, C. (2023). Fluorescence microscopy study of the intracellular sulfur globule protein SgpD in the purple sulfur bacterium *Allochromatium vinosum*. *Microorganisms* 11:1792. doi: 10.3390/microorganisms11071792

Labrenz, M., Grote, J., Mammitzsch, K., Boschker, H. T. S., Laue, M., Jost, G., et al. (2013). *Sulfurimonas* gotlandica sp. nov., a chemoautotrophic and psychrotolerant epsilonproteobacterium isolated from a pelagic redoxcline, and an emended description of the genus Sulfurimonas. *Int. J. Syst. Evol. Microbiol.* 63, 4141–4148. doi: 10.1099/ijs.0.048827-0

Lagesen, K., Hallin, P., Rødland, E. A., Staerfeldt, H.-H., Rognes, T., and Ussery, D. W. (2007). RNAmmer: consistent and rapid annotation of ribosomal RNA genes. *Nucleic Acids Res.* 35, 3100–3108. doi: 10.1093/nar/gkm160

Le Moine Bauer, S., Lu, G.-S., Goulaouic, S., Puzenat, V., Schouw, A., Barreyre, T., et al. (2023). Structure and metabolic potential of the prokaryotic communities from the hydrothermal system of Paleochori Bay, Milos, Greece. *Front. Microbiol.* 13:1060168. doi: 10.3389/fmicb.2022.1060168

Lentini, V., Gugliandolo, C., Bunk, B., Overmann, J., and Maugeri, T. L. (2014). Diversity of prokaryotic community at a shallow marine hydrothermal site elucidated by Illumina sequencing technology. *Curr. Microbiol.* 69, 457–466. doi: 10.1007/s00284-014-0609-5

Lu, G.-S., LaRowe, D. E., Fike, D. A., Druschel, G. K., Iii, W. P. G., Price, R. E., et al. (2020). Bioenergetic characterization of a shallow-sea hydrothermal vent system: Milos Island, Greece. *PLoS One* 15:e0234175. doi: 10.1371/journal.pone.0234175

McGinnis, S., and Madden, T. L. (2004). BLAST: at the core of a powerful and diverse set of sequence analysis tools. *Nucleic Acids Res.* 32, W20–W25. doi: 10.1093/nar/gkh435

Mehta, M. P., Butterfield, D. A., and Baross, J. A. (2003). Phylogenetic diversity of nitrogenase (nifH) genes in deep-sea and hydrothermal vent environments of the Juan de Fuca ridge. *Appl. Environ. Microbiol.* 69, 960–970. doi: 10.1128/AEM.69.2.960-970.2003

Meier, D. V., Pjevac, P., Bach, W., Hourdez, S., Girguis, P. R., Vidoudez, C., et al. (2017). Niche partitioning of diverse sulfur-oxidizing bacteria at hydrothermal vents. *ISME J.* 11, 1545–1558. doi: 10.1038/ismej.2017.37

Meyer, F., Paarmann, D., D'Souza, M., Olson, R., Glass, E., Kubal, M., et al. (2008). The metagenomics RAST server – a public resource for the automatic phylogenetic and functional analysis of metagenomes. *BMC Bioinform.* 9:386. doi: 10.1186/1471-2105-9-386

Mino, S., Kudo, H., Arai, T., Sawabe, T., Takai, K., and Nakagawa, S. (2014). *Sulfurovum aggregans* sp. nov., a hydrogen-oxidizing, thiosulfate-reducing chemolithoautotroph within the Epsilonproteobacteria isolated from a deep-sea hydrothermal vent chimney, and an emended description of the genus Sulfurovum. *Int. J. Syst. Evol. Microbiol.* 64, 3195–3201. doi: 10.1099/ijs.0.065094-0

Müller, A. L., Kjeldsen, K. U., Rattei, T., Pester, M., and Loy, A. (2015). Phylogenetic and environmental diversity of DsrAB-type dissimilatory (bi)sulfite reductases. *ISME J.* 9, 1152–1165. doi: 10.1038/ismej.2014.208

Muyzer, G., de Waal, E. C., and Uitterlinden, A. G. (1993). Profiling of complex microbial populations by denaturing gradient gel electrophoresis analysis of polymerase chain reaction-amplified genes coding for 16S rRNA. *Appl. Environ. Microbiol.* 59, 695–700. doi: 10.1128/aem.59.3.695-700.1993

Nomikou, P., Krassakis, P., Kazana, S., Papanikolaou, D., and Koukouzas, N. (2021). The volcanic relief within the Kos-Nisyros-Tilos tectonic graben at the eastern edge of the Aegean volcanic arc, Greece and geohazard implications. *Geosciences* 11:231. doi: 10.3390/geosciences11060231

O'Brien, C. E., Giovannelli, D., Govenar, B., Luther, G. W., Lutz, R. A., Shank, T. M., et al. (2015). Microbial biofilms associated with fluid chemistry and megafaunal colonization at post-eruptive deep-sea hydrothermal vents. *Deep Sea Res. Part II Top. Stud. Oceanogr.* 121, 31–40. doi: 10.1016/j.dsr2.2015.07.020

Patwardhan, S., Foustoukos, D. I., Giovannelli, D., Yücel, M., and Vetriani, C. (2018). Ecological succession of sulfur-oxidizing epsilon- and gammaproteobacteria during colonization of a shallow-water gas vent. *Front. Microbiol.* 9:2970. doi: 10.3389/fmicb.2018.02970

Patwardhan, S., Phan, J., Smedile, F., and Vetriani, C. (2023). The genome of *Varunaivibrio sulfuroxidans* strain TC8T, a metabolically versatile alphaproteobacterium from the Tor Caldara gas vents in the Tyrrhenian Sea. *Microorganisms* 11:1366. doi: 10.3390/microorganisms11061366

Patwardhan, S., Smedile, F., Giovannelli, D., and Vetriani, C. (2021). Metaproteogenomic profiling of chemosynthetic microbial biofilms reveals metabolic flexibility during colonization of a shallow-water gas vent. *Front. Microbiol.* 12:638300. doi: 10.3389/fmicb.2021.638300

Pereira, I. A. C., Ramos, A. R., Grein, F., Marques, M. C., Da Silva, S. M., and Venceslau, S. S. (2011). A comparative genomic analysis of energy metabolism in sulfate reducing bacteria and archaea. *Front. Microbiol.* 2:69. doi: 10.3389/fmicb.2011.00069

Pérez-Rodríguez, I., Bohnert, K. A., Cuebas, M., Keddis, R., and Vetriani, C. (2013). Detection and phylogenetic analysis of the membrane-bound nitrate reductase (Nar) in pure cultures and microbial communities from deep-sea hydrothermal vents. *FEMS Microbiol. Ecol.* 86, 256–267. doi: 10.1111/1574-6941.12158

Piednoël, M., and Bonnivard, E. (2009). DIRS1-like retrotransposons are widely distributed among Decapoda and are particularly present in hydrothermal vent organisms. *BMC Evol. Biol.* 9:86. doi: 10.1186/1471-2148-9-86

Precht, E., and Huettel, M. (2004). Rapid wave-driven advective pore water exchange in a permeable coastal sediment. *J. Sea Res.* 51, 93–107. doi: 10.1016/j.seares.2003.07.003

Price, R. E., and Giovannelli, D. (2017). "A review of the geochemistry and microbiology of marine shallow-water hydrothermal vents" in Reference module in earth systems and environmental sciences. eds. J. K. Cochran, H. J. Bokuniewicz and P. L. Yager (Oxford, U.K.: Elsevier). doi: 10.1016/B978-0-12-409548-9.09523-3

Price, R. E., Lesniewski, R., Nitzsche, K. S., Meyerdierks, A., Saltikov, C., Pichler, T., et al. (2013). Archaeal and bacterial diversity in an arsenic-rich shallow-sea hydrothermal system undergoing phase separation. *Front. Microbiol.* 4:158. doi: 10.3389/fmicb.2013.00158

Prieto-Barajas, C. M., Valencia-Cantero, E., and Santoyo, G. (2018). Microbial mat ecosystems: structure types, functional diversity, and biotechnological application. *Electron. J. Biotechnol.* 31, 48–56. doi: 10.1016/j.ejbt.2017.11.001

Puzenat, V., Escartín, J., Martelat, J.-E., Barreyre, T., Le Moine Bauer, S., Nomikou, P., et al. (2021). Shallow-water hydrothermalism at Milos (Greece): nature, distribution, heat fluxes and impact on ecosystems. *Mar. Geol.* 438:106521. doi: 10.1016/j.margeo.2021.106521

Reeder, J., and Knight, R. (2010). Rapidly denoising pyrosequencing amplicon reads by exploiting rank-abundance distributions. *Nat. Methods* 7, 668–669. doi: 10.1038/nmeth0910-668b

Reyes, C., Schneider, D., Lipka, M., Thürmer, A., Böttcher, M. E., and Friedrich, M. W. (2017). Nitrogen metabolism genes from temperate marine sediments. *Mar. Biotechnol.* 19, 175–190. doi: 10.1007/s10126-017-9741-0

Roux, S., Faubladier, M., Mahul, A., Paulhe, N., Bernard, A., Debroas, D., et al. (2011). Metavir: a web server dedicated to virome analysis. *Bioinformatics* 27, 3074–3075. doi: 10.1093/bioinformatics/btr519

Schine, C. M. S., Alderkamp, A.-C., van Dijken, G., Gerringa, L. J. A., Sergi, S., Laan, P., et al. (2021). Massive Southern Ocean phytoplankton bloom fed by iron of possible hydrothermal origin. *Nat. Commun.* 12:1211. doi: 10.1038/s41467-021-21339-5

Schuler, C. G., Havig, J. R., and Hamilton, T. L. (2017). Hot spring microbial community composition, morphology, and carbon fixation: implications for interpreting the ancient rock record. *Front. Earth Sci.* 5:97. doi: 10.3389/feart.2017.00097

Sciutteri, V., Smedile, F., Vizzini, S., Mazzola, A., and Vetriani, C. (2022). Microbial biofilms along a geochemical gradient at the shallow-water hydrothermal system of Vulcano Island, Mediterranean Sea. *Front. Microbiol.* 13:840205. doi: 10.3389/fmicb.2022.840205

Sievert, S. M., Brinkhoff, T., Muyzer, G., Ziebis, W., and Kuever, J. (1999). Spatial heterogeneity of bacterial populations along an environmental gradient at a shallow submarine hydrothermal vent near Milos Island (Greece). *Appl. Environ. Microbiol.* 65, 3834–3842. doi: 10.1128/AEM.65.9.3834-3842.1999

Sievert, S. M., Kuever, J., and Muyzer, G. (2000). Identification of 16S ribosomal DNA-defined bacterial populations at a shallow submarine hydrothermal vent near Milos Island (Greece). *Appl. Environ. Microbiol.* 66, 3102–3109. doi: 10.1128/AEM.66.7.3102-3109.2000

Sievert, S. M., and Vetriani, C. (2012). Chemoautotrophy at deep-sea vents: past, present, and future. *Oceanography* 25, 218–233. doi: 10.5670/oceanog.2012.21

Sievert, S. M., Wieringa, E. B. A., Wirsen, C. O., and Taylor, C. D. (2007). Growth and mechanism of filamentous-sulfur formation by *Candidatus Arcobacter sulfidicus* in opposing oxygen-sulfide gradients. *Environ. Microbiol.* 9, 271–276. doi: 10.1111/j.1462-2920.2006.01156.x

Smirnov, A. Y., Mourokh, L. G., and Nori, F. (2009). Kinetics of proton pumping in cytochrome c oxidase. *J. Chem. Phys.* 130:235105. doi: 10.1063/1.3155213

Springael, D., and Top, E. M. (2004). Horizontal gene transfer and microbial adaptation to xenobiotics: new types of mobile genetic elements and lessons from ecological studies. *Trends Microbiol.* 12, 53–58. doi: 10.1016/j.tim.2003.12.010

Tang, K., Liu, K., Jiao, N., Zhang, Y., and Chen, C.-T. A. (2013). Functional metagenomic investigations of microbial communities in a shallow-sea hydrothermal system. *PLoS One* 8:e72958. doi: 10.1371/journal.pone.0072958

Tarasov, V. G. (2006). "Effects of shallow-water hydrothermal venting on biological communities of coastal marine ecosystems of the Western Pacific" in *Advances in Marine Biology*. eds. A. J. Southward, C. M. Young and L. A. Fuiman (London, U.K.: Academic Press (Elsevier)) vol. 50, 267–421. doi: 10.1016/S0065-2881(05)50004-X

Tarasov, V. G., Gebruk, A. V., Mironov, A. N., and Moskalev, L. I. (2005). Deep-sea and shallow-water hydrothermal vent communities: two different phenomena? *Chem. Geol.* 224, 5–39. doi: 10.1016/j.chemgeo.2005.07.021

Truong, D. T., Franzosa, E. A., Tickle, T. L., Scholz, M., Weingart, G., Pasolli, E., et al. (2015). MetaPhlAn2 for enhanced metagenomic taxonomic profiling. *Nat. Methods* 12, 902–903. doi: 10.1038/nmeth.3589

Vetriani, C., Voordeckers, J. W., Crespo-Medina, M., O'Brien, C. E., Giovannelli, D., and Lutz, R. A. (2014). Deep-sea hydrothermal vent *Epsilonproteobacteria* encode a conserved and widespread nitrate reduction pathway (nap). *ISME J.* 8, 1510–1521. doi: 10.1038/ismej.2013.246

Vigil-Stenman, T., Ininbergs, K., Bergman, B., and Ekman, M. (2017). High abundance and expression of transposases in bacteria from the Baltic Sea. *ISME J.* 11, 2611–2623. doi: 10.1038/ismej.2017.114

Wang, L., Cheung, M. K., Kwan, H. S., Hwang, J.-S., and Wong, C. K. (2015). Microbial diversity in shallow-water hydrothermal sediments of Kueishan Island, Taiwan as revealed by pyrosequencing. *J. Basic Microbiol.* 55, 1308–1318. doi: 10.1002/jobm.201400811

Wang, L., Cheung, M. K., Liu, R., Wong, C. K., Kwan, H. S., and Hwang, J.-S. (2017). Diversity of total bacterial communities and chemoautotrophic populations in sulfur-rich sediments of shallow-water hydrothermal vents off Kueishan Island, Taiwan. *Microb. Ecol.* 73, 571–582. doi: 10.1007/s00248-016-0898-2

Wang, Q., Garrity, G. M., Tiedje, J. M., and Cole, J. R. (2007). Naive Bayesian classifier for rapid assignment of rRNA sequences into the new bacterial taxonomy. *Appl. Environ. Microbiol.* 73, 5261–5267. doi: 10.1128/AEM.00062-07

Wang, S., Jiang, L., Hu, Q., Cui, L., Zhu, B., Fu, X., et al. (2021). Characterization of *Sulfurimonas hydrogeniphila* sp. nov., a novel bacterium predominant in deep-sea hydrothermal vents and comparative genomic analyses of the genus Sulfurimonas. *Front. Microbiol.* 12:626705. doi: 10.3389/fmicb.2021.626705

Weissgerber, T., Dobler, N., Polen, T., Latus, J., Stockdreher, Y., and Dahl, C. (2013). Genome-wide transcriptional profiling of the purple sulfur bacterium *Allochromatium vinosum* DSM 180T during growth on different reduced sulfur compounds. *J. Bacteriol.* 195, 4231–4245. doi: 10.1128/jb.00154-13

Wenzhöfer, F., Holby, O., Glud, R. N., Nielsen, H. K., and Gundersen, J. K. (2000). In situ microsensor studies of a shallow water hydrothermal vent at Milos, Greece. *Mar. Chem.* 69, 43–54. doi: 10.1016/S0304-4203(99)00091-2

Westcott, S. L., and Schloss, P. D. (2015). De novo clustering methods outperform reference-based methods for assigning 16S rRNA gene sequences to operational taxonomic units. *PeerJ* 3:e1487. doi: 10.7717/peerj.1487

Wirsen, C. O., Sievert, S. M., Cavanaugh, C. M., Molyneaux, S. J., Ahmad, A., Taylor, L. T., et al. (2002). Characterization of an autotrophic sulfide-oxidizing marine *Arcobacter* sp. that produces filamentous sulfur. *Appl. Environ. Microbiol.* 68, 316–325. doi: 10.1128/AEM.68.1.316-325.2002

Wu, S., Zhu, Z., Fu, L., Niu, B., and Li, W. (2011). WebMGA: a customizable web server for fast metagenomic sequence analysis. *BMC Genomics* 12:444. doi: 10.1186/1471-2164-12-444

Xie, S., Wang, S., Li, D., Shao, Z., Lai, Q., Wang, Y., et al. (2021). *Sulfurovum indicum* sp. nov., a novel hydrogen- and sulfur-oxidizing chemolithoautotroph isolated from a deep-sea hydrothermal plume in the northwestern Indian Ocean. *Int. J. Syst. Evol. Microbiol.* 71:004748. doi: 10.1099/ijsem.0.004748

Yücel, M. (2013). Down the thermodynamic ladder: a comparative study of marine redox gradients across diverse sedimentary environments. *Estuar. Coast. Shelf Sci.* 131, 83–92. doi: 10.1016/j.ecss.2013.07.013

Yücel, M., Gartman, A., Chan, C. S., and Luther, G. W. (2011). Hydrothermal vents as a kinetically stable source of iron-sulphide-bearing nanoparticles to the ocean. *Nat. Geosci.* 4, 367–371. doi: 10.1038/ngeo1148

Yücel, M., Sievert, S. M., Vetriani, C., Foustoukos, D. I., Giovannelli, D., and Le Bris, N. (2013). Eco-geochemical dynamics of a shallow-water hydrothermal vent system at Milos Island, Aegean Sea (eastern Mediterranean). *Chem. Geol.* 356, 11–20. doi: 10.1016/j.chemgeo.2013.07.020

The microbiology and geochemistry of the shallow-water hydrothermal vents of the Gulf of Naples, Italy

Bernardo Barosa[1†], Carmela Celentano[1], Flavia Migliaccio[1,2], Sara Claudia Diana[1,3], Ana Clara Pelliciari Silva[1], Matteo Selci[1,4], Luca Tonietti[1,5,6], Deborah Bastoni[1], Martina Cascone[1], Alessia Bastianoni[1], Monica Correggia[1], Luciano di Iorio[1], Roy Price[7], Stefano Caliro[8], Marco Milazzo[1,3], Alessandro Aiuppa[1,3], Costantino Vetriani[4,9], Angelina Cordone[1], Donato Giovannelli[1,4,10,11,12*]

1 Department of Biology, University of Naples "Federico II", Naples, Italy
2 National Biodiversity Future Center, Italy
3 Department of Earth and Sea Sciences, University of Palermo, Italy National Biodiversity Future Center, Palermo, Italy
4 Department of Marine and Coastal Science, Rutgers University, New Brunswick, NJ, USA
5 Department of Science and Technology, University of Naples, Parthenope, Naples, Italy
6 INAF-OAC, Osservatorio Astronomico di Capodimonte, Naples, Italy
7 School of Marine and Atmospheric Sciences, Stony Brook, NY, United States
8 Istituto Nazionale di Geofisica e Vulcanologia(INGV), Napoli, Italy
9 Department of Biochemistry and Microbiology, Rutgers University, New Brunswick, NJ, USA
10 Istituto per le Risorse Biologiche e Biotecnologiche Marine, Consiglio Nazionale delle Ricerche, CNR-IRBIM, Ancona, Italy
11 Earth-Life Science Institute, Tokyo Institute of Technology, Ookayama, Tokyo, Japan
12 Marine Chemistry & Geochemistry Department - Woods Hole Oceanographic Institution, MA, USA

***Correspondence:** Donato Giovannelli donato.giovannelli@unina.it

Abstract

Shallow-water hydrothermal vents are dynamic ecosystems that occur below 200 m in tectonically active regions of the planet. While their geochemical composition has been investigated in several locations, knowledge about the microbial diversity they harbour remains scarce. Moreover, the relationships between hydrothermal fluid chemistry, geological settings and microbial community structure in shallow vents have not been explored in detail. Here, we investigate the interplay between fluid geochemistry and microbial diversity in two underwater volcanic regions in the Gulf of Naples, Italy, one under the influence of the Somma-Vesuvio volcano and the other located within the underwater portion of the Campi Flegrei caldera. By combining 16S rRNA amplicon sequencing with geochemical measurements, and by contextualizing it with previous geochemical measurements done in the region, we found that hydrothermal fluid chemistry, influenced by the geological setting where the vents are hosted, plays a key role in shaping microbial ecological niches, and imposes strong selective pressures on the resident microbial communities. We additionally describe two new shallow vent sites, contributing to the characterization of the hydrothermalism in the area and unveiling the biodiversity associated with shallow-water hydrothermalism in the region.

Keywords: Shallow-water hydrothermal vents, microbial diversity, geochemistry, biodiversity, Gulf of Naples, Campi Flegrei

1 Introduction

Hydrothermal vents are dynamic marine ecosystems that occur in tectonically active regions of the planet and in proximity to active volcanic regions, where geothermal heat drives fluid circulation in the crust (German and Seyfried, 2014). The resulting hydrothermal fluids enriched in reduced compounds, metals and volatiles mix with oxidised seawater, promoting a redox thermodynamic disequilibrium that fuels highly diverse microbial communities that employ different metabolic strategies (Amend et al., 2003, 2011; Rogers and Amend, 2005, 2006; Dahle et al., 2015, 2018; Price et al., 2015; Rucker et al., 2022). In contrast to their deep-sea counterparts, shallow-water hydrothermal vents (SWHV) occur closer to the surface (below 200 m), and are strongly influenced by solar radiation (Price and Giovannelli, 2017). In these ecosystems chemotrophy and phototrophy co-occur, making SWHVs high energy environments capable of sustaining complex trophic networks (Tarasov et al., 2005; Gomez-Saez et al., 2017; Price and Giovannelli, 2017; Barosa et al., 2023). Due to the shallow depths and consequent decrease in pressure, it is possible to find abundant free-gas phases formed by the exsolution of dissolved volatile gases (Barge and Price, 2022), as well as intense tidal fluctuations and dynamic forcing (Yücel et al., 2013; Price and Giovannelli, 2017; Barge and Price, 2022; Barosa et al., 2023). Additionally, their general proximity to land masses entails a higher transport of terrigenous carbon and phytodetritus into these systems. (Price and Giovannelli, 2017).

Previous studies conducted in shallow-water hydrothermal vents have demonstrated a highly diverse microbial consortia inhabiting these ecosystems (Cardigos et al., 2005; Rusch et al., 2005; Manini et al., 2008; Maugeri et al., 2010, 2013; Giovannelli et al., 2013; Gugliandolo et al., 2015; Sciutteri et al., 2022; Silva et al., 2025b). SWHVs were recently proposed to be a possible cradle for the origin of life or the early evolution of microbial metabolism (Barge and Price, 2022; Rucker et al., 2022). Thermodynamic mapping of exergonic reactions has demonstrated a high energy landscape available for microbial metabolism (Amend et al., 2003; Rogers and Amend, 2005, 2006; Rogers et al., 2007; Price et al., 2015; Lu et al., 2020). Depending on the typology of the hydrothermal system, niche stratification can be observed, with a shift from sites dominated by chemolithoautotrophic and sulfur utilising microbial communities to an increase of phototrophic and heterotrophic communities (Giovannelli et al., 2013; Gugliandolo et al., 2015; Fagorzi et al., 2019; Barosa et al., 2023; Silva et al., 2025b).

Differences in fluid geochemistry and the geological setting where hydrothermal systems are hosted have been shown to impose strong controls on the resident microbial communities (Fullerton et al., 2021; Colman et al., 2023; Sims et al., 2023; Upin et al., 2023). As water percolates into the crust, fluids are transformed by subsurface processes, such as temperature dependent water-rock-gas reactions, the release of metals and other elements from the host lithologies, as well as phase separation events (Tivey, 2007; German and Seyfried, 2014; Price et al., 2015). As such, the

composition of each hydrothermal fluid can be, to some degree, unique to every hydrothermal system, reflecting changes in rock type, shape and size of the heat sources, composition of the primary volatiles, geochemical reactions happening during fluid ascent, timescales of fluid-rock interaction (German and Seyfried, 2014; Ely et al., 2023). The typology of the system also exerts control on how the fluids are being discharged at the surface. For instance, hydrothermal systems hosted close to a heat source (e.g. magmatic chamber or intrusions) or with direct channelling to the surface, usually present higher temperatures and more focused flows, compared to more diffuse fluids, where there is a higher degree of mixing between the hydrothermal fluids with seawater (Von Damm and Lilley, 2004; Scheirer et al., 2006). This mixing also constrains the possible niches occupied by microbial communities, given the variance in electron donors/acceptors available, as well as different carbon sources. However, the extent to which these different geochemical landscapes constrain shallow-water hydrothermal vents communities has not been explored in detail.

A previous study conducted in SWHV of the Aeolian archipelago (Italy) reported that microbial communities changed according to the different geochemical regimes found within the different islands, following large-scale trends in volcanic activity (Barosa et al., 2023). Here, we combine 16S rRNA amplicon sequencing with geochemical and physico-chemical measurements of the shallow-water hydrothermal vents present within two volcanic regions of the Gulf of Naples, in the Campania region, Italy, to investigate how the geochemistry and typology of the hydrothermal systems in the area structure the microbial communities. The Gulf of Naples is characterized by the presence of active volcanisms, with three active volcanoes in the area that are either surrounded or extend at sea. Given the recent signs of unrest with increasing seismic activity of the Campi Flegrei volcano (Astort et al., 2024; Giudicepietro et al., 2025), this study may provide baseline microbiological data for future research aimed at understanding shifts in microbial communities in response to changes in volcanic activity.

2 Experimental Procedures

2.1 Campi Flegrei and Somma-Vesuvius volcanic complexes

Naples's area is characterized by the presence of three active volcanoes: the Ischia volcanic complex, the Campi Flegrei caldera and the Somma-Vesuvius volcanic complex. The gulf is characterized by intense hydrothermal activity, with numerous submarine hydrothermal systems reported in the region (Figure 1) (De Astis et al., 2004; Aiello et al., 2010; Kerrison et al., 2011; Calosi et al., 2013; Torrente and Milia, 2013; Passaro et al., 2014b; Somma et al., 2016; Donnarumma et al., 2019; Baldrighi et al., 2020; Bellec et al., 2020; Sacchi et al., 2020).

The Campi Flegrei caldera is a significant and historically active volcanic field situated along the Neapolitan Tyrrhenian coastline of Italy. The distinctive geomorphology of the Pozzuoli Bay area has been shaped by two major explosive eruptions: the Campanian Ignimbrite approximately 39,000 years ago (Rosi et al., 1996) and the Neapolitan Yellow Tuff around 15,000 years ago (Orsi et al., 1992). The southern part of the caldera is now submerged (the Pozzuoli Bay area), and is hence characterised by intense underwater hydrothermal activity. The area has been characterized by uplifting and intense seismic events (Astort et al., 2024; Giudicepietro et al., 2025), and the inland and submarine geothermal features are constantly monitored to understand the state of unrest of the volcano. The last eruption is dated 1538, with the formation of Monte Nuovo.

On the western side of the city of Naples, the Somma-Vesuvius volcanic complex originated from a sequence of eruptions through time, starting from the construction of the Somma edifice (>20,000 years ago) that was later (partially) dismantled in a sequence of Plinian eruptions between 20,000 to 1,871 years ago. These eruptions gave rise to the formation of a summit caldera, measuring 4.9 by 3.4 kilometres in an east-west elongated configuration (Bertagnini et al., 1998), topped by the young (post-caldera) Vesuvius cone. Mild hydrothermal activity has been ongoing at Vesuvius since its last eruption in 1944. Key indicators of this activity include: (a) weak fumarolic emissions, accompanied by diffuse soil CO_2 degassing in the crater area (Chiodini et al., 2001; Frondini et al., 2004); (b) CO_2-rich groundwaters along the southern flank of Vesuvius and in the adjacent plain (Caliro et al., 2011); and (c) episodic seismic activity with epicentres concentrated within the crater (Caliro et al., 2011). The toe-shaped morphology on the seafloor located in the southwestern side of the Somma-Vesuvius is explained by two flank collapses in the Late Pleistocene (Passaro et al., 2014a).

2.2 Sampling and site description

Samples were collected from June to October 2020 during the FEAMP20 expedition on the shallow-water hydrothermal vents present on the Gulf of Naples (Figure 1) following a large-scale sampling approach (Giovannelli et al., 2022). More specifically, samples were collected at the region of Campi Flegrei caldera: Secca delle Fumose (SF) and Gabbiano (GB), at the region of Campi Flegrei caldera rim: Capo Miseno (CM), and the region of Somma-Vesuvius: Bagno Conte (BC). The most interesting sites, Secca delle Fumose (geyser) and Capo Miseno, were sampled twice, and indicated as SF_G2 and CM2, respectively (Table 1). All samples were retrieved by scuba divers, and in order to get a broader characterization of the vent environment, three types of samples were collected at each site: sediments, fluids, and biofilms. Fluids were sampled through the insertion of a silicon tube in the selected vent orifice (7-15 cm), and filtered through Sterivex 0.22 µm filter membranes. The sediments were collected in the vent orifice (top 1-2 cm), and biofilms were collected at or in the vicinity of the vents. For geochemical analyses, fluids were filtered (0.22 µm) and treated with nitric acid (final concentration of 2 %). In the laboratory, Sterivex filters and

sediments were stored at -20 °C until DNA extraction, while the samples for geochemical analyses were stored at 4 °C. Physico-chemical parameters for each sample site were measured *in-situ* using a multiparametric probe (HANNA, HI98196), a refractometer (Fisherbrand ™), and a field thermometer.

2.3 Geochemical Analysis

The concentrations of major cations (sodium-Na^+, potassium-K^+, magnesium-Mg^{2+}, ammonia-NH_4^+, and calcium-Ca^+) and anions (chlorine-Cl^-, sulfate-SO_4^{2-} and bromide-Br^-) of the sampled fluids were measured (in duplicates) using ion chromatography (ECO, IC Metrohm). Calibration curves for the ion species were measured in the range of 0.1 and 200 ppm with an $R \geq 0.999$. All samples were filtered (0.22 µm) and diluted to a conductivity of 600 µS/cm (Correggia et al., 2023a). All dilutions were made using 18.2 MΩ/cm type I water, also used as a blank for blank subtractions. Anions were run using a 3.2 mM Na_2CO_3 + 1 mM $NaHCO_3$ mobile phase on a Metrosep A Supp 5 column equipped with a 0.15 M ortho-Phosphoric acid suppressor. The flow of the anionic eluent was 0.7 ml min^{-1} for 30 min. Cations were run using a 2.5 mM HNO_3 + 0.5 mM $(COOH)_2 \times 2H_2O$ mobile phase on a Metrosep C4 column. The flow of the cationic eluent was 0.9 ml min^{-1} with a total separation of 35 min. Data acquisition and analysis were carried out through MagIC Net 3.3 software. Calibration curves were defined using certified CPA chem external multi-ion standards for each of the anions and cations analysed in this study (1000 mg/L). Additionally, the concentration of biologically relevant trace elements (i.e. Fe, Zn, As, Rb, Sr, Mo and Cs), were measured (in triplicates) using an Agilent inductively coupled plasma mass spectrometer (Agilent ICP-MS 7900) following the standard operating practice developed at the Giovannelli Lab (Correggia et al., 2023b). Calibration curves covered a concentration range between 0.01 to 100 ppb, and were run using Agilent certified multistandard 2A (10 µg/mL of Ag, AI, As, Ba, Be, Ca, Cd, Co, Cr, Cs, Cu, Fe, Ga, K, Li, Mg, Mn, Na, Ni, Pb, Rb, Se, Sr, TI, U, V, Zn). Additionally, we contextualised the geochemistry of these hydrothermal systems with published data from the region found in the literature. The visualisation and statistical analysis on geochemical data were carried out in the R statistical software version 4.1.2 (Core, 2021) and ggplot2 packages (Wickham, 2011).

2.4 DNA Extraction and Amplicon Sequencing

DNA extraction was performed using the DNeasy PowerSoil Kit (QIAGEN), following the manufacturer's instructions, with an extra elution step. When low DNA yields were obtained, a modified phenol-chloroform DNA extraction method was used, adapted for shallow-water hydrothermal vent conditions (Giovannelli et al., 2013, 2016b). Briefly, 850 µl of extraction buffer (50 mM Tris-HCl pH 8, 20 mM EDTA pH 8, 100 mM NaCl) was added to 0.5 g of sediment and sterivex filters. Followed with 100 µl of Lysozyme (100 mg/ml) and 5 µl of Proteinase K, with a step

of incubation at 37 °C for 30 min after each supplementation step, and followed by 1 min of vortexing. Subsequently, 50 µl of 20 % SDS was added to the samples and incubated for 30 min at 65 °C, with regular mixing, followed by a vortexing step for 1 min. Samples were then centrifuged for 3 min at 14,000 × g. The supernatant was collected and transferred to a phenol:chloroform:isoamyl alcohol (25:24:1) solution, followed by centrifugation for 3 min at 14,000 × g. The aqueous phase was collected and transferred to a solution of chloroform:isoamyl alcohol (24:1) and centrifuged for 3 min at 14,000 × g. The supernatant was collected and supplemented with Na-acetate (0.1 vol) and isopropanol (0.7 vol), and incubated at -20 °C for 2 h. The precipitated DNA was further washed with 70% cold ethanol and re-suspended in 50 µl of Tris-HCL. DNA was visualised with agarose gel electrophoresis and quantified spectrophotometrically and spectrofluorimetrically (NanoDrop and Qubit, respectively). The successfully extracted DNA was sequenced at the Integrated Microbiome Resource (IMR, https://imr.bio) using primers targeting the V4-V5 region (515FB = GTGYCAGCMGCCGCGGTAA and 926R = CCGYCAATTYMTTTRAGTTT515FB - 926R) of the 16S rRNA gene, using an Illumina V3 sequencing MiSeq.

2.5 Bioinformatic and statistical analysis

The raw sequencing data were analysed using the DADA2 package (Callahan et al., 2017). Quality profile analysis was carried out after trimming the primers and adapters, where only the sequences with a quality call for each base between 20 and 40 were kept for downstream analysis. Amplicon sequencing variants (ASVs) were estimated through error profiling, and taxonomy was assigned to each ASV with the SILVA database, release 138 (Quast et al., 2013). Amplicon variant abundance tables and taxonomic assignments were used to create a phyloseq object to further calculate diversity indices and investigate the microbial diversity, as previously reported (Cordone et al., 2022, 2023; Barosa et al., 2023). Sequences belonging to Mitochondria, Eukaryotes, Chloroplasts, groups related to human pathogens and common DNA extraction contaminants (Sheik et al., 2018), as well as the sequenced blanks, were removed from the dataset. The remaining reads represented 95 % of the original reads, with 178671 reads assigned to 4612 ASVs. Diversity analyses were carried out using the Phyloseq package (McMurdie and Holmes, 2013) with the relative abundance values set to 100 %. Beta diversity was investigated using the Jaccard diversity index (Unweighted and Weighted) as implemented in the vegan package (Oksanen et al., 2018). The obtained ordination was used to investigate the correlation between the environmental and geochemical variables using environmental fitting (*envfit* and *ordisurf* functions). ASV taxonomic classification was further carried out using the EzBioCloud database (Yoon et al., 2017), as well as blasted against the nucleotide database of the National Center for Biotechnology Information (NCBI). All statistical calculations, data processing, and visualisation were carried out in the R statistical software version 4.1.2 (Core, 2021) and ggplot2 packages (Wickham, 2011). All the sequences analysed in this study are available through the

European Nucleotide Archive (ENA) under project accession PRJEB67762, under the ENA Umbrella project CoEvolve PRJEB55081. A complete R script containing all the steps of our analysis is available at https://github.com/giovannellilab/Barosa_et_al_Feamp20_16S with DOI: 10.5281/zenodo.14966493, together with all the environmental and geochemical data.

3 Results

3.1 Site description and physico-chemical parameters

The samples were collected in three different locations belonging to two different volcanic regions (Figure 1), the Campi Flegrei caldera (SF_G1, SF_G2, SF_EF, and GB) and caldera rim (CM1 and CM2), and the Somma-Vesuvius area (BC). Venting in the SF_G1 site, known by local divers as the geyser, occurs in a rocky bottom and it is characterized by intense focused emission surrounded by yellow, orange and white bacterial mats and mineral precipitates. No free gas is visible at this site. Venting in the SF_EF site, located in close proximity to SF_G1, occurs in a field of large rocks . Gas bubbles are visible and run against the rocks determining the distribution of abundant white biofilms. Venting at site GB is diffuse and occurs through sediments covered with white particles. Minimal free gas is present in the area. The site CM, located in the Campi Flegrei caldera rims is characterized by diffuse gas emission in a rocky area and the presence of a larger more focused opening named “the flute”, covered with white filamentous biofilms. The site BC, in the region of Somma-Vesuvius, is located at the shoreline, and characterised by white particles in suspension and an intense smell of “rotten eggs” characteristic of H_2S.

The physico-chemical parameters of the shallow-water hydrothermal vents of the Gulf of Naples sampled in this study are shown in Table 1. Vent temperatures varied from 26.3 °C in the SWHV of CM1 to 71 °C in SF_G1. The salinity ranged from 17.65 PSU in BC to 38.37 PSU in CM2. Dissolved oxygen (DO) values ranged from 43 % in GB to 92 % in CM2. The oxidation-reduction potential (ORP) was negative for all the sampling sites with the exception of CM2, in which the value is 54.2 mV. The pH was slightly acidic for every sampled shallow-water vent (average pH of 5.73). The conductivity for each site is around 50 mS/cm, with the exception of BC, in which the value is 28.7 mS/cm. The total dissolved solid (TDS) ranged between 14.31 ppt TDS in BC to 28.76 ppt TDS in CM2.

3.2 Geochemical Results

The concentrations of the major and minor elements (and respective measurement errors reported in % RSD) of the shallow-water hydrothermal vents sampled in this study are presented in Table 2 and Table 3, respectively. Chloride (Cl^-) ranged from 10,030.06 ppm in the BC site to 21,094.04 ppm at CM1. Bromide (Br^-) values ranged from 34.27 ppm in BC to 72.48 ppm in CM1, whereas sulfate

(SO_4^{2-}) ranged from 1,377.55 ppm in BC to 2,920.13 ppm in SF_EF. Sodium (Na^+) values ranged from 5,844.84 ppm in BC to 12,783.86 ppm in SF_EF, while ammonium (NH_3^+) ranged from 33.28 ppm in GB to 40.30 ppm in SF_G2. Potassium (K^+), magnesium (Mg^{2+}), and calcium (Ca^{2+}) concentrations ranged from 198.47 ppm in BC to 598.43 ppm in GB, 606.89 ppm in BC to 1,395.17 ppm in CM1, and 434.79 ppm in SF_EF to 497.28 ppm in SF_G2, respectively.

The trace elements measured in this study are presented in Table 3. Manganese (Mn) concentrations ranged from 0.0037 ppm in CM2 to 3.1 ppm in GB, while iron (Fe) concentrations ranged from 0.011 ppm in CM2 to 11.12 ppm in GB. Zinc (Zn) and Arsenic (As) concentrations ranged from 0.023 ppm in SF_EF2 to 0.46 ppm in CM1, and 0.011 ppm in SF_EF2 to 2.45 ppm in SF_G2 in SF_G2, respectively. Rubidium (Rb) concentrations ranged from 0.12 ppm in BC to 3.23 ppm in GB. Strontium (Sr) and Caesium (Cs) values ranged from 8.11 ppm in BC to 13.3 in SF_G1, and 0.002 ppm in CM1 to 1.73 ppm in SF_G1, respectively. Molybdenum (Mo) concentrations ranged from 0 ppm in BC to 0.012 ppm in SF_EF2. Seawater element concentrations were obtained from Price et. al., 2015.

Principal Component Analysis (PCA, Figure 2A) constructed using the physico-chemical characteristic of each site and major ion composition shows that sites clustering according to the geographic locations where venting occurs, with the exception of SF_EF. Site BC, located under the influence of the Somma-Vesuvius volcanic complex, presented the most diverse geochemistry compared to all the other sites investigated and clustered on its own (Figure 2A). The concentrations of chloride plotted against sodium suggest that all the fluids are of seawater origin and mixed with lower salinity deeply-derived fluids with the exception of BC, that might be the results of meteoric recharge mixing with seawater and shows much lower salinities (Figure 2B). The mixing plots of the other major ions (Figure 2D–E) support this trend, revealing three distinct clusters (consistent with the PCA results). Sites SF_EF, CM1, and CM2 exhibit concentrations similar to seawater, indicating a higher degree of fluid mixing with background seawater, compared to sites SF_G1, SF_G2, and GB. The higher Fe concentrations observed at site GB (Figure 2F) suggest increased rock leaching, possibly influenced by the local host lithology.

3.3 Microbial Diversity

The microbial diversity of the shallow-water vents of the Gulf of Naples was investigated using the V4-V5 regions of the 16S rRNA gene. A total of 4,612 ASVs were identified (after quality check and filtering steps, see methods for details).

The sites SF_G1, SF_G2, SF_EF, and GB are in the Campi Flegrei caldera region (Figure 3). The site SF_G1, represented only by a fluid sample, was dominated by the Aquificota phylum, followed by Chloroflexi, Desulfurobacterota, and an unidentified phylum, at lower abundances. Within Aquificota,

Hydrogenothermus was the most abundant genus in this site (63.0 % average relative abundance). Within Chloroflexi, the most abundant family was *Anaerolineaceae*, with no classification down to the genus level (8.8 % average relative abundance). Within Desulfurobacterota, the most abundant genera belonged to the *Thermodesulforhabdus* and *Thermosulfurimonas* (4.5 % and 3.0 % average relative abundance, respectively). An unidentified phylum was also present in lower abundances (2.1 % average relative abundance). The site SF_G2, composed of both fluid and sediment samples, was dominated by members belonging to the phyla Proteobacteria, Cyanobacteria and Bacteroidota, at lower abundances. Within Proteobacteria, the most abundant family belonged to *Thiomicrospiraceae*, with no further classification down to the genus level (5.2 % average relative abundance across fluid and sediment samples), followed by a gammaproteobacterial unidentified ASV (3.0 % average relative abundance across fluid and sediment samples). Additionally, it was possible to identify the genera *Thiogranum*, and *Woeseia*, the Sars11 clade, and the genus *Thiohalophilus* (2.4 %, 2.3 %, and 2.2 % average relative abundance across fluid and sediment samples, respectively). Within Cyanobacteria, the most abundant genus belonged to *Synechococcus* CC9902 (3.6 % average relative abundance across fluid and sediment samples). Within Bacteroidota, the most abundant family belonged to *Cryomorphaceae*, with no further taxonomic classification (2.2 % average relative abundance across fluid and sediment samples).

The site SF_EF has as most abundant members, ASVs affiliated to the Bacteroidota phylum, with Calditrichota, Desulfurobacterota, Halobacterota, and Campylobacterota, present in lower abundances. Within Bacteroidota, the most abundant ASV belongs to the clade bacteroidetes VC2.1 Bac22 (5.0 % average relative abundance across the fluid and sediment samples), and to the families *Lentimicrobiaceae*, *Melioribacteraceae*, and *Bacteroidetes* BD2-2 (3.8 %, 3.1 %, and 2.1 % average relative abundance across fluid and sediment samples, respectively). Within Calditrichota, Desulfurobacterota, Halobacterota, and Campylobacterota, ASVs were affiliated with the genera *Calditrix*, *Desulfovibrio*, *Methanofolis*, and *Sulforovum*, respectively (3.3 %, 2.7 %, 2.7 %, 2.5% average relative abundance across fluid and sediment samples, respectively).

The site GB, located near both SF_G1 and SF_G2, is the one in this region closest to land. This site is composed of both fluid and sediment samples, and dominated by members belonging to the Bacteroidota phylum, with Acidobacterota, Desulfurobacterota, Nanoarchaeota, and an unidentified phylum, present at lower abundances. Within Bacteroidota, the most abundant genus belongs to *Marinifilum* (7.6 % average relative abundance across fluid and sediment samples), followed by the clade PHOS-HE36 and family *Cyclobacteriaceae*, which could not be resolved to the genus level (5.9 % and 2.5 % average relative abundance across fluid and sediment samples, respectively). Additionally, it was possible to identify the clade lheB3-7 (2.2 % average relative abundance across fluid and sediment sample, as well as an ASV belonging to an unidentified phylum (3.9 % average relative abundance across fluid and sediment sample). Within Acidobacteriota, the genus

Thermotomaculum was present in higher abundances (2.5 % average relative abundance across fluid and sediment samples). Within Desulfurobacteriota and Nanoarchaeota, it was possible to identify the family *Desulfosarcinaceae* and the clade SCGC_AAA011-D5, with no further taxonomic classification (2.1% average relative abundance in both the fluid and sediment samples).

The sites CM1 and CM2 are located within the Campi Flegrei caldera rim region. The site CM1, composed of both fluid and sediment samples, was dominated by the phylum Bacteroidota and Proteobacteria, with Campylobacterota present at lower abundances. Within Bacteroidota, the most abundant family belonged to the *Flavobacteriaceae*, where it was possible to identify the genera *Lutibacter*, *Olleya*, and *Maritimimonas* (8.0 %, 3.7 %, and 2.0 % average relative abundance across fluid and sediment samples, respectively). Additionally, one ASV could not be resolved to the genus level (5.1 % average relative abundance in both the fluid and sediment samples). The ASVs belonging to the families *Saprospiraceae* and *Cryomorphaceae* were not possible to classify down to the genus level (4.2 % and 2.6 % average relative abundance across fluid and sediment samples). Within Proteobacteria, the most abundant family belonged to the *Rhodobacteraceae*, where one ASV could not be classified to the genus level, and the other to the genus *Actibacterium* (3.8 % and 2.1 % average relative abundance across fluid and sediment samples). The family *Thiotrichaceae* could not be resolved to the genus level (3.0 % average relative abundance across fluid and sediment samples). Within Campylobacterota, *Sulfurovum* was the most abundant genus (2.5 % average relative abundance across fluid and sediment samples). The site CM2 was dominated by the phylum Bacteroidota and Proteobacteria in higher abundances, with Cyanobacteria, Campylobacterota, and Planctomycetota present at lower abundances. Within Bacteroidota, the most abundant family belonged to *Cyclobacteriaceae*, with no further taxonomic classification (2.3 % average relative abundance across the fluid and sediment samples). Within Proteobacteria, *Woesia* was the most abundant genus (4.3 % average relative abundance across fluid and sediment samples), followed by the SAR 11 and B2M28 clades, with no classification down to the genus level (2.5 % and 2.2 % average relative abundance across the fluid and sediment samples). Within Cyanobacteria, Campylobacterota and Plactomycetota, *Synechococcus* CC9902, *Sulfurovum* and *Rubripirellula* were the most abundant genera (3.5 %, 2.2 %, and 2.2 % average relative abundance across the fluid and sediment samples, respectively).

The BC site located within the Somma-Vesuvius volcanic area, was dominated by members belonging to the Bacteroidota and Proteobacteria phyla, with Desulfurobacterota present at lower abundances (Figure 3). Within Bacteroidota, the most abundant order belongs to the *Flavobacteriales*, with the most abundant ASV not resolved to the genus level (13.3 % average relative abundance across fluid and sediment samples), followed by the clade n7 marine group (9.8 % average relative abundance across fluid and sediment samples), and the genus *Artictiflavibacter* (2.3 % average relative abundance across fluid and sediment samples). The order *Ignavibacteriales* was dominated by the

clade LheB3-7 (4.0 % average relative abundance across fluid and sediment samples), followed by the Bacteroidetes VC2.1 Bac22 clade (4.6 % average relative abundance across fluid and sediment samples). Within Proteobacteria, the most abundant genera belong to *Thiomicrorhabdus* (7.8 % average relative abundance across fluid and sediment samples), followed by *Thioclava* (3.8 % average relative abundance across fluid and sediment samples), and *Cocleimonas* (2.7 % average relative abundance across fluid and sediment samples). The low abundance phylum Desulfurobacteriota was dominated by the genus *Desulfobulbus* (2.1 % average relative abundance across fluid and sediment samples).

The biofilm samples were collected in the vicinity of the vent orifice (Figure 4). At the Campi Flegrei region, in SF_G1 and SF_G2 sites (two biofilms were collected - SF_G2A and SF_G2B), the biofilm communities were dominated by ASVs belonging to the Aquificota phyla, more specifically to *Hydrogenothermus* genus (49 %, 37.4 %, and 87.4 % relative abundance, respectively), with other phyla present at lower abundances. On the other hand, at the site CM2, the biofilms were instead dominated by ASVs belonging to the class Gammaproteobacteria (36.9 % relative abundance), with no classification down to the genus level, and the genus *Thiothrix* at lower abundances (8.4 % relative abundance). At the site BC, the most abundant ASVs were affiliated to the genus *Thiothrix* (30.7 % relative abundance).

In order to understand the role of the measured geochemical and environmental parameters in constraining the distribution of the microbial communities inhabiting the sampled shallow-water hydrothermal vents, we performed both abundance weighted and unweighted (presence-absence) multivariate ordination (nMDS) based on the Jaccard dissimilarity indexes. We found that the microbial communities are separated according to the different settings where the vents occur, as well as to fluid geochemistry observed in our geochemical analysis (Figure 2A, Figure 5A and 5B, and Supplementary Figure 2 for nMDS based on the unweighted Jaccard index). The clustering based on the geographic location is statistically significant in both the weighted, as well as the unweighted jaccard based nMDS, taking into account the volcanic region (ADONIS, $n = 7$, $p = 0.034$ and adj.p = 0.005), as well as the geochemical regime (ADONIS, $n = 7$, $p = 0.034$ and adj.p = 0.004). Environmental fitting performed on the weighted Jaccard nMDS show that: salinity, total dissolved solids, conductivity, and the concentrations of Na, Cl, and Br, were statistically correlated with the changes in betadiversity (adj.p < 0.05). Salinity and Sr concentrations were statistically correlated with the unweighted jaccard based nMDS (adj.p < 0.05) (Supplementary Table 2).

4 Discussion

Coupled geochemical and microbiological analyses are fundamental to understanding the geosphere-biosphere feedback in natural ecosystems (Giovannelli et al., 2022). In hydrothermal

systems, both continental and marine hosted, geosphere-biosphere coupling is much stronger compared to other ecosystems, since the microbial communities largely rely on compounds and elements provided by the hydrothermal fluids and derived from fluid-rock interactions (Dahle et al., 2018; Fullerton et al., 2021; Barosa et al., 2023; Colman et al., 2023; Basili et al., 2024). In the present study, we analysed the geochemistry of hydrothermal fluids collected from the shallow-water hydrothermal vents of the Gulf of Naples, occurring within two different volcanic regions, Campi Flegrei and Somma-Vesuvius (Figure 1). We also report the geochemical characterization of two new shallow-water hydrothermal vent sites (CM1/2, and GB) that, to our knowledge, have never been described in the literature before. We contextualised the geochemistry of these hydrothermal systems with previous studies done in the region.

4.1 Geochemistry of the shallow-water vents of the Gulf of Naples

On the seafloor, the ascent of hydrothermal fluids is facilitated through the permeability of lithospheric fault systems, allowing a more focused channelling of subsurface fluids to the surface (Pearce et al., 2019). All the sampled sites are located within proximity to fault systems (see geological maps in Tramparulo et al., 2018 and Aucelli et al., 2020), which might facilitate both recharging and discharge.

Three major groups of venting fluid geochemistry can be identified using the major ions composition (Table 2 and Figure 2A-E). The first two groups occur within the Campi Flegrei caldera and are hosted in Campania ignimbrite rocks, characterizing the area and can be recognized by their fluid chemistry using classic diagnostic plots for hydrothermal systems (Price et al., 2015). In end-member hydrothermal fluids, Mg^{2+} is depleted due to high temperature water-rock reactions, and it can therefore be used as a tracer to infer the degree of mixing with seawater (Price et al., 2015; Di Napoli et al., 2016). Ion concentrations, including Mg^{2+} in the first group of samples, composed of the fluids from the sites CM1, CM2, and SF_EF, had concentrations and compositions similar to seawater, suggesting a high degree of mixing between the venting hydrothermal fluids and seawater. By contrast, a second group of samples, from GB, SF_G1, and SF_G2, presented a lower degree of mixing, as suggested by the lower Mg^{2+} concentrations and the presence of NH_4^+. In seawater, NH_4^+ is present in trace amounts, as it is readily assimilated by phytoplankton and oxidised by nitrifying microorganisms (Karl et al., 2008; O'Connor Šraj et al., 2017), while high concentrations of NH_4^+ have been reported in hydrothermal springs within the Campi Flegrei region (Sieland, 2009). This suggests a higher contribution of primary hydrothermal fluids to these sites. Additionally, sites SF_G1 and SF_G2 have similar fluid chemistry with respect to previous geochemical data collected in 2006, highlighting the stability of the system (Di Napoli et al., 2016).

The third group, represented only by the site BC, occurs within a different host lithology in the southern portion of the Gulf of Naples (carbonates - Figure 1). The site location in the intertidal zone and the low concentrations of Cl^- and Na^+ compared to the other sites suggest mixing with groundwaters before discharge. A previous study done in the region has shown that the fluids of the vents present in this region are a mixture of seawater and groundwater end-members, as a result of saltwater intrusion into fractured and karstified aquifers, which could account for the differences in fluid chemistry seen here (Baiocchi et al., 2010).

The fluids from the site GB, SF_G1 and SF_G2 were enriched in elements such as Rb, Cs, Fe, As, and Mn. It has been demonstrated that some elements, such as Rb and Cs, can be efficiently extracted from basalt at higher temperatures (Palmer and Edmond, 1989). Cs/Rb ratios in the SF_G1/G2 fluids are high, suggesting equilibration with mafic rocks at depth (Palmer and Edmond, 1989). Sites GB, SF_G1 and SF_G2 were also enriched in As, which can be leached from host lithologies at high temperatures. Arsenic, in the form AsO_3^{3-} and AsO_4^{3-} is an important electron donor and acceptor for microorganisms and it has already been reported in high concentrations in multiple shallow-water hydrothermal systems (Aiuppa et al., 2006; Pichler et al., 2006; Leal-Acosta et al., 2013; Price et al., 2013; Ruiz-Chancho et al., 2013). Fluids from SF_G1/SF_G2, and GB, were also enriched in Mn and Fe, although with different concentrations (GB site had higher concentrations of Fe and Mn). These elements are frequently enriched in hydrothermal fluids (Tebo and Mandernack, 1993; Scholten et al., 2019), indicating that these fluids could be equilibrating within similar host lithologies. The difference in temperature (more than 30 °C), Fe, and Mn, observed between SF_G1/SF_G2, and GB, could be due to the mixing with seawater as the fluids approach the surface, and/or different water-rock reactions (for instance, in the upflow zone - secondary mineral precipitations), respectively.

The PCA analysis (Figure 2A) shows that the concentrations of the fluids from the shallow-water hydrothermal vents CM1, CM2, and SF_EF cluster together and therefore have similar fluid chemistry. Their similar chemistry, with respect to seawater in the major ions biplots (Figure 2- B-E), suggests a higher degree of mixing at these locations (i.e., a lower ratio between hydrothermal fluid vs seawater). The sites GB, SF_G1, and SF_G2, had similar fluid chemistry between each other (clustering together in the PCA analysis), and were located within the same region within the Campi Flegrei caldera (see Figure 1).

Noble gases, due to their inert properties, can serve as valuable geochemical tracers (Hilton et al., 2002). Helium, for instance, has two stable isotopes: ^3He and ^4He. ^3He is primordial and has been stored in the mantle following Earth's accretion 4.56 Gyr. In contrast, ^4He is produced continuously on Earth through the radioactive decay of U and Th (Barry et al., 2022, Hilton et al., 2002). The mean ratio of $^3He/^4He$ for arc gases is approximately 5.4 ± 1.9 Ra (Ra = 1.39×10^6, Hilton et al., 2002; Ozima and Podosek, 2002). Changes in this ratio can provide information about the origin of volatiles

in hydrothermal systems (i.e. crust and/or mantle derived) (Hilton et al., 2002). A previous study measured $^{3}He/^{4}He$ in both shallow-water hydrothermal vents, as well as in-land geothermal wells and fumaroles in the Campi Flegrei volcanic region (Tedesco et al., 1990). The authors found that there is no significant difference in the $^{3}He/^{4}He$ ratio between the sites ($^{3}He/^{4}He$ ratios ranging between 2.0 and 3.2 Ra), thus suggesting a common source of helium in the two regions. Notably, however, $^{3}He/^{4}He$ ratios have been shown to decrease towards the margins of the Campi Flegrei caldera. A lower $^{3}He/^{4}He$ ratio in the peripheral manifestations could be due to greater distances from the magmatic source and the primary location of degassing, or mixing with crustal derived volatiles higher in ^{4}He (Tedesco et al., 1990). One of the lowest $^{3}He/^{4}He$ values measured in Campi Flegrei was found close to where the CM1 and CM2 sites were sampled in the present study. Additionally, Orlando et al. (2011), through the analysis of gas ratios of H_2, Ar, CH_4, and CO_2, found that gases from the Secca della Fumosa region (SF site in this work) are equilibrated at approximately 250 °C, compared to lower equilibration temperatures in samples collected from the Capo Miseno region (150 °C). Even though we did not directly measure gases in this work, the aforementioned studies suggest that the CM1 and CM2 vents occur further away from the main magmatic gas outflow path than, for instance, the vents present in the SF region, supporting regional differences in geochemistry of the fluids controlled by regional difference in volcanism. Since the shape, size and distance to the heat source has been acknowledged to be one of the most important parameters dictating the chemistry of hydrothermal fluids (German and Seyfried, 2014), this could explain both the divergence in fluid chemistry measured in CM1 and CM2, as well as the possible higher mixing with seawater as the fluids approach the surface.

Taken together these results highlight how even in such small scales, regional differences in the host lithologies and geological background can have an impact in the hydrothermal fluid chemistry.

4.2 Microbial Diversity

The microbial communities inhabiting the shallow-water hydrothermal vents of the Gulf of Naples, were mostly dominated by ASVs belonging to Proteobacteria and Bacteroidota, with other phyla present at lower abundances (Figure 3). Dominant groups have been previously reported from other shallow-water hydrothermal environments (Zhang et al., 2012; Giovannelli et al., 2013; Gomez-Saez et al., 2017; Price and Giovannelli, 2017, 2019; Barosa et al., 2023). The inherent characteristics of SWHV, such as the presence of both sunlight and geochemical energy, coupled with organic and inorganic carbon sources, reflect both the diversity of taxa as well as the metabolic strategies found in these ecosystems (Price and Giovannelli, 2017). For instance, in the present study, we consistently find ASVs associated with groups known to perform chemolithoautotrophy, chemoheterotrophy, heterotrophy, and photoautotrophy. The differences in their distribution, however, may be related to the topology of the hydrothermal system, as well as to fluid geochemistry and mixing patterns. The

mixing of hydrothermal fluids with seawater during ascent and venting creates dynamic mixing zones, generating a plethora of microbial niches with diverse combinations of electron donors and acceptors, suggesting that hydrothermal systems with a higher degree of mixing could support a greater diversity of ecological niches to be explored by the resident microbial communities.

The Campi Flegrei venting sites SF_G1 and SF_G2 were collected at the same location, on two different occasions. They present remarkably different communities. For instance, SF_G1 has the most abundant ASVs related to taxa commonly found in high temperature shallow-water hydrothermal systems (Barosa et al., 2023). At this site, the majority of the ASVs were associated with the genus *Hydrogenothermus*, with the ASV affiliated with the species *Hydrogenothermus marinus* (99.5 % similarity; supplementary table 1). Members belonging to this genus are thermophilic, chemolithoautotrophic bacteria, coupling the oxidation of hydrogen to inorganic carbon fixation using the rTCA cycle (Stöhr et al., 2001). Other abundant ASVs were affiliated with the family *Anaerolineceae*, within Chloroflexi. This family is known to harbour genera employing widely diverse metabolic strategies with anaerobic growth (Bedoya-Urrego and Alzate, 2024). Furthermore, it was also possible to find ASVs related to known groups associated with sulfur metabolism, such as *Thermodesulforhabdus*, which is a thermophilic, acetate-oxidizing, sulfur-reducing bacterium (Beeder et al., 1995), as well as *Thermosulfurimonas,* which is a group known to perform the disproportionation of sulfide to sulfate (Slobodkin et al., 2012). In contrast, samples from site SF_G2 present marked differences in the microbial communities. On one hand, we detected a high abundance of ASVs related to chemolithoautotrophs, such as *Thiomicrospiraceae,* known sulfur-oxidizing thermophilic bacteria, and *Thiogranum,* obligate sulfur-oxidizing, chemolithoautotrophic bacteria (Mori et al., 2015). On the other hand, we found the presence of ASVs affiliated with groups commonly found in open seawater, such as photoautotrophic taxa *Syneccococus* and SAR11 clade, suggesting mixing with seawater. The difference between these two sampling times could be explained by multiple factors, such as changes in the community over time due to the entrainment of seawater in the hydrothermal system or sampling errors that collected a variable amount of seawater during the sampling of SF_G2. The latter seems more plausible given the similar geochemistry and temperature of the fluids (~68 °C, providing the same selective pressures). Additionally, the microbial communities of the SF_G2 site are more similar to other sampled locations in the study, which are associated with more diffuse and seawater-mixed hydrothermal fluids.

The site SF_EF was sampled approximately 80 meters from SF_G1/2, and was located in an area of vigorous diffuse gas degassing and low temperature anomaly. The geochemistry was very different from the sites SF_G1 and SF_G2, and showed similar chemical composition to seawater (Figure 2-B). At this location, most of the high abundance ASVs are affiliated with known chemoorganotrophs. For instance, the family *Lentimicrobiaceae* has been shown to grow chemoorganotrophically using a narrow range of carbohydrates under anaerobic conditions (Sun et al., 2016). There is a high

abundance of ASVs related to known groups that use nitrogen species known to be present in seawater (N_2O, NO_2^-, NO_3^-) as electron acceptors. The Bacteroidetes VC2.1Bac22 clade, which is an uncultured clade distributed in marine ecosystems, including hydrothermal systems, has been shown, through MAG analysis, to play key roles in complex organic carbon mineralization. It has also been suggested to play equally important roles in N_2O sinks in deep-sea hydrothermal systems (Leng et al., 2022, p. 202). High abundance ASVs related to members belonging to the *Calditrix* genus were recovered from the same sample. The type species of this genus, *Calditrix abissi*, couples the oxidation of hydrogen to the reduction of nitrate, using organic carbon to build biomass (Kublanov et al., 2017). The family *Melioribacteraceae* was affiliated with highly abundant ASVs, and are known facultative anaerobic chemoorganotrophic bacteria, which can use Fe^{3+}, nitrite (NO_2^-), and As^{5+}, as electron acceptors (Podosokorskaya et al., 2013). The presence of ASVs affiliated with known sulfate-reducing chemoorganotrohic groups was also present, such as *Desulfovibrio*, which are known mesophilic, hydrogenotrophic, sulfate-reducing bacteria previously isolated from a deep-sea hydrothermal system (Alazard et al., 2003). At this site, there were also ASVs affiliated to the species *Methanofolis fontis* (99.47 % similarity; supplementary table 1), which has been isolated from deep-sea sediments, and it is a mesophilic, hydrogenotrophic methanogen (Chen et al., 2020).

Chemolithoautotrophic bacteria are present in high abundances, such as AVS related to the genus *Sulfurovum*, a sulfur and thiosulfate-oxidizing bacterium that uses oxygen or nitrate as the electron acceptor (Inagaki et al., 2004; Giovannelli et al., 2016a). The site GB, from all the sites within the Campi Flegrei caldera, was the closest to land. Similar to the other sites in this region, the ASVs with higher abundances were affiliated with known chemoorganotrophs, chemolithoautotrophs, as well as heterotrophic groups. The most abundant ASVs were affiliated with the species *Marinifilm fragile* (100 % similarity; supplementary Table 1), isolated from a tidal flat sediment in Korea. This bacterium was described as being facultatively anaerobic, moderately halophilic, and was also identified in shallow-water hydrothermal vent systems (Na et al., 2009; Barosa et al., 2023). It was also possible to identify the clade PHOS-HE36, which some previous studies have suggested to be composed of denitrifying bacteria (Xin et al., 2023). A recent study showed that the relative abundance of PHOS-HE36 gradually increased as the Mn^{2+} concentrations increased, as an indication of the strengthening of denitrification (Jiang et al., 2024). This site has the highest concentration of Mn^{2+} measured (Table 3), and therefore indicates a possible relationship between the metals that are being released from the hydrothermal system and the types of metabolism found (Giovannelli, 2023). The family *Cyclobacteriaceae* was also affiliated with abundant ASVs, which have been demonstrated to have wide physiological properties, such as growth temperature and salinity range, and have also been observed in hot springs and mud volcanoes (Dworkin et al., 2006). Similarly to SF_EF, it was possible to identify the family *Melioribacteraceae*. Heterotrophic groups associated with *Thermotomaculum* were affiliated with some ASVs, which are thermophilic, heterotrophic

bacteria, initially isolated from deep-sea hydrothermal systems (Izumi et al., 2012). ASVs at this site were also affiliated with the family *Desulfosarcinaceae,* which includes groups associated with sulfate-reducing bacteria (Watanabe et al., 2021). Overall, the shallow-water hydrothermal vents hosted within the Campi Flegrei region were populated by ASVs affiliated with a mixture known chemolithoautotrophic, chemoorganotrophic, and heterotrophic groups, which heavily relied on nitrogen species as electron acceptors, and hydrogen as electron donors, and used organic as well as inorganic carbon to build biomass. These types of metabolisms have been described before in these types of ecosystems in previous studies (Price and Giovannelli, 2017; Barosa et al., 2023).

The shallow-water hydrothermal vents hosted in the Campi Flegrei caldera rim are represented here by the sites CM1 and CM2. These vents have fluid chemistry similar to seawater, suggesting a higher degree of mixing as the fluids approach the surface. At these shallow-water hydrothermal vents, the microbial communities were dominated by ASVs associated with groups known to perform heterotrophic lifestyles, common marine taxa, as well as chemolithoautotrophic and phototrophic groups at lower abundances. In the site CM1, it was possible to identify ASVs affiliated with the *Lutibacter* genus, commonly found in marine environments as well as deep-sea hydrothermal vents, and shown to reduce nitrate to nitrite (Le Moine Bauer et al., 2016). Similar to other shallow-water hydrothermal vents, it was possible to identify ASVs affiliated with *Thiotrichaceae,* which can grow chemolithoautotrophically or chemolithoheterotrophically in the presence of hydrogen sulfide and/or thiosulfate or chemoorganoheterotrophically, as well as *Sulfurovum*. Similarly, at the site CM2, the most abundant ASVs were affiliated with the family *Cyclobacteriaceae*, which are present in a wide variety of environments, including hot springs, and where some species have been shown to degrade polysaccharides and other complex molecules (Dworkin et al., 2006). It was also possible to find ASVs related to common marine heterotrophic bacteria, such as *Woesia*, which have also been recently described in other shallow-water hydrothermal environments (Barosa et al., 2023). At this site, we also retrieved ASVs related to known photoautotrophic taxa, *Synechococcus* CC9902, that is widely distributed in marine environments, and is regarded as one of the most important components of photosynthetic picoplankton (Kim et al., 2018), as well as SAR11, chemoheterotrophic alphaproteobacteria accounting for 25 % of all plankton (Giovannoni, 2017). Notwithstanding, there were still present ASVs related to chemolithoautotrophic taxa, such as in the case of *Sulfurovum*. At both these sites, the increase of groups associated with heterotrophic metabolisms in the high abundance ASVs, as well as common marine taxa, sheds light on the complexities inherent to the mixing ratios observed in shallow-water hydrothermal systems. Vents hosted further away from a heat source, and where hydrothermal fluids mix to a higher degree with seawater, present lower temperatures and the presence of increased members associated with marine taxa and heterotrophic metabolisms. This pattern was also observed in the Aeolian archipelago, especially in the islands with less pronounced volcanic activity (Barosa et al., 2023).

The site BC was located within the area of influence of the Somma-Vesuvius volcano. The geochemistry of these fluids was the most divergent compared to all the other sites of the Campi Flegrei region. As discussed in the geochemistry section, these differences could be due to difference in the host rocks between BC, occurring in carbonates in contact with volcanic deposits, compared to the Campi Flegrei sites occurring within trachytic ignimbrites, by diverse primary fluids and mixing regimes between the two areas, or most likely a combination of both. In the BC site was possible to find the presence of ASVs related to common marine taxa, as well as high abundances of ASVs affiliated to groups capable of sulfur oxidation, such as the genus *Thiomicrorhabdus, Thioclava,* and *Cocleimonas* (Sorokin et al., 2005; Tanaka et al., 2011; Kojima and Fukui, 2019). From all the sites, BC is the one with the lowest oxidation reduction potential, suggestive of a highly reducing environment. This is also supported by the very low concentrations of SO_4^{2-}, coupled with a very strong smell of "rotten eggs" at the location, characteristic of the presence of H_2S. Enzymes catalyzing the oxidation of sulfur species, as noted in (Hay Mele et al., 2023), are heavily based on the trace metals Fe and Mo. These specific metals were present in very low abundances at this site, especially Mo, below the detection limit in all dilutions conducted pre-measurements. Microbial communities inhabiting strongly reducing environments undergo selective pressures to exploit the abundance of "free" electrons for their metabolic needs. This could imply heavy scavenging of the specific metals needed to perform these reactions, possibly explaining their low abundance in this particular site. The relationship between metal availability and microbial distribution and metabolism has been suggested in recent studies, and this could provide yet another hint on how these relationships happen in complex natural environments (Giovannelli, 2023; Hay Mele et al., 2023).

At sites SF_G1 and SF_G2 in the Campi Flegrei region, the biofilms sampled in the vicinity of the vents were mostly composed of ASVs affiliated with the Aquificota phylum, more specifically with the genus *Hydrogenothermus.* Interestingly, previous studies that analyzed the microbial communities of biofilms in both deep-sea and shallow-water hydrothermal systems report a community composed mainly of sulfur-oxidizing groups belonging to Campylobacterota and the class Gammaproteobacteria (Gulmann et al., 2015; O'Brien et al., 2015; Sciutteri et al., 2022; Barosa et al., 2023). Members belonging to the Aquificota, on the other hand, have been identified in biofilms of high temperature deep-sea vents (Fullerton et al., 2024). This suggests that both the availability of electron donors and acceptors, as well as the temperature of the system, can have important roles in constraining the establishment of bacterial biofilms in natural hydrothermal systems. For this reason, Secca delle Fumose, due to its easy access, can serve as an ideal laboratory to understand biofilm dynamics in hydrothermal systems.

The beta-diversity analysis (Figure 5) coupled with permutational multivariate analysis (ADONIS) shows that the microbial communities from the shallow-water hydrothermal vents hosted in different

settings, that is, the Campi Flegrei caldera, Campi Flegrei caldera rim, and the Somma-Vesuvius regions, are statistically different from one another (Figure 5A). That takes into account the most abundant groups, as well as the rare species. Interestingly, the vents separated by type of fluid chemistry are also statistically different. Differences between microbial communities inhabiting geologically and geographically distinct shallow-water hydrothermal vents have been previously reported for the shallow vents of the Aeolian archipelago (Barosa et al., 2023). This suggests that the geological setting where the vents occur and the consequent difference in hydrothermal fluid chemistry can impose controls on microbial distribution. Geological controls on the microbial diversity have also been observed on land for deeply sourced seeps in the volcanic regions of Costa Rica, Peru, and Bolivia (Fullerton et al., 2021; Colman et al., 2023; Sims et al., 2023; Upin et al., 2023). In SWHV, however, the complex mixing with seawater, the presence of sunlight, tidal forcing, and organic matter inputs to the system, could overlap, cross and influence geological and geochemical processes, also playing a key role in mediating microbial diversity and distribution. These parameters are in themselves a *property* of each individual hydrothermal system. For instance, recent studies have demonstrated that in deeply sourced seeps of Costa Rica, even though chemolithoautotrophic communities were responding to changes in geochemistry, no such pattern was observed for secondary consumers, i.e, heterotrophs (Paul et al., 2023). The quality and abundance of fresh organic matter might play an important role in controlling the abundance of taxa associated with heterotrophic metabolic strategies. In SWHV, organic matter can be either produced by chemolithoautotrophs, phototrophs, as well as imported to the system from the water column or terrigenous input from nearby landmasses (Price and Giovannelli, 2017). In the shallow-water hydrothermal vents of the Aeolian archipelago, the presence of fresh organic matter in some sites was associated with the higher abundance of heterotrophic groups (Barosa et al., 2023). Gases from volcanic origin, such as H_2, CO_2, H_2S, and CH_4, due to their key roles in microbial redox metabolism as electron donors and acceptors, might also play a key role in shaping ecological niches for microbial exploitation in these systems.

The *ordisurf* analysis conducted here (Figure 5C-H) shows how the groups that have similar fluid chemistry (as seen in the PCA analysis on the geochemistry section), cluster closely, illustrating their similar microbial community structure. As previously discussed, it follows that the nature of any given hydrothermal system, such as its proximity to the magmatic heat source, has a direct influence on the types of temperature dependent water-rock-gas reactions happening during fluid trajectory, and consequent fluid chemistry, dictating also the degree to which the upflowing fluids mix with seawater. This highlights the importance of taking a multidisciplinary sampling approach to study geothermal environments, such as the one suggested by Giovannelli at al., 2022. Additionally, in order to untangle the complex mixing ratios in these systems, we further suggest an approach based on the background concept introduced in Cascone at al., 2025. By sampling background seawater, and similar to what is

currently done in geochemical analysis, it can allow us to provide a microbiological "end-member" to gain further knowledge on life inhabiting these dynamic ecosystems.

5 Conclusion

The Gulf of Naples shows intense underwater hydrothermalism as a function of the volcanic activity in the area. In the present study, we describe both the geochemistry as well as the microbiology of the SWHV occurring within two different volcanic regions, Campi Flegrei and Somma-Vesuvius. Through geochemical analysis, we found that on the SWHV sampled, hydrothermal fluid chemistry is contingent on the region where the vents occur, with the distance from the heat source possibly playing a key role in dictating the chemistry of the fluids, corroborated by gas geochemistry measurements conducted in the past. Additionally, we found diverse microbial consortia inhabiting these SWHV, with a high abundance of ASVs affiliated with known chemolithoautotrophic, heterotrophic, and photoautotrophic groups. This is consistent with previous studies conducted in other shallow-water hydrothermal systems, and therefore, can be regarded as a definite characteristic of these dynamic systems. Notably, here the distribution of the ASVs is suggested to be related to differences in hydrothermal fluid geochemistry as a function of fluid mixing landscapes, as well as the vent's location (Campi Flegrei caldera, Campi Flegrei caldera rim, and Somma-Vesuvius). The chemistry of hydrothermal fluids, as a response to water-rock-gas reactions at depth, can strongly influence the availability/diversity of ecological niches to be exploited by microorganisms, through differences in electron donors and acceptors, as well as organic and inorganic carbon sources. On the other hand, the geological background and location of hydrothermal systems, and the consequent diffusivity of the fluids approaching the surface, can generate complex mixing ratios with seawater, which, coupled with sunlight, tidal fluctuations, and organic matters, can also play key roles in constraining microbial distribution and composition in SWHV. As the Campi Flegrei volcano continues to exhibit signs of unrest with increasing seismic activity, this work provides an important baseline for future studies aiming at understanding how microbial communities respond to geochemical shifts driven by volcanic processes. In this context, our findings could contribute valuable insights for the development of long-term monitoring strategies within highly geodynamic systems.

6 Data Availability Statement

Sequences are available through the European Nucleotide Archive (ENA) with bioproject accession number PRJEB67762 under the Umbrella Project CoEvolve PRJEB55081. A complete R script containing all the steps to reproduce our analysis is available at https://github.com/giovannellilab/Barosa_et_al_FEAMP_shallow_vent_diversity permanently stored with DOI: 10.5281/zenodo.14966493.

7 Conflict of Interest

The authors declare no conflict of interest.

8 Author Contributions

BB carried out data analysis, geochemical experiments and wrote the first draft of the manuscript. BB, CC, MS, SD, MC, AB, MCO, and LD produced the geochemical and microbiological data. CC performed DNA extractions. CC, MS, DB, MC, RP, CV, and DG planned the expedition and collected the samples. RP, CV, AC, and DG supervised the study. All authors contributed equally to the final version of the manuscript.

9 Funding

This work was funded by the European Research Council (ERC) under the European Union's Horizon 2020 research and innovation program (grant agreement No. 948972, acronym COEVOLVE) to DG. The work received funding also from PO FEAMP Campania 2014–2020 (DRD691 n. 35 of 15 March 2018). We also acknowledge the project "National Biodiversity Future Center – NBFC," project code: CN_00000033, Concession Decree No: 1034 of June 17, 2022 adopted by the Italian Ministry of University and Research. APS is supported by the European Union's Horizon 2020 research and innovation programme under the Marie Skłodowska-Curie PhD Cofund CRESCENDO (Grant Agreement No. 101034245). FM was supported by the "National Biodiversity Future Center - NBFC", project code CN_00000033, Concession Decree No. 1034 of 17 June 2022 adopted by the Italian Ministry of University and Research. Partial support to REP was provided from the NASA Habitable Worlds program under grants 80NSSC20K0228 and 80NSSC24K0076. LT and MC are partially funded by the PhD program PON "Ricerca e Innovazione" 2014–2020, DM n. 1061 (10 August 2021) and n. 1233 (30 July 2020) by the Ministero dell'Università e della Ricerca (MUR),

10 Acknowledgments

The authors wish to thank the Pozzuoli diving centre (Centro Sub Pozzuoli) and Guglielmo Fragale for providing diving logistics necessary to carry out the sampling.

11 References

Aiello, G., Marsella, E., and Stefano, R. (2010). Three-dimensional magneto-seismic reconstruction of the 'Torre del Greco' submerged volcanic structure (Naples Bay, Southern Tyrrhenian Sea, Italy): implications for Vesuvius's marine geophysics and volcanology. *Surf. Geophys.* 8, 17–32. doi: 10.3997/1873-0604.2009037

Aiuppa, A., Avino, R., Brusca, L., Caliro, S., Chiodini, G., D'Alessandro, W., et al. (2006). Mineral control of arsenic content in thermal waters from volcano-hosted hydrothermal systems:

Insights from island of Ischia and Phlegrean Fields (Campanian Volcanic Province, Italy). *Chem. Geol.* 229, 313–330. doi: 10.1016/j.chemgeo.2005.11.004

Alazard, D., Dukan, S., Urios, A., Verhé, F., Bouabida, N., Morel, F., et al. (2003). *Desulfovibrio hydrothermalis* sp. nov., a novel sulfate-reducing bacterium isolated from hydrothermal vents. *Int. J. Syst. Evol. Microbiol.* 53, 173–178. doi: 10.1099/ijs.0.02323-0

Amend, J. P., McCollom, T. M., Hentscher, M., and Bach, W. (2011). Catabolic and anabolic energy for chemolithoautotrophs in deep-sea hydrothermal systems hosted in different rock types. *Geochim. Cosmochim. Acta* 75, 5736–5748. doi: 10.1016/j.gca.2011.07.041

Amend, J. P., Rogers, K. L., Shock, E. L., Gurrieri, S., and Inguaggiato, S. (2003). Energetics of chemolithoautotrophy in the hydrothermal system of Vulcano Island, southern Italy. *Geobiology* 1, 37–58. doi: 10.1046/j.1472-4669.2003.00006.x

Astort, A., Trasatti, E., Caricchi, L., Polcari, M., De Martino, P., Acocella, V., et al. (2024). Tracking the 2007–2023 magma-driven unrest at Campi Flegrei caldera (Italy). *Commun. Earth Environ.* 5, 506. doi: 10.1038/s43247-024-01665-4

Aucelli, P. P. C., Mattei, G., Caporizzo, C., Cinque, A., Troisi, S., Peluso, F., et al. (2020). Ancient Coastal Changes Due to Ground Movements and Human Interventions in the Roman Portus Julius (Pozzuoli Gulf, Italy): Results from Photogrammetric and Direct Surveys. *Water* 12, 658. doi: 10.3390/w12030658

Baiocchi, A., Di Paola, A., and Lotti, F. (2010). Seawater intrusion in carbonate aquifers: The case of the spring group of castellammare di stabia (Naples, Southern Italy). *Ital. J. Eng. Geol. Environ.*, 5–20. doi: 10.4408/IJEGE.2010-02.O-01

Baldrighi, E., Zeppilli, D., Appolloni, L., Donnarumma, L., Chianese, E., Russo, G. F., et al. (2020). Meiofaunal communities and nematode diversity characterizing the Secca delle Fumose shallow vent area (Gulf of Naples, Italy). *PeerJ* 8, e9058. doi: 10.7717/peerj.9058

Barge, L. M., and Price, R. E. (2022). Diverse geochemical conditions for prebiotic chemistry in shallow-sea alkaline hydrothermal vents. *Nat. Geosci.* 15, 976–981. doi: 10.1038/s41561-022-01067-1

Barosa, B., Ferrillo, A., Selci, M., Giardina, M., Bastianoni, A., Correggia, M., et al. (2023). Mapping the microbial diversity associated with different geochemical regimes in the shallow-water hydrothermal vents of the Aeolian archipelago, Italy. *Front. Microbiol.* 14, 1134114. doi: 10.3389/fmicb.2023.1134114

Barry, P. H., De Moor, J. M., Chiodi, A., Aguilera, F., Hudak, M. R., Bekaert, D. V., et al. (2022). The Helium and Carbon Isotope Characteristics of the Andean Convergent Margin. *Front. Earth Sci.* 10, 897267. doi: 10.3389/feart.2022.897267

Basili, M., Rogers, T. J., Nakagawa, M., Yücel, M., De Moor, J. M., Barry, P. H., et al. (2024). Subsurface microbial community structure shifts along the geological features of the Central American Volcanic Arc. *PLOS ONE* 19, e0308756. doi: 10.1371/journal.pone.0308756

Bedoya-Urrego, K., and Alzate, J. F. (2024). Phylogenomic discernments into *Anaerolineaceae* thermal adaptations and the proposal of a candidate genus Mesolinea. *Front. Microbiol.* 15, 1349453. doi: 10.3389/fmicb.2024.1349453

Beeder, J., Torsvik, T., and Lien, T. (1995). *Thermodesulforhabdus norvegicus* gen. nov., sp. nov., a novel thermophilic sulfate-reducing bacterium from oil field water.

Bellec, L., Cambon-Bonavita, M.-A., Durand, L., Aube, J., Gayet, N., Sandulli, R., et al. (2020). Microbial Communities of the Shallow-Water Hydrothermal Vent Near Naples, Italy, and Chemosynthetic Symbionts Associated With a Free-Living Marine Nematode. *Front. Microbiol.* 11, 2023. doi: 10.3389/fmicb.2020.02023

Bertagnini, A., Landi, P., Rosi, M., and Vigliargio, A. (1998). The Pomici di Base plinian eruption of Somma-Vesuvius. *J. Volcanol. Geotherm. Res.* 83, 219–239. doi: 10.1016/S0377-0273(98)00025-0

Caliro, S., Chiodini, G., Avino, R., Minopoli, C., and Bocchino, B. (2011). Long time-series of chemical and isotopic compositions of Vesuvius fumaroles: evidence for deep and shallow processes. doi: 10.4401/ag-5034

Callahan, B. J., McMurdie, P. J., and Holmes, S. P. (2017). Exact sequence variants should replace operational taxonomic units in marker-gene data analysis. *ISME J.* 11, 2639–2643. doi: 10.1038/ismej.2017.119

Calosi, P., Rastrick, S. P. S., Graziano, M., Thomas, S. C., Baggini, C., Carter, H. A., et al. (2013). Distribution of sea urchins living near shallow water CO_2 vents is dependent upon species acid–base and ion-regulatory abilities. *Mar. Pollut. Bull.* 73, 470–484. doi: 10.1016/j.marpolbul.2012.11.040

Cardigos, F., Colaço, A., Dando, P. R., Ávila, S. P., Sarradin, P.-M., Tempera, F., et al. (2005). Shallow water hydrothermal vent field fluids and communities of the D. João de Castro Seamount (Azores). *Chem. Geol.* 224, 153–168. doi: 10.1016/j.chemgeo.2005.07.019

Cascone, M., Bastianoni, A., Selci, M., Correggia, M., di Iorio, L., Cordone, A., et al. (2025) Deeply-sourced springs of the Argentina backarc as windows into the subsurface. Submitted.

Chen, S.-C., Teng, N.-H., Lin, Y.-S., Lai, M.-C., Chen, H.-H., and Wang, C.-C. (2020). *Methanofollis fontis* sp. nov., a methanogen isolated from marine sediment near a cold seep at Four-Way Closure Ridge offshore southwestern Taiwan. *Int. J. Syst. Evol. Microbiol.* 70, 5497–5502. doi: 10.1099/ijsem.0.004440

Chiodini, G., Marini, L., and Russo, M. (2001). Geochemical evidence for the existence of high-temperature hydrothermal brines at Vesuvio volcano, Italy. *Geochim. Cosmochim. Acta* 65, 2129–2147. doi: 10.1016/S0016-7037(01)00583-X

Colman, D. R., Veach, A., Stefánsson, A., Wurch, L., Belisle, B. S., Podar, P. T., et al. (2023). Tectonic and geological setting influence hot spring microbiology. *Environ. Microbiol.* 25, 2481–2497. doi: 10.1111/1462-2920.16472

Cordone, A., D'Errico, G., Magliulo, M., Bolinesi, F., Selci, M., Basili, M., et al. (2022). Bacterioplankton Diversity and Distribution in Relation to Phytoplankton Community Structure in the Ross Sea Surface Waters. *Front. Microbiol.* 13, 722900. doi: 10.3389/fmicb.2022.722900

Cordone, A., Selci, M., Barosa, B., Bastianoni, A., Bastoni, D., Bolinesi, F., et al. (2023). Surface Bacterioplankton Community Structure Crossing the Antarctic Circumpolar Current Fronts. *Microorganisms* 11, 702. doi: 10.3390/microorganisms11030702

Correggia, M., Di Iorio, L., Bastianoni, A. B., Yucel, M., Cordone, A., and Giovannelli, D. (2023a). Standard operating procedure for the analysis of major ions in hydrothermal fluids by ion chromatography. *Open Res. Eur.* 3, 94. doi: 10.12688/openreseurope.15605.1

Correggia, M., Di Iorio, L., Bastianoni, A. B., Yücel, M., Cordone, A., and Giovannelli, D. (2023b). Standard Operating Procedure for the analysis of trace elements in hydrothermal fluids by Inductively Coupled Plasma Mass Spectrometry (ICP-MS). *Open Res. Eur.* 3, 90. doi: 10.12688/openreseurope.15699.1

Dahle, H., Le Moine Bauer, S., Baumberger, T., Stokke, R., Pedersen, R. B., Thorseth, I. H., et al. (2018). Energy Landscapes in Hydrothermal Chimneys Shape Distributions of Primary Producers. *Front. Microbiol.* 9, 1570. doi: 10.3389/fmicb.2018.01570

Dahle, H., Økland, I., Thorseth, I. H., Pederesen, R. B., and Steen, I. H. (2015). Energy landscapes shape microbial communities in hydrothermal systems on the Arctic Mid-Ocean Ridge. *ISME J.* 9, 1593–1606. doi: 10.1038/ismej.2014.247

De Astis, G., Pappalardo, L., and Piochi, M. (2004). Procida volcanic history: new insights into the evolution of the Phlegraean Volcanic District (Campania region, Italy). *Bull. Volcanol.* 66, 622–641. doi: 10.1007/s00445-004-0345-y

Di Napoli, R., Aiuppa, A., Sulli, A., Caliro, S., Chiodini, G., Acocella, V., et al. (2016). Hydrothermal fluid venting in the offshore sector of C ampi Flegrei caldera: A geochemical, geophysical, and volcanological study. *Geochem. Geophys. Geosystems* 17, 4153–4178. doi: 10.1002/2016GC006494

Donnarumma, L., Appolloni, L., Chianese, E., Bruno, R., Baldrighi, E., Guglielmo, R., et al. (2019). Environmental and Benthic Community Patterns of the Shallow Hydrothermal Area of Secca Delle Fumose (Baia, Naples, Italy). *Front. Mar. Sci.* 6, 685. doi: 10.3389/fmars.2019.00685

Dworkin, M., Falkow, S., Rosenberg, E., Schleifer, K.-H., and Stackebrandt, E. eds. (2006). *The Prokaryotes*. New York, NY: Springer New York. doi: 10.1007/0-387-30747-8

Ely, T. D., Leong, J. M., Canovas, P. A., and Shock, E. L. (2023). Huge Variation in H_2 Generation During Seawater Alteration of Ultramafic Rocks. *Geochem. Geophys. Geosystems* 24, e2022GC010658. doi: 10.1029/2022GC010658

Fagorzi, C., Del Duca, S., Venturi, S., Chiellini, C., Bacci, G., Fani, R., et al. (2019). Bacterial Communities from Extreme Environments: Vulcano Island. *Diversity* 11, 140. doi: 10.3390/d11080140

Frondini, F., Chiodini, G., Caliro, S., Cardellini, C., Granieri, D., and Ventura, G. (2004). Diffuse CO2 degassing at Vesuvio, Italy. *Bull. Volcanol.* 66, 642–651. doi: 10.1007/s00445-004-0346-x

Fullerton, H., Smith, L., Enriquez, A., Butterfield, D., Wheat, C. G., and Moyer, C. L. (2024). Seafloor incubation experiments at deep-sea hydrothermal vents reveal distinct biogeographic signatures of autotrophic communities. *FEMS Microbiol. Ecol.* 100, fiae001. doi: 10.1093/femsec/fiae001

Fullerton, K. M., Schrenk, M. O., Yücel, M., Manini, E., Basili, M., Rogers, T. J., et al. (2021). Effect of tectonic processes on biosphere–geosphere feedbacks across a convergent margin. *Nat. Geosci.* 14, 301–306. doi: 10.1038/s41561-021-00725-0

German, C. R., and Seyfried, W. E. (2014). "Hydrothermal Processes," in *Treatise on Geochemistry*, (Elsevier), 191–233. doi: 10.1016/B978-0-08-095975-7.00607-0

Giovannelli, D. (2023). Trace metal availability and the evolution of biogeochemistry. *Nat Rev Earth Environ* 4, 597–598. doi: 10.1038/s43017-023-00477-y

Giovannelli, D., Barry, P. H., de Moor, J. M., Jessen, G. L., Schrenk, M. O., and Lloyd, K. G. (2022). Sampling across large-scale geological gradients to study geosphere–biosphere interactions. *Front. Microbiol.* 13, 998133. doi: 10.3389/fmicb.2022.998133

Giovannelli, D., Chung, M., Staley, J., Starovoytov, V., Le Bris, N., and Vetriani, C. (2016a). *Sulfurovum riftiae* sp. nov., a mesophilic, thiosulfate-oxidizing, nitrate-reducing chemolithoautotrophic epsilonproteobacterium isolated from the tube of the deep-sea hydrothermal vent polychaete Riftia pachyptila. *Int. J. Syst. Evol. Microbiol.* 66, 2697–2701. doi: 10.1099/ijsem.0.001106

Giovannelli, D., d'Errico, G., Fiorentino, F., Fattorini, D., Regoli, F., Angeletti, L., et al. (2016b). Diversity and Distribution of Prokaryotes within a Shallow-Water Pockmark Field. *Front. Microbiol.* 7. doi: 10.3389/fmicb.2016.00941

Giovannelli, D., d'Errico, G., Manini, E., Yakimov, M., and Vetriani, C. (2013). Diversity and phylogenetic analyses of bacteria from a shallow-water hydrothermal vent in Milos island (Greece). *Front. Microbiol.* 4. doi: 10.3389/fmicb.2013.00184

Giovannoni, S. J. (2017). SAR11 Bacteria: The Most Abundant Plankton in the Oceans. *Annu. Rev. Mar. Sci.* 9, 231–255. doi: 10.1146/annurev-marine-010814-015934

Giudicepietro, F., Avino, R., Bellucci Sessa, E., Bevilacqua, A., Bonano, M., Caliro, S., et al. (2025). Burst-like swarms in the Campi Flegrei caldera accelerating unrest from 2021 to 2024. *Nat. Commun.* 16, 1548. doi: 10.1038/s41467-025-56723-y

Gomez-Saez, G. V., Pop Ristova, P., Sievert, S. M., Elvert, M., Hinrichs, K.-U., and Bühring, S. I. (2017). Relative Importance of Chemoautotrophy for Primary Production in a Light Exposed Marine Shallow Hydrothermal System. *Front. Microbiol.* 8, 702. doi: 10.3389/fmicb.2017.00702

Gugliandolo, C., Lentini, V., Bunk, B., Overmann, J., Italiano, F., and Maugeri, T. L. (2015). Changes in prokaryotic community composition accompanying a pronounced temperature shift of a shallow marine thermal brine pool (Panarea Island, Italy). *Extremophiles* 19, 547–559. doi: 10.1007/s00792-015-0737-2

Gulmann, L. K., Beaulieu, S. E., Shank, T. M., Ding, K., Seyfried, W. E., and Sievert, S. M. (2015). Bacterial diversity and successional patterns during biofilm formation on freshly exposed basalt surfaces at diffuse-flow deep-sea vents. *Front. Microbiol.* 6. doi: 10.3389/fmicb.2015.00901

Hay Mele, B., Monticelli, M., Leone, S., Bastoni, D., Barosa, B., Cascone, M., et al. (2023). Oxidoreductases and metal cofactors in the functioning of the earth. *Essays Biochem.* 67, 653–670. doi: 10.1042/EBC20230012

Inagaki, F., Takai, K., Nealson, K. H., and Horikoshi, K. (2004). *Sulfurovum lithotrophicum* gen. nov., sp. nov., a novel sulfur-oxidizing chemolithoautotroph within the ε-Proteobacteria isolated from Okinawa Trough hydrothermal sediments. *Int. J. Syst. Evol. Microbiol.* 54, 1477–1482. doi: 10.1099/ijs.0.03042-0

Izumi, H., Nunoura, T., Miyazaki, M., Mino, S., Toki, T., Takai, K., et al. (2012). *Thermotomaculum hydrothermale* gen. nov., sp. nov., a novel heterotrophic thermophile within the phylum Acidobacteria from a deep-sea hydrothermal vent chimney in the Southern Okinawa Trough. *Extremophiles* 16, 245–253. doi: 10.1007/s00792-011-0425-9

Jiang, Z., Huang, X., Wang, S., Xiong, J., Xie, C., and Chen, Y. (2024). Divalent manganese

stimulates the removal of nitrate by anaerobic sludge. *RSC Adv.* 14, 2447–2452. doi: 10.1039/D3RA07088C

Karl, D. M., Bidigare, R. R., Church, M. J., Dore, J. E., Letelier, R. M., Mahaffey, C., et al. (2008). "The Nitrogen Cycle in the North Pacific Trades Biome," in *Nitrogen in the Marine Environment*, (Elsevier), 705–769. doi: 10.1016/B978-0-12-372522-6.00016-5

Kerrison, P., Hall-Spencer, J. M., Suggett, D. J., Hepburn, L. J., and Steinke, M. (2011). Assessment of pH variability at a coastal CO2 vent for ocean acidification studies. *Estuar. Coast. Shelf Sci.* 94, 129–137. doi: 10.1016/j.ecss.2011.05.025

Kim, Y., Jeon, J., Kwak, M. S., Kim, G. H., Koh, I., and Rho, M. (2018). Photosynthetic functions of *Synechococcus* in the ocean microbiomes of diverse salinity and seasons. *PLOS ONE* 13, e0190266. doi: 10.1371/journal.pone.0190266

Kojima, H., and Fukui, M. (2019). *Thiomicrorhabdus aquaedulcis* sp. nov., a sulfur-oxidizing bacterium isolated from lake water. *Int. J. Syst. Evol. Microbiol.* 69, 2849–2853. doi: 10.1099/ijsem.0.003567

Kublanov, I. V., Sigalova, O. M., Gavrilov, S. N., Lebedinsky, A. V., Rinke, C., Kovaleva, O., et al. (2017). Genomic Analysis of *Caldithrix abyssi*, the Thermophilic Anaerobic Bacterium of the Novel Bacterial Phylum Calditrichaeota. *Front. Microbiol.* 8. doi: 10.3389/fmicb.2017.00195

Le Moine Bauer, S., Roalkvam, I., Steen, I. H., and Dahle, H. (2016). *Lutibacter profundi* sp. nov., isolated from a deep-sea hydrothermal system on the Arctic Mid-Ocean Ridge and emended description of the genus Lutibacter. *Int. J. Syst. Evol. Microbiol.* 66, 2671–2677. doi: 10.1099/ijsem.0.001105

Leal-Acosta, M. L., Shumilin, E., Mirlean, N., Delgadillo-Hinojosa, F., and Sánchez-Rodríguez, I. (2013). The impact of marine shallow-water hydrothermal venting on arsenic and mercury accumulation by seaweed *Sargassum sinicola* in Concepcion Bay, Gulf of California. *Environ. Sci. Process. Impacts* 15, 470. doi: 10.1039/c2em30866e

Leng, H., Zhao, W., and Xiao, X. (2022). Cultivation and metabolic insights of an uncultured clade, Bacteroidetes VC2 .1 Bac22 (*Candidatus Sulfidibacteriales* ord. nov.), from deep‐sea hydrothermal vents. *Environ. Microbiol.* 24, 2484–2501. doi: 10.1111/1462-2920.15931

Lu, G.-S., LaRowe, D. E., Fike, D. A., Druschel, G. K., Gilhooly, W. P., Price, R. E., et al. (2020). Bioenergetic characterization of a shallow-sea hydrothermal vent system: Milos Island, Greece. *PLOS ONE* 15, e0234175. doi: 10.1371/journal.pone.0234175

Manini, E., Luna, G. M., Corinaldesi, C., Zeppilli, D., Bortoluzzi, G., Caramanna, G., et al. (2008). Prokaryote Diversity and Virus Abundance in Shallow Hydrothermal Vents of the Mediterranean Sea (Panarea Island) and the Pacific Ocean (North Sulawesi-Indonesia). *Microb. Ecol.* 55, 626–639. doi: 10.1007/s00248-007-9306-2

Maugeri, T. L., Gugliandolo, C., and Lentini, V. (2013). Diversity of prokaryotes at a shallow submarine vent of Panarea Island (Italy) by high-throughput sequencing. *Atti Della Accad. Perloritana Dei Pericolanti Cl. Sci. Fis. Mat. E Nat.* 91, A1-1-A1-9. doi: 10.1478/AAPP.912A1

Maugeri, T. L., Lentini, V., Gugliandolo, C., Cousin, S., and Stackebrandt, E. (2010). Microbial Diversity at a Hot, Shallow-Sea Hydrothermal Vent in the Southern Tyrrhenian Sea (Italy). *Geomicrobiol. J.* 27, 380–390. doi: 10.1080/01490450903451518

Mori, K., Suzuki, K., Yamaguchi, K., Urabe, T., and Hanada, S. (2015). *Thiogranum longum* gen. nov., sp. nov., an obligately chemolithoautotrophic, sulfur-oxidizing bacterium of the family *Ectothiorhodospiraceae* isolated from a deep-sea hydrothermal field, and an emended description of the genus Thiohalomonas. *Int. J. Syst. Evol. Microbiol.* 65, 235–241. doi: 10.1099/ijs.0.070599-0

Na, H., Kim, S., Moon, E. Y., and Chun, J. (2009). *Marinifilum fragile* gen. nov., sp. nov., isolated from tidal flat sediment. *Int. J. Syst. Evol. Microbiol.* 59, 2241–2246. doi: 10.1099/ijs.0.009027-0

O'Brien, C. E., Giovannelli, D., Govenar, B., Luther, G. W., Lutz, R. A., Shank, T. M., et al. (2015). Microbial biofilms associated with fluid chemistry and megafaunal colonization at post-eruptive deep-sea hydrothermal vents. *Deep Sea Res. Part II Top. Stud. Oceanogr.* 121, 31–40. doi: 10.1016/j.dsr2.2015.07.020

O'Connor Šraj, L., Almeida, M. I. G. S., McKelvie, I. D., and Kolev, S. D. (2017). Determination of trace levels of ammonia in marine waters using a simple environmentally-friendly ammonia (SEA) analyser. *Mar. Chem.* 194, 133–145. doi: 10.1016/j.marchem.2017.06.008

Orlando, V., Franco, T., Dario, T., Robert, P. J., and Antonio, C. (2011). Submarine and Inland Gas Discharges from the Campi Flegrei (Southern Italy) and the Pozzuoli Bay: Geochemical Clues for a Common Hydrothermal-Magmatic Source. *Procedia Earth Planet. Sci.* 4, 57–73. doi: 10.1016/j.proeps.2011.11.007

Orsi, G., D'Antonio, M., Vita, S. de, and Gallo, G. (1992). The Neapolitan Yellow Tuff, a large-magnitude trachytic phreatoplinian eruption: eruptive dynamics, magma withdrawal and caldera collapse. *J. Volcanol. Geotherm. Res.* 53, 275–287. doi: 10.1016/0377-0273(92)90086-S

Palmer, M. R., and Edmond, J. M. (1989). Cesium and rubidium in submarine hydrothermal fluids: Evidence for recycling of alkali elements. *Earth Planet. Sci. Lett.* 95, 8–14. doi: 10.1016/0012-821X(89)90163-5

Passaro, S., Genovese, S., Sacchi, M., Barra, M., Rumolo, P., Tamburrino, S., et al. (2014a). First hydroacoustic evidence of marine, active fluid vents in the Naples Bay continental shelf (Southern Italy). *J. Volcanol. Geotherm. Res.* 285, 29–35. doi: 10.1016/j.jvolgeores.2014.08.001

Passaro, S., Genovese, S., Sacchi, M., Barra, M., Rumolo, P., Tamburrino, S., et al. (2014b). First hydroacoustic evidence of marine, active fluid vents in the Naples Bay continental shelf (Southern Italy). *J. Volcanol. Geotherm. Res.* 285, 29–35. doi: 10.1016/j.jvolgeores.2014.08.001

Paul, R., Rogers, T. J., Fullerton, K. M., Selci, M., Cascone, M., Stokes, M. H., et al. (2023). Complex organic matter degradation by secondary consumers in chemolithoautotrophy-based subsurface geothermal ecosystems. *PLOS ONE* 18, e0281277. doi: 10.1371/journal.pone.0281277

Pearce, R. K., Sánchez de la Muela, A., Moorkamp, M., Hammond, J. O. S., Mitchell, T. M., Cembrano, J., et al. (2019). Interaction between hydrothermal fluids and fault systems in the in the Southern Andes revealed by magnetotelluric and seismic data. Geophysics. doi: 10.1002/essoar.10501143.1

Pichler, T., Amend, J. P., Garey, J., Hallock, P., Hsia, N. P., Karlen, D. J., et al. (2006). A natural laboratory to study arsenic geobiocomplexity. *Eos Trans. Am. Geophys. Union* 87, 221–225.

doi: 10.1029/2006EO230002

Podosokorskaya, O. A., Kadnikov, V. V., Gavrilov, S. N., Mardanov, A. V., Merkel, A. Y., Karnachuk, O. V., et al. (2013). Characterization of *Melioribacter roseus* gen. nov., sp. nov., a novel facultatively anaerobic thermophilic cellulolytic bacterium from the class *Ignavibacteria*, and a proposal of a novel bacterial phylum *Ignavibacteriae*. *Environ. Microbiol.* 15, 1759–1771. doi: 10.1111/1462-2920.12067

Price, R. E., and Giovannelli, D. (2017). "A Review of the Geochemistry and Microbiology of Marine Shallow-Water Hydrothermal Vents," in *Reference Module in Earth Systems and Environmental Sciences*, (Elsevier), B9780124095489095233. doi: 10.1016/B978-0-12-409548-9.09523-3

Price, R. E., and Giovannelli, D. (2019). "Marine Shallow-Water Hydrothermal Vents: Geochemistry," in *Encyclopedia of Ocean Sciences*, 346–352. doi: 10.1016/b978-0-12-409548-9.11015-2

Price, R. E., LaRowe, D. E., Italiano, F., Savov, I., Pichler, T., and Amend, J. P. (2015). Subsurface hydrothermal processes and the bioenergetics of chemolithoautotrophy at the shallow-sea vents off Panarea Island (Italy). *Chem. Geol.* 407–408, 21–45. doi: 10.1016/j.chemgeo.2015.04.011

Price, R. E., Lesniewski, R., Nitzsche, K. S., Meyerdierks, A., Saltikov, C., Pichler, T., et al. (2013). Archaeal and bacterial diversity in an arsenic-rich shallow-sea hydrothermal system undergoing phase separation. *Front. Microbiol.* 4. doi: 10.3389/fmicb.2013.00158

Quast, C., Pruesse, E., Yilmaz, P., Gerken, J., Schweer, T., Yarza, P., et al. (2013). The SILVA ribosomal RNA gene database project: improved data processing and web-based tools. *Nucleic Acids Res.* 41, D590–D596. doi: 10.1093/nar/gks1219

Rogers, K. L., and Amend, J. P. (2005). Archaeal diversity and geochemical energy yields in a geothermal well on Vulcano Island, Italy. *Geobiology* 3, 319–332. doi: 10.1111/j.1472-4669.2006.00064.x

Rogers, K. L., and Amend, J. P. (2006). Energetics of potential heterotrophic metabolisms in the marine hydrothermal system of Vulcano Island, Italy. *Geochim. Cosmochim. Acta* 70, 6180–6200. doi: 10.1016/j.gca.2006.08.046

Rogers, K. L., Amend, J. P., and Gurrieri, S. (2007). Temporal Changes in Fluid Chemistry and Energy Profiles in the Vulcano Island Hydrothermal System. *Astrobiology* 7, 905–932. doi: 10.1089/ast.2007.0128

Rosi, M., Vezzoli, L., Aleotti, P., and De Censi, M. (1996). Interaction between caldera collapse and eruptive dynamics during the Campanian Ignimbrite eruption, Phlegraean Fields, Italy. *Bull. Volcanol.* 57, 541–554. doi: 10.1007/BF00304438

Rucker, H. R., Ely, T. D., LaRowe, D. E., Giovannelli, D., and Price, R. E. (2022). Quantifying the bioavailable energy in an ancient hydrothermal vent on Mars and a modern Earth-based analogue. doi: 10.1101/2022.09.09.507253

Ruiz-Chancho, M. J., Pichler, T., and Price, R. E. (2013). Arsenic occurrence and speciation in Cyclope neritea, a gastropod inhabiting the arsenic-rich marine shallow-water hydrothermal system off Milos Island, Greece. *Chem. Geol.* 348, 56–64. doi: 10.1016/j.chemgeo.2012.05.017

Rusch, A., Walpersdorf, E., deBeer, D., Gurrieri, S., and Amend, J. P. (2005). Microbial communities

near the oxic/anoxic interface in the hydrothermal system of Vulcano Island, Italy. *Chem. Geol.* 224, 169–182. doi: 10.1016/j.chemgeo.2005.07.026

Sacchi, M., Passaro, S., Molisso, F., Matano, F., Steinmann, L., Spiess, V., et al. (2020). "The holocene marine record of unrest, volcanism, and hydrothermal activity of Campi Flegrei and Somma–Vesuvius," in *Vesuvius, Campi Flegrei, and Campanian Volcanism*, (Elsevier), 435–469. doi: 10.1016/B978-0-12-816454-9.00016-X

Scheirer, D. S., Shank, T. M., and Fornari, D. J. (2006). Temperature variations at diffuse and focused flow hydrothermal vent sites along the northern East Pacific Rise. *Geochem. Geophys. Geosystems* 7, 2005GC001094. doi: 10.1029/2005GC001094

Scholten, L., Schmidt, C., Lecumberri-Sanchez, P., Newville, M., Lanzirotti, A., Sirbescu, M.-L. C., et al. (2019). Solubility and speciation of iron in hydrothermal fluids. *Geochim. Cosmochim. Acta* 252, 126–143. doi: 10.1016/j.gca.2019.03.001

Sciutteri, V., Smedile, F., Vizzini, S., Mazzola, A., and Vetriani, C. (2022). Microbial Biofilms Along a Geochemical Gradient at the Shallow-Water Hydrothermal System of Vulcano Island, Mediterranean Sea. *Front. Microbiol.* 13, 840205. doi: 10.3389/fmicb.2022.840205

Sheik, C. S., Reese, B. K., Twing, K. I., Sylvan, J. B., Grim, S. L., Schrenk, M. O., et al. (2018). Identification and Removal of Contaminant Sequences From Ribosomal Gene Databases: Lessons From the Census of Deep Life. *Front. Microbiol.* 9. doi: 10.3389/fmicb.2018.00840

Silva, A. C. P., Migliaccio, F., Barosa, B., Gallucci, L., Yücel, M., Foustoukos, D., et al. (2025a). Hydrodynamic flow and benthic boundary layer interactions shape the microbial community in Milos shallow water hydrothermal vents. Front. Microbiol. 16, 1649514. doi: 10.3389/fmicb.2025.1649514

Sims, K. W. W., Messa, C. M., Scott, S. R., Parsekian, A. D., Miller, A., Role, A. L., et al. (2023). The dynamic influence of subsurface geological processes on the assembly and diversification of thermophilic microbial communities in continental hydrothermal systems. *Geochim. Cosmochim. Acta* 362, 77–103. doi: 10.1016/j.gca.2023.10.021

Slobodkin, A. I., Reysenbach, A.-L., Slobodkina, G. B., Baslerov, R. V., Kostrikina, N. A., Wagner, I. D., et al. (2012). *Thermosulfurimonas dismutans* gen. nov., sp. nov., an extremely thermophilic sulfur-disproportionating bacterium from a deep-sea hydrothermal vent. *Int. J. Syst. Evol. Microbiol.* 62, 2565–2571. doi: 10.1099/ijs.0.034397-0

Somma, R., Iuliano, S., Matano, F., Molisso, F., Passaro, S., Sacchi, M., et al. (2016). High-resolution morpho-bathymetry of Pozzuoli Bay, southern Italy. *J. Maps* 12, 222–230. doi: 10.1080/17445647.2014.1001800

Sorokin, D. Yu., Tourova, T. P., Spiridonova, E. M., Rainey, F. A., and Muyzer, G. (2005). *Thioclava pacifica* gen. nov., sp. nov., a novel facultatively autotrophic, marine, sulfur-oxidizing bacterium from a near-shore sulfidic hydrothermal area. *Int. J. Syst. Evol. Microbiol.* 55, 1069–1075. doi: 10.1099/ijs.0.63415-0

Stöhr, R., Waberski, A., Völker, H., Tindall, B. J., and Thomm, M. (2001). H*ydrogenothermus marinus* gen. nov., sp. nov., a novel thermophilic hydrogen-oxidizing bacterium, recognition of *Calderobacterium hydrogenophilum* as a member of the genus *Hydrogenobacter* and proposal of the reclassification of *Hydrogenobacter acidophilus* as *Hydrogenobaculum acidophilum* gen. nov., comb. nov., in the phylum ' Hydrogenobacter/Aquifex .'

Sun, L., Toyonaga, M., Ohashi, A., Tourlousse, D. M., Matsuura, N., Meng, X.-Y., et al. (2016).

Lentimicrobium saccharophilum gen. nov., sp. nov., a strictly anaerobic bacterium representing a new family in the phylum Bacteroidetes, and proposal of *Lentimicrobiaceae* fam. nov. *Int. J. Syst. Evol. Microbiol.* 66, 2635–2642. doi: 10.1099/ijsem.0.001103

Tanaka, N., Romanenko, L. A., Iino, T., Frolova, G. M., and Mikhailov, V. V. (2011). *Cocleimonas flava* gen. nov., sp. nov., a gammaproteobacterium isolated from sand snail (Umbonium costatum). *Int. J. Syst. Evol. Microbiol.* 61, 412–416. doi: 10.1099/ijs.0.020263-0

Tarasov, V. G., Gebruk, A. V., Mironov, A. N., and Moskalev, L. I. (2005). Deep-sea and shallow-water hydrothermal vent communities: Two different phenomena? *Chem. Geol.* 224, 5–39. doi: 10.1016/j.chemgeo.2005.07.021

Tebo, B., and Mandernack, K. W. (1993). Manganese scavenging and oxidation at hydrothermal vents tid in vent plumes.

Tedesco, D., Allard, P., Sano, Y., Wakita, H., and Pece, R. (1990). Helium-3 in subaerial and submarine fumaroles of Campi Flegrei caldera, Italy. *Geochim. Cosmochim. Acta* 54, 1105–1116. doi: 10.1016/0016-7037(90)90442-N

Tivey, M. K. (2007). Generation of Seafloor Hydrothermal Vent Fluids and Associated Mineral Deposits. *Oceanography*, 65.

Torrente, M. M., and Milia, A. (2013). Volcanism and faulting of the Campania margin (Eastern Tyrrhenian Sea, Italy): a three-dimensional visualization of a new volcanic field off Campi Flegrei. *Bull. Volcanol.* 75, 719. doi: 10.1007/s00445-013-0719-0

Tramparulo, F. D. A., Vitale, S., Isaia, R., Tadini, A., Bisson, M., and Prinzi, E. P. (2018). Relation between alternating open/closed-conduit conditions and deformation patterns: An example from the Somma-Vesuvius volcano (southern Italy). *J. Struct. Geol.* 112, 138–153. doi: 10.1016/j.jsg.2018.05.008

Upin, H. E., Newell, D. L., Colman, D. R., and Boyd, E. S. (2023). Tectonic settings influence the geochemical and microbial diversity of Peru hot springs. *Commun. Earth Environ.* 4, 112. doi: 10.1038/s43247-023-00787-5

Von Damm, K. L., and Lilley, M. D. (2004). "Diffuse flow hydrothermal fluids from 9° 50′ N East Pacific Rise: Origin, evolution and biogeochemical controls," in *Geophysical Monograph Series*, eds. W. S. D. Wilcock, E. F. DeLong, D. S. Kelley, J. A. Baross, and S. Craig Cary (Washington, D. C.: American Geophysical Union), 245–268. doi: 10.1029/144GM16

Watanabe, M., Galushko, A., Fukui, M., and Kuever, J. (2021). "*Desulfosarcinaceae*," in *Bergey's Manual of Systematics of Archaea and Bacteria*, ed. W. B. Whitman (Wiley), 1–4. doi: 10.1002/9781118960608.fbm00329

Xin, X., Li, B., Liu, X., Yang, W., and Liu, Q. (2023). Starting-up performances and microbial community shifts in the coupling process (SAPD-A) with sulfide autotrophic partial denitrification (SAPD) and anammox treating nitrate and ammonium contained wastewater. *J. Environ. Manage.* 331, 117298. doi: 10.1016/j.jenvman.2023.117298

Yoon, S.-H., Ha, S.-M., Kwon, S., Lim, J., Kim, Y., Seo, H., et al. (2017). Introducing EzBioCloud: a taxonomically united database of 16S rRNA gene sequences and whole-genome assemblies. *Int. J. Syst. Evol. Microbiol.* 67, 1613–1617. doi: 10.1099/ijsem.0.001755

Yücel, M., Sievert, S. M., Vetriani, C., Foustoukos, D. I., Giovannelli, D., and Le Bris, N. (2013). Eco-geochemical dynamics of a shallow-water hydrothermal vent system at Milos Island,

Aegean Sea (Eastern Mediterranean). *Chem. Geol.* 356, 11–20. doi: 10.1016/j.chemgeo.2013.07.020

Zhang, Y., Zhao, Z., Chen, C.-T. A., Tang, K., Su, J., and Jiao, N. (2012). Sulfur Metabolizing Microbes Dominate Microbial Communities in Andesite-Hosted Shallow-Sea Hydrothermal Systems. *PLoS ONE* 7, e44593. doi: 10.1371/journal.pone.0044593

Figure Legends

Figure 1. Map depicting the shallow-water hydrothermal vents sampled. **A -** Regional map of Italy (red square indicating the sampled locations). **B -** Map of the Gulf of Naples**.** Coloured points represent the different locations sampled in the present study, along the bathymetry depiction of the region. Grey points are known shallow-water hydrothermal vents from the literature (De Astis et al., 2004; Aiello et al., 2010; Kerrison et al., 2011; Calosi et al., 2013; Torrente and Milia, 2013; Passaro et al., 2014b; Somma et al., 2016; Donnarumma et al., 2019; Baldrighi et al., 2020; Bellec et al., 2020; Sacchi et al., 2020).

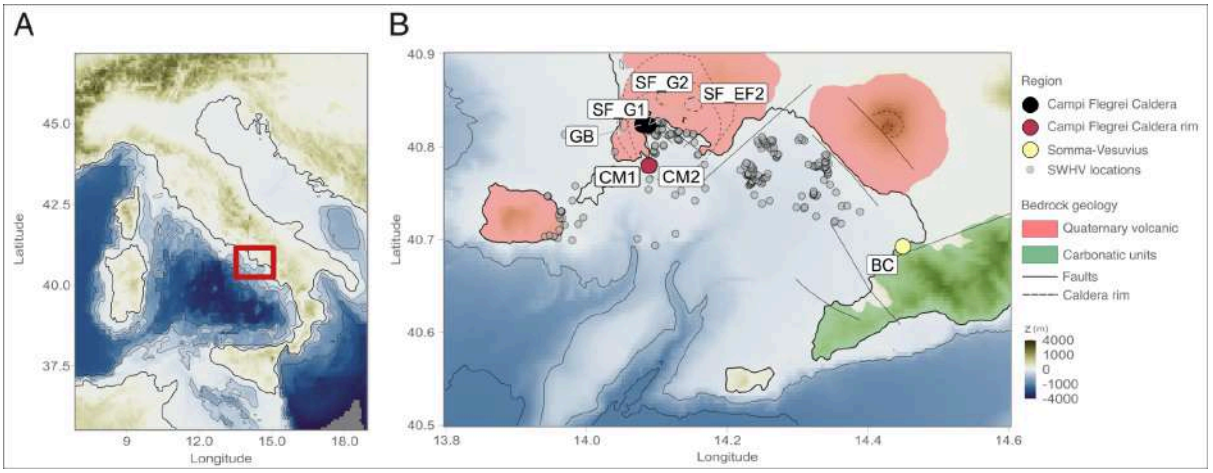

Figure 2. Geochemical data measured at the different shallow-water hydrothermal vents of the Campi Flegrei region and Somma-Vesuvius. Seawater concentrations were taken from Price et al., 2015**. A)** Principal component analysis (PCA) with geochemical data measured (major ions and trace elements; see Table 2 and 3). **B)** Biplot Cl^- against Na^+ **C)** Biplot Cl^- against Mg^{2+} **D)** Biplot Br^{2-} against Cl^- **E)** Biplot SO_4^{2-} against Cl^- and **F)** Biplot Fe against Mg^{2+}. Values reported in ppm and errors related to the measurements are reported in Table 2 and 3.

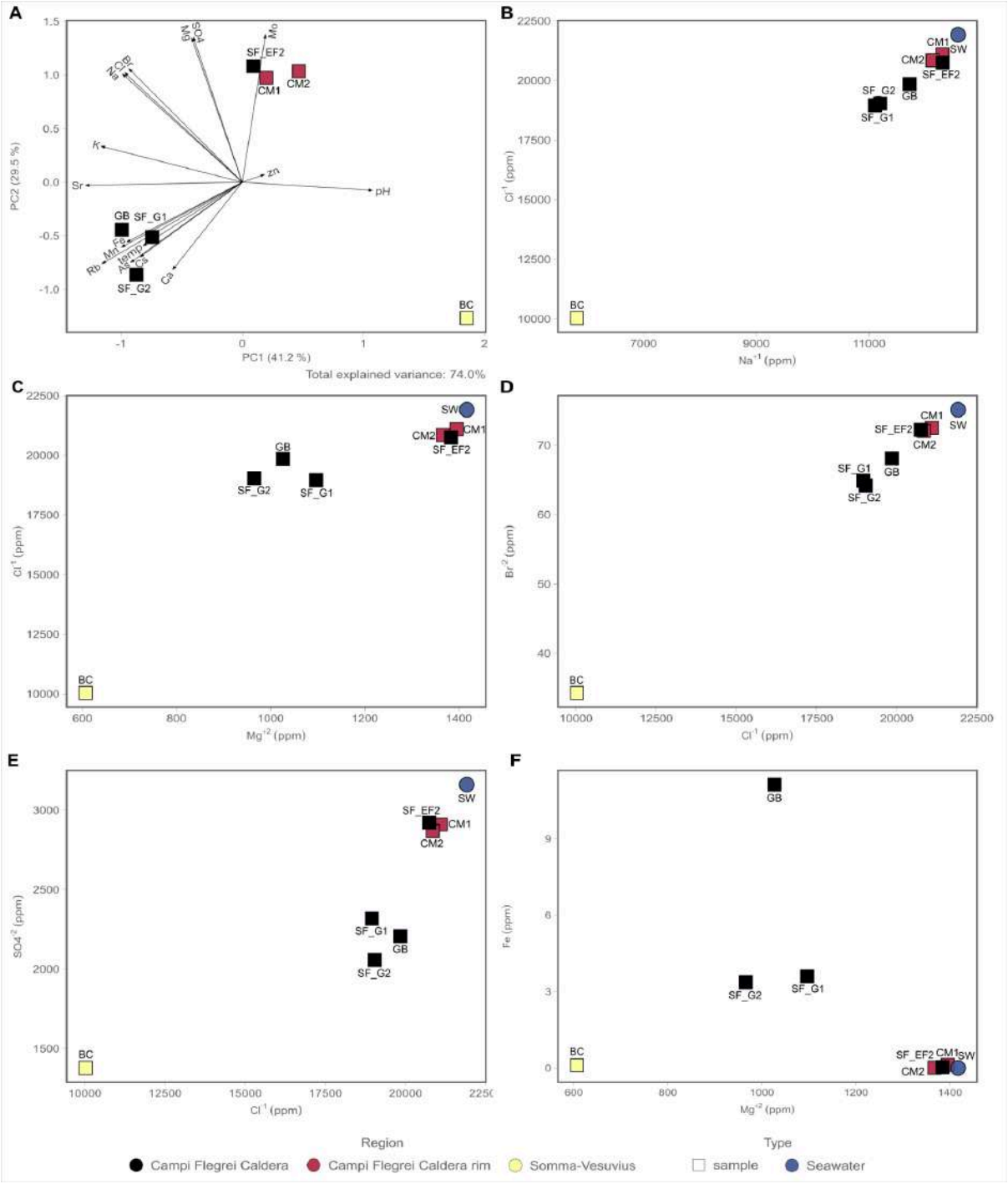

Figure 3. Microbial community composition of the different shallow-water hydrothermal vents sampled, with the two matrices, sediments and fluids. A) Phylum taxonomic rank; B) Order taxonomic rank.

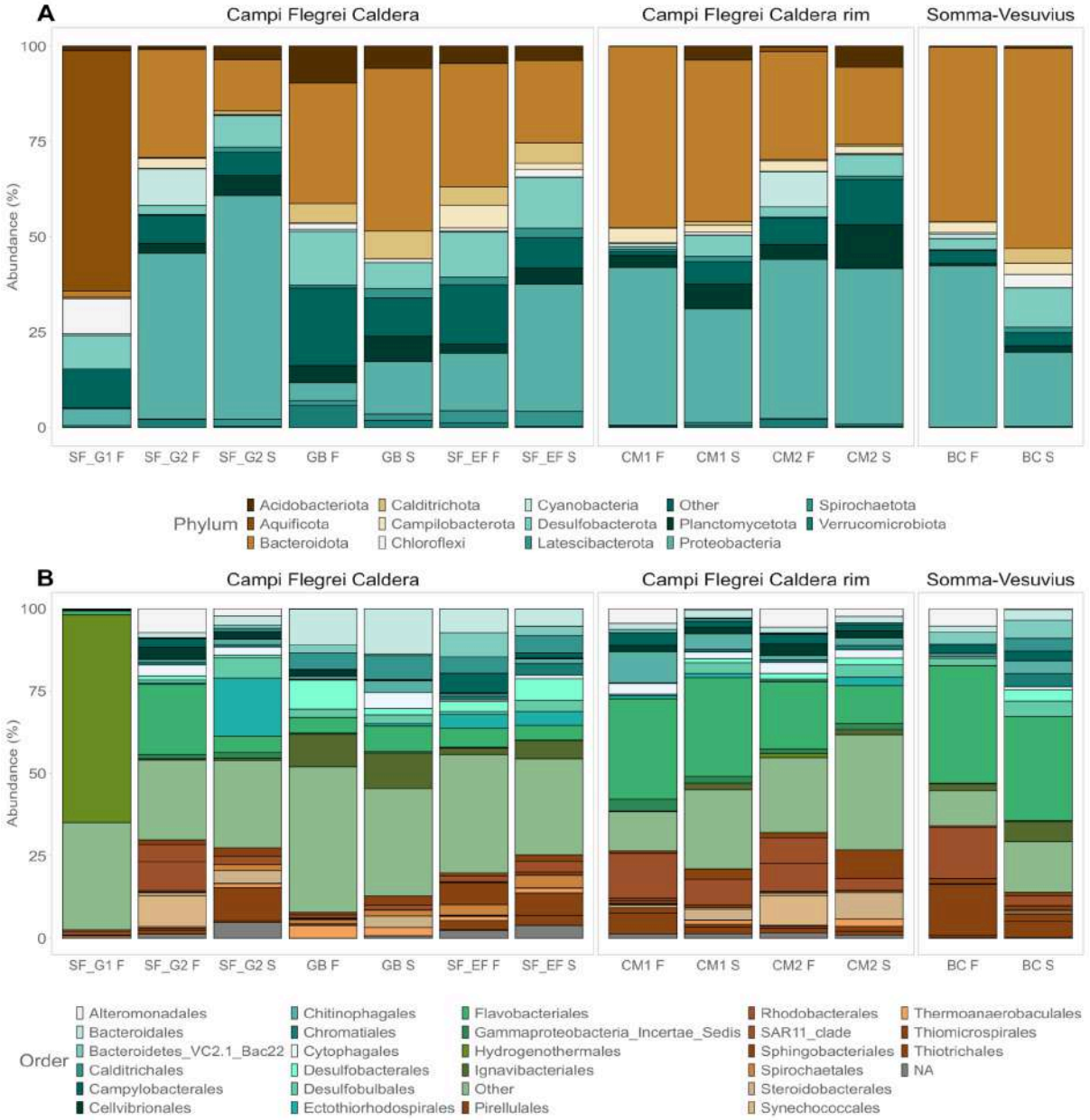

Figure 4. Microbial community composition of the biofilms sampled around the different shallow-water hydrothermal vents studied here: A) Phylum taxonomic rank; B) Order taxonomic rank.

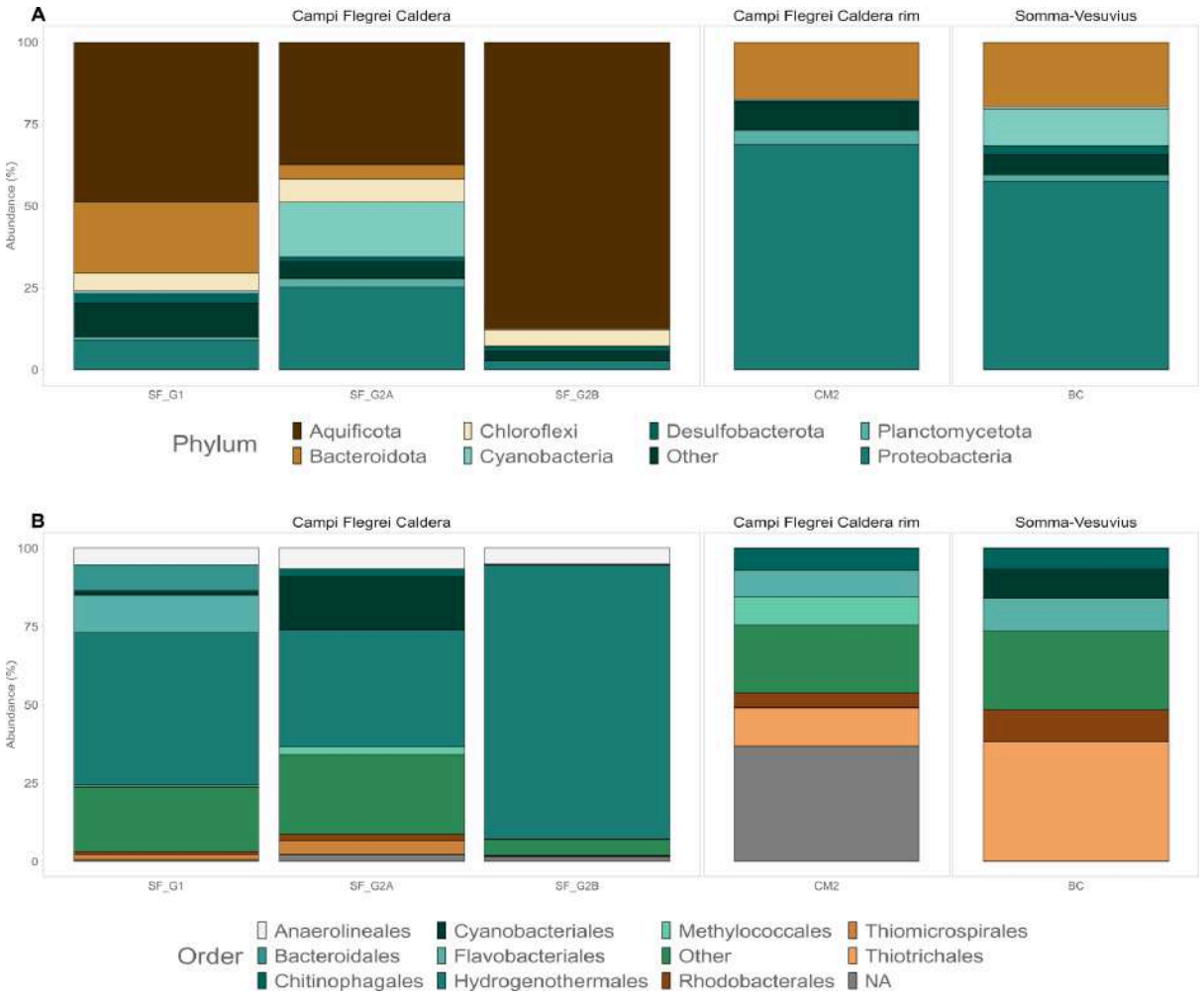

Figure 5. Beta-diversity analysis based on Non-metric multidimensional scaling (nMDS) using the Weighted Jaccard similarity index. A) nMDS coloured by sampling region, B) nMDS coloured by geochemistry (clusters seen on the PCA analysis of the geochemical data) and C-H) *ordisurf* analysis of the most significant variables.

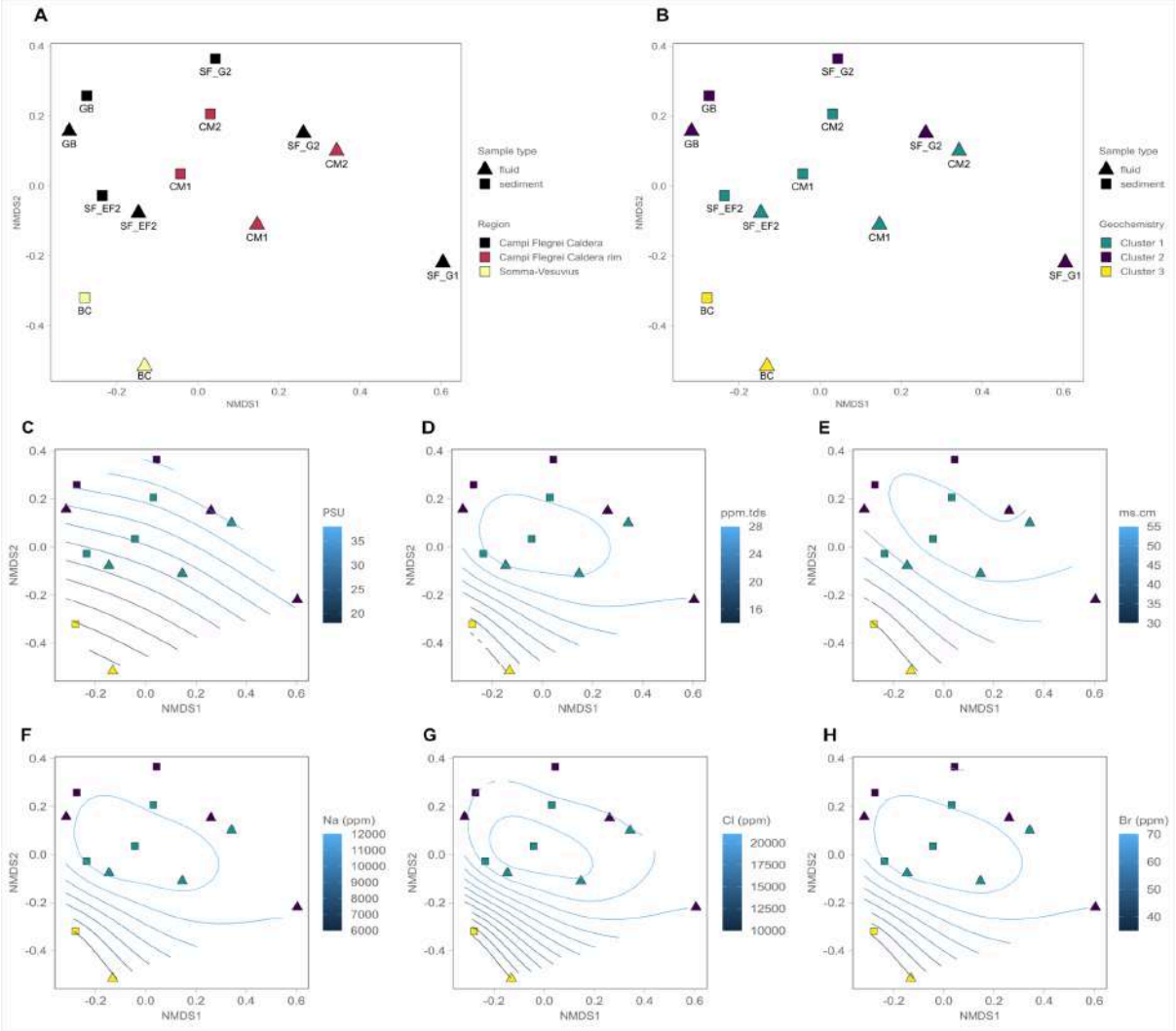

Tables

Table 1. Location (GPS coordinates), Depth, and the Physico-chemical parameters measured on the venting fluids at the different sampled locations. ORP - Oxido-reduction potential; DO - Dissolved oxygen; mS/cm - Conductivity; ppt tds - Total dissolved solids.

Site	Latitude (°N)	Longitude (°E)	Depth (m)	Temp (ºC)	Salinity (PSU)	DO (%)	ORP (mV)	pH	SPC (mS/cm)	TDS (ppm)
CM1	40.77955	14.08835	7	26.3	27.54	55	-115.4	5.87	56.58	28.35
CM2	40.77955	14.08835	8.3	27	38.37	92	54.2	6.3	57.54	28.76
GB	40.82375	14.0789	5.4	28	35.41	43	-145.2	5.33	53.64	26.8
SF_EF2	40.82305556	14.0875	10	34	26.5	75	-173	5.25	NA	28.5
SF_G1	40.82305556	14.0875	13.3	71	34.06	50.8	-159	5.45	51.8	25.9
SF_G2	40.82305556	14.0875	12.9	68.9	34.5	51.8	-142	5.61	52	26.1
BC	40.688578	14.454745	-0.5	26.4	17.65	53.7	-226.2	6.3	28.66	14.31

Table 2. Concentrations (ppm) of the major anions and cations of the different sampled shallow-water hydrothermal vents (error ± in % RSD). Seawater (SW) values were obtained from Price et al., 2015.

Site	Cl^- (ppm)	Br^- (ppm)	SO_4^{2-} (ppm)	Na^+ (ppm)	NH_4^+ (ppm)	K^+ (ppm)	Mg^{2+} (ppm)	Ca^{2+} (ppm)
CM1	21094.04 ± 0.08	72.48 ± 0.38	2909.92 ± 0.12	12456.39 ± 0.04	NA	401.85 ± 0.81	1395.68 ± 0.71	462.97 ± 1.32
CM2	20846.61 ± 0.09	72.06 ± 0.79	2868.06 ± 0.15	12246.10 ± 0.00	NA	394.59 ± 0.53	1366.58 ± 0.1	435.08 ± 0.09
GB	19842.83 ± 0.08	68.07 ± 0.03	2206.67 ± 0.05	11868.50 ± 0.05	33.28 ± 2.59	598.43 ± 0.81	1026.30 ± 0.05	479.80 ± 1.28
SF_EF2	20741.32 ± 0.07	72.20 ± 0.91	2920.13 ± 0.06	12783.86 ± 0.03	NA	406.04 ± 0.99	1383.97 ± 0.13	434.79 ± 0.69
SF_G1	18952.08 ± 0.08	64.86 ± 0.44	2316.92 ± 0.01	11233.85 ± 0.05	40.08 ± 0.55	384.93 ± 0.24	1096.45 ± 0.24	444.47 ± 0.33
SF_G2	19033.28 ± 0.04	64.18 ± 0.66	2057.21 ± 0.20	11297.79 ± 0.01	40.30 ± 0.21	412.15 ± 0.06	965.41 ± 0.72	497.28 ± 0.43
BC	10030.06 ± 0.06	34.27 ± 0.36	1377.55 ± 0.09	5844.84 ± 0.02	NA	198.47 ± 0.77	606.89 ± 0.06	461.07 ± 0.74
SW	21910	75.11	3160.4	12581	NA	430	1417	444.9

Table 3. Concentrations (ppm) of the trace elements of the different sampled shallow-water hydrothermal vents (error ± in % RSD).

Site	Mn (ppm)	Fe (ppm)	Zn (ppm)	As (ppm)	Rb (ppm)	Sr (ppm)	Mo (ppm)	Cs (ppm)
CM1	0.061 ± 2	0.113 ± 1.7	0.457 ± 1.8	0.022 ± 1.2	0.158 ± 1	11.403 ± 0.2	0.011 ± 4.3	0.002 ± 4.2
CM2	0.004 ± 4.9	0.011 ± 4.2	0.033 ± 7.1	0.020 ± 3.8	0.148 ± 0.8	10.232 ± 0.8	0.012 ± 1.2	0.005 ± 3.3
GB	3.099 ± 06	11.123 ± 1.1	0.171 ± 3.1	0.513 ± 1	3.237 ± 0.6	11.488 ± 0.5	0.001 ± 6.2	0.170 ± 0.7
SF_EF2	0.007 ± 6.8	0.034 ± 4.7	0.023 ± 9.6	0.011 ± 0.9	0.146 ± 1.4	10.712 ± 0.4	0.012 ± 1.5	0.004 ± 1.4
SF_G1	1.184 ± 2.9	3.591 ± 3.1	0.186 ± 3.7	1.909 ± 2.3	2.430 ± 2.4	13.262 ± 1.9	0.001 ± 3.7	1.730 ± 2.8
SF_G2	1.131 ± 0.8	3.361 ± 1.2	0.048 ± 0.6	2.447 ± 0.4	2.424 ± 0.2	13.074 ± 1	0.002 ± 6.5	1.645 ± 0.6
BC	0.047 ± 4.5	0.098 ± 3.8	0.194 ± 2.3	0.011 ± 4.9	0.121 ± 1.4	8.111 ± 0.6	0.000 (NA)	0.006 ± 1.3